DEVELOPMENT OF A THERMODYNAMIC

DATABASE, EVALUATION OF EXPERIMENTAL

ENTHALPY DEPARTURE DATA, AND MODELING

PHASE BEHAVIOR IN WEAK AQUEOUS

ELECTROLYTE MIXTURES

By

ERIC LAWRENCE MAASE

Bachelor of Science
University of Maryland
College Park, Maryland
1993

Master of Science
Colorado School of Mines
Golden, Colorado
1995

Submitted to the Faculty of the
Graduate College of the
Oklahoma State University
in partial fulfillment of
the Degree of
DOCTOR OF PHILOSOPHY
December 2004

DEVELOPMENT OF A THERMODYNAMIC

DATABASE, EVALUATION OF EXPERIMENTAL

ENTHALPY DEPARTURE DATA, AND MODELING

PHASE BEHAVIOR IN WEAK AQUEOUS

ELECTROLYTE MIXTURES

Dissertation Approved:

<u>   Jan Wagner   </u>
Dissertation Adviser

<u>   Khaled A. M. Gasem   </u>

<u>   Arland H. Johannes   </u>

<u>   John Chandler   </u>

<u>   A. Gordon Emslie   </u>
Dean of the Graduate College

ACKNOWLEGEMENTS

TABLE OF CONTENTS

LIST OF TABLES

LIST OF FIGURES

NOMENCLATURE

a, b, c, d   Regression coefficients

T   Temperature

P, p   Pressure

°C   Temperature, Degrees Celsius

K   Temperature, Kelvin

K or K_{VLE} Vapor / Liquid Equilibrium Constant

T_r Reduced Temperature

T_c Critical Temperature

p_c Critical Pressure

v_c Critical Volume

C_p° Ideal gas heat capacity at constant pressure

C_u° Ideal gas heat capacity at constant volume

C_{ij} SRK or PR-EOS binary interaction parameter

D_{ij} SRK or PR-EOS interaction parameter

A Helmholtz energy

$A - A^\circ$	Helmholtz energy departure function
H°	Ideal gas enthalpy
$H - H^\circ$	The enthalpy departure function
$H(T, p)$	Enthalpy of a pure fluid or fluid mixture
$H(T^\circ, p^\circ)$ Or H°	Enthalpy at a defined reference state
$G(T, p)$	Gibbs free energy of a pure fluid or fluid mixture
$G(T^\circ, p^\circ)$ Or G°	Gibbs free energy at a defined reference state
$\Delta \bar{G}^\circ_{r,T,P}$	Gibbs free energy of a reaction at standard state conditions
$\Delta \bar{G}_{i,T,P}$	Gibbs free energy of a component at T and P
$\Delta \bar{G}^\circ_{i,T,P}$	Gibbs free energy of a component at standard state
$\Delta \bar{G}^\circ_{f,T_r,P_r}$	Gibbs free energy of formation of a component at standard state
Q	Activity product
K or K_r	Chemical Equilibrium Constant
$S - S^\circ$	Entropy departure function from ideal gas state
(pvT)	Pressure-volume-temperature properties
R	Ideal Gas law constant
M_i	Molal concentration of a molecular species

m_j	Molal concentration of ionic or soluble molecular species
m_{vi}	Molal concentrations of the molecular species in the vapor phase
m_{Li}	Molal concentrations of the molecular species in the liquid phase
λ_j	Combination parameter; Stoichiometry of Elements in Molecule
υ_{ei}	Atoms of each element present in the molecular formula for each
m_e	Total molality of an element e species
z	Charge of ionic species
B	Solvent constant related to dielectric constant of the medium
$\overset{\circ}{a}$	Debye-Hückel, Ion size parameter
d	Debye-Hückel hard sphere diameter of an ion
g_i^{DH}	Debye-Hückel activity coefficient
H	Henry's Law constant
$\dot{B}$	Davies Equation, B-dot coefficient
β	Bromley Equation, Beta parameter
a	SRK, PR EOS Parameter
m	SRK, PR EOS parameter
a_i, b_i	SRK, PR EOS pure component parameters
a, b	SRK, PR EOS mixing parameters

g_{ij}	PR-EOS Enthalpy Calculation parameter (Defined in Equation. ?-?)
a	Debye-Hückel factor
b_{ik}	Debye-Hückel interaction parameter between species i and k
$l_{i,j}(I)$	Ionic strength dependent second virial coefficient
$t_{i,j,k}$	Triplet interaction parameter
D_{ij}	Second virial coefficient
E_{ijk}	Third virial coefficient
r_i	Stoichiometric coefficient of a reactant species
R_i	Reactant species
p_i	Stoichiometric coefficient of a product species
P_i	Product species
x_i	Mole fraction of component i in liquid phase
y_i	Mole fraction of component i in vapor phase
f_v	Vapor Phase Fugacity coefficient
f_l	Liquid Phase Fugacity coefficient
a	Activity
g_i	Activity coefficient
M^+	Cation species

X^-	Anion species
$\bar{G}^{\circ}_{T_r,P_r}$	Standard state Gibbs free energy at T and P
$\bar{G}^{\circ}_{T,P}$	Standard state Gibbs free energy at defined reference state
$-\bar{S}^{\circ}_{T_r,P_r}$	Entropy at standard state reference
$\bar{C}^{\circ}_{P_r}$	Isobaric heat capacity standard state reference
$\bar{V}^{\circ}_{T_r}$	Isothermal volume at the standard state reference
d_i	Dissociation fraction

ACRONYMS

DEV$_i$ Point Deviation

$$DEV_i = \left(H_{i,Calc} - H_{i,Exp} \right)$$

%DEV$_i$ Percent Deviation

$$\%DEV_i = 100 \times \frac{\left(H_{i,Calc} - H_{i,Exp} \right)}{H_{i,Exp}}$$

BIAS   Bias; Multiple Point Error Measure

$$BIAS @ \frac{\sum_{i=1}^{NPTS} \left(DEV_i \right)}{NPTS}$$

AAD   Average absolute deviation; Multiple Point Error Measure

$$AAD \equiv \frac{\sum\limits_{i=1}^{NPTS} \left| DEV_i \right|}{NPTS}$$

%AAD   Percent average absolute deviation; Multiple Point Error Measure

$$AAD \equiv \frac{\sum\limits_{i=1}^{NPTS} \left| \%DEV_i \right|}{NPTS}$$

RMSE   Root-Mean-Square-Error; Multiple Point Error Measure

$$RMSE \equiv \sqrt{\frac{\sum\limits_{i=1}^{NPTS} \left(DEV_i \right)^2}{NPTS}}$$

L   Denotes Liquid Phase

V   Denotes Vapor Phase

L-V-V   Liquid-Vapor Phase, Vapor measurement

L-L-V   Liquid-Vapor Phase, Liquid measurement

NPTS   Number of data points

EOS   Equation of State

PR, PR-EOS   Peng-Robinson Cubic Equation of State

SRK, SRK-EOS Soave-Redlich-Kwong Cubic Equation of State

GPA   Gas Processors Association

NRTL   Non-Random Two-Liquid Theory

UNIQUAC   Universal Quasi-Chemical Theory

SUBSCRIPTS

  i i^{th} component / species

  j j^{th} component / species

  r   Reaction

  e   Element

  l   Liquid

  v   Vapor

  Calc   Calculated

  Exp   Experimental

SUPERSCRIPTS

  °   Degrees Temperature

  °   Standard State Temperature and Pressure Conditions

GREEK SYMBOLS

  ω Pitzer Accentric factor

SECTION ONE

ORGANIZATION AND EVALUATION OF EXPERIMENTAL DATA

CHAPTER I

INTRODUCTION

The Gas Processor's Association (GPA) is a cooperative research organization sponsored by a consortium of energy sector companies. The GPA directs research in thermodynamics and physical properties areas, focusing on gases, light hydrocarbons, and process solvents for the recovery and purification of natural gas, liquefied petroleum gas and substitute gas [2]. Sponsor companies receive the economic benefits from the cooperative research. By dividing the cost of research among multiple companies, the participating organizations acquire valuable research for a fraction of the cost of other alternatives.

A recent research goal focused on the organization and continuing maintenance of the extensive compilation of thermodynamic data, including enthalpy departure data, gathered by the GPA over many years research. The GPA commissioned Project 921, Enthalpy Database Development and Maintenance, to compile, evaluate, and maintain experimental enthalpy, heat of solution and isothermal enthalpy departure data for pure fluids and mixtures of interest to the gas processing industry [3].

In this context, the database primary use is: 1) evaluate enthalpy prediction methods and computer models, 2) develop new or system-specific correlations, and 3) provide experimental measurements for direct application in process engineering calculations.

ORGANIZATION OF EXPERIMENTAL DATA

The primary purpose of the GPA Thermodynamic Database is to provide a basis for evaluating and developing enthalpy and phase equilibrium prediction methods and computer programs and to provide experimental measurements for direct application (interpolation) in process engineering calculations. In this context, the development of the GPA Thermodynamic Database was undertaken with two main features in mind. First, it is restricted to data applicable to gas processing operations. Second, it contains only data generated by the GPA Research Program and evaluated outside data. The bottom-line benefits of the GPA Research Program are well-documented [1-4], and consolidation of enthalpy and phase equilibrium data from the GPA Research Programs in a single source is an added feature of the Database.

The enthalpy and phase equilibrium database development was initiated in 1981 under GPA Projects 806 and 822 by Tom Daubert at The Pennsylvania State University and the joint guidance of the GPA Phase Equilibria and Enthalpy Steering Committees [5]. It contained only vapor-liquid equilibrium data and enthalpy departures for pure hydrocarbons and acid gases and binary mixtures of these compounds with each other and with water. As development continued, vapor-liquid-liquid (both aqueous and non-aqueous), vapor-liquid-solid, and vapor-liquid-hydrate data were included in the phase equilibrium database, and the enthalpy database was extended to multicomponent mixtures [6-8].

EVALUATION OF ENTHALPY DATA

Accurate enthalpy data are crucial for design as well as operation of efficient chemical processes. Improper design of equipment leads, at best, to over-expenditure of capital and unnecessary higher operating costs. While many equations exist for enthalpy prediction for different groups of fluids at desired pressures, temperatures, phases, and compositions, no single equation exists which accurately predicts enthalpy of all fluid, or fluid mixture, at any process conditions. Experimental enthalpy data are necessary for evaluation of the equations used for enthalpy prediction, and to provide more exact data than engineering models are able to provide. Available experimental enthalpy data accuracy may be questionable when taken from multiple sources, each perhaps with a unique reference state and experimental background. The Gas Processors' Association (GPA) maintains a thermodynamic database including enthalpy data. The accuracy of the enthalpy data in this database is evaluated with the application of equations of state and statistical analysis. The Peng-Robinson equation of state and statistical analysis [1] are employed in this evaluation.

The GPA continually compiles research results into a common database, with the goals of efficient distribution, consolidation of similar and related research data, and as a source of verifiably precise and reliable experimental data. This database, available to sponsor companies, helps produce more accurate and efficient process designs, as well as improving simulations of existing equipment and improving efficiency. The economic benefits from improved design in industry can be staggering, not only yielding lower capital costs, but also reducing operating costs for the lifetime of the designed equipment. To meet these goals, the data of the database must meet the highest standards possible for

thermodynamic consistency, experimental verification (original source verification), and

include evaluations of the data 'reliability.'

CHAPTER II

GPA THERMODYNAMIC DATABASE

INTRODUCTION

In 1993, Oklahoma State University assumed responsibility for the enthalpy and phase equilibrium database development and maintenance under GPA Projects 921 and 925. Flat-file databases are inherently slow and unwieldy systems to search efficiently, and part of these projects involved conversion of the basic data structures to a relational database model [9] that includes pure-component physical properties. The current version of the GPA Thermodynamic Database is a software application written in Microsoft Access Basic™. The user can interactively search the database using several predefined queries and export selected records to text files or Microsoft Excel™ spreadsheets. Alternatively, users with experience in structured query language (SQL) or Microsoft Access™ can develop customized queries.

There are seven basic data categories in the GPA Database. Table 1 summarizes the number of data sets and data points in each category. As shown in Tables 2 and 3, the data sets in each category cover a wide range of temperatures, pressures, and compositions. In addition, the physical properties for the 109 pure components from

Figure 23-2 of the GPSA Engineering Data Book [10] are included in the GPA Thermodynamic Database.

A data input form has been developed for each category, and users can use these input forms to add additional data sets to the Database. These user-added records are identified and preserved during updates of the GPA Thermodynamic Database.

A unique feature of the GPA Thermodynamic Database is the open structure that allows SQL compliant applications, such as Visual Basic™ or Visual C++™, to interface with the data tables. Users can develop applications to cross-reference data to in-house programs or other applications, i.e., Microsoft Excel™.

ENTHALPY DATA

Background

GPA enthalpy research projects have resulted in the publication of experimental pure component and mixture enthalpies for systems of interest to the gas processing industry. However, most of the published data were based on different reference states. To eliminate this variation in the reported data, the GPA enthalpy data were converted to two common reference states: the ideal gas state at 0 K, and the elemental states at 25 °C. Lenoir (1973) [11] undertook the development of techniques for data conversion in GPA Project 733.

Under GPA Projects 806 and 822-91 [8], all the experimental enthalpy data in the GPA Enthalpy Databank were presented as enthalpy departures. This was done to provide

appropriate means for evaluating predictive models, and for individual companies to evaluate their in-house correlations.

The GPA Enthalpy Databank contains experimental isothermal enthalpy departure data (Tables A4, A5, and A6) and enthalpy of solution data (Tables A7, A8, and A9) for pure fluids and mixtures of interest to the gas processing industry. The intended use of these data are primarily to (1) evaluate enthalpy prediction methods and computer models, (2) develop new or system-specific correlations, and (3) provide experimental measurements for direct application in process engineering.

ENTHALPY DATA QUALITY ASSURANCE

Several procedures have been employed to assess the quality of the enthalpy data in the GPA database.

Data Entry Checks.

All records for pure component systems have been compared to the original references to verify the correct entry of temperature, pressure, and composition. In most instances, the enthalpy data cannot be checked against the original references, because the original measurements have been converted to enthalpy departures.

Equation-of-State Data Screening.

The content of the enthalpy departure databank was examined for gross errors and outliers. A Peng-Robinson equation of state (EOS) was used to screen and evaluate the GPA enthalpy data. Data for pure fluids and binary, ternary, and multi-component mixtures in the sub-cooled and superheated regions were examined. Data points that

exhibit higher than expected deviations between the experimental (raw and smoothed) and EOS predicted enthalpy departures have been identified for further examination. In contrast to previous evaluations described in GPA RR-69 and RR-81 [12, 13], the single-phase enthalpy departures were calculated directly and not within the vapor-liquid equilibrium framework. In addition, the original Peng-Robinson mixing rules, which utilize pure fluid critical properties and accentric factors, were used.

Data entry checks and handling of outliers have been concerned with errors and omissions related to temperature, pressure, composition, and phase code entries. As noted above, entries for the enthalpy departure values in the database cannot be directly compared to the original measurements. The original enthalpy data have been smoothed and/or manipulated to generate enthalpy departure values, which were entered into the GPA Enthalpy Databank.

The criteria used to identify data points exhibiting larger-than-expected deviations between the reported and predicted enthalpy departures are summarized in Table A10. The methodology applied and the analyses used to identify data records meriting further examination are described in detail by Rastogi [14], Twoomey [15], and this work develop three-dimensional deviation plots to help detect systematic trends in deviations, and develop systematic analysis methods of the equation-of-state calculation approach.

Records exhibiting larger-than-expected deviations were not deleted from the database. They are flagged with a code corresponding to the criteria in Table A10.

Loop Closure Analysis.

Software was developed to implement a loop-closure analysis [14]. Reproducing the loop closure results reported in earlier GPA studies validated the procedure. Loop-closure errors are less than 1 percent for the 14 data sets amenable to this type of analysis.

PHASE EQUILIBRIA DATA

The original phase-equilibrium data banks described in GPA Research Report RR-64C (Daubert, 1993) included vapor-liquid equilibrium data (commonly referred to as K-values), bubble-point and dew-point data, vapor-liquid-liquid and vapor-liquid-solid equilibrium data, and hydrate equilibrium data. During 1999, amine-solvent equilibrium data were added to the new relational database as part of GPA Project 925. In addition, data from GPA Research Reports have been included, as they became available.

The dew-point and bubble-point data can be summarized in several ways. Table A11 presents the data by the components in each data set. Other summaries based on the phase condition and the number of components are shown in Tables A12 and A13, respectively.

The vapor-liquid-equilibrium data are summarized in Tables A14 and A15. Summarizing the data by system composition is unwieldy due to the large number of components represented in vapor-liquid-equilibrium data sets. The vapor-liquid-liquid and vapor-liquid-solid data and hydrate data are summarized in Tables A16 and A17, respectively.

PHASE EQUILIBRIA DATA QUALITY ASSURANCE

Procedures similar to those used to assess the quality of the enthalpy data were used to assess the quality of phase equilibria records in the database.

Data Entry Checks.

All records have been compared to the original references to verify the correct entry of temperature, pressure, and phase compositions. During this process, the original source was reviewed to determine whether the records represented raw or smoothed data. Both types of data were entered into the database, if they were published.

The point-by-point verification of records against the original reference resulted in the addition of approximately 4,200 new records for the existing references. In addition, some of the dew and bubble-point data sets (phase boundary conditions) included critical conditions. These records were identified with a "CP" phase condition identifier.

EOS Data Screening.

Few of the bubble-point, dew-point, and vapor-liquid equilibrium data sets are amenable to point or integral tests for thermodynamic consistency. An equation-of-state screening approach was used to identify those records exhibiting larger than expected deviations from a Peng-Robinson equation of state (EOS) [16].

Vapor-liquid equilibrium records usually do not include feed compositions or relative quantities of the vapor and liquid phases. Therefore, the liquid phase composition was used in bubble-point calculations at the system temperature, and the predicted pressure and vapor compositions were compared to the experimental values to identify outliers.

The criteria outlined in Table A10 were used to identify data points exhibiting larger-than-expected deviations, and these records were flagged with the corresponding criterion number. The methodology applied and the analyses used to identify data records meriting further examination are similar to those described by Rastogi [14] and Twomey [15] for enthalpy departure records. No records have been deleted; all data from the original publications have been preserved.

DATABASE STRUCTURE AND USE

A simplified representation of the structure of the GPA Thermodynamic Database is shown in Figure 1, where each of the blocks represents one or more data tables in the relational database.

The data set number is the primary key which links references, authors, components, and data type to the data records for each of the seven categories of data. The relational structure of records representing individual data points within each of the categories is dictated by the format in which data are typically reported. For example, dew and bubble point, vapor-liquid equilibrium, vapor-liquid-liquid, and vapor-liquid-solid solid equilibrium data tables are very similar. At the data-point level, the state variables – temperature and pressure – are stored in one table and the phase compositions are stored in a second table. The structure of the hydrate data records includes the phase equilibrium data, but a second table is needed to store the overall concentration of inhibitors. Distinct data tables and relations are required to accommodate the enthalpy departure, enthalpy of solution, and amine data.

The reference, authors, and component tables contain "descriptive" information for each data set. Queries included in the Database use these tables for search options. Users may search the database by data type or types and the number of components in the system. The results of a search can be reported in user specified units for temperature, pressure, and enthalpy and filtered by setting temperature and pressure ranges.
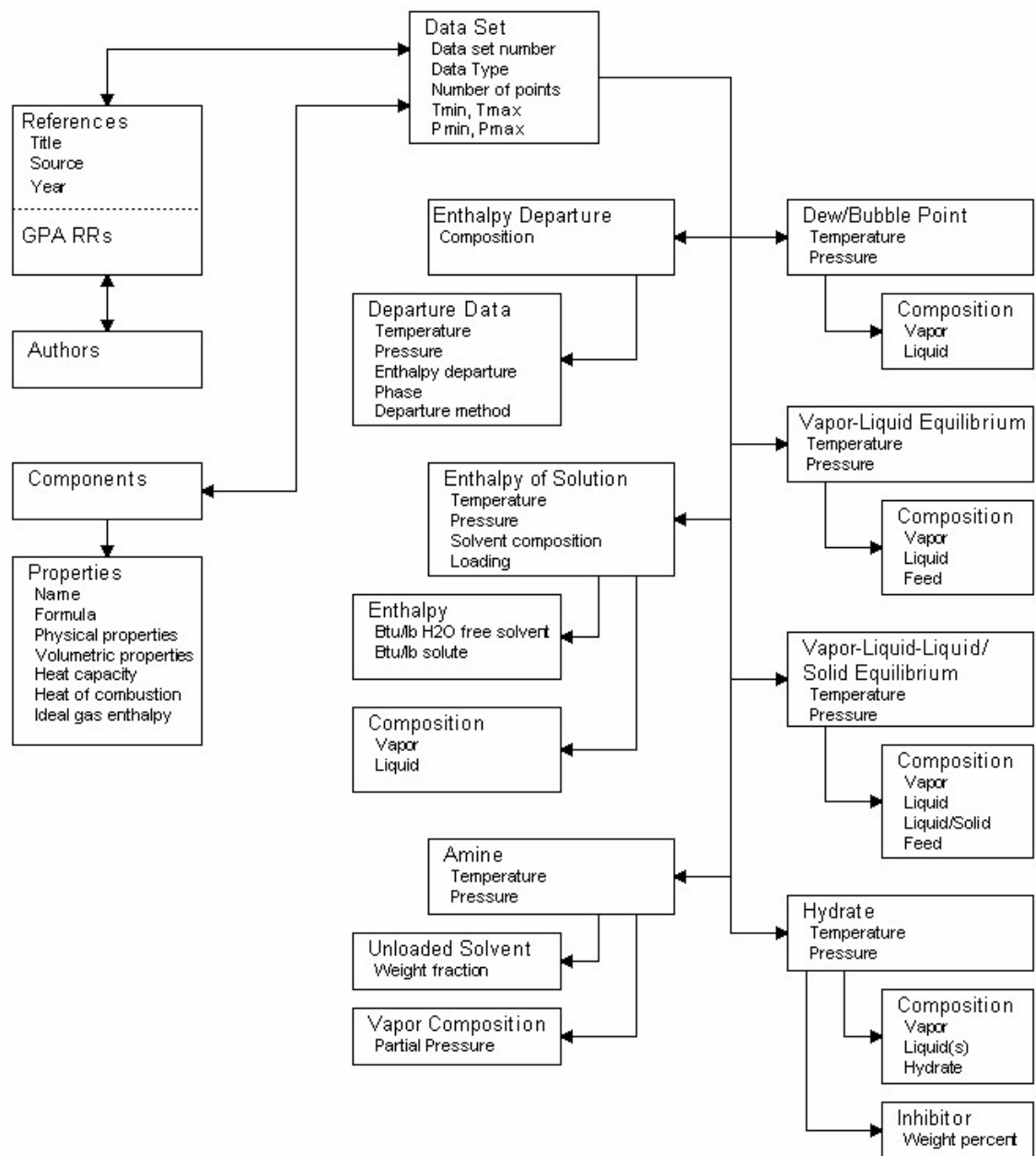
Figure 1 - GPA Database tables relationships.

INSTALLATION

The installation application was developed with InstallShield™ 5.51 with scripts from SageKey Software, Inc. for Microsoft Access 97™. The Database can be installed under Windows 95, Windows 98, or Windows NT (Versions 3.5 or 4.0).

DATABASE INTERFACE

The GPA Database interface is menu, or "form" driven. The main menu shown in Figure 2 - Main menu. presents options available to users in a three-column layout. The left column contains search functions, and the middle column has informational functions. Data entry and editing functions are in the right column.

In addition to primary search features, three additional types of searches are programmed in the Database and available from both the main and search menus. The Database can be searched for references using a data type, a component, or an author as the keyword. To provide convenient access to data from GPA Research Reports, an option has been included that generates a list of Research Reports from the references table. The user can then select a specific Research Report to be used as the keyword to retrieve the data records. Finally, the user can access the physical properties from Figure 23-2 of the GPSA Engineering Data Book [10] for a component. Figure 3 shows a screen with the "General Properties" tab selected. Note that the user can navigate the component list and launch a component and data type search from this screen.
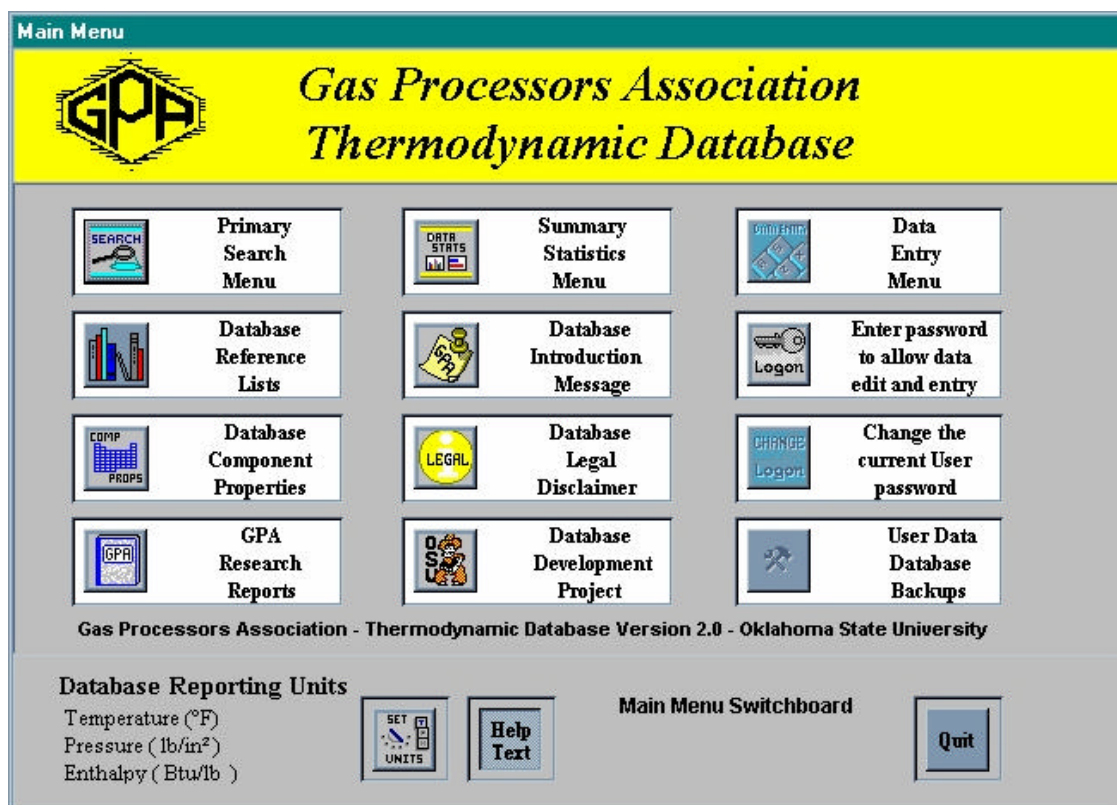
Figure 2 - Main menu.

Applications have also been written in Microsoft Access Basic™ to allow administrators of the Database to add records. User-added records and be edited and deleted. Data input forms are provided for data type, number of components, reference, authors, and units. Each data type requires a separate form for the data set and data point records. The use of these forms and the underlying applications assure that all of the relational links between tables are established. User-added records are identified and preserved during updates of the GPA Thermodynamic Database.
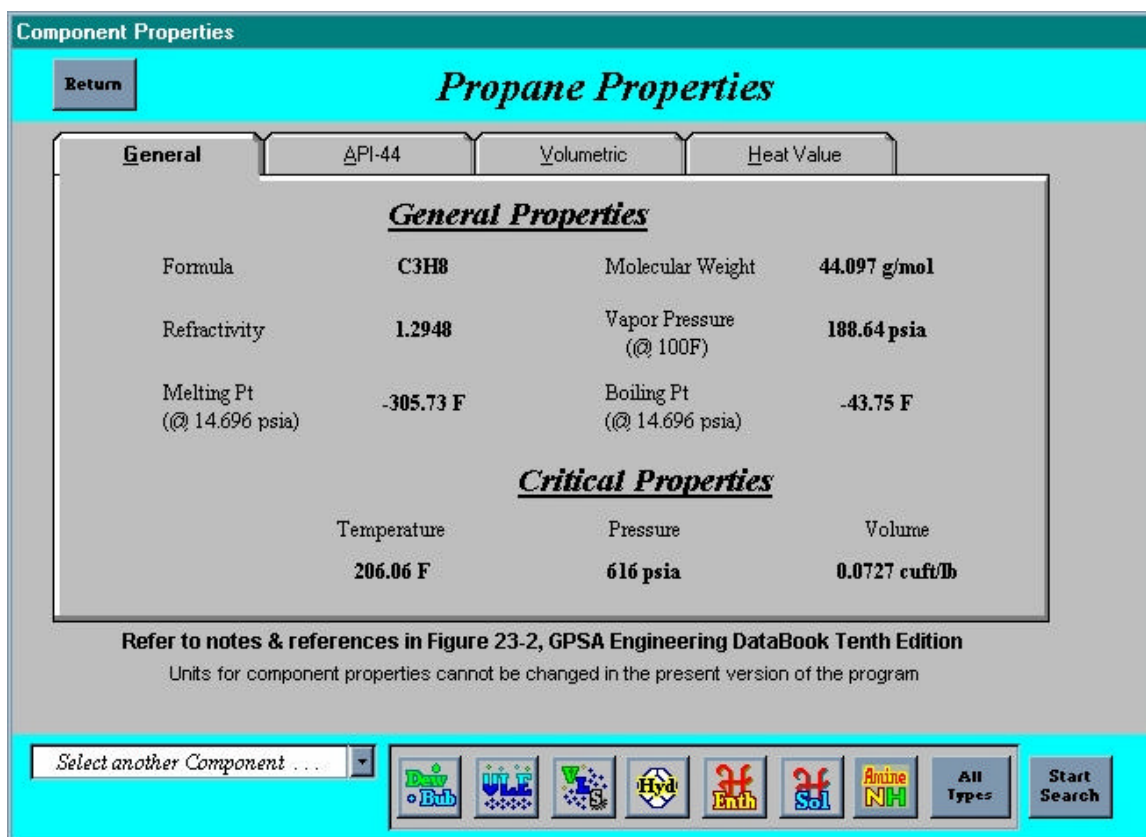
Figure 3. Physical properties for propane.

Search Example.

An example two-component search is used to illustrate the main forms and functions of the GPA Thermodynamic Database.

The Primary Search Menu shown in Figure 4 consists of three essential parts that are enclosed by the 'boxes' on the form. The first of these is along the top and comprises the data types for the search. As an example, the Dew/Bubble, Vapor-Liquid Equilibrium (VLE), Vapor-Liquid-Liquid-Solid Equilibrium (VLS), and Enthalpy Departure data have been selected in Figure 4.

Figure 4. Search menu.

The second search criterion is the number of components in the systems. In the example, "Any" ensures that all mixtures are returned. The third criterion is the search method: components, authors, or all records. As shown in Figure 4, a search by components is desired. Initiating the search opens the dialog boxes in Figure 5. The user specifies the number and name(s) of the desired components. Analogous sets of dialog interactions occur for an author name search, where up to two author names may form the basis of a search.

In Figure 5, two components are specified as search criteria: methane and carbon dioxide. The search opens the "Search Results Map" form, Figure 6, providing an overview of the records found. The results map sorts records by data type and number of components.

18
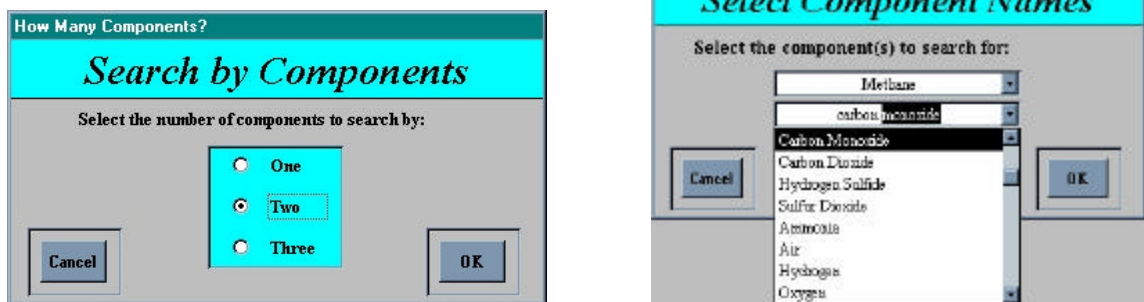
Figure 5. Component search dialogs.

Components, reference, and note information using a tabbed-control interface present a summary of each data set. At the bottom of the form, the total number of records for each data type are presented. In this example there are 10 Dew/Bubble, 20 VLE, 9 VLS, 15 Hydrate and 5 Enthalpy Departure data sets.
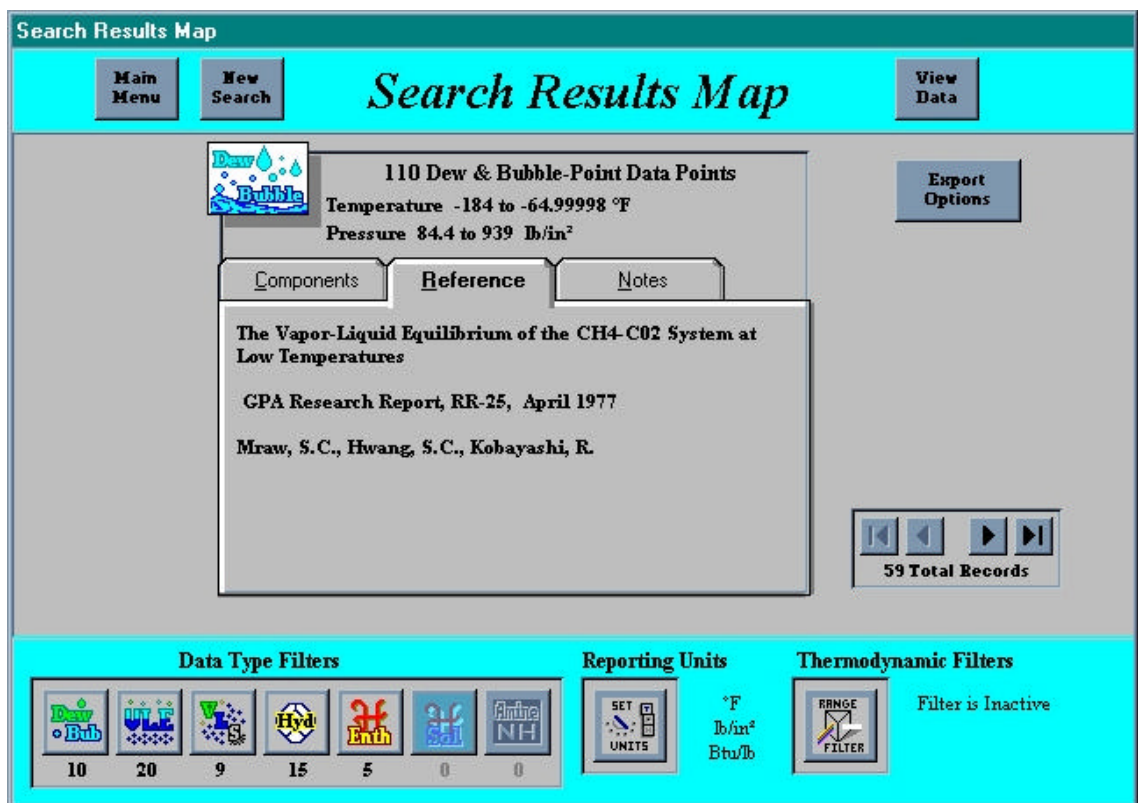
Figure 6. Search result map: data type filters.

The "Data Type Filters" buttons can be used to browse the search results by data type. As an example, selecting the "H-Enth," button, which represents enthalpy departure data, results in the summary map shown in Figure 7. Only the five enthalpy-departure data sets are included. Temperature and pressure filters are also available to the user.
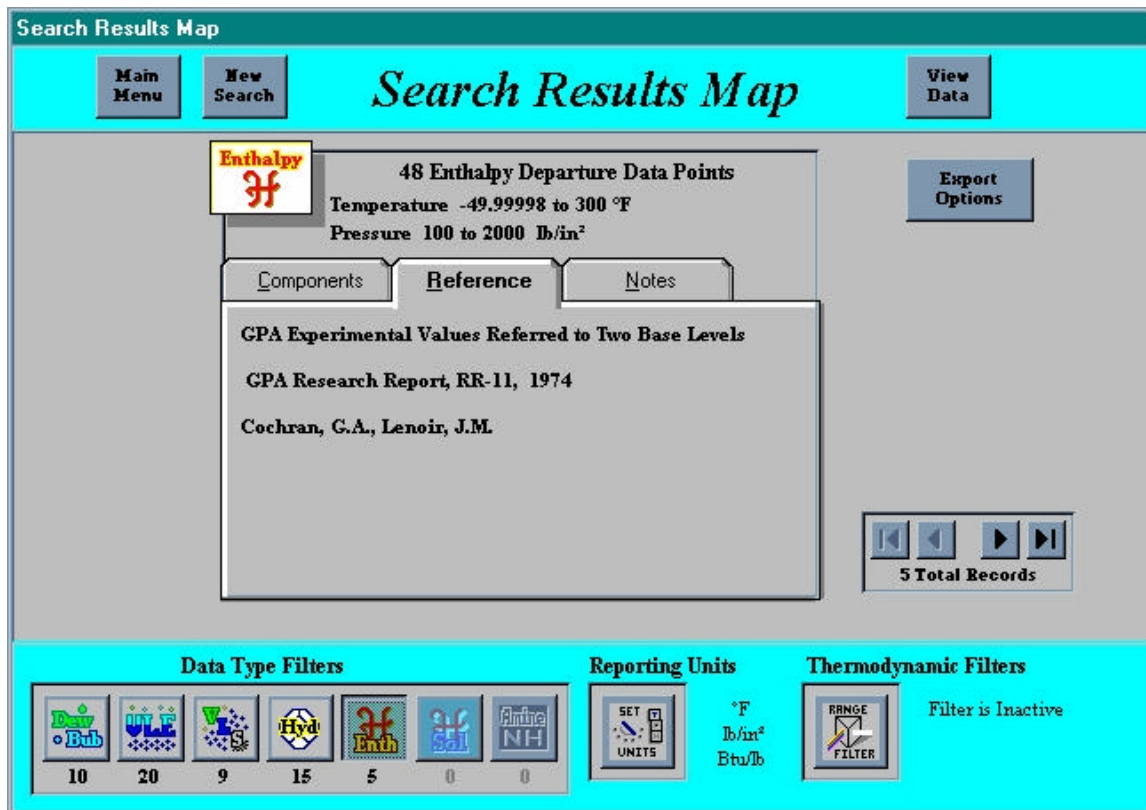
Figure 7. Search result map.

The "View Data" button opens the data point form. Figure 8 is the form for the first record of the enthalpy-departure data set from Figure 7. In this example, the absolute enthalpy of the mixture has also been selected. Enthalpy is calculated from the enthalpy-departure data record and the API-44 ideal gas constants [17] from the component properties table.

Figure 8. Data records: enthalpy departure.

Exporting Records.

The "Output Points" function, available on each data point form, allows the user to export data records as *.xls, *.txt, or *.html files. The structures of the different data types create problems in exporting the results of searches. Because there is no common format for the data point records, a more generic export option is available from the "Search Results Map" (Figure 6). The "Export Options" button opens the screen in Figure 9 that enables the export of all records found in the search.
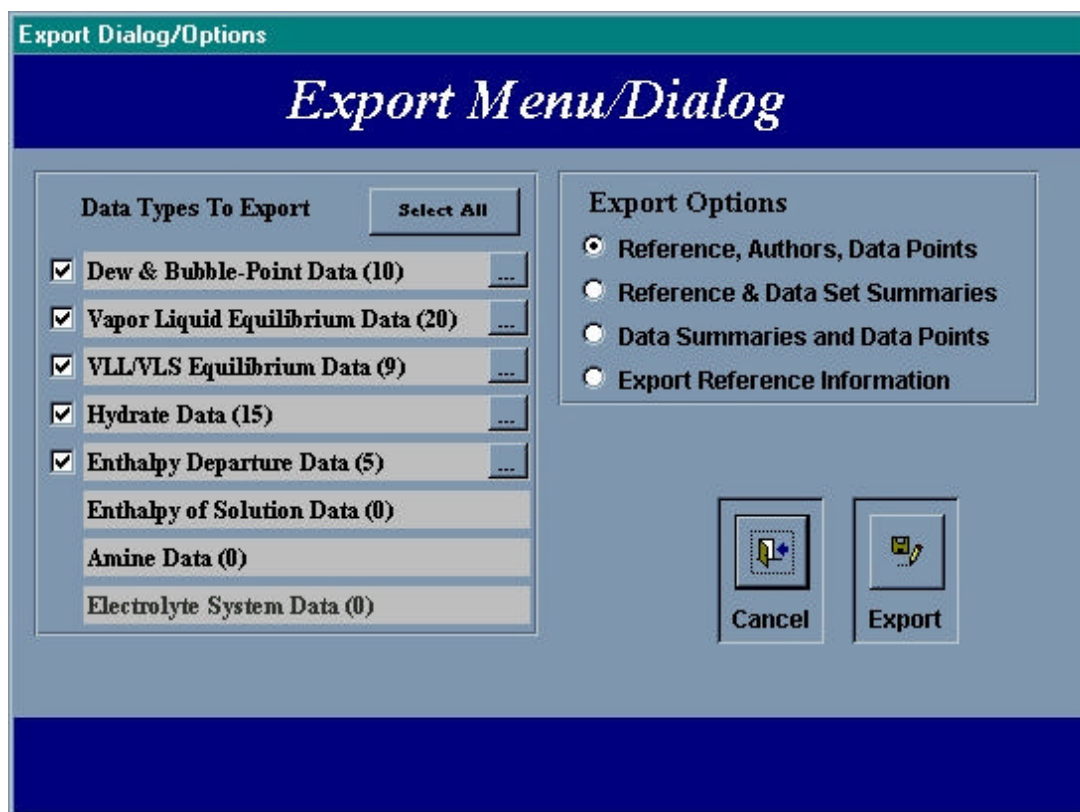
Figure 9. Export dialog.

The check boxes can be used to select the data type(s) that will be exported to a single file. Recall that the data point record can be quite different between data types, and exporting the results of a search by data type can facilitate subsequent manipulation of the data point records. The "…" buttons to the right of the checked data types in Figure 9 provide expanded list views that allow data sets within each data type to be included or excluded from the report. This is accomplished through the "Data Type Export" form shown in Figure 10.. This form allows the user to browse the summary information for each data set by data type and select those data sets to include in the output file.

The "Export Options" radio buttons shown in Figure 9 can be used to select the types of information to export. For example, references, authors, and data points for tagged data sets can be selected; or only the references without the data can be exported.
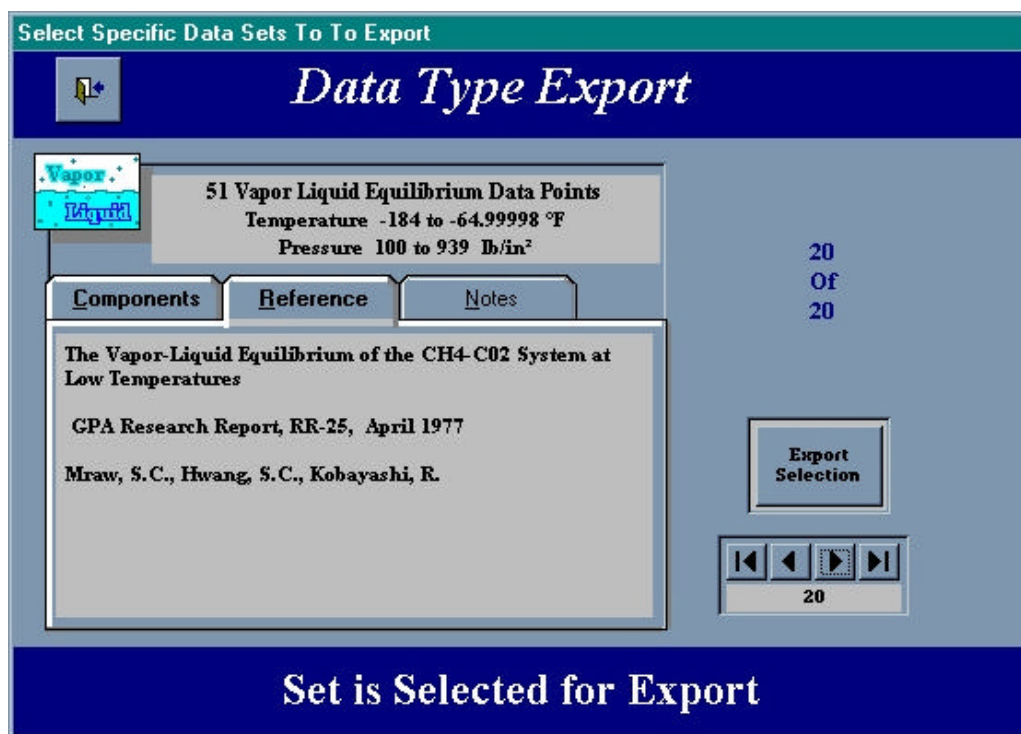
Figure 10. Export dialog: data set.

CHAPTER SUMMARY

The GPA thermodynamic database consists of data compiled by the Gas Processor's Association containing over 900 data sets of more than 45,000 experimental data points organized in seven categories: dew/bubble, vapor-liquid, vapor-liquid-solid, hydrate, enthalpy departure, enthalpy of solution, and amine solution data. Evaluations of data quality were made based on comparisons with original source references and equation-of-state screening methods. The data are organized in a relational database structure using Microsoft Access™.

An interface based on forms provides access to the database contents. Through a main menu form searches are available based on component or reference information. Through a primary search menu form searches may be further defined based on specific data type, number of components, and component name. An additional option allows searches to be restricted to specific temperature and pressure ranges. Search results are reported using individual data type forms and data may be exported as text files.

A stand-alone application of the GPA database was developed with InstallShield™ 5.51 with scripts from SageKey Software, Inc. for Microsoft Access 97™. The database is currently available for Microsoft Windows.

REFERENCES

1.   Jones, S., et al. Simultaneous Removal of Water and BTEX from Feed Gas for a Cryogenic Plant. in Seventy-Eight GPA Annual Convention. 1999. Nashville, Tennessee.

2.   Ng, H.-J., J.J. Carroll, and J. Maddocks. Impact of Thermophysical Properties Research on Acid Gas Injection Process Design. in Seventy-Eighth GPA Annual Convention. 1999. Nashville, Tennessee.

3.   Lyddon, L.G., et al. Applications and Benefits to the Gas Processing Industry of the GPA Research Program. in Seventy-Eighth GPA Annual Convention. 1999. Nashville, Tennessee.

4.   Hegarty, M. and D. Hawthorne. Application of BTEX/Amine VLE Data at Hanlan Robb Gas Plant. in Seventy-Eighth GPA Annual Convention. 1999. Nashville, Tennessee.

5.   Daubert, T.E., Development of GPA Data Bank of Selected Enthalpy and Equilibria Values. 1983, Gas Processors Association: Tulsa, Oklahoma.

6.   Daubert, T.E., GPA Data Bank of Selected Enthalpy and Equilibria Values. 1986, Gas Processors Association: Tulsa, Oklahoma.

7.   Daubert, T.E., GPA Data Bank of Selected Enthalpy and Equilibria Values. 1990, Gas Processors Association: Tulsa, Oklahoma.

8.   Daubert, T.E., GPA Data Bank of Selected Enthalpy and Equilibria Values. 1993, Pennsylvania State University: University Park, Pennsylvania.

9.   Sanghavi, P., Design and Development of a Thermodynamic Database Using the Relational Data Model. 1992, Oklahoma State University: Stillwater, Oklahoma.

10. Engineering Data Book. Eleventh Edition ed, ed. G.P.S. Association. 1998, Tulsa, Oklahoma.

11. Lenoir, J.M., GPA Experimental Enthalpy values Referred to Two Base Levels. 1973, Gas Processors Association: Tulsa, Oklahoma.

12. Daubert, T.E., Evaluation of GPA*SIM Computer Program with GPA Data Bank of Selected Enthalpy Values. 1983, Gas Processors Association: Tulsa, Oklahoma.

13. Daubert, T.E., Evaluation of Peng-Robinson Computer Program with GPA Data Bank of Selected Enthalpy Values. 1984, Gas Processors Association: Tulsa, Oklahoma.

14. Rastogi, A., Evaluation and Maintenance of an Enthalpy Database, in Chemical Engineering. 1996, Oklahoma State University: Stillwater, Oklahoma.

15. Twomey, D.W., Evaluation and a New Reporting Method for Enthalpy Data, in Chemical Engineering. 1998, Oklahoma State University: Stillwater, Oklahoma. p. 141.

16. Wong, S.-H., Evaluation of Vapor-Liquid-Equilibrium Database Using Error Analyses Based on an Equation of State and Statisical Methods. 1999, Oklahoma State University: Stillwater, Oklahoma.

17. Institute, A.P., Technical Data Book--Petroleum Refining. Revision 7 ed, ed. T.E. Daubert and R.P. Danner. 1983, New York, New York: API.

CHAPTER III

ENTHALPY DEPARTURE CALCULATIONS WITH THE PENG-ROBINSON EQUATION OF STATE

INTRODUCTION

Accurate enthalpy data are crucial for design as well as operation of efficient chemical processes. Improper design of equipment leads, at best, to over-expenditure of capital and unnecessary higher operating costs. Although, many equations exist for enthalpy prediction for different groups of fluids at desired pressures, temperatures, phases, and compositions, no single equation exists which accurately predicts enthalpy of all fluid, or fluid mixture, at any process conditions.

Experimental enthalpy data are necessary for evaluation and development of the equations used for enthalpy prediction. Such data must meet the highest standards possible for thermodynamic consistency, experimental verification (original source verification), and include evaluations of the data's 'reliability.'

The quality of the experimental enthalpy data provided in the Gas Processor's Association Thermodynamic database [1, 2] is evaluated by modeling pure and binary systems with an equation of state (EOS). Statistical based comparisons of the

experimental data with EOS predictions provides estimates of individual data point quality and assessment of EOS suitability for accurately modeling the systems examined.

EVALUATIONS OF ENTHALPY DATA

Direct comparisons of the current enthalpy data in the database to the values in the literature would be ideal [1]. However, since the data were compiled over several decades, with data taken from various experimental techniques and reported in various reference states, a comprehensive effort in 1974 undertaken by Cochran and Lenoir [3] converted the GPA enthalpy database to two common reference states: the ideal gas state at 0 K, and elemental states at 25°C. Although this data conversion effort facilitates the use of the entire enthalpy database, it is neither possible nor practical to compare the enthalpy departure data in the database directly with the original literature values. Evaluation is possible using calculations based on an equation of state.

The Enthalpy Equation

According to the phase rule, for a homogeneous substance of constant composition, fixing the values of two intensive properties establishes its state. Therefore, the molar or specific enthalpy of a substance may be expressed as a function of two other state variables. The two state variables chosen are temperature and pressure:

$$H = H(T, p) \qquad (3.1\text{-}1)$$

The enthalpy of a compound can be expressed as a summation of three quantities [4] :

$$H(T,p) = \left[H(T,p) - H(T,p^\circ) \right] + \left[H(T,p^\circ) - H(T^\circ, p^\circ) \right] + H(T^\circ, p^\circ) \qquad (3.1\text{-}2)$$

Where

$$H\left(T,p\right) \qquad\qquad = \qquad\qquad \text{Enthalpy of a pure fluid or fluid mixture}$$

$$\left[H\left(T,p\right)-H\left(T,p^{\circ}\right)\right] \qquad = \qquad \text{Enthalpy departure function (pressure)}$$

$$\left[H\left(T,p^{\circ}\right)-H\left(T^{\circ},p^{\circ}\right)\right] \qquad = \qquad \text{Ideal Gas departure function (temperature)}$$

$$H\left(T^{\circ},p^{\circ}\right) \qquad\qquad = \qquad\qquad \text{Enthalpy at a defined reference state}$$

For notational convenience, the enthalpy departure function and the ideal gas enthalpy difference will, hereafter, be denoted as $H - H^{\circ}$ and H°, respectively. Accordingly, an equation of state allows calculation of the enthalpy of a fluid or fluid mixture for a point-by-point comparison with data in the database.

Ideal Gas Enthalpy Determination

The ideal gas enthalpy is calculated using an exact relation of type given as:

$$H^{\circ} = H^{\circ}\left(T,P^{\circ}\right) - H^{\circ}\left(T^{\circ},P^{\circ}\right) = \int_{T^{\circ}}^{T} C_{p}^{\circ} dT \qquad\qquad (3.1\text{-}3)$$

where H° is the ideal gas enthalpy, C_{p}° the ideal gas heat capacity at constant pressure, and T the absolute temperature. The choice of the functional form of heat capacity in most correlations is polynomial [5, 6]:

$$C_{p}^{\circ} = a + bT + cT^{2} + dT^{3} + \dots \qquad\qquad (3.1\text{-}4)$$

In the United States, and for substances of interest to the energy sector, the regression coefficients (a, b, c, d) are usually generated from the C_{p}° data of API Research Project

44 and the Thermodynamic Research Center (TRC) Data Project [5, 6]. The constants

being derived from conventional least-squares methods, which minimizes the sum of the

squares of either the absolute deviations or percentage deviations with respect to reported

C_p° data. Improvements in accuracy are possible by increasing the number of constants

in the correlation.

A drawback of the polynomial form of heat capacity correlations is that although greater

accuracy in the fitting of the individual property may be achieved, it is at the expense of

thermodynamic consistency [7]. This is because actual heat capacity behavior is not

constrained to follow any particular polynomial.

A more elaborate and thermodynamically consistent choice for heat capacity correlations

have the form [8, 9] shown below :

$$C_p^\circ = a + b\exp\left(\frac{-c}{T^n}\right) \tag{3.1-5}$$

This equation is derived from theoretical considerations; however, it is not readily

amenable to integration, i.e., a series expansion or a numerical integration procedure is

required. Still, the predicted values of C_p° are more accurate than those calculated from

the polynomial equation with four constants [8].

More rigorous equations for calculating the ideal gas heat capacity and enthalpy have

been proposed based on statistical mechanical arguments [7-9].

Although the theoretically based forms for ideal heat capacity are fundamentally based

and more accurate numerically, the additional computational requirements often

outweigh the benefits of the polynomial-based expressions.

Heat capacity correlations of the polynomial form are, by far, the most popular means of computing ideal gas enthalpy values. Polynomial forms provide reasonable accuracy and allow straightforward calculation of ideal gas enthalpies by analytical integration. With the typical errors in ideal gas enthalpy predictions of polynomial expressions ordinarily less than 0.5% on average for any component, with a maximum error of 1% in the temperature range of any fit, the commonly employed polynomial forms are sufficiently robust for most process design needs [6].

ENTHALPY DEPARTURE FUNCTION DETERMINATION

The enthalpy departure function, $H - H^\circ$, is obtained from the pressure-volume-temperature (pvT) properties of the fluid under study. An equation of state (EOS) capable of describing the (pvT) behavior of the fluid offers the most efficient means for determining enthalpy departure functions.

For any pressure-explicit EOS, the departure function for the Helmholtz energy A is developed first using the appropriate fundamental property relations. Then, any other desired departure function is calculable [4], as shown below:

$$H - H^\circ = \left(A - A^\circ\right) + T\left(S - S^\circ\right) + RT\left(Z - 1\right) \tag{3.1-6}$$

$$A - A^\circ = -\int_{\infty}^{v}\left(p - \frac{RT}{v}\right)dV - RT In\frac{v}{v^\circ} \tag{3.1-7}$$

$$S - S^\circ = -\int_{\infty}^{v}\left[\left(\frac{\partial p}{\partial T}\right)_v - \frac{R}{v}\right]dV + R\ln\frac{v}{v^\circ} \tag{3.1-8}$$

For a specific EOS, the right-hand side expressions of the above equations have to be evaluated.

EQUATION-OF-STATE ENTHALPY PREDICTIONS

Adachi [10] completed a reasonably comprehensive study involving the comparative capabilities of eleven cubic equations of state for paraffins ranging from methane to decane. The Peng-Robinson EOS [6] yielded lower deviations for enthalpy departure values than the Schmidt and Wenzel [11], Soave-Redlich-Kwong [12], and Harmens and Knapp [13] equations of state. The PR EOS predictions were similar to those of Kumar and Starling [14]. However, the equation of state of Adachi, et al. [15] yielded the best enthalpy departure prediction results. Further reviews of enthalpy prediction methods can be found elsewhere [16, 17].

In 1984, Daubert [1] used the PR EOS for enthalpy departure predictions and comparisons with selected enthalpy values in the GPA databank. The database has seen much growth and maintenance since that time. Daubert showed that the PR EOS predicted enthalpy departures very well for light hydrocarbons and gases. As the molecular weight increased, the accuracy decreased, specifically for pentane and heavier components.

Although the PR equation does have limitations for heavier hydrocarbons, there remain several advantages [16]:

- Capable of handling multiphase natural gas systems over wide temperature and pressure ranges
- Applicable to multi-component systems with established mixing rules
- Provides accuracy with acceptable computational speed

32

As the present work is primarily concerned with calculations of enthalpy departure relative to experimental data, concerns regarding accuracy are not a hindrance to application of the statistical procedure outlined. The relative deviation between points is of greater importance than whether the PR EOS accurately predicts enthalpy departures over a range of temperatures and pressures.

Peng-Robinson Equation of State (PR EOS)

The PR EOS as used in this study is as follows [18]:

$$p = \frac{RT}{(v-b)} - \frac{a_c \mathbf{a}}{(v^2 + 2bv - b^2)} \tag{3.1-9}$$

where

$$b_i = 0.07780 \frac{RT_{c_i}}{P_{c_i}} \tag{3.1-10}$$

$$a_i = 0.45724 \frac{R^2 T_{c_i}^2}{P_{c_i}} \tag{3.1-11}$$

$$\mathbf{a} = \left[1 + m\left(1 - T_r^{0.5}\right) \right]^2 \tag{3.1-12}$$

$$m = 0.37464 + 1.54266\mathbf{v} - 0.26992\mathbf{v}^2 \tag{3.1-13}$$

The mixing rules employed are:

$$a = \sum\sum z_i z_j a_{ij} \tag{3.1-14}$$

$$a\mathbf{a} = \sum\sum x_i x_j (a\mathbf{a})_{ij} \tag{3.1-15}$$

$$(a\boldsymbol{a})_{ij} = \left[(a\boldsymbol{a})_i \, (a\boldsymbol{a})_i \right]^{\frac{1}{2}} \left(1 - C_{ij} \right) \qquad (3.1\text{-}16)$$

$$b = \sum \sum x_i \, x_j \, (a\boldsymbol{a})_{ij} \qquad (3.1\text{-}17)$$

$$b_{ij} = 0.5 \left(b_i + b_j \right) \left(1 - Dij \right) \qquad (3.1\text{-}18)$$

where C_{ij} is an adjustable, empirically determined "binary interaction parameter" which characterizes the interactions between component i and component j.

The PR equation of state requires pure-component properties, critical temperature, T_c, critical pressure, p_c, and accentric factor, ω. Molecular weights of the substances are also necessary to report enthalpy departures on a unit mass basis. All pure-fluid values of T_c, p_c, and ω used are those given by Daubert [1], with the exception of cis-2-pentene, ethylcyclohexane, cis-decalin, transdecalin, tetralin, and hexadecane which are taken from Reid et al. [4]. All values are in Appendix D.

Enthalpy Departure Function for the PR EOS

The enthalpy departure function $H - H^\circ$ as given by the PR EOS is:

$$H - H^\circ = a_c \left[\frac{\left(\boldsymbol{a} - T \dfrac{d\boldsymbol{a}}{dT} \right)}{2\sqrt{2b}} \right] \ln \left[\frac{\boldsymbol{n} - 0.414b}{\boldsymbol{n} + 2.414b} \right] + pv - RT \qquad (3.1\text{-}19)$$

with

$$\frac{d\boldsymbol{a}}{dT} = \left(\frac{-\boldsymbol{a}}{T_c} \right) \frac{\left(m T_r^{-0.5} \right)}{1 + m \left(1 - T_r^{-0.5} \right)} \qquad (3.1\text{-}20)$$

To extend (3.1-19), and (3.1-20) to multi-component systems, mixing rules are applied. Using equations (3.1-14) and (3.1-17), the PR EOS enthalpy departure equations for mixtures is obtained as:

$$H - H^\circ = \left[\frac{\displaystyle\sum_{i=1}^{n}\sum_{j=1}^{n} z_i z_j \boldsymbol{g}_{ij} T - a}{2\sqrt{2}b}\right] In\left[\frac{v - 0.414b}{v + 2.414b}\right] + pv - RT \qquad (3.1-21)$$

With

$$\boldsymbol{g}_{ij} = a_{ij}\left[\frac{-0.5 m_i T_{ri}^{-.05}}{T_{ci}\left(1 + m_i\left(1 - T_{ri}^{0.5}\right)\right)} - \frac{-0.5 m_j T_{rj}^{-.05}}{T_{cj}\left(1 + m_j\left(1 - T_{rj}^{0.5}\right)\right)}\right] \qquad (3.1-22)$$

Further discussion, including a detailed derivation of the enthalpy departure function for the PR EOS may be found elsewhere [16].

Equation of State Software

The enthalpy departure models for the PR EOS was incorporated into GEOS, a thermodynamic software package for calculating volumetric, phase equilibrium, and calorimetric properties [16]. The software has the capability to handle multiple systems simultaneously. To validate the enthalpy departures generated by GEOS, predictions are confirmed using APEN PLUS™ simulation software.

The program inputs needed to perform the enthalpy departure predictions and to make comparisons with the experimental enthalpies included: the pure-fluid critical properties, temperature, pressure, feed composition, experimental enthalpy departures as reported in the GPA database, and the option to calculate vapor or liquid enthalpy. In enthalpy

departure calculations, the predictive ability of the PR EOS is employed, in that, the mixing rules are used without empirically based corrections (i.e., the interaction parameters are $C_{ij}=0$).

ENTHALPY DEPARTURE DATA CALCULATIONS

Over thirteen thousand single-phase experimental data points are available. These data points are classified into three system types: pure-components, binary, and multicomponent mixtures. Within these systems, data points are further classified by the phases present and the phase measured experimentally. The GPA Database denotes specific phase information such as vapor (V) and liquid (L). Two additional phase designations of "liquid-liquid-vapor" (L-L-V) and "liquid-vapor-vapor" (L-V-V) signify vapor-liquid equilibria and the phase measured experimentally [19]. The PR EOS has been applied for enthalpy departure calculations on an experimental database consisting of over 13,000 points of specific temperature, pressure, and composition. A brief summary of the database studied is outlined in Table 1, and a more comprehensive description is given in Appendix E.

Table 1. Enthalpy Data Summary

System	Phase	# Comps	# Points	# Refs
Pure Components	L	19	1,466	23
	V	18	1,437	24
Binary Systems	L	21	4,134	24
	V	22	6,110	30
	Totals	22	13,147	30

Each of the available data points is evaluated by calculations with the PR EOS, an example of these is shown in Table 2.

Table 2. Sample Enthalpy Calculations

System: Pure Cyclohexane (V)

PT	T(F)	P	H_{EX}	H_{PR}	DEV	%DEV	L/N	REF
1								
$\vdots$	$\vdots$	$\vdots$	$\vdots$	$\vdots$	$\vdots$	$\vdots$	$\vdots$	$\vdots$
31	482.4	300	-24.4	-19.0	5.44	-22.3	0	584
32	472.6	300	-24.5	-19.6	4.93	-20.1	0	584
33	459.7	300	-23.4	-20.5	2.94	-12.6	0	584
$\vdots$	$\vdots$	$\vdots$	$\vdots$	$\vdots$	$\vdots$	$\vdots$	$\vdots$	$\vdots$

Included in the calculations are two measurements of the error for an individual data point: deviation (*DEV*) and percent deviation (*%DEV*). Deviation is defined as

$$DEV_i = \left(H_{i,Calc} - H_{i,Exp} \right) \tag{3.1-23}$$

which is a measure of the numerical difference between the model prediction and the experimental value. Percent deviation, given by

$$\%DEV_i = 100 \times \frac{\left(H_{i,Calc} - H_{i,Exp} \right)}{H_{i,Exp}} \tag{3.1-24}$$

quantifies error relative to the magnitude of the experimental enthalpy departure value.

Due to the presence of random variation, which are not carefully documented, it can be difficult to determine whether or not all of the data in a data set are of equal quality. As a result, most process modeling procedures treat all of the data equally when using it to estimate the unknown parameters in the model. Most methods also use a single estimate of the amount of random variability in the data for computing prediction and calibration uncertainties. Treating all of the data in the same way yields simpler, easier-to-use models. Nevertheless, the decision to treat the data in this manner may produce less than an optimum model. An evaluation of the database of experimental data is possible by

37

considering the experimental source, measured phase, and thermodynamic conditions that define individual data points. Grouping data point deviations, into datasets, allow statistical comparisons to aid evaluations of the quality of each individual data points comprising a dataset.

Quantifications of Error

Data quality cannot be measured point-by-point since it is clear from direct observation of the data that the amount of error in each point varies. However, working with groups of single-point errors, there are several possible quantifications describing of the overall error for a number of data points (NPTS).

The bias (BIAS) of a series of deviations is defined as:

$$BIAS = \frac{\sum_{i=1}^{NPTS}\left(DEV_i\right)}{NPTS} \qquad (3.1\text{-}25)$$

and quantifies preferential trends in the deviations. Bias values indicate if a group of errors tend to over or under predict, i.e. if calculated values are higher or lower on average for the set of points examined.

Another measure, the average absolute deviation (AAD) is an indicator of the magnitude of the error for a set of deviations, is defined as:

$$AAD = \frac{\sum_{i=1}^{NPTS}\left|DEV_i\right|}{NPTS} \qquad (3.1\text{-}26)$$

and provides an overall impression of the average error which would be expected for a series of deviations. Additionally, percent average absolute deviation (%AAD)

38

$$\% AAD = \frac{\sum_{i=1}^{NPTS} \left| \% DEV_i \right|}{NPTS} \qquad (3.1\text{-}27)$$

is the corresponding form based on the percent deviation formula. Average absolute deviation can provide effective indicators, but this measurement of error tends to bias near-zero property values.

Another error measure providing an overall indicator of the error for a set of deviations is the Root-Mean-Square Error (RMSE):

$$RMSE = \sqrt{\frac{\sum_{i=1}^{NPTS} \left(DEV_i \right)^2}{NPTS}} \qquad (3.1\text{-}28)$$

The formula for RMSE is similar to that of standard deviation of population. Since the standard deviation of the data at each set of explanatory variable values is the square root of its variance, the standard deviation of the data for each different combination of explanatory variables can also be used to measure data quality. Data points that have the same underlying average squared error, or variance, are considered to be of equal quality.

RMSE is an indicator of the gross expected deviation for enthalpy predictions on a particular component. The AAD measure indicates average absolute deviation for the component, while the BIAS indicates the tendency of the calculations to under or over prediction. As AAD and BIAS scale the same, a BIAS error may only be as large as the corresponding AAD. A positive BIAS, which is numerically equal to the AAD, is indicative of a component where the EOS consistently over predicts enthalpy. Similarly, negative BIAS values indicate under prediction tendency. A negative BIAS of the same magnitude of the AAD for the component indicates the EOS is consistently under

39

predicting enthalpy departures. Although analysis is primarily dependent on RMSE, the other error measures are also useful.

Evaluation Criteria

The criteria developed identified data points whose differences between reported and predicted deviation were larger than expected within a data set, and are marked accordingly in the GPA Database. In order to evaluate the data, a list of criteria is used [16]:

Table 3. Outlier Criteria Applied in Evaluation

#	Criteria
1	Data-entry errors not noted by inspection
2	Data points exhibiting deviations in the calculated enthalpy departure values that are greater than twice the root-mean-square error (RMSE) and do not represent a consistent trend in the entire data set. Near critical points were given special attention
3	Data points showing an abrupt change in the deviation sign
4	Data values showing gross systematic errors; these are identified by the disagreement in the deviations among reported data sets for the same system at identical conditions

When using an equation of state to predict enthalpy, the researcher needs to be aware of some potential pitfalls. Special attention is required near the critical point, when approaching the phase envelope, and in high temperature and high-pressure regions. This evaluation typically found large deviations in these regions. Without additional verification methods, such data may only be flagged when not conclusively determined as outliers or good data. The data distribution is important to help identify the areas where the equation of state has potential problems.

EVALUATION OF ENTHALPY DEPARTURE DATA

Although each of the single point-by-point evaluations may not be directly compared to literature references, useful evaluation is possible by construction of analyses based on the variables defining our database of experimental enthalpy departure points. Many variables define the scope of our database, including temperature and pressure, as well as phase measured. Additional information such as the reference source for each data point and component classification are considered. The Venn diagram shown (Figure 11) is for pure-component data and outlines combinations illustrating the possibilities.

Any individual data point is a member of various groups of data having similar characteristics. Each data point is a specific component (e.g., methane, tetralin), specific phase measured (e.g., vapor, liquid), and original source reference. Grouping of individual data points provide error measurement criteria for the data points within the group. A consistency test of an individual data point is the analysis of the data point deviation as compared with the group error measurement. The basis used to define a data point grouping, and the calculated group error measures, define various levels of analysis. Three levels of analysis are applied in the evaluation process and are referred to as internal consistency, external consistency, and composite analysis.
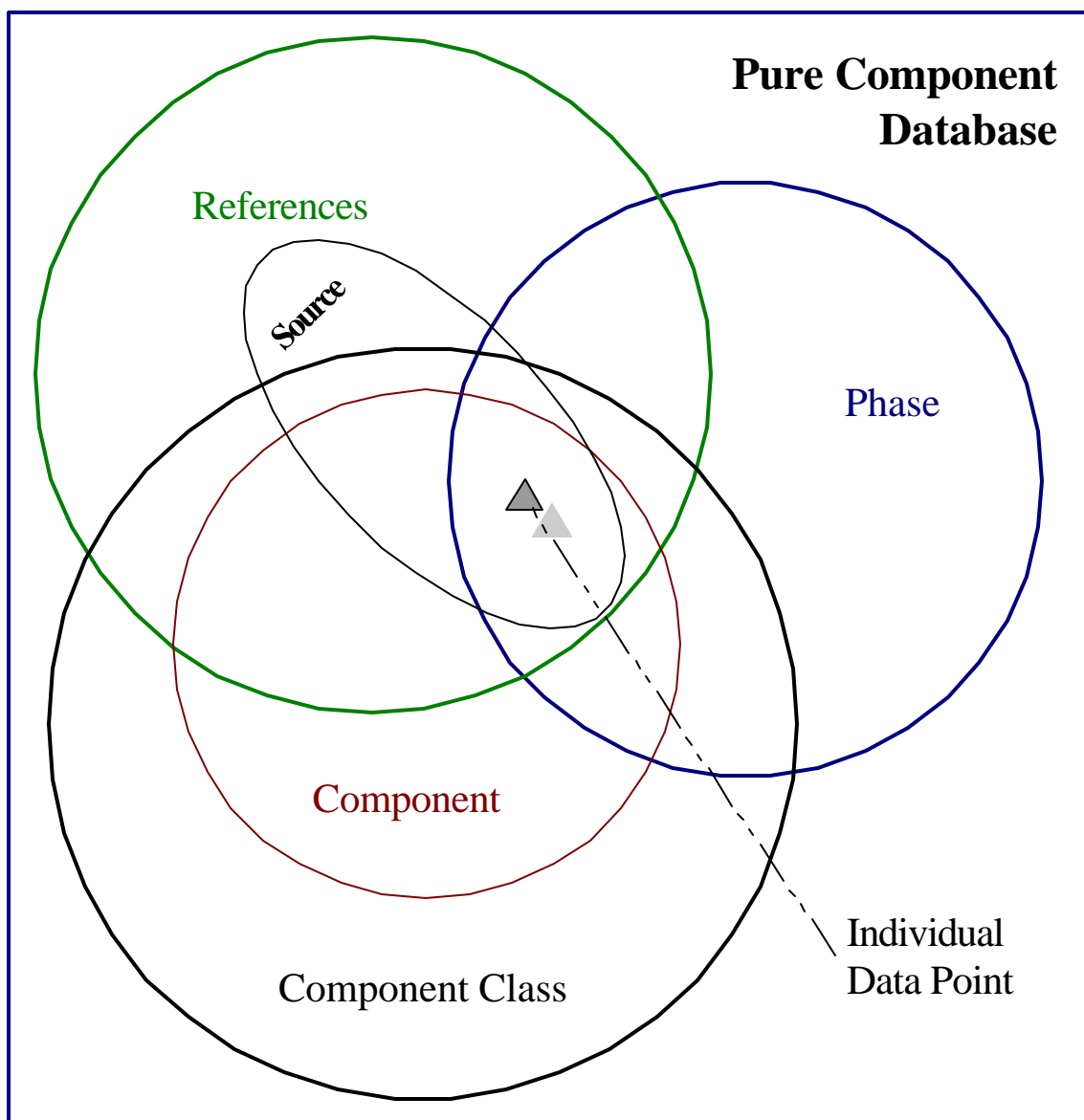
Figure 11. Analysis by Combination: Venn Diagram for Pure-Component Data

Internal Consistency

Each reference source ordinarily includes multiple experiments performed at various temperatures and pressures for a specific component and phase. The data point for a specific reference source for a given component and phase defines an individual data set. Internal consistency subsequently refers to the analysis of individual data point deviations by comparison with error measures based on all data points from the same reference, for the same component, in the same phase as the data point being evaluated.

Evaluations of internal consistency, by considering only the original reference source, are able to provide information regarding both the experimental precision of the source as well as information about the ability of the PR EOS to calculate the enthalpy deviation for the particular component of interest.

External Consistency

External consistency commonly refers to the accuracy of experimental data when compared with reliable literature data. In this study, external consistency is similarly defined. Error measures for data sets incorporating data points from all reference sources, which measure the specific component in the particular phase of interest, provide the comparison test criteria for individual points.

Evaluations of external consistency, by considering all experimental data available for a specific component and phase, are able to provide information regarding the ability of the PR EOS to calculate the enthalpy deviation for the particular component of interest. More specifically, with observable consistency in experimental data from multiple reference sources, the external consistency evaluation provides an assessment of the

ability of the equation of state to model the data examined. External consistency evaluations prove valuable, as ordinarily the thermodynamic range of the data points is broader in temperature and pressure when considering multiple references and the possibility of overlapping thermodynamic conditions can aid in evaluations of data points at experimental measurement limits for an individual reference source.

Composite Evaluation

Composite analysis refers to evaluations based on homologous components, e.g., comparisons of the consistency of results for two normal paraffins such as methane and propane. The composite analysis is based on an examination of data set deviations by phase and component classification.
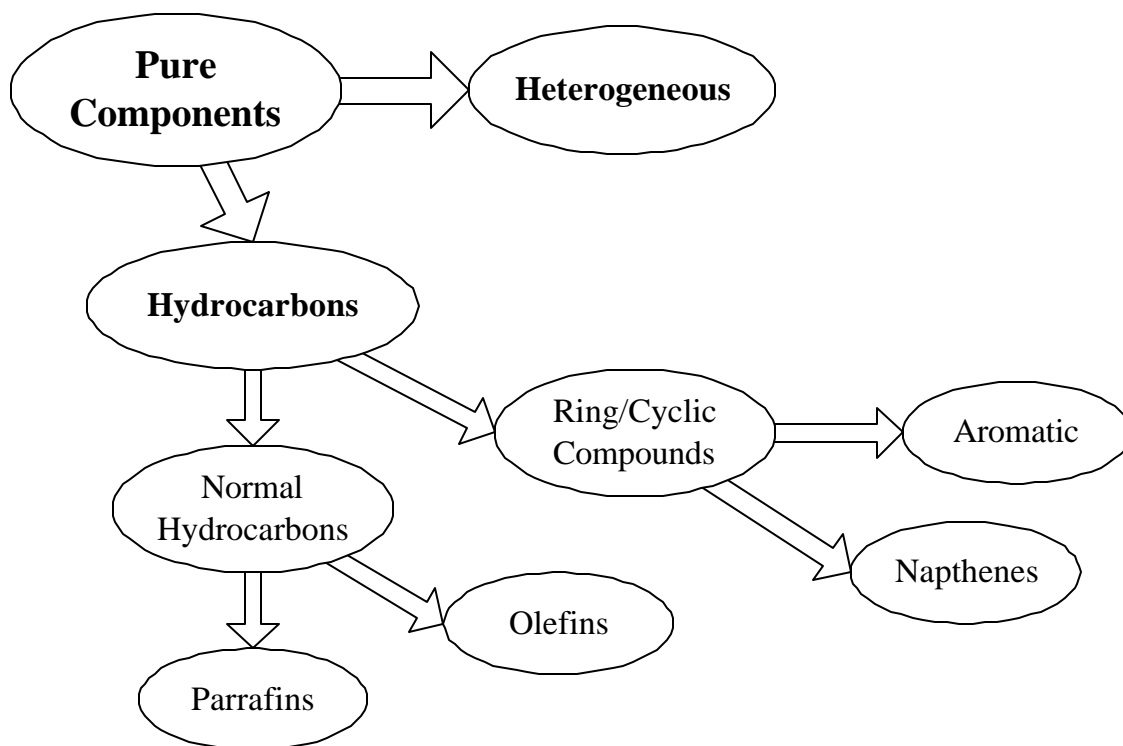
Figure 12. Pure-Component Classification

All components in the database are classified into groups and sub groups, as outlined in Figure 12. Hydrocarbons are grouped as paraffins, olefins, napthenes, or aromatic compounds. The group of normal hydrocarbons may also be considered in groups of either straight chain or branched compounds. Heterogeneous compounds are all those compounds, which are not hydrocarbons, e.g. nitrogen, water, etc.

The evaluation of the enthalpy departure data of the GPA database proceeds by first examining the internal consistency of data sets. In the second step, external consistency is evaluated, combining component data sets from multiple reference sources. The final evaluation consists of composite analysis, with similar components compared. In each evaluation step various data points may be determined as outliers or flagged data by the criteria outlined in Table 3. As evaluation proceeds into external and composite analysis the outlier points previously found in internal evaluation, or external evaluations, are exempted from the data set error analysis, creating what is termed a smooth data set for comparison. The exclusion of previously determined outliers is particularly important in the final composite analysis evaluation.

Several examples of the internal, external consistency evaluations are discussed illustrating the principles of these steps and outlining the formation of smooth data employed in composite analysis evaluations.

INTERNAL AND EXTERNAL CONSISTENCY EXAMPLES

Three systems are examined as examples of internal and external consistency. The first system, methane vapor, outlines the basic procedure applied in all evaluations. Liquid pentane is employed as an example of how the limitations of the EOS and thermodynamic constraints are considered during the evaluation procedure. Finally, the internal, source, and thermodynamic evaluations of liquid cyclohexane are discussed.

Vapor Methane

Vapor methane enthalpy departure data of the GPA Database is graphed as a function of temperature in Figure 13. The available data are graphed based on specific pressure values over a temperature range. Overall, the data from Reference #578 has a RMSE of 12.4 Btu/lb. Within this reference, three data points at 1000, 1500, and 2000 psia, all at -100°F, are of interest as each is greater than twice the RMSE of the entire data set. Figure 14 graphs the deviation, or error, for the methane (V) data showing the magnitude of the deviations more clearly.

Thermodynamically, these conditions are at high pressure and low temperature, and well above the methane critical point and as such, little aid is available to assess the quality of the data from a theoretical basis. The additional data points from reference # 573 confirm the higher temperature beginnings of the isobars but are of no help at the lower temperatures. Without additional experimental data at lower temperatures along the isobars of interest, the three data points may not be conclusively classified as outliers. The three points are flagged based on criteria #2 from Table 3.

Table 4 shows the summary results for the methane (V) references, and raw and smooth compiled results for both references.

Table 4. Methane (V) Enthalpy Departure Error Analysis

Data Set	RMSE	AAD	%AAD	BIAS	Max Dev (Low)	Max Dev (High)	NPTS
Ref#573	3.87	3.71	14.4	-3.71	-5.05	-2.03	4
Ref#578	12.35	5.89	8.5	2.88	-3.77	46.28	21
All (Raw)	11.42	5.54	9.4	1.83	-5.05	46.28	25
All (Smooth)	2.71	2.39	7.9	-1.83	-5.05	3.41	22

The procedure described is atypical of the evaluations performed on all data points. Beginning with examinations based on the phase and reference source, data are examined for internal consistency. The evaluation then expands to include other appropriate references and the errors, trends, and information available. As an overall concern, all data point calculations are considered based on the trend in the results, comparison with other references, and especially considering thermodynamic constraints.

includes both raw and smoothed datasets, e.g., internal consistency tests were performed

and 12 data points exceeding twice the RMSE of the respective reference are noted.

Table 5. Pentane (L) Enthalpy Evaluation Summary

Ref#	Data	RMSE	AAD	%AAD	BIAS	Max Dev (Low)	Max Dev (High)	NPTS
#458 -200	raw	5.26	4.06	3.7	4.05	-0.06	10.0	13
	smooth	3.37	2.56	2.2	2.55	-0.06	6.7	10
#585	raw	1.60	1.19	1.0	1.07	-0.97	5.7	71
	smooth	1.60	1.19	1.0	1.07	-0.97	5.7	71
#663	raw	4.34	3.44	3.0	3.44	0.01	10.4	57
	smooth	3.06	2.55	2.1	2.55	0.01	6.6	48
All	raw	3.38	2.36	2.1	2.30	-0.97	10.4	141
	smooth	2.40	1.80	1.5	1.73	-0.97	6.7	129

All three references include data points along the 400 psia isobar which is graphed in

Figure 15. As shown, the experimental points begin to deviate from the calculated values

as the temperature approaches 350°F. Figure 16 provides a three dimensional plot of

calculated deviations for all liquid n-pentane data, and provides explanations for the

observed deviation errors with the inclusion of additional phase equilibrium information.

Pentane (L) Enthalpy Departure at 400psia

Figure 15. Enthalpy Departure for Pentane (L) at 400psia
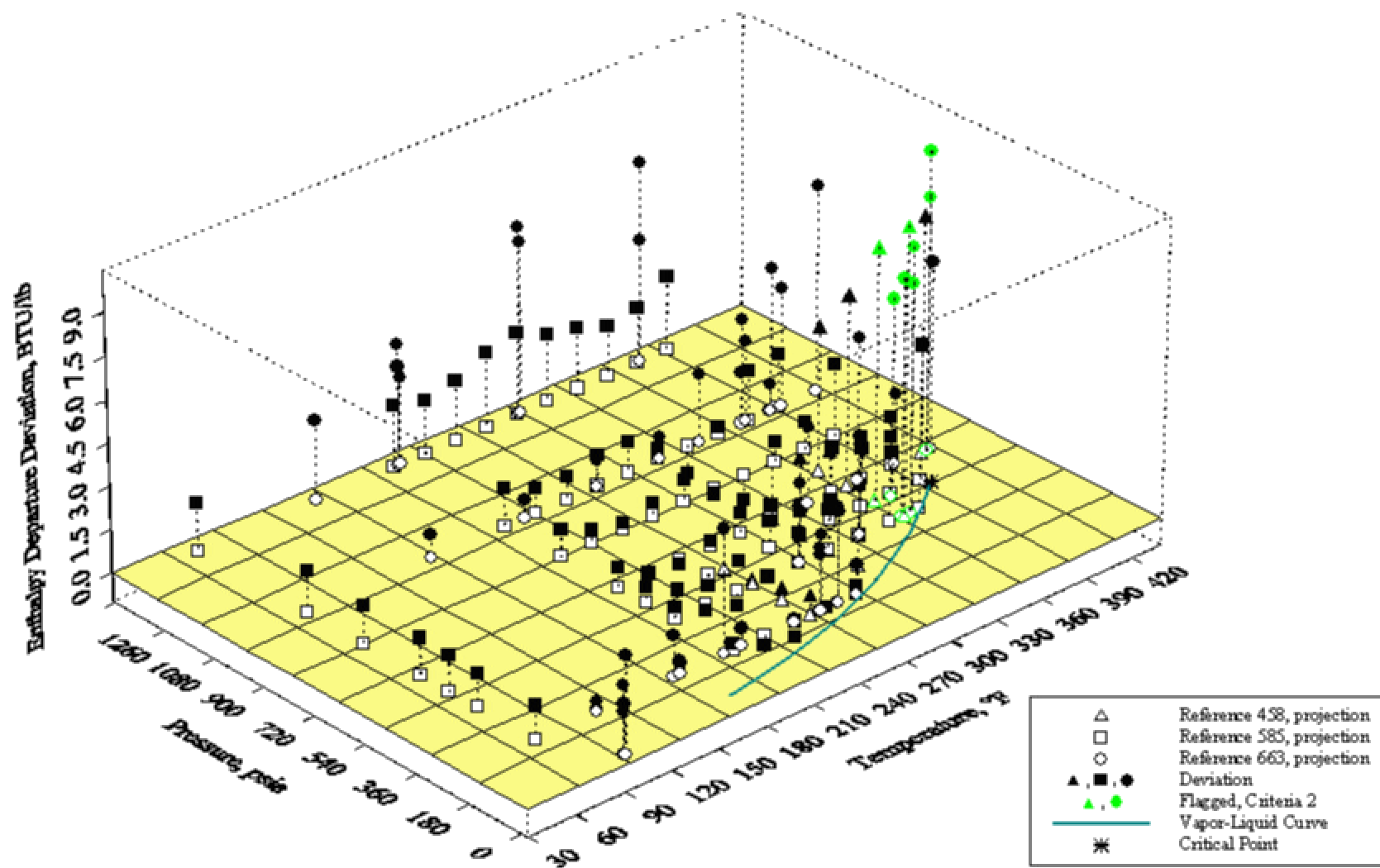
Figure 16. 3-D Enthalpy Departure Deviation for Pentane (L)

All three experimental reference sources are deviating as temperature increases. This is expected. Consideration of the phase envelope and the critical point are required for accurate evaluation of these experimental data points. For pure pentane, the saturation temperature at 400 psia is approximately 361°F. Additionally, the critical point of pentane is 385.5°F and 488.8 psia [1] (PR calculations determine the EOS based critical point as 382.98°F and 477.9 psia). In the region near the vapor-liquid coexistence curve and when approaching the critical point, special care is required as the deviation of data points in these regions is expected to increase. This approach to a phase equilibrium boundary and the critical point must be considered to ensure that data points exhibiting larger than expected deviations in these regions are not incorrectly identified as outliers. An observable and consistent trend of deviations from multiple sources also provides an assessment of the EOS applicability approaching the vapor-liquid curve and critical point.

In the liquid pentane system along the 400 psia isobar described, only 4 experimental data points are flagged under Criterion #2, and the remaining points are considered as accurate, given the constraint represented by the phase boundary and critical point. The evaluation of the experimental points in these boundary regions is reliant upon consideration of the consistency among the three available reference sources.

Liquid Cyclohexane

The liquid cyclohexane system contains several different examples of interest. The liquid cyclohexane data of the GPA Database is summarized in Table 6. Of the original 128 liquid phase data points, a total of 10 points are flagged as possible outliers.

Table 6. Liquid Cyclohexane Enthalpy Evaluation Summary

Ref#	Data	RMSE	AAD	%AAD	BIAS	Max Dev (Low)	Max Dev (High)	NPTS
#584	raw	2.99	2.12	1.7	1.22	-4.69	10.7	69
	smooth	2.04	1.65	1.3	0.83	-2.54	5.2	64
#677	raw	3.02	2.17	2.0	0.56	-3.01	9.3	59
	smooth	2.08	1.66	1.5	-0.11	-3.01	5.4	54
All	raw	3.01	2.15	1.9	0.92	-4.69	10.7	128
	smooth	2.06	1.66	1.4	0.40	-3.01	5.4	118

During the assessment of internal consistency, eight data points are initially flagged by the criteria outlined. As shown in Figure 17, the data points, which exceed twice the RMSE, are concentrated in a trend. This rise in deviation is likely due to limitations in the equation of state, which gives poor predictions in the critical region ($T_c \approx 540°F$, $p_c \approx$ 590 psia for cyclohexane). On the other hand, as already discussed, these results may be due to a systematic error in the experimental data. No conclusions for these data points are made and the data remain flagged under Criterion #2.

Two additional points are identified as outliers. Our discussion focuses on these outliers and their determination.

In Figure 17, the data point at 512.1°F and 1000.0 psia has a deviation exceeding three times the RMSE, while no other data point in the 1000.0 psia isobar exceeds twice the RMSE. As such, this data point is identified as an outlier.
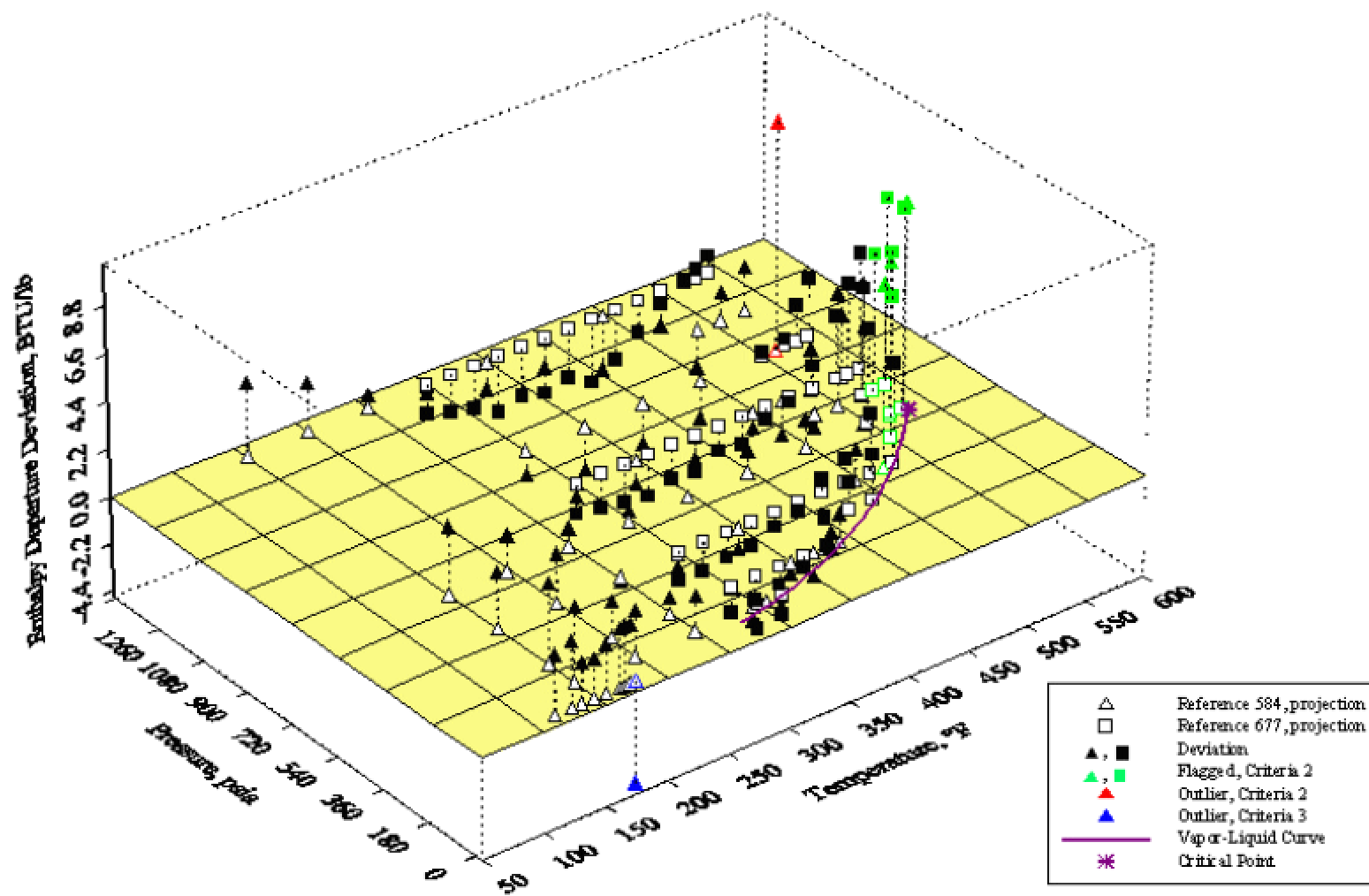
Figure 17. 3-D Enthalpy Departure Deviation for Cyclohexane (L)

The second unique data point at 181°F and 15.40 psia from reference #584 has a deviation of –4.7 Btu/lb. Although this deviation is within twice the RMSE, when compared with other points along the 15.4 psia isobar shows an abrupt change in deviation sign. Its deviation is 6 Btu/lb from the nearest point in the isobar, clearly showing this point is a likely outlier.

The examples from the three systems examined, methane vapor, liquid pentane, and liquid cyclohexane, are typical of the procedure employed in internal and external consistency evaluations. The resultant constructions of smooth data from the internal and external evaluation are critical for the final composite analysis evaluation.

COMPOSITE ANALYSIS – PURE COMPONENTS

In the initial composite analysis evaluation, data is organized as shown in Figure 18. The bar chart shows three error measures for pure component enthalpy departures within the database (the numbers in parenthesis indicate total number of data points available). In Figure 19, the error analysis of the pure component data are organized by compound classification. It is important to note that the results shown are for smoothed data sets, as determined by the internal and external consistency evaluations described previously, for each component in all available phases. Several of the pure component systems contain notable trends.
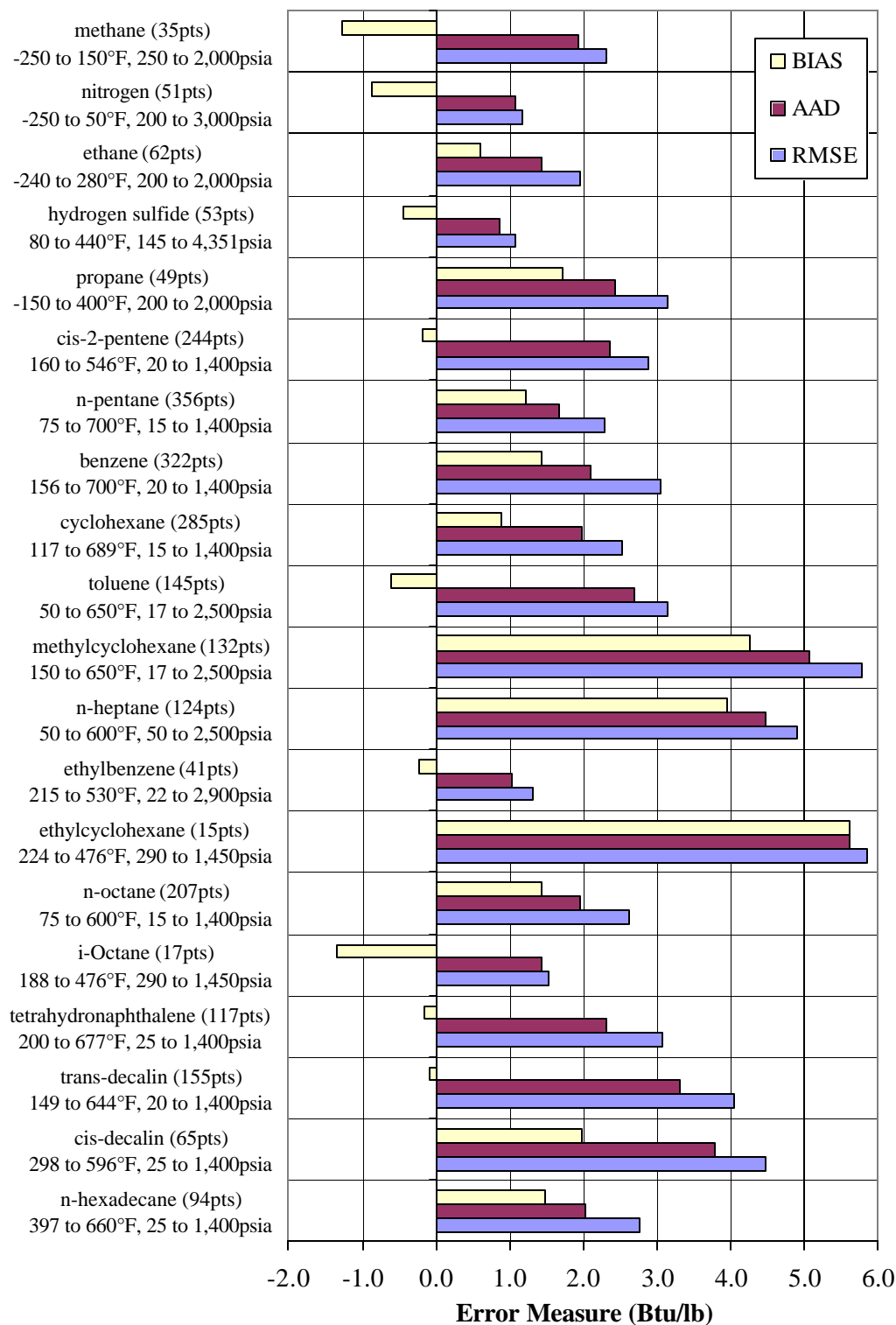
Figure 18. Pure Component Data Evaluation Summary
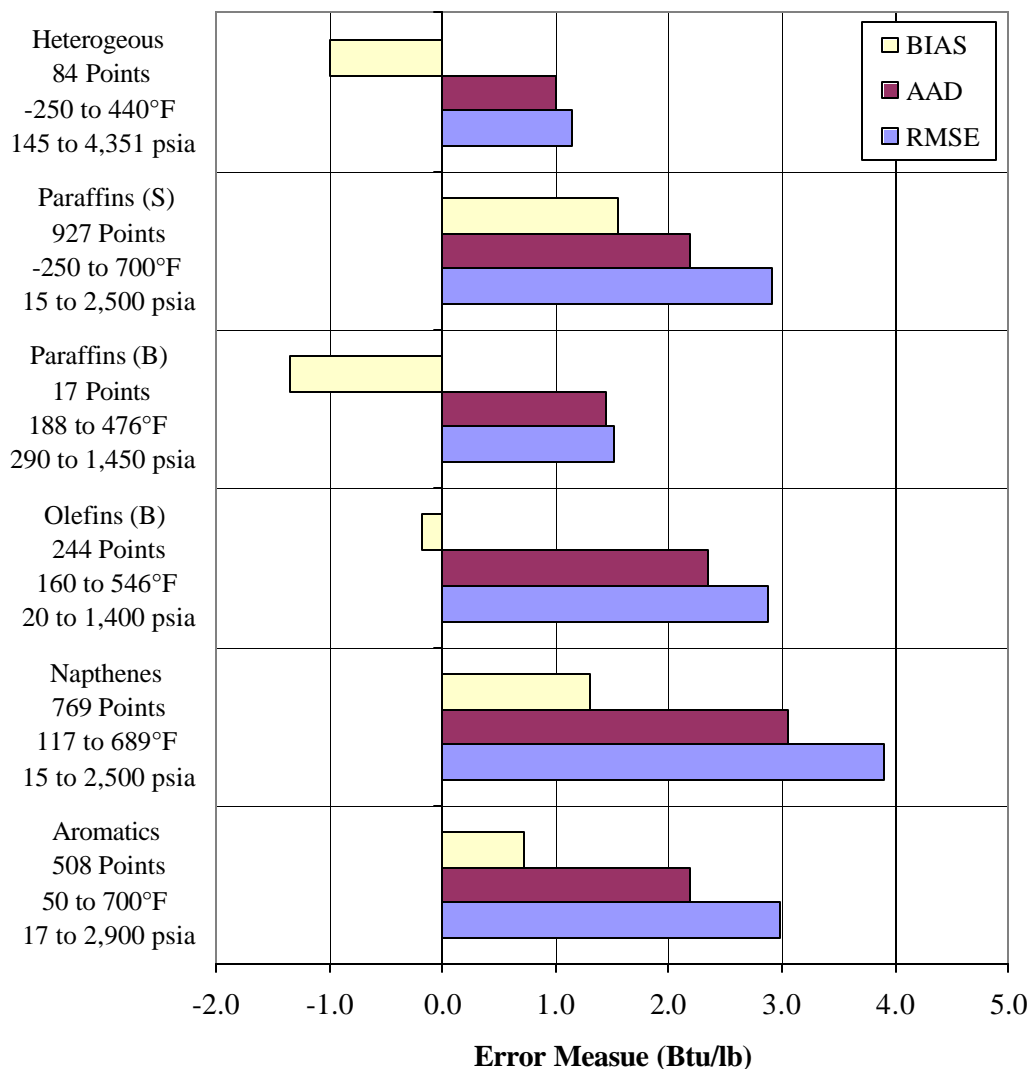
Figure 19. Pure-Component Evaluation Summary by Class

Several analyses are facilitated from the organization of pure and grouped component error. As with internal and external consistency, the systems of interest in a composite evaluation are identified by conditions including larger than expected RMSE, those with high AAD combined with high BIAS values, and systems that show behavior unusual as compared to components of the similar class. The examples that follow demonstrate composite analysis of heptane, i-octane, ethyl- and methylcyclohexane, and cyclohexane data.

Liquid Heptane

Of the 154 heptane data points, 105 are liquid phase measurements. Although the RMSE of the vapor points is similar to the RMSE of the liquid points a questionable trend is discernable in the liquid data. Figure 20 presents the error analysis the liquid heptane results as compared with results of other paraffin systems and hydrocarbons excluding the liquid heptane points.
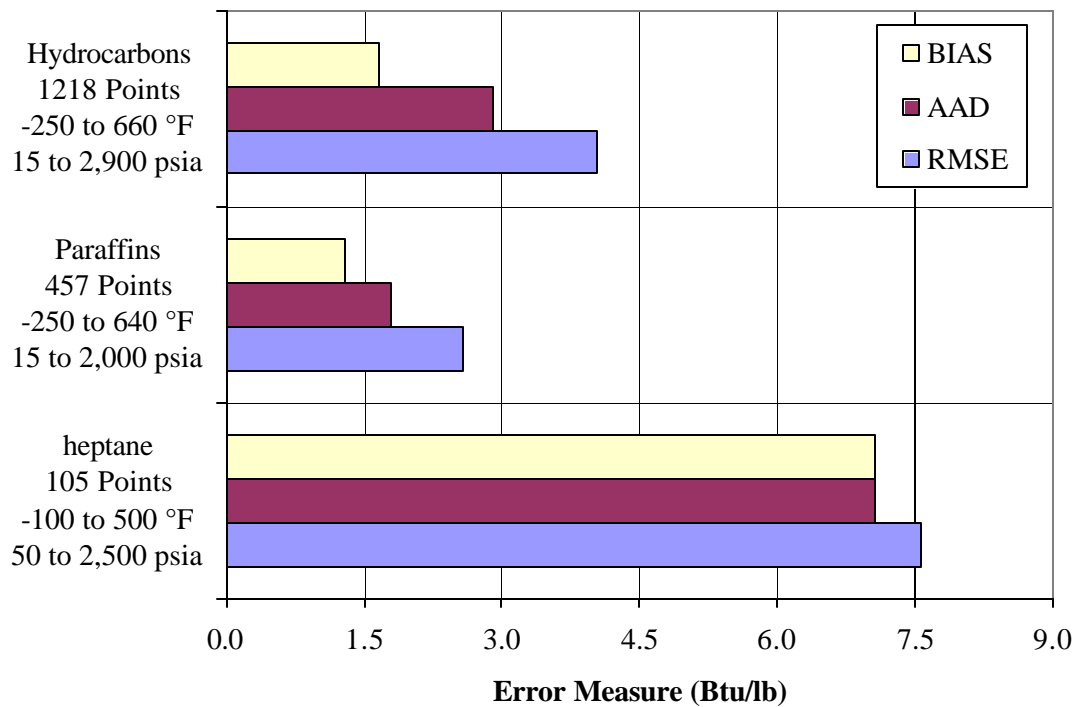
Figure 20. Heptane (L) System Evaluation

As shown, the RMSE for liquid heptane is twice the expected value for a normal liquid paraffin system, as well as nearly double that of the entire liquid hydrocarbon database. In accordance with the internal consistency analysis, the entire system should be flagged as suspect. The additional results showing that liquid heptane has numerically identical BIAS and AAD error measures, indicating the entire system is over-predicted by the

EOS. This is unusual when compared with other paraffin results. These trends suggest that the entire liquid heptane data set be flagged under Criteria #2.

Liquid i-Octane

The error measurements of the 17 experimental i-octane data presented Figure 21 are from a single reference source and are all liquid-phase measurements. While the RMSE of the experimental data is excellent, at 1.8 Btu/lb, this value is based on a small number of data points. Of interest in this data is the numerically large negative BIAS. This negative BIAS is questionable when compared with other paraffin, and hydrocarbon data groups. The entire data set is flagged, and additional investigation is needed.
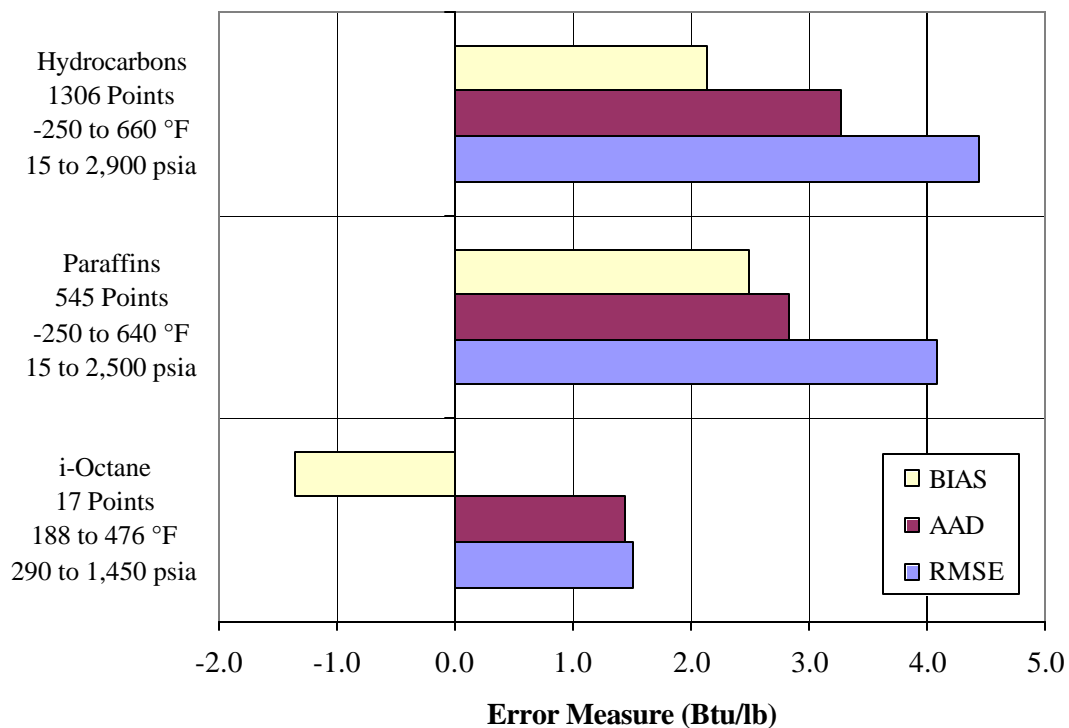
Figure 21. i-Octane System Evaluation

Vapor and Liquid Methylcyclohexane and Liquid Ethylcyclohexane

Enthalpy departures calculations for methylcyclohexane and ethylcyclohexane components are consistently over predicted (BIAS and AAD numerically large). The RMSE of these components, as shown in Figure 22 are significantly larger than similar components in various classes but do not exceed twice the RMSE of any group. While not exceeding the twice RMSE criteria, the liquid ethylcyclohexane and vapor methylcyclohexane data sets do exhibit unusual BIAS values (all over predictions) which are inconsistent with the comparable component classes. At present these systems are flagged as requiring additional consideration.

The examples discussed are typical of composite analysis evaluation. The completed evaluation allows some conclusions to be drawn regarding the ability of the PR EOS to predict enthalpy departure data.
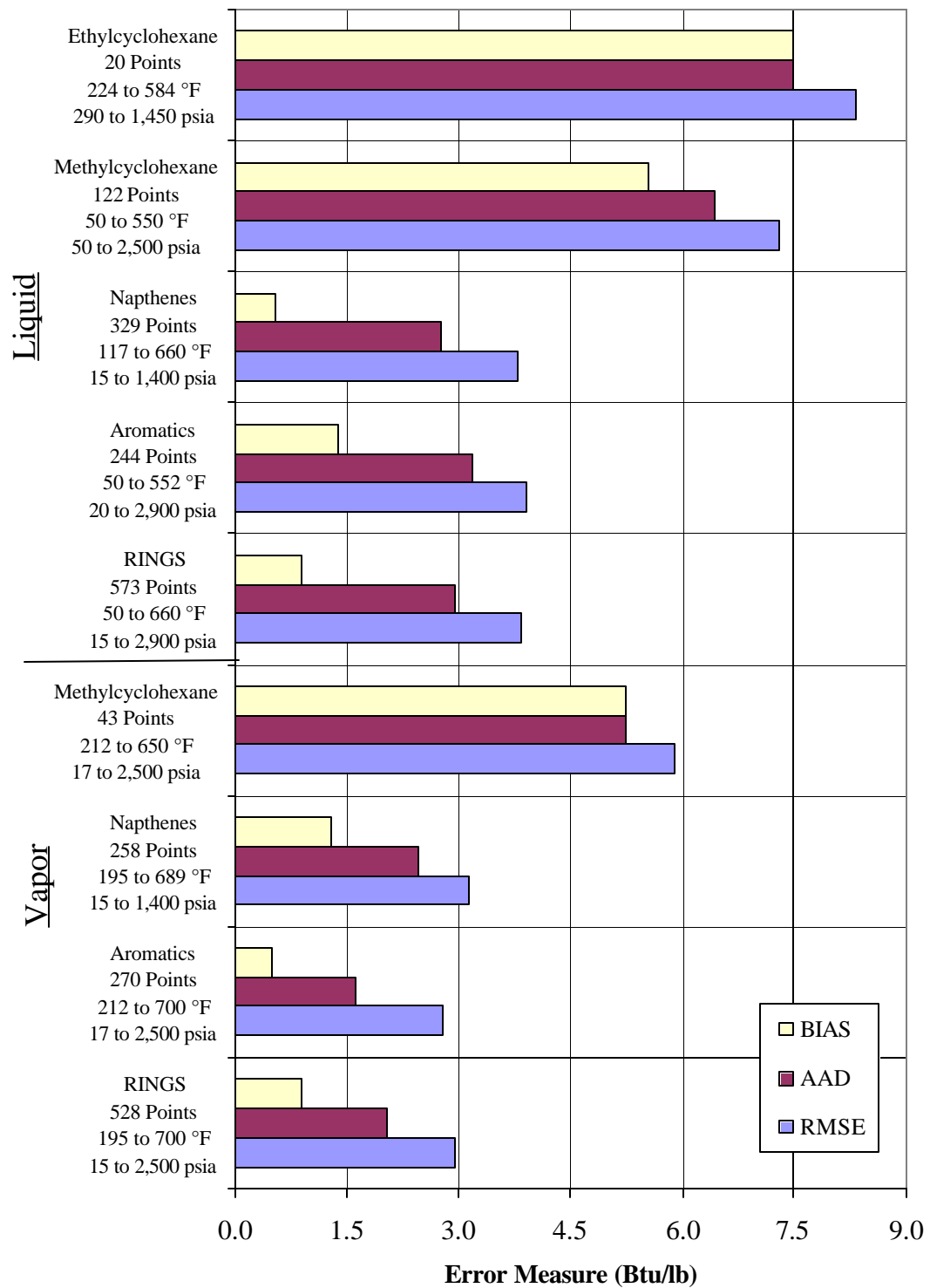
Figure 22. Methyl- and Ethylcyclohexane Composite Evaluation

PR EOS Predictions of Pure Component Enthalpy Departure

The final smoothed data error analysis of pure component enthalpy departure data, organized by component group, is given in Table 7. The groups include ring compounds split into napthenes and aromatics, branched olefins (B), normal paraffins (S), branched paraffins (B), and heterogeneous components.

Table 7. Pure-Component Enthalpy Departure Evaluation by Group

GROUP	RMSE	AAD	%AAD	BIAS	Max Dev (Low)	Max Dev (High)	NPTS
Aromatics	3.0	2.2	14.4	0.7	-5.9	7.8	508
Napthenes	3.9	3.1	33.7	1.3	-9.4	9.5	769
Olefins (B)	2.9	2.3	8.5	-0.2	-6.7	7.6	244
Paraffins (B)	1.5	1.4	1.4	-1.3	-2.0	0.9	17
Paraffins (S)	2.9	2.2	8.7	1.6	-5.2	7.6	927
Heterogeous	1.1	1.0	7.3	-1.0	-2.3	0.0	84
TOTAL	3.2	2.4	17.1	1.0	-9.4	9.5	2,569

The table also reports maximum deviation values for each group as low and high values which represent the maximum deviation found among over prediction and under predictions. It is worth noting these maximum as outer limits of the departure deviation calculations the majority of data points lie within these bounds as evident by the RMSE and BIAS error measures. The graphs of Figure 23 and Figure 24 provide error analysis summaries for pure component vapor and liquid phase points. Each figure gives the RMSE, AAD, and BIAS error for each group, and also reports the number of data points, the temperature range (to the nearest degree) and the pressure range (to the nearest psi).
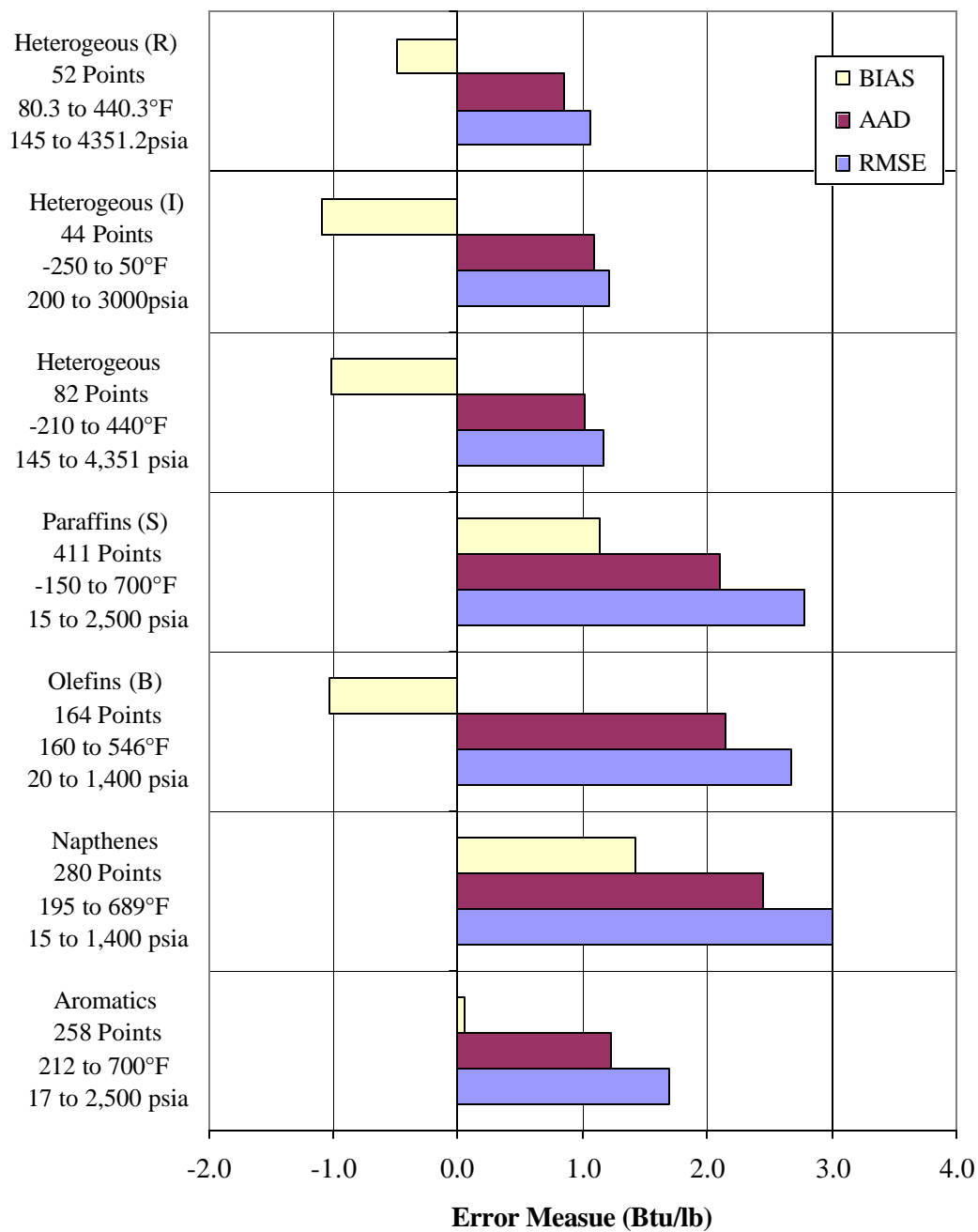
Figure 23. PR EOS Evaluation of Vapor Pure Component Enthalpy Departure Data
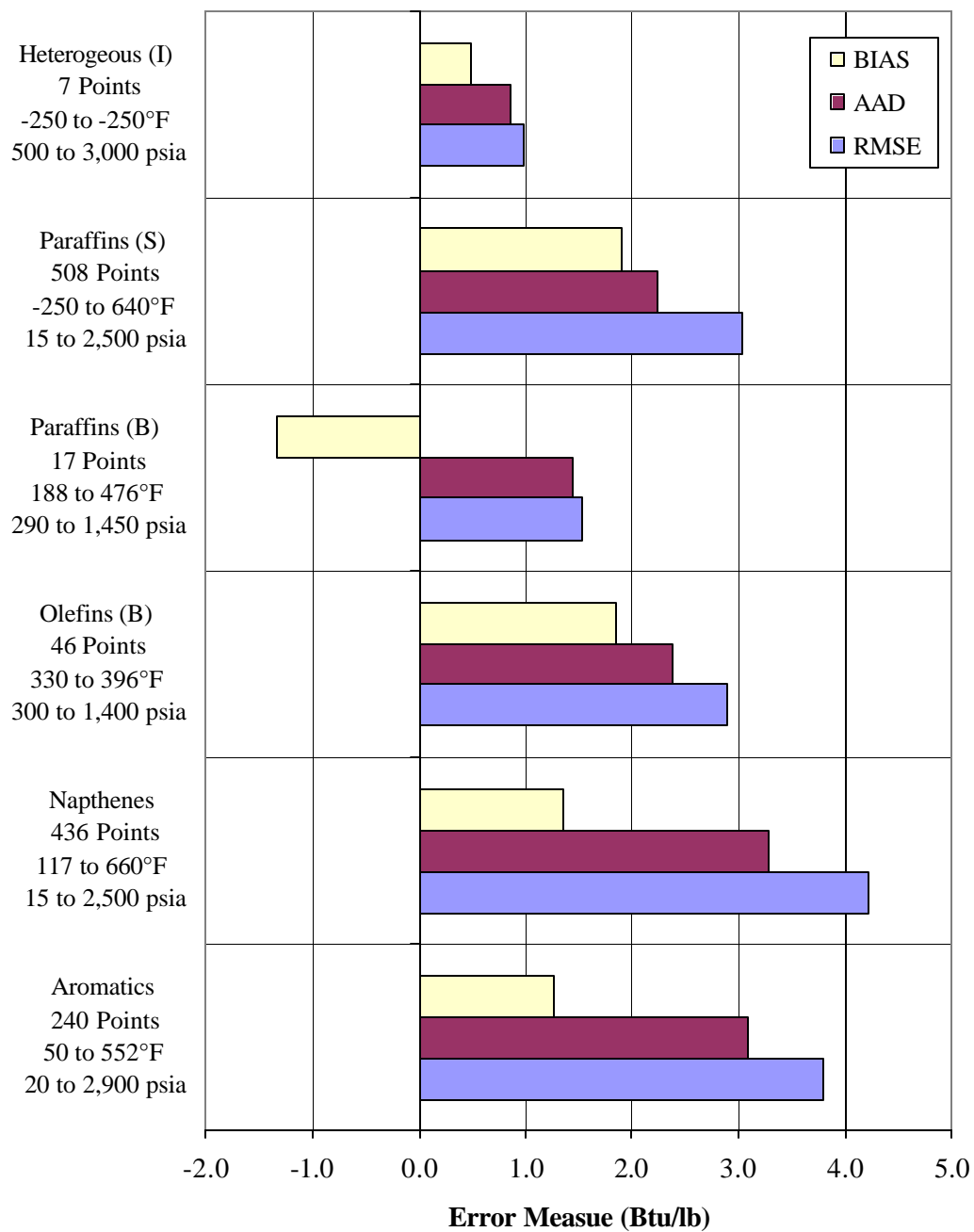
Figure 24. PR EOS Evaluation of Liquid Pure Component Enthalpy Departure Data

In liquid phase data, it is notable that the branched paraffins examined, which are from the i-octane system discussed, exhibit a noticeable negative BIAS. These results are appear atypical when compared with normal paraffins (straight) and olefins (branched) but are not identified as outliers in light of the similar observation for vapor phase branched paraffins (Figure 23). Additional experimental data are needed to determine the validity of the trend observed in the equation-of-state calculations.

As shown, the RMSE of pure vapor phase enthalpy departure is within 3.0 Btu/lb among all groups (Figure 23). Overall 90% of the vapor data points examined are within 4.5 Btu/lb. For liquid phase data, the RMSE of liquid enthalpy departure data is within 4.2 Btu/lb on average (Figure 24), with 90% of the data examined within 6.0 Btu/lb.

The analysis of the pure component data is valuable when evaluating binary system data. The observed trend for pure heterogeneous compounds (Figure 23) and pure methane (Figure 18) which exhibit negative BIAS in vapor phase data are important considerations when examining binary mixtures including methane or a heterogeneous component. Also evident in Figure 18 for the methane, ethane, propane results there is a negative to positive BIAS trend, which should be considered in binary data evaluations.

BINARY SYSTEMS

Binary data evaluations are similar to the procedure described in detail for pure component systems, by considering internal consistency, external consistency, and a composite analysis. There are additional features necessary for binary system evaluations in the external and composite evaluation process. Examples from benzene-hexadecane, methane-propane, and pentane-octane clarify the evaluation process as applied to binary data.

In an external evaluation data are considered by comparison with additional reference sources, the benzene-hexadecane data shown in Figure 25 provides an example. As shown, the RMSE differs from one source to another, i.e., data points at identical compositions available from different reference sources.

An additional consideration necessary for external consistency evaluations includes examination of the error analysis results across the composition range of the binary system. The methane-propane vapor data shown in Figure 26 is a notable example of the possibility of a composition effect on the calculated enthalpy departure.
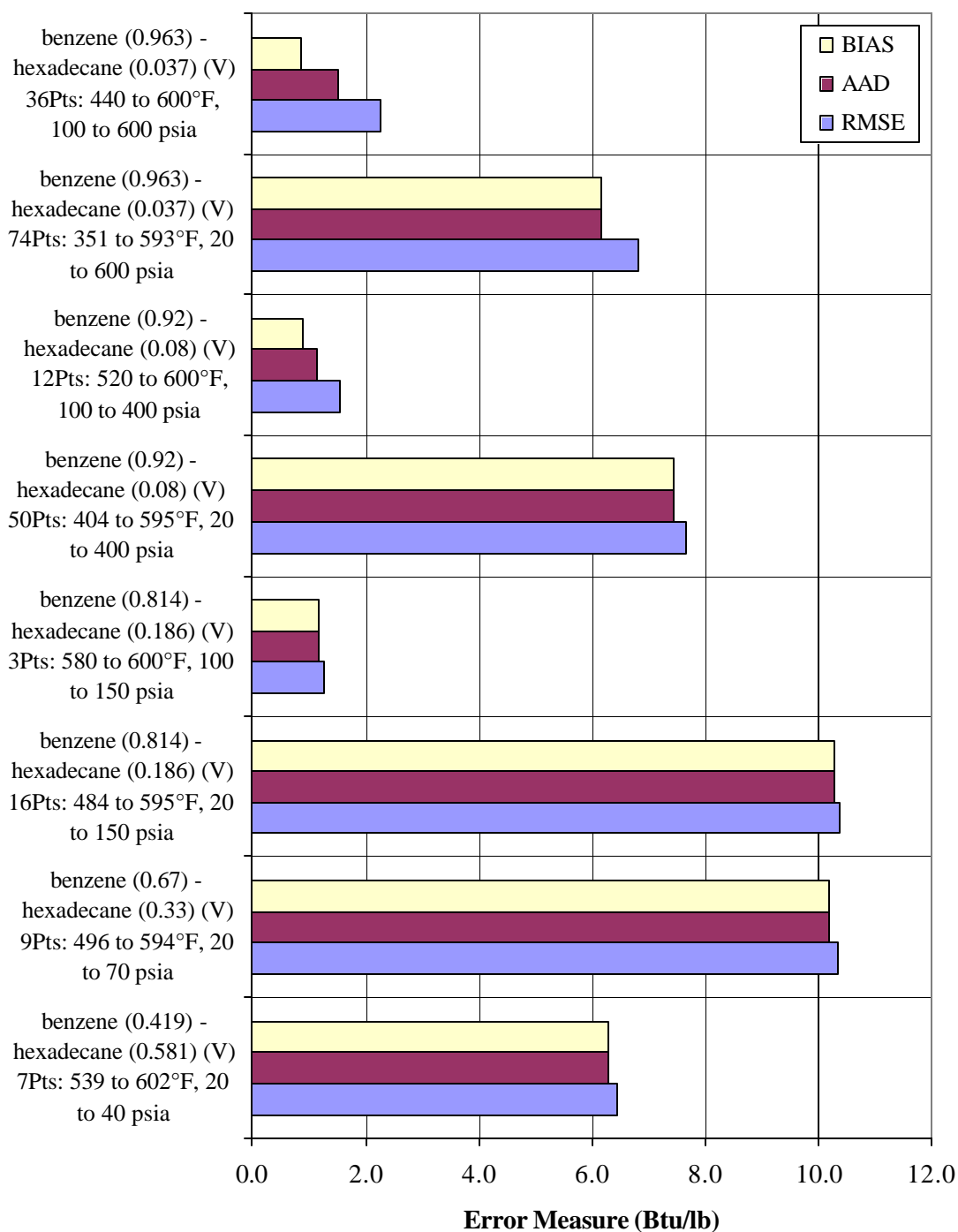
Figure 25. Benzene-Hexadecane Vapor: Analysis by Composition and Source
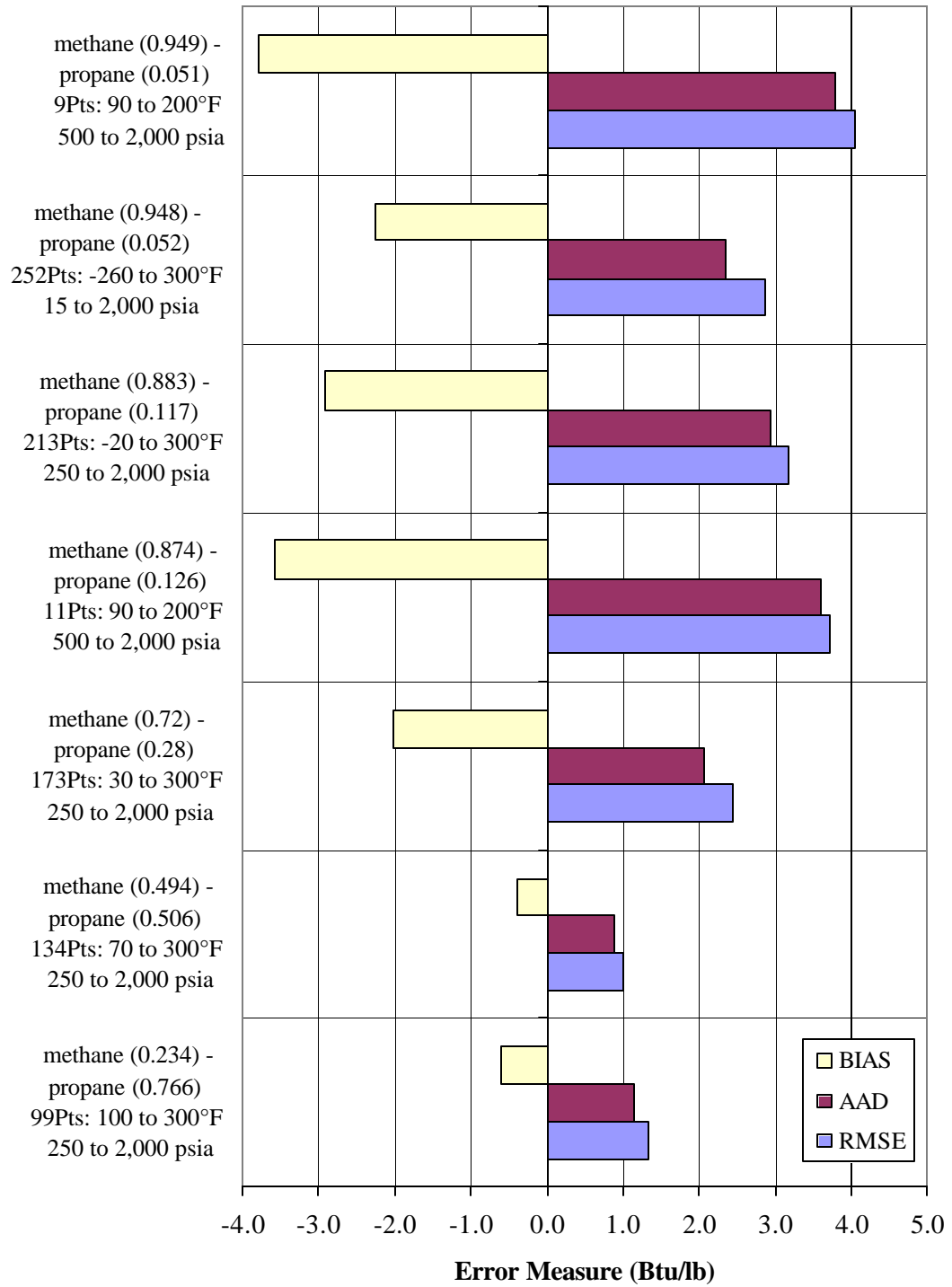
Figure 26. Methane-Propane Liquid Data Evaluation: Effects of Composition

There is a clear trend in the binary in which methane rich systems are more negative in BIAS and have higher RMSE. In the methane-propane binary data evaluations, where data points exhibiting deviations greater than twice the RMSE of the data set as a whole are identified as outliers, each mole fraction combination is considered individually. Application of a mole fraction-based consistency evaluation on this binary system is crucial to avoid incorrectly identifying points as outliers in the methane rich composition region when applying evaluation criteria based on a lower RMSE based on the entire composition range.

The composition dependent results for the methane-propane system are unusual, the more common occurrence is that shown in Figure 27 for the pentane-octane binary system. As shown in either the liquid or vapor data there is no discernable trend as a function of composition.

The composition effects on the error analysis represent the additional consideration necessary for consistent and accurate evaluation of binary data sets. In addition to the evaluation consideration based on composition effects the analysis of each pure component (as available) serves as a guideline to a binary composed of the components being examined. The final smoothed evaluation summary for binary systems include the data shown in Figure 28.
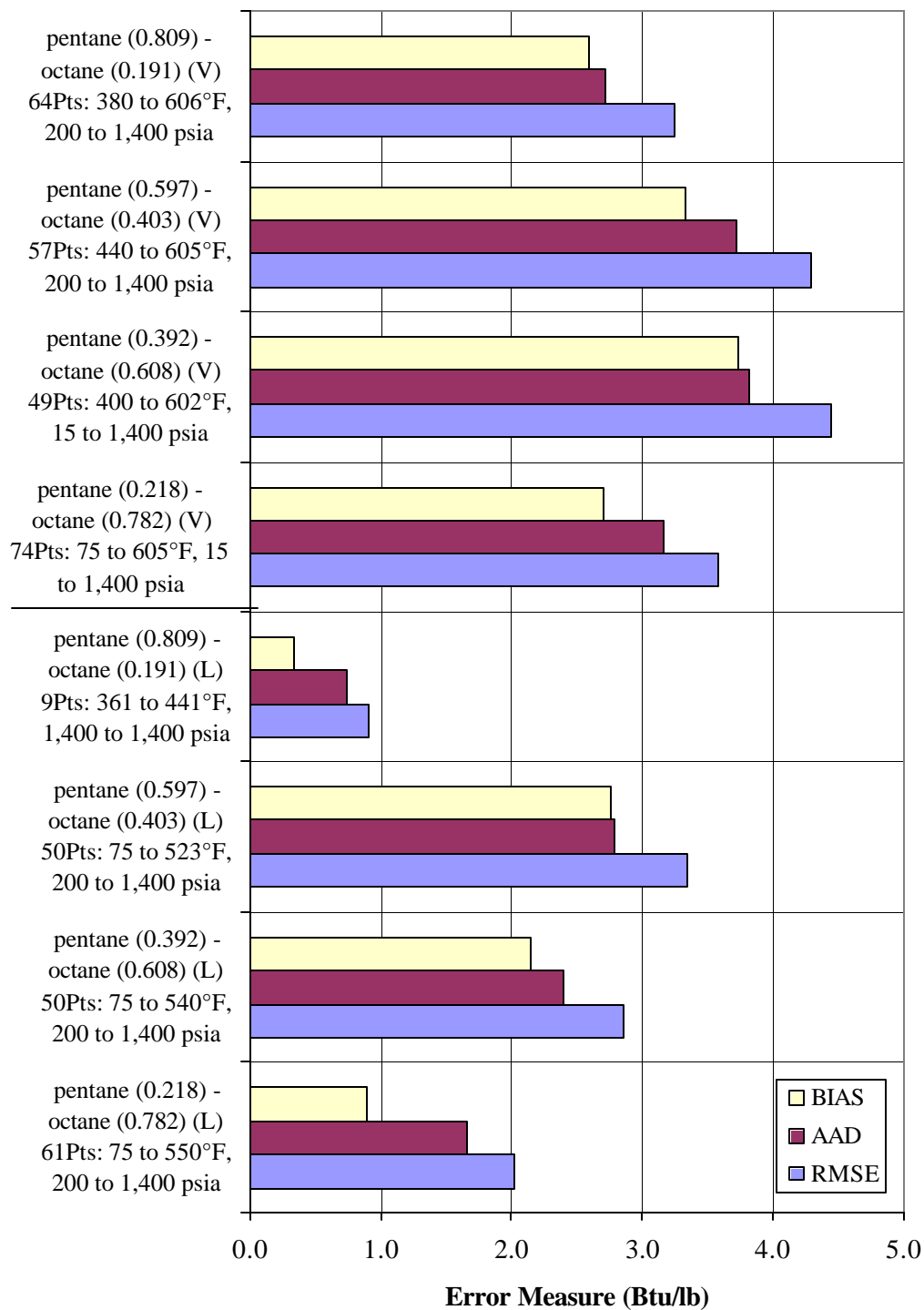
Figure 27. Pentane-Octane Error Analysis

71
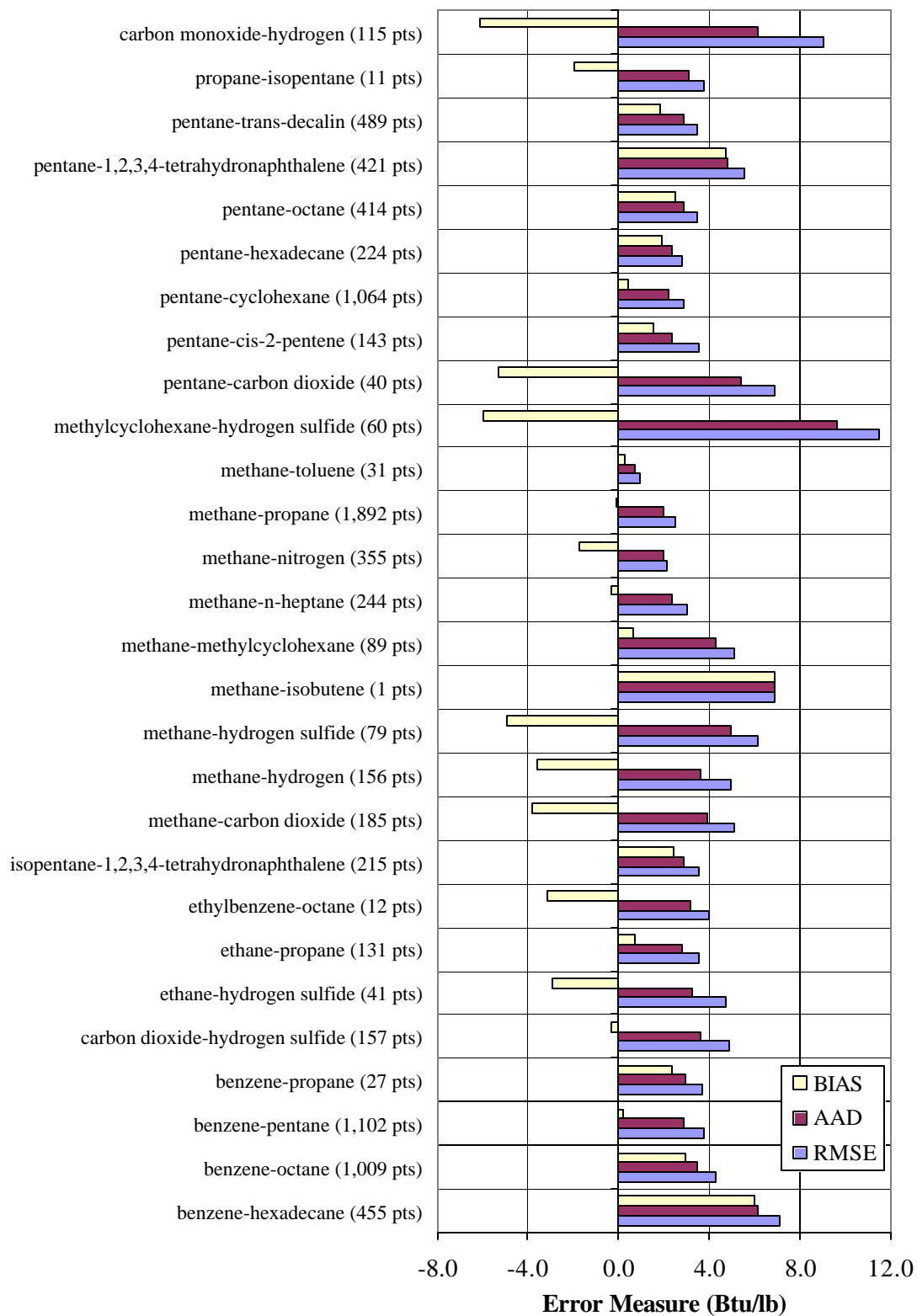
Figure 28. Binary Systems Error Analysis Summary

PR EOS Predictions of Binary Systems Enthalpy Departure

Similar to pure systems binary combinations are also grouped by clas, with the results of this organization is given in Table 8. The table also reports maximum deviation values for each group as low and high values which represent the maximum deviation found among over prediction and under predictions.

Table 8. Binary System Evaluation by Group

GROUP	RMSE	AAD	%AAD	BIAS	Max Dev (low)	Max Dev (high)	NPTS
Parrafin-Parrafin	2.8	2.2	12.6	0.4	-8.0	8.0	2,917
Parrafin-Olefin	3.5	2.4	4.1	1.5	-2.9	11.9	143
Parrafin-Ring	4.3	3.3	17.5	2.0	-12.1	13.3	4,914
Parrafin-Hetero	4.1	3.0	31.0	-2.9	-12.2	6.6	777
Ring-Hetero	8.8	7.5	26.2	-3.0	-15.4	15.2	49
Hetero-Hetero	4.9	3.6	12.0	-0.3	-12.8	12.9	157
Total	3.9	2.9	16.8	1.0	-15.4	15.2	8,957

The maximum deviation observed (high and low) are greater than for pure systems. The graphs of Figure 29 and Figure 30 provide error analysis summaries for binary vapor and liquid phase data sets. Each figure gives the RMSE, AAD, and BIAS error for each group, and also reports the number of data points, the temperature range (to the nearest degree) and the pressure range (to the nearest psi). Both liquid and vapor phase binary systems which include heterogeneous components exhibit negative BIAS and significantly greater RMSE than other systems.

For vapor phase data, the RMSE of enthalpy departure data is within 4.0 Btu/lb on average (Figure 29), with 90% of the data examined within 5.0 Btu/lb.
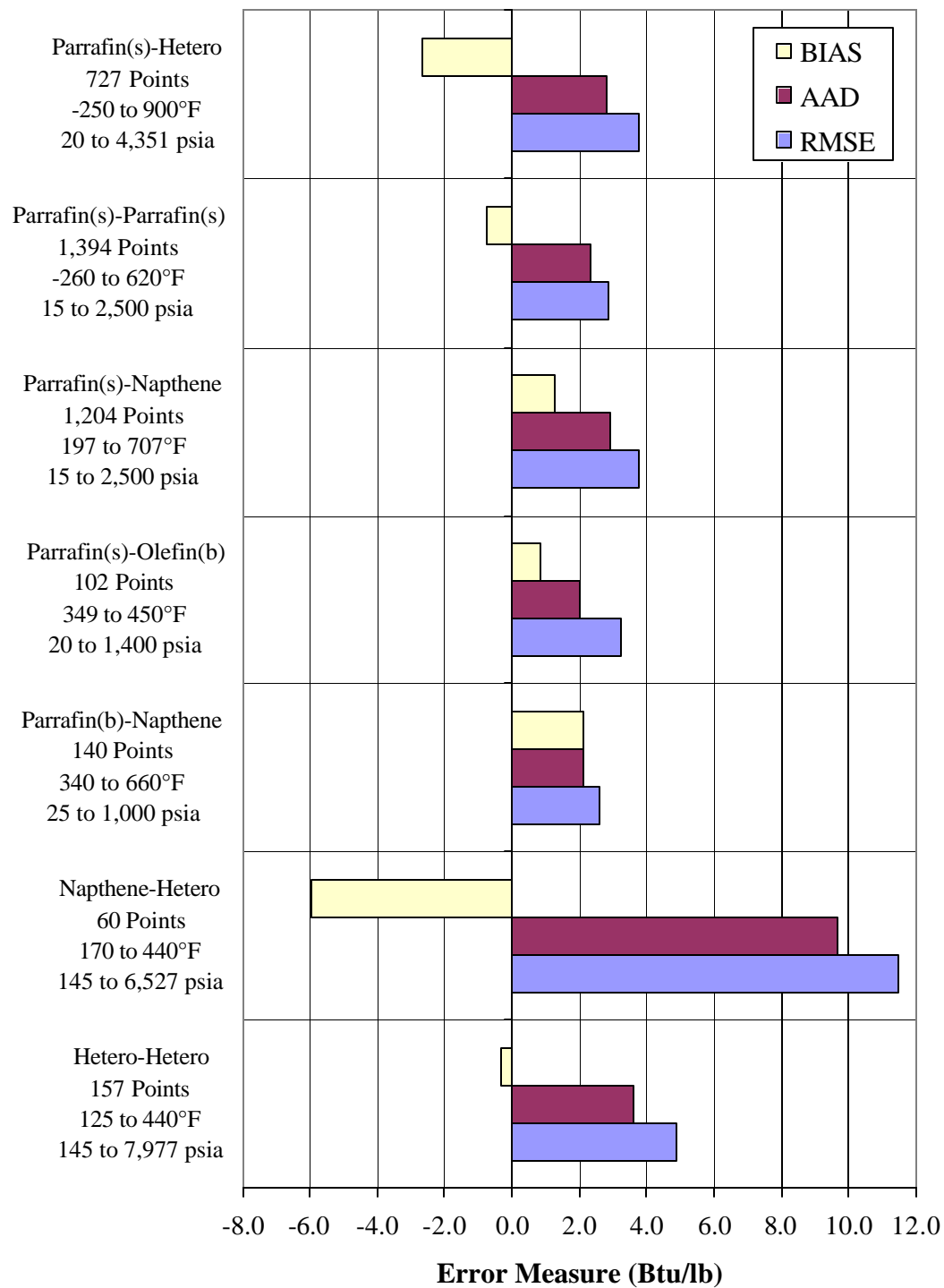
Figure 29. Binary Vapor Phase Data Analysis by Group

74
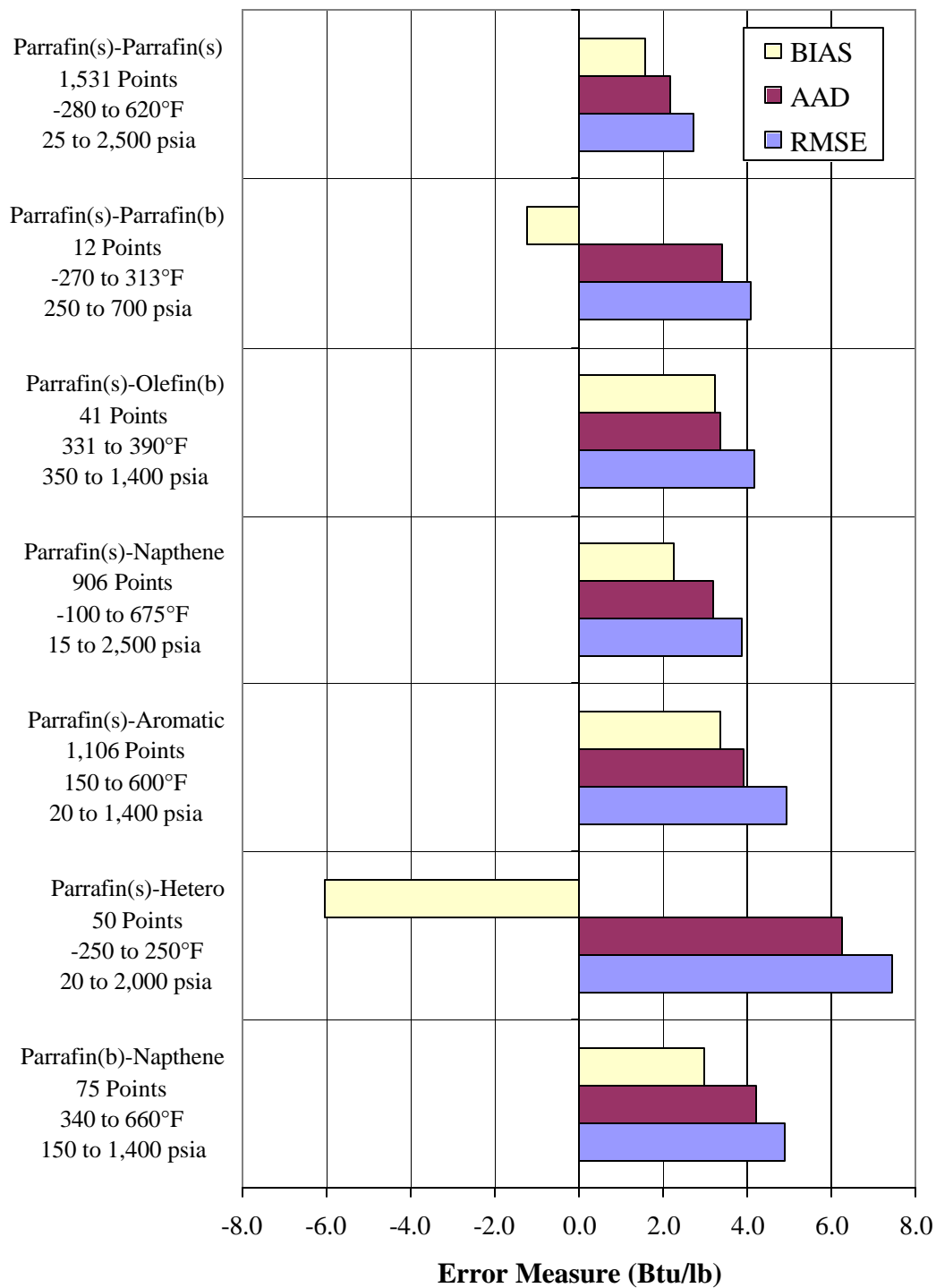
Figure 30. Binary Liquid Phase Data Error Analysis by Group

As shown, the RMSE of binary liquid phase enthalpy departure data is within 4.5 Btu/lb when excluding heterogeneous components (Figure 30). With the exception of heterogeneous components, 90% of the liquid phase data examined are within 4.5 Btu/lb.

Binary systems show larger error measures overall when compared with the corresponding pure component data. The observed trends found in pure component data are also found in binary systems. Systems, which include a heterogeneous component, exhibit larger BIAS values indicating a tendency for the equation of state to under predicting the enthalpy departure for these systems.

SUMMARY

The enthalpy data contained within the Gas Processors Association Database are evaluated for reliability. Enthalpy departure prediction using the Peng-Robinson equation of state are used for data quality assessment of experimental enthalpy departure data. This work identifies less than one percent of the total data as flagged data, of which only a small percentage are outliers. Additional composite evaluation based on component classification identifies suspect outliers and data sets exhibiting larger than expected deviations.

For pure components, the Peng-Robinson equation of state is found to adequately estimate the enthalpy departure of a liquid phase within 4.5 Btu/lb and corresponding vapor phase to within 6.0 Btu/lb. For purely hydrocarbon components the equation-of-state predictions improve, and are expected to be within 4.5 Btu/lb for liquid phases and 4.0 Btu/lb for vapor phases. Binary systems with one or both components consisting of a

heterogeneous compound exhibit significantly larger RMSE, indicating the equation of state under predicts the enthalpy departure of these mixtures.

Overall the Peng-Robinson equation of state showed an average deviation of 2 to 6 Btu/lb for the entire databank, giving slightly better predictions for pure systems compared to binary systems, and slightly better for normal paraffins compared with other compounds. In both pure and binary systems, heterogeneous components tend to be under predicted by the equation of state.

REFERENCES

1.   Daubert, T.E., *GPA Data Bank of Selected Enthalpy and Equilibria Values*. 1993, Pennsylvania State University: University Park, Pennsylvania.

2.   Wagner, J., et al., *GPA Thermodynamic Database*. 2000, Gas Processors Association: Tulsa.

3.   Cochran, G.A. and J.M. Lenoir, *GPA Experimental Values Referred to Two Base Levels*. 1974.

4.   Reid, R.C., J.M. Prausnitz, and B.E. Poling, *The Properties of Gases & Liquids*. Fourth ed. 1987, New York: McGraw-Hill, Inc. 741 pgs.

5.   Passut, C.A. and R.P. Danner, *Correlation of Ideal Gas Enthalpy, Heat Capacity, and Entropy.* Ind. Eng. Chem. Process Des. Dev., 1972. 11(No. 4): p. 543-546.

6.   Thinh, T.P., et al., *Equations Improve C_p^* Predictions.* Hydrocarbon Processing, 1971(January): p. 98-104.

7.   Aly, F.A. and L.L. Lee, *Self-Consistent Equations for Calculating the Ideal Gas Heat Capacity, Enthalpy, and Entropy.* Fluid Phase Equilibria, 1981. 6: p. 169-179.

8.   Yuan, S.C. and Y.I. Mok, *New Look at Heat Capacity Prediction.* Hydrocarbon Processing, 1968. 47(No. 3): p. 133-136.

9.   Duran, J.L., et al., *Predict Heat Capacity More Accurately.* Hydrocarbon Processing, 1976. 55(No. 8): p. 153-156.

10.   Adachi, Y., H. Sugie, and B.C.Y. Lu, *Taking Advantage of Available Cubic Equations of State.* The Canadian Journal of Chemical Engineering, 1990. 68(August): p. 639-644.

11.   Schmidt, G. and H. Wenzel, *A Modified van der Waals Type Equation of State.* Chemical Engineering Science, 1980. 35(No. 7): p. 1503-1512.

12.   Soave, G., *Equilibrium Constants from a Modified Redlich-Kwong Equation of State.* Chemical Engineering Science, 1972. 27: p. 1197-1203.

13.   Harmens, A. and H. Knapp, *Three Parameter Cubic Equation of State for Normal Substances.* Ind. Eng. Chem. Process Des. Dev., 1975. 14: p. 209.

14.   Kumar, K.H. and K.E. Starling, *The Most General Density-Cubic Equation of State: Application to pure Nonpolar Fluids.* Ind. Eng. Chem. Fundam., 1982. 21(No. 3): p. 255-262.

15.   Adachi, Y., H. Sugie, and B.C.-Y. Lu, *Evaluation of Cubic Equation of State.* Journal of Chemical Engineering of Japan, 1984. 17(No. 16): p. 624-631.

16.   Rastogi, A., M.S., *Evaluation and Maintenance of an Enthalpy Database*, Chemical Engineering, Oklahoma State University, Stillwater, Oklahoma, 1996.

17.   Row, K.Y., Ph.D., *Evaluation of the Modification of the PGR Equation of State for Selected Pure Components*, Chemical Engineering, Oklahoma State University, Stillwater, Oklahoma, 1998.

18.   Peng, D.-Y. and D.B. Robinson, *A New Two-Constant Equation of State.* Ind. Eng. Chem. Fundam., 1976. 15: p. 59-64.

19.   Lenoir, J.M., *GPA Experimental Enthalpy values Referred to Two Base Levels*. 1973, Gas Processors Association: Tulsa, Oklahoma.

CHAPTER IV

ENTHALPY DEVIATION: EVALUATION USING 3-DIMENSIONAL GRAPHS

EVALUATIONS OF ENTHALPY DATA

The four criteria by which data points are evaluated are, at times, difficult to interpret. Visualization of the data graphically makes trends and possible errors in the data more obvious. Graphs aid in interpretation of the output from the enthalpy prediction model. Greater accuracy resulting from a clearer view of the data under evaluation is the goal of the enthalpy plots.

PREVIOUS GRAPHICAL METHOD

One example of a graphical analysis is given for liquid heptane data, as shown in Figure 31. In this representation, calculated and experimental enthalpy departure data are graphed as a function of temperature, as grouped by pressure. The trends and error of calculated enthalpy departures are easily depicted for the four series (two pressures) shown. In order to examine trends in temperature and pressure simultaneously, all available date are placed on a single graph. However, the inset graph shows a complication as series overlap one another.
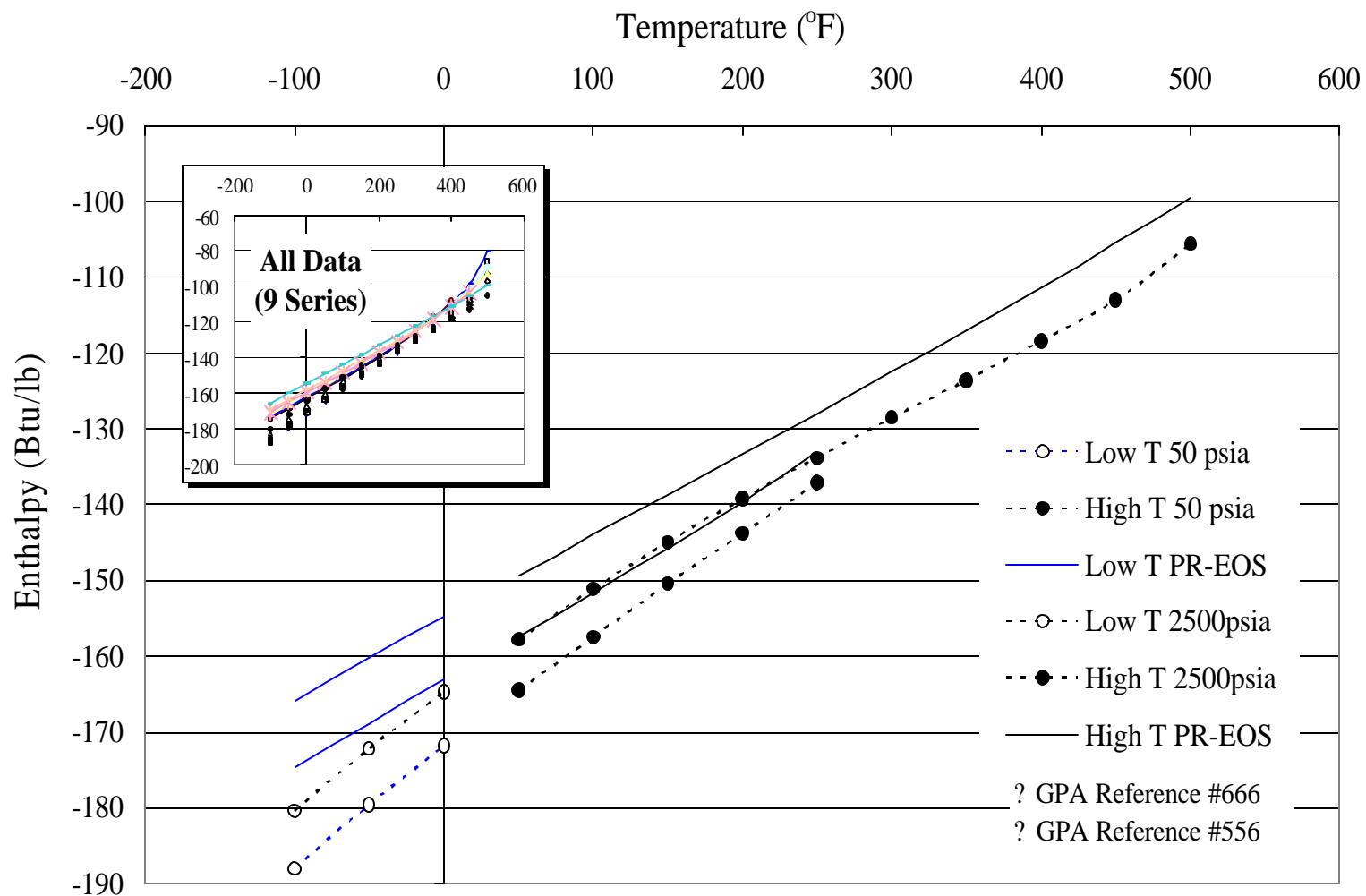
Figure 31 - Enthalpy Departure for Heptane Liquid: Source and Trend Consistency

81

Trend plots, such as in Figure 31, are valuable for representing agreement in calculated and experimental deviations. Unfortunately, such plots ordinarily exhibit the overlap behavior demonstrated and alternative graphing is necessary to resolve individual data points. As a starting point for development of a new graphical method, the old graphical approach is evaluated. One approach to error analysis compares experimental to calculated values by means of deviation plots. Figure 32 represents an example of a deviation plot for enthalpy departure data as a function of temperature.
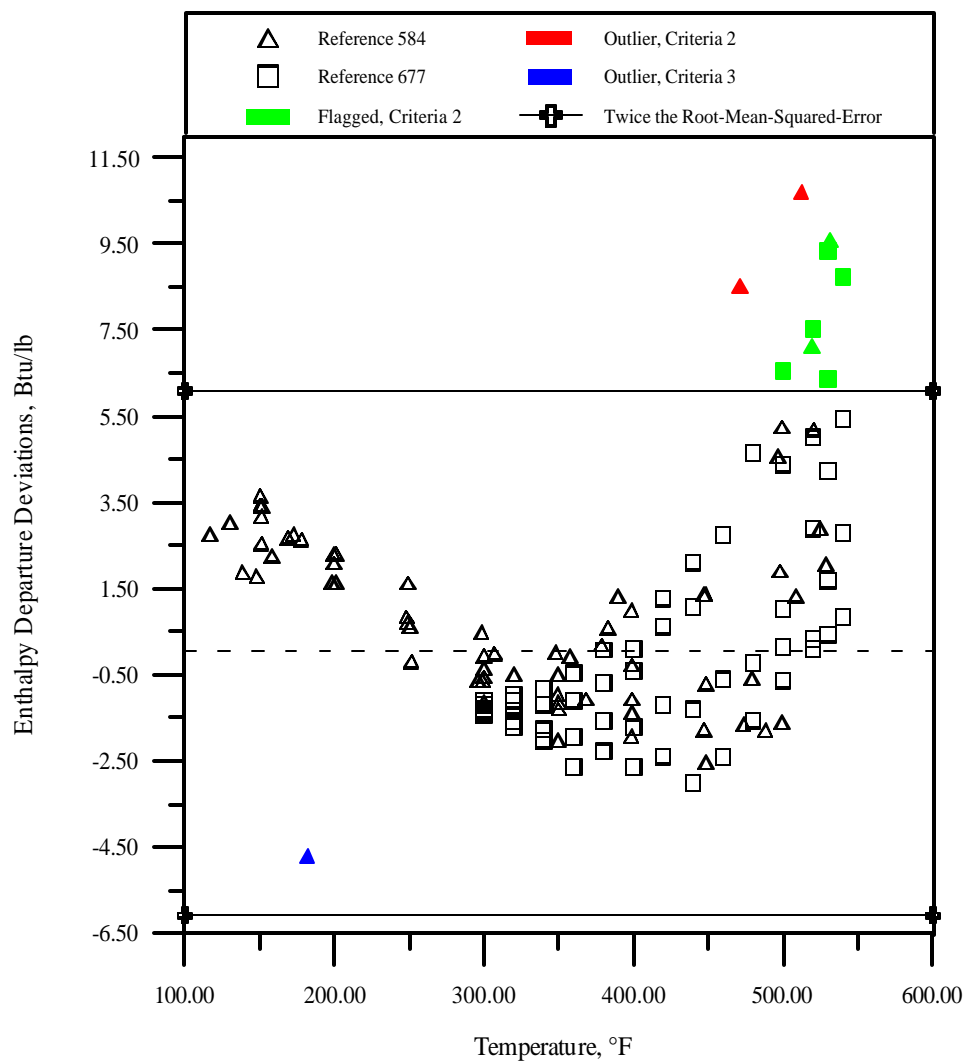
Figure 32 - Enthalpy Departure Deviations with Temperature: Cyclohexane (L)

With the primary criterion being the root-mean-squared error (twice the RMSE) comparison to data point deviations, plots of enthalpy departure deviations with pressure or temperature are valuable. Figure 32 presents enthalpy deviations as a function of temperature and includes the zero deviation line and boundaries representing twice the RMSE (positive and negative), which seems sufficient to identify suspect outliers.

On Figure 32, a discernable trend in temperature is evident. The deviation at lower temperatures is initially positive, turns negative then shoots to high positive values, eventually exceeding twice the RMSE around 450°F. While numerous data points are clearly approaching the critical temperature, from this plot alone it is indeterminate which, if any, of the graphed data points are simultaneously nearing the critical pressure.

A similar plot, shown in Figure 33, depicts the same data as a function of pressure. As in the previous representation, points exceeding twice the RMSE are clearly shown. Data points showing an abrupt change in deviation sign are also identified as outliers.

Trends in pressure are not as obvious. The deviation changes positive to negative along the same isobar, yielding no useful trend information. The temperature range along any isobar or the pressure range along any isotherm cannot be seen at all.

However, these plots show that determination of outliers from data following a normal trend in deviation from the equation-of-state calculations can be difficult, particularly when insufficient data exists in the needed range of temperature and pressure.
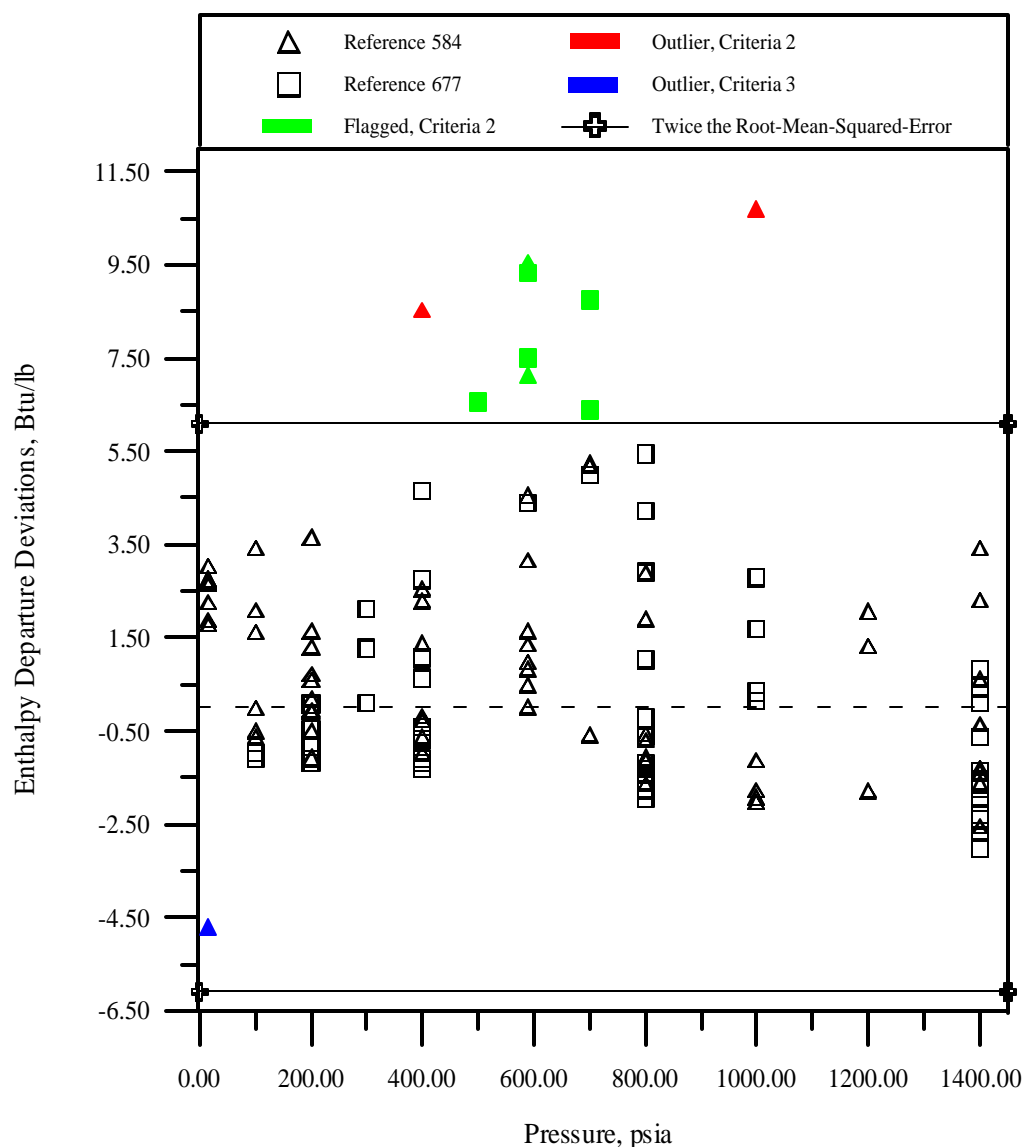
Figure 33 - Enthalpy Departure Deviations with Pressure: Liquid Cyclohexane

As described, both graphs are necessary for data point evaluations. With excessive deviation expected near the phase envelope, around the critical region, and as the system exceeds the critical point into non-ideal regions of high temperature and pressure, a third graph, including data variations as functions of temperature with pressure, is crucial to both the scope of the data and relationship of data points to these important phase boundaries.

Realistically, analysis of three graphs simultaneously is both inconvenient and difficult. To see the deviation trends with both temperature and pressure along with the scope of the data, a three-dimensional representation is desirable.

An improved graph should address several goals. It should be easy to understand and read. The plot should enable the reader to distinguish between different references for the system and give a clear picture of the temperature and pressure scope of the data. The deviation of the enthalpy data should be clearly represented to allow for easy sighting of trends and points where deviations abruptly change. Additional beneficial features would include representation of the vapor-liquid equilibrium boundaries and critical point of the system of interest.

THREE DIMENSIONAL SURFACE PLOTS

The first attempt to see the trends and the scope of the data is with a three-dimensional surface plot.

Figure 34 presents liquid cyclohexane data with temperature and pressure on the x-y plane, and percent enthalpy departure deviation along the z-axis. Figure 34 represents to the enthalpy departure deviation as a function of temperature and pressure. This general surface representation seems useful, but it can be easily misinterpreted.
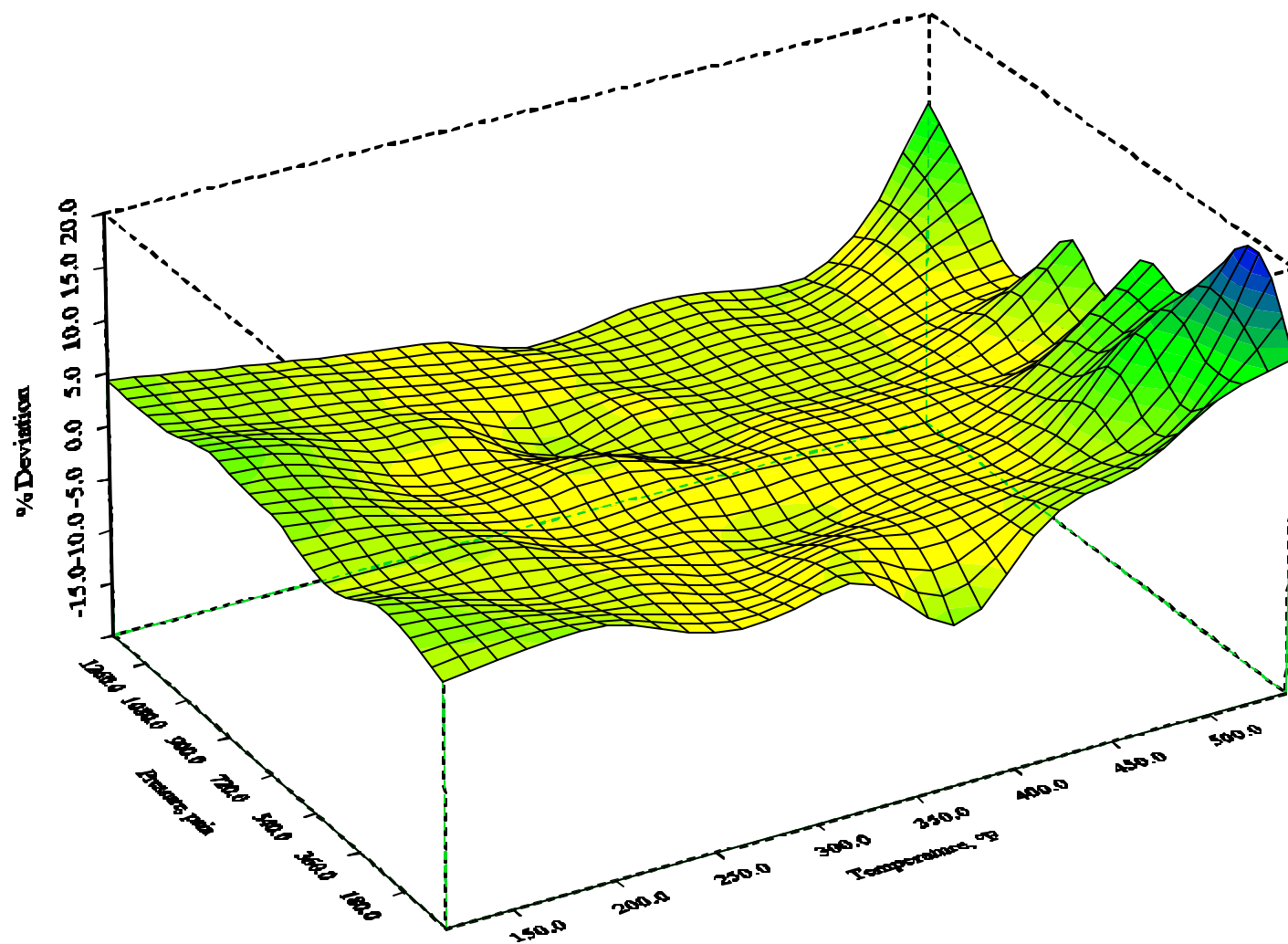
Figure 34 - Surface map of Enthalpy Departure Deviations: Cyclohexane (L)

Figure 35 shows a similar surface plot with additional markers for enthalpy departure deviations overlaid. There are three main areas of interest on this figure. First, in the high temperature, moderate pressure region there is a large spike in deviation. This is due to a single point, while all the surrounding points show relatively smaller deviations. The spike is not representative of the data set, being a lone data point, and is identified as an outlier compared to the surrounding points. The second area of interest is at high temperature and pressure. This area shows a large deviation trend although no data appearing to be significantly larger than any surrounding points. The third area occurs at low temperature and moderate pressure. Although this region contains no data the surface shows an increase in deviation, which may or may not be correct. Along with these phenomena, the surface extrapolates errors more than double the maximum error of the data. The smoothing function, a cubic spline (interpolation), is the source of all the phenomena described.
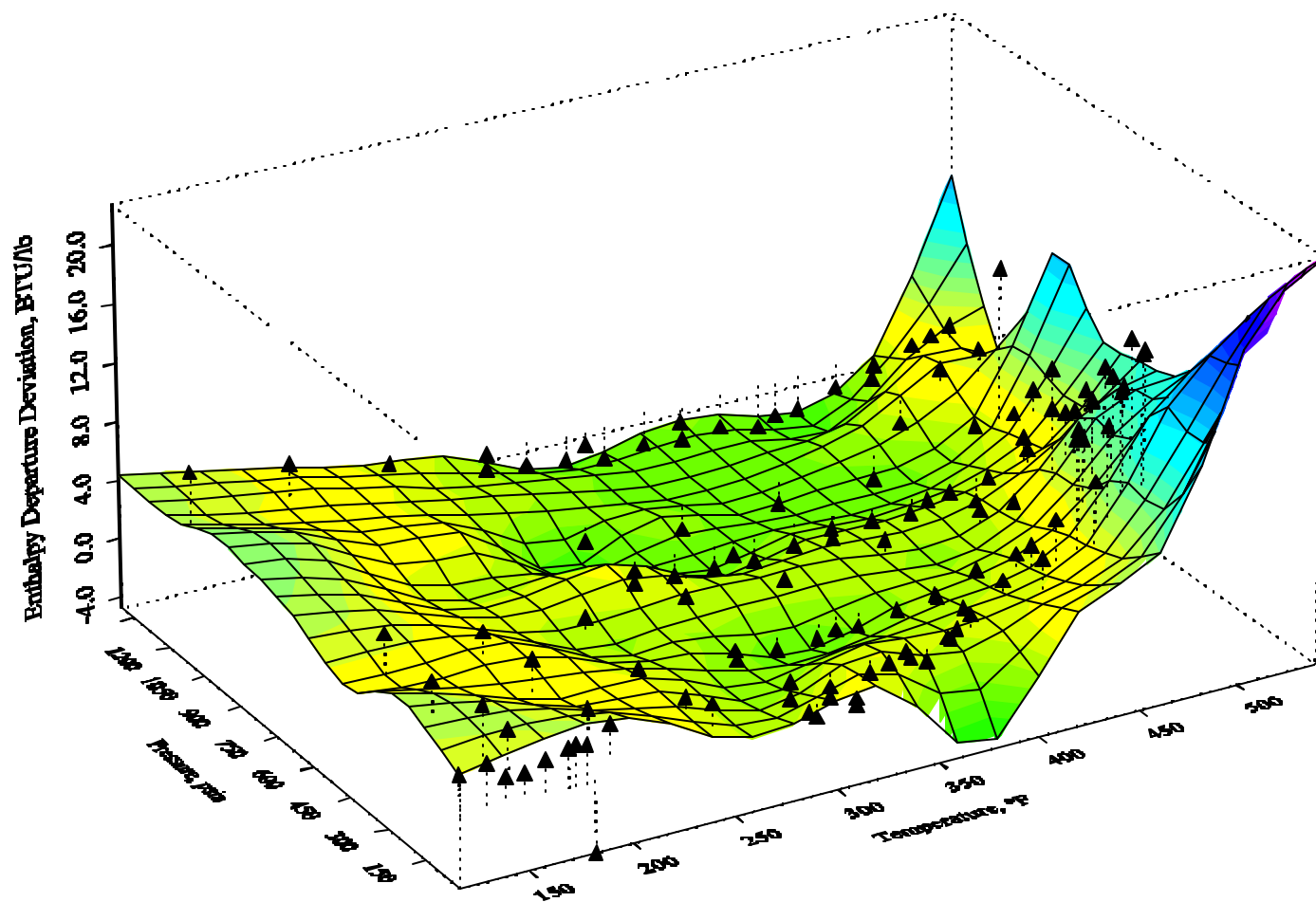
Figure 35 - Points and Surface map of Enthalpy Departure Deviations: Cyclohexane

A surface plot initially seems to be a good choice for analyzing deviations. However, without well-behaved data systematically covering the entire thermodynamic range, added complications to graphical evaluation may be introduced by the interpolated/extrapolated surface. While the surface plot has its shortcomings, the question remains on how to combine the simplicity of a two-dimensional plot with the ability to visualize temperature and pressure ranges simultaneously.

THREE DIMENSIONAL DATA POINT PLOTS

An improved three-dimensional plot is formed by combining the two-dimensional representations of deviations with temperature (Figure 32) and deviations with pressure (Figure 33) with a zero-reference plane. A flat grid, or x-y plane, at zero deviation is inserted on the deviation plot providing scope in the temperature and pressure scale. This provides interpretation of the temperature and pressure ranges. Data point deviations are then plotted on the graph, with deviation on the z-axis. Each point is connected by dotted drop-down line to a corresponding position on the temperature-pressure plane. These drop-down lines help the user quickly identify the corresponding projection of the deviation plot onto the temperature-pressure plane. Now, the figure has each point represented twice, once in a two-dimensional temperature-pressure plot, then again with a corresponding point showing the enthalpy departure deviation. The length of the drop line represents the amount of deviation.
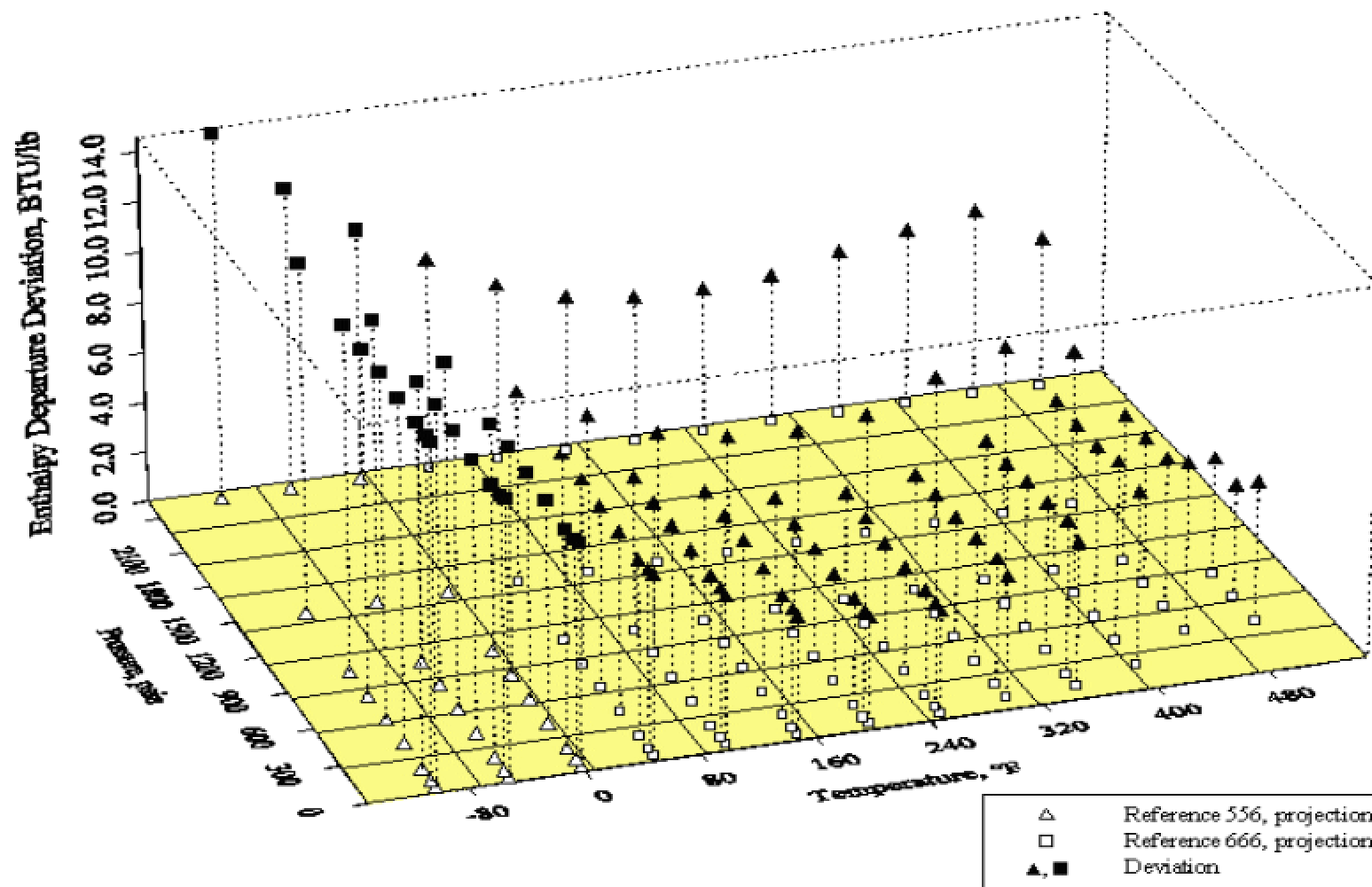
Figure 36. 3-D Enthalpy Departure Deviation for Heptane (L)

The three-dimensional data point plot in Figure 36 for the liquid heptane system overcomes the problems described by Figure 31. In Figure 36, unlike the original representation, the isobars are differentiated, the two sources of the experimental data are obvious, and trends in both temperature and pressure are discernable.

Color facilitates quick evaluation of the figure. Black represents deviations considered typical, or normal, for the system. Additional colors represent points of interest that fall under one of the four criteria. In a final modification, vapor-liquid equilibrium information either from an experimental source or from EOS-based calculations are incorporated into the plot.

Figure 37 represents the final version of the new method of plotting applied to the liquid cyclohexane system. For the cyclohexane data, the data point showing an abrupt change in deviation shows clearly. One point in the high temperature, moderate pressure range shows significant deviation from any of the surrounding points, and is outside twice the RMSE. This point is identified as an outlier. The cluster of data points in the high temperature and low-pressure range also show deviations over twice the RMSE, but these data are following a trend. The temperature is increasing along a narrow band of pressure, and the deviations are steadily increasing, unlike the data point around the same temperature and at a higher pressure. On the two-dimensional plots, the point at 400 psia was called an outlier; it is now seen to be part of a trend.
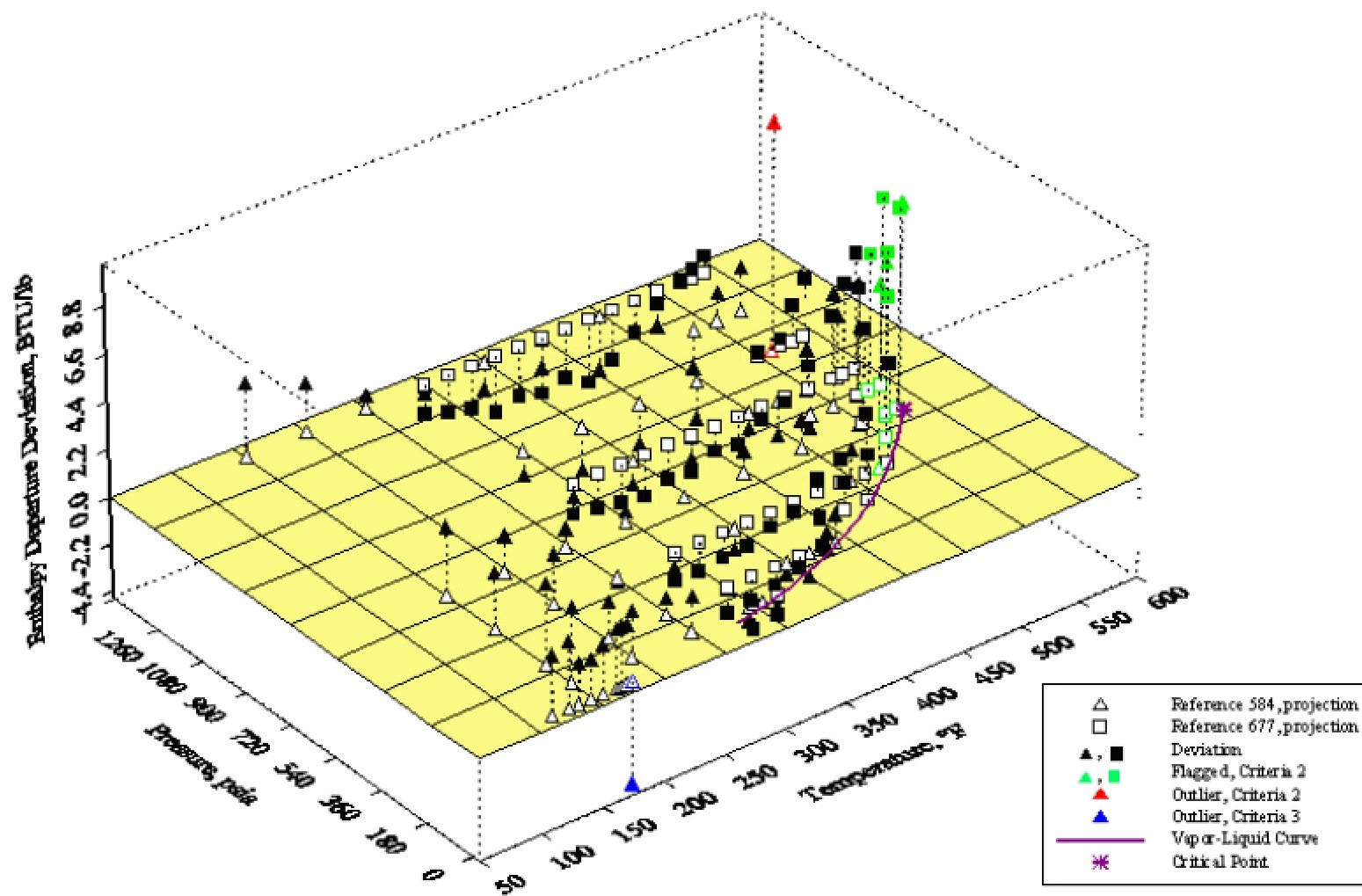
Figure 37. 3-D Enthalpy Departure Deviation for Cyclohexane (L)

Other useful information emerges from this graph. In the mid-range temperatures covering the entire pressure range, the Peng-Robinson equation of state agrees with the experimental data. Several isobars are seen that correspond with Figure 33. The data concentrates in the higher temperature region but covers a wider pressure range at lower temperatures. The change from positive to negative and back to positive deviations is seen on this figure, which are consistent with Figure 33.

Figure 37 has the advantages of Figure 32 and Figure 33, while incorporating the benefits of the temperature-pressure plot. It also has the advantage of a surface plot where trends are easily identified, and outliers stand out. At the same time, the three-dimensional representation remains easy to understand using colors and drop lines. The ability to incorporate vapor-liquid equilibrium also provides an additional benefit to immediate evaluation. This type of plot proved to be crucial throughout the data evaluation.

SUMMARY

When used in conjunction with direct comparisons and equations of state, three-dimensional plotting of enthalpy data proves to be useful in obtaining an accurate evaluation. Major shortcomings of the equations of state plainly show up on the graphs. Trends in excessive deviation commonly appear near the phase envelope, around the critical region, and as the system exceeded the critical point into non-ideal regions of high temperature and pressure. The two-dimensional temperature-pressure plot contained on the deviation plots give a quick reference tool to determine whether any system contains sufficient data in the region of the users' interest. The deviation plots also prove useful when comparing two models against each other. The plots quickly reveal the temperature trend mentioned above.

SECTION TWO

WEAK ELECTROLYTE VAPOR-LIQUID EQUILIBRIUM

CHAPTER I

INTRODUCTION

Electrolyte systems, particularly aqueous electrolyte mixtures, are an important component of both natural and industrial processes. A fundamental understanding of electrolyte mixtures is crucial for interpreting natural phenomenon and vital for effective design and operation of chemical process separations. More accurate thermodynamic models and better comprehension of the underlying chemistry and physics are needed to improve the design of separation equipment. There is a growing interest in the correlation and prediction of thermodynamic properties of aqueous electrolyte systems, since the applications are useful to both natural and industrial processes.

In contrast to the abundant research on aqueous strong electrolytes, significantly less material is available regarding weak electrolyte solutions. Whereas strong electrolytes undergo complete dissociation, a weak electrolyte forms ionic species by partial dissociation. While dissociation is often assumed to be a minor consequence, this distinction significantly increases the complexity of thermodynamic equilibrium modeling [1].

This work describes an extension and improvement of a vapor-liquid equilibrium solution method for weak electrolyte solutions. Although numerous weak electrolytes exist, this

96

study focuses on carbon dioxide (CO_2), hydrogen sulfide (H_2S), sulfur dioxide (SO_2) and ammonia (NH_3), all of which occur in both industrial processing and natural systems. Additional considerations include the ability to model systems with strong electrolytes (salts), as well as solutions of mixed weak and strong electrolytes.

VAPOR-LIQUID EQUILIBRIUM IN ELECTROLYTE SYSTEMS

Thermodynamically, at any given temperature and pressure, the criteria for equilibrium require equality of the chemical potential of each component present to be equal in all phases. There is extensive research regarding the development of models to represent chemical potentials of components in vapor and liquid phases across broad ranges of temperature and pressure. Abundant work also exists that discusses the mathematical solution methods necessary for finding unique answers to phase equilibrium problems.

Strong electrolytes, such as sodium chloride (NaCl), are present predominantly as either a solid or liquid at temperatures and pressures of interest. When combined with water these strong electrolytes dissociate completely, or as completely as possible, based on solid solubility equilibrium constraints. Other common strong electrolytes are strong acids or bases, which are also predominantly either solids or liquids.

Two common assumptions for systems of strong electrolytes are: (1) ionic species cannot distribute into a vapor or non-aqueous liquid phase, and (2) all interactions of ions are strictly limited to the aqueous phase. For strong electrolytes that completely dissociate, explicit chemical equilibria can be removed from the vapor-liquid equilibrium problem when applying these assumptions.

Unlike strong electrolytes, many weak electrolytes are often vapor phase components. These components, normally of low solubility in an aqueous medium, partially dissociate into ionic species. Hence, from an overall view, components will have an 'apparent' solubility, that assumes no reactions occur. This 'apparent' solubility is the sum of soluble molecular species and the chemically related ionic species concentrations.

A complete thermodynamic description of weak electrolyte systems must explicitly consider chemical equilibria, mass balances, and electroneutrality.

THE WEAK ELECTROLYTE SYSTEM

Many molecular species are reactive in an aqueous phase. These species, when in vapor states, are soluble in an aqueous phase and subsequently react with liquid water, hydrogen ions, or hydroxide ions to form ionic species. Figure 38 describes the generic reactive gas - water problem.
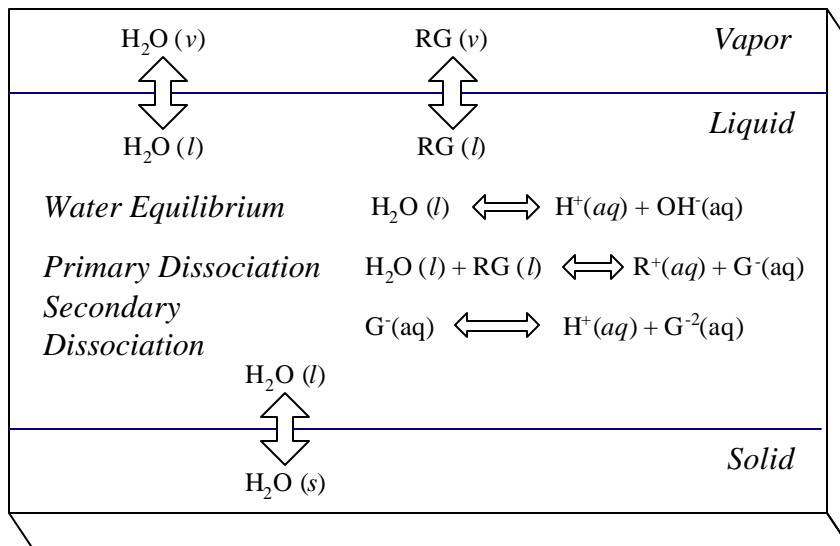
Figure 38 - Generic Reactive Gas (RG) - Water Equilibrium

The initial solubility of the specie of interest may range from almost complete miscibility (NH_3) to nearly immiscible behavior (CO_2). In the aqueous phase, reactions include primary and secondary dissociations, but other reactions are possible.

The modeling of electrolyte mixtures requires awareness and quantification of possible reactions, a description of the thermodynamics of all species, and mass balances that appropriately account for vapor species, soluble molecular species, and derived ionic species.

VAPOR-LIQUID EQUILIBRIUM FRAMEWORK

An outline introduced by Edwards et al. [2] provides a basic thermodynamic framework for dilute aqueous electrolyte systems. The equilibrium between the vapor and liquid phase is described by application of Henry's constants for the solubility of molecular solute(s).

$$y_i \boldsymbol{j}_i P = H_i m_i \boldsymbol{g}_i \qquad (2.1\text{-}1)$$

Where y_i, P, H_i, and m_i are, for a component i, the mole fraction in the vapor phase, total pressure, Henry's constant for the gas in pure water, and the molality in the liquid phase.

Edwards, et al. [2] use an equation of state to describe vapor phase non-idealities. Henry's constants and chemical equilibrium "dissociation" constants provide ideal-liquid mixture properties.

The present work employs a model outlined by Friedman [3] and extended by Lin [4] and has similar requirements. An equation of state describes vapor and liquid phase

equilibrium of molecular components, chemical equilibrium constants describe dissociation of reactive species, and an activity coefficient model accounts for liquid phase ionic species.

THERMODYNAMIC BASIS AND CONVENTIONS

Electrolyte solutions with both molecular and ionic species include three types of interactions: ion-ion, molecule-molecule, and ion-molecule. Thermodynamic properties are strongly dependent not only on long-range electrostatic forces between the ions, but also on short-range forces between the ions, solvent molecules, and undissociated electrolytes [1].

The activity of a species is a thermodynamic property, which relates directly to the excess Gibbs free energy. Specifically,

$$\bar{G}_i^E = RT \ln(a_i) \tag{2.1-2}$$

where R is the gas law constant, and T is absolute temperature. Activities, a, describe the non-ideal behavior of the mixture. In non-electrolyte systems, the common definition of activities is a function of an activity coefficient, $\boldsymbol{g}_i$ and mole fraction of the component present in the system.

$$a_i = \boldsymbol{g}_i x_i \tag{2.1-3}$$

In contrast, for dissolved species the activity coefficient is defined as

$$a_i = \boldsymbol{g}_i m_i \tag{2.1-4}$$

where m_i is the concentration of the dissolved specie in moles per kilogram of solvent, or molality. The final form of the Gibbs free energy of an electrolyte, or dissolved species is given as

$$\overline{G}_i = \overline{G}_i^\circ + RT \ln\left(g_i m_i\right) \tag{2.1-5}$$

The differences in the electrolyte and non-electrolyte definitions are both necessary and important to note. In the non-electrolyte definition, the activity coefficient conforms to a symmetric convention where the activity of any species approaches unity as the mole fraction of the component approaches one. In an electrolyte solution, such a convention would have little meaning, as the existence of the solvent phase (usually an aqueous phase) is a necessary requirement for the existence of the ionic species. As the molality of the ionic component increases, the solute phase is continuously present. Thus, in the electrolyte convention the activity of a dissolved component approaches unity as the concentration of the specie approaches zero, or the infinite dilution condition. As the concentration of the electrolyte specie increases, an upper limit based on solubility of the component occurs (long before the corresponding mole fraction of the specie would approach unity). Hence, the activity coefficient defined by Equation (2.1-4) conforms to an asymmetric convention. An important consequence of this convention is that the activity of a solvent medium, ordinarily water, is defined differently than ionic or dissolved species, and calculated by equation(s) that specifically describe the solvent.

In addition to the need for caution when working simultaneously with both mole fraction and molality scales, other features such as standard state definitions based on a molality scale are important to note in any application of these activity definitions [5].

CHEMICAL EQUILIBRIUM

Consider a general, stoichiometrically balanced, aqueous-phase reaction involving R molecular reactants and P aqueous ionic products. A generic reaction expression is

$$r_1 R_1 + r_2 R_2 + r_3 R_3 + \ldots + r_n R_n \Leftrightarrow p_1 P_1 + p_2 P_2 + p_3 P_3 + \ldots + p_n P_n \qquad (2.1\text{-}6)$$
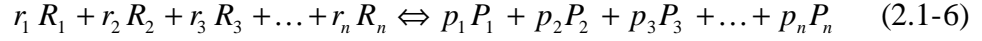
The chemical potential is the partial molar Gibbs free energy, or

$$m_i \equiv \left(\frac{\partial G}{\partial n_i} \right)_{T,p,n_j} \qquad (2.1\text{-}7)$$

with the chemical potential of any species is given by

$$m_i = m_i^\circ + RT \ln a_i \qquad (2.1\text{-}8)$$

where m_i° is the chemical potential at standard state conditions, R is the gas constant, T is the absolute temperature, and a_i is the activity of the species of interest.

For equilibrium, the chemical potential or Gibbs free energy of the reactants must be equal to the chemical potential or Gibbs free energy of the products of the reaction, or

$$\sum_{i=1}^{r} r_i \, \overline{G}_i = \sum_{i=1}^{p} p_i \, \overline{G}_i \qquad (2.1\text{-}9)$$

Combining equations (2.1-5) and (2.1-9) and rearranging as a ratio of products to reactants gives a definition of the chemical equilibrium constant:

$$K = \frac{\left(g_{P_1} m_{P_1} \right)^{p_1} \left(g_{P_2} m_{P_2} \right)^{p_2} \left(g_{P_3} m_{P_3} \right)^{p_3} \cdots \left(g_{P_P} m_{P_P} \right)^{p_P}}{\left(g_{R_1} m_{R_1} \right)^{r_1} \left(g_{R_2} m_{R_2} \right)^{r_2} \left(g_{R_3} m_{R_3} \right)^{r_3} \cdots \left(g_{R_R} m_{R_R} \right)^{r_R}} \qquad (2.1\text{-}10)$$

Equilibrium constants are functions of temperature and pressure, but they are not a function of composition [5]. The equilibrium constants, when combined with activity coefficients, determine unique equilibrium concentrations of each reactant and product.

The addition of chemical reactions to the vapor-liquid equilibrium problem complicates the mass balance constraint. The nature of the reactive species (charged ions) also adds a new constraint to the problem, a charge balance.

MASS AND CHARGE BALANCES

In electrolyte mixtures, the mass balance constraint is extended to include the additional species contributed by reactions. Thus, the total mass of a molecular compound is the sum of the amount present in the vapor, in the liquid phase as dissolved specie, and in the liquid phase as derived ionic species. On a molal concentration basis, the mass constraint is given as

$$M_i = m_{vi} + m_{Li} + \sum_{j=1}^{N_S} \lambda_{ij} m_j \qquad (2.1\text{-}11)$$

Where, M_i is total molal concentration of a molecular species i, and m_{vi} and m_{Li} are molal concentrations of the molecular species in the vapor and liquid phases, respectively. The summation is over all ionic species, where λ_j is a stoichiometric coefficient relating the molecular species to each chemically derived product species (ionic species), and m_j is the molal concentration of ionic species. In practice, correctly applying a molecular balance is complicated by accurate qualification of stoichiometric coefficients.

Alternatively, an atomic basis of the following form may be applied, mathematically

$$m_e = \sum_{i=1}^{N} \boldsymbol{n}_{ei} m_i \qquad (2.1\text{-}12)$$

In this equation, m_e is the total molality of an element e, and m_i is the molality of each chemical species present in the system. The parameter $\boldsymbol{n}_{ei}$ refers to the number of atoms of each element present in the molecular formula for each species. For example, the species NH_4Cl would have parameter $\nu_N=1$, $\nu_H=4$, and $\nu_{Cl}=1$ for elemental balances on nitrogen, hydrogen, and chlorine. The ionic species from this molecular specie are NH_4^+ with $\nu_N=1$, $\nu_H=4$, and Cl^- with $\nu_{Cl}=1$. These stoichiometric coefficients provide a mass balance that correctly accounts for all species present in an electrolyte mixture.

Due to the presence of charged species, an additional constraint to ensure electroneutrality of the mixture is necessary. The charge balance is given by

$$\sum_{ions} z_i m_i = 0 \qquad (2.1\text{-}13)$$

where z_i is the ionic charge and m_i the molality of ion i.

SUMMARY

Any multiphase equilibrium modeling effort requires attention to satisfying thermodynamic equilibrium, i.e. chemical potential equality of all species in all phases, a minimum Gibbs free energy of the system, and appropriate focus on the mass balance constraint. In weak electrolyte systems, several additional features are introduced into the problem. While the complication to the mass balance and the new charge balance constraint affect the methodology of obtaining solutions, the basis of the equilibrium

model rests on accurate and reasonable methods for determining chemical dissociation

constants and activity coefficients.

REFERENCES

1.   Prausnitz, J.M., R.N. Lichtenthaler, and E.G. de Azevedo, *Molecular Thermodynamics of Fluid-Phase Equilibria*. 3rd ed. 1999, Upper Saddle River, New Jersey: Prentice Hall. 860 pgs.

2.   Edwards, T.J., et al., *Thermodynamics of Aqueous Solutions Containing Volatile Weak Electrolytes.* AIChE Journal, 1975. **21**: p. 248-259.

3.   Friedemann, J.D., Ph.D. Dissertation, *The Simulation of Vapor-Liquid Equilibria in Ionic Systems*, School of Chemical Engineering, Oklahoma State University, Stillwater, Oklahoma, 1987.

4.   Lin, F., M.S., *Vapor-Liquid Equilibrium in Aqueous Solutions Containing Weak and Strong Electrolytes*, School of Chemical Engineering, Oklahoma State University, Stillwater, Oklahoma, 1994.

5.   Anderson, G.M. and D.A. Crerar, *Thermodynamics in Geochemistry The Equilibrium Model*. 1993, New York: Oxford University Press. 588 pgs.

CHAPTER II

LITERATURE REVIEW

ACTIVITY MODELS

Activity models suitable for non-electrolyte systems are numerous, and many of these efforts find broad acceptance in process modeling. In contrast, no comprehensive model has been formalized or accepted by industry for electrolyte systems. Standard means for modeling electrolyte systems are inadequate for wide ranges of temperature, pressure, and concentration [1, 2].

The solubility of a gas in an aqueous salt solution can be less or greater than that in pure water. This solubility decrease or increase is referred to as "salting out" or "salting in" phenomena. This behavior, attributed to the interactions between ions and water molecules, has a direct impact on the solubility of non-polar and polar gases in water. Activity models attempt to predict this non-ideal behavior.

Two research goals run concurrently throughout the literature regarding modeling ionic systems. One goal focuses on models specifically for more accurate descriptions of ionic solutions. Among this group are empirical extensions of the Debye-Hückel model, virial activity models of which the most broadly used is Pitzer's ion interaction model, and hydration models. The second goal concentrates on improvements in predictions of

phase equilibrium. Among this group are empirical models, and the incorporation of electrolytes in local composition models and equations of state.

A review of the principle contributions from research in these areas, and a summary review of current progress in statistical thermodynamic fluid theories and simulation work is given in the following sections.

The beginnings of modern electrolyte theory are best defined by the work of Debye and Hückel in 1923 [3]. The Debye-Hückel theory represents a limiting law behavior in electrolyte models. Due to the overwhelming importance of this theory to all subsequent research, a review of the Debye-Hückel model begins this discussion.

Debye-Hückel Theory

The Debye-Hückel theory is based on the assumption that charged species, having fixed diameters (initial theory assumed point charges with negligible diameter) interact with each other in a continuous dielectric medium (background potential field). With this basis, interionic potentials are formed, and a concise equation for the activity coefficient of an ionic species is derived using the principles of statistical mechanics.

The final, simple expression for mean ionic activity coefficient, the Debye-Hückel limiting law, is

$$\ln g_{\pm} = -A \left| z_{+} z_{-} \right| \sqrt{I} \tag{2.2-1}$$

The coefficient A is temperature dependent, and I is the ionic strength of the solution. The ionic strength is defined as

$$I = \frac{1}{2} \sum m_i z_i^2 \tag{2.2-2}$$

108

where m_i is the molality of component i, and z_i is the charge of the ionic specie. This equation is valid only in dilute mixtures, up to approximately 0.001 molal concentrations [4, 5].

Better agreement with experimental results for concentrations to 0.1 molality are achieved by the introduction of finite ion sizes into the Debye-Hückel equation [6]:

$$\ln g_\pm = -\frac{A\left|z_+z_-\right|\sqrt{I}}{1+Bd\sqrt{I}}$$

(2.2-3)

In this equation, d is the hard sphere diameter of the ions and B a solvent constant related to the dielectric constant of the medium of interest. In practice the Debye-Hückel, and extended Debye-Hückel equations exhibit the characteristic behavior that

as I → 0, activities approach 1.0; and

as I → ∞, calculated activities decrease monotonically.

The theory is based explicitly on bng-range electrostatic effects and is often called the "Debye-Hückel limiting law." Other interactions that were ignored, such as short-range forces and hydration effects, provide one impetus for improvements to models based on Debye-Hückel behavior. The Debye-Hückel equation, Equation (2.2-3), successfully predicts activity coefficients in mixtures up to ionic strengths of approximately 0.1 molal. The complexities, basis, and drawbacks of the assumptions of the derivation have been well documented [7].

Empirical Extensions to Debye-Hückel Theory

In the traditional engineering approach, improvements on the Debye-Hückel equation have been attempted by adding semi-empirical corrections. One successful variant of the Debye-Hückel equation is by Davies [5],

$$\log \boldsymbol{g}_i = -Az_i^2 \left[\frac{\sqrt{I}}{1+\sqrt{I}} - 0.3I \right]$$ (2.2-4)

The Davies equation, with the additional empirical term of 0.3 I, no longer decreases monotonically, but retains accurate behavior as $I \rightarrow 0$. The equation performs moderately well for solutions of up to 0.3 to 0.5 molal ionic strengths [4, 5].

Another common variant of Debye-Hückel is the B-Dot model [8, 9].

$$\log \boldsymbol{g}_i = -\frac{Az_i^2\sqrt{I}}{1+\overset{\circ}{a}B\sqrt{I}} + \dot{B}I$$ (2.2-5)

The ion size parameter, $\overset{\circ}{a}$, remains fixed while the coefficients A, B, and $\dot{B}$ vary with temperature, and are fit to experimental data by regression. The B-dot model has been widely applied in geochemical speciation programs [10-13]. The original equation accurately models solutions with ionic strengths of 0.3 to 1 .0 molal.

In a similar fashion, Bromley [14, 15] developed a model combining a Debye-Hückel term with an single empirical term. Bromley found that suitable values for this empirical parameter could be estimated by assuming additivity of the individual cations and anions. The procedure successfully correlated experimental results for strong electrolytes up to about 6 molality with one parameter for each salt. The immediate benefit is a model

capable of providing estimates of activity coefficients, when no experimental data is available.

Edwards et al. [16] established the basic thermodynamic framework to correlate vapor-liquid equilibrium for dilute aqueous electrolyte solutions. In their work, liquid phase activity coefficients, g_i, were obtained from a modification similar to Bromley's method,

$$\ln g_i = -\frac{a\, z_i^2 \sqrt{I}}{1+\sqrt{I}} + 2 \sum_{k \neq water} b_{ik} m_k$$

(2.2-6)

where a is the Debye-Hückel factor and b_{ik} is the interaction parameter between species i and k. The original model is able to predict multi-solute systems without ternary parameters, but it remains limited to low ionic strength solutions.

In an engineering approach to the problem, Meissner and Tester [17] found that plotting the reduced mean activity coefficient ($g_\pm^{1/z^+z^-}$) as a function of total ionic strength of the solution at 25°C forms a family curves for single strong electrolyte solutions. This graphical method allows estimation of mean activity coefficients when given one experimental value at a known ionic strength for a single electrolyte. Meissner and Kusik [18] were able to extend their graphical approach to correlate multi-salt solutions at high temperatures with algebraic equations describing the family of curves and using one parameter for each strong electrolyte. Predictions of the mean activity coefficients with the correlation for solutions ranging from 3 to 15 molality agree within 20% error with experimental data.

Patawardhan and Kumar [19, 20] successfully correlated mixed electrolyte solution properties, including vapor pressure and heats of vaporization, by correlation of an

111

overall reduced ionic coefficient, Γ, developed by relating ionic strength to the vapor pressure of an electrolyte mixture.

The empirical relationships developed by Meissner, et al. [17, 18, 21, 22] and those of Patwardhan and Kumar [19, 20] remain quite useful for approximating the properties of electrolyte solutions in the absence of appropriate experimental data. The variants on the Debye-Hückel model, although adequate for many applications, are limited to lower ionic strength solutions, and further improvements have not been forthcoming. The development of a virial-based model by Pitzer supplanted these empirical approaches.

Virial Activity Models

Virial equations, sometimes called specific interaction or phenomenological equations, offer a very different approach than the original Debye-Hückel theory. The basis of the model rests on the conceptual similarity of an electrolyte mixture to that of an imperfect gas, the original source of application of the virial equation model.

The method requires little or no information regarding any explicit distribution of species, and in the simplest form, recognizes only the existence of free ions. The virial method does not account implicitly for the reduction of free ion activity by the formation of ion pairs and complexes. Rather, it describes electrostatic interactions, ion hydration, and species distribution.

Although several virial based models have been formulated, one specific form commonly called Pitzer's equations has been widely applied to both industrial processes and natural systems.

Pitzer Activity Model

Pitzer [23-27] proposed a system of virial equations expanding the Debye-Hückel approach to represent the thermodynamic properties of electrolyte solutions. The most important contribution of his work was to include the effect of short-range forces. Pitzer proposed the following expression for the excess Gibbs free energy:

$$\frac{G^E}{RTn_w M_w} = f(I) + \sum_i \sum_j m_i m_j \boldsymbol{l}_{i,j}(I) + \sum_i \sum_j \sum_k m_i m_j m_k \boldsymbol{t}_{i,j,k} \qquad (2.2\text{-}7)$$

The first term is a modified Debye-Hückel equation expressing the effect of the long-range electrostatic forces. The correction for short-range binary interactions between ions is taken into account by the parameter $\boldsymbol{l}_{i,j}(I)$, which is the ionic strength dependent second virial coefficient. A ternary parameter $\boldsymbol{t}_{i,j,k}$ is the correction term for triple ion interactions and is assumed independent of ionic strength. The activity coefficient expression follows from differentiation of (2.2-7), resulting in

$$\ln \boldsymbol{g}_i = \ln \boldsymbol{g}_i^{DH} + \sum_j D_{ij}(I) m_j + \sum_j \sum_k E_{ijk} m_j m_k \qquad (2.2\text{-}8)$$

In this equation, $\boldsymbol{g}_i^{DH}$ is a Debye-Hückel term, D_{ij} is the second virial coefficient, which is considered a function of ionic strength, and E_{ijk} is the third virial coefficient.

Unlike a vapor virial equation of state, in which second and/or third virial constants may be experimentally confirmed, the electrolyte-based formalism cannot be compared directly to experimental data. Thus, application of the model requires fitting the constants to experimental data, and the derived parameters are neither unique, nor universal. Pitzer's equations are semi-empirical.

Pitzer's final equations have the same limitations as any virial method [2] in addition to their semi-empirical nature. There are two advantages of the model: (1) the equations are easily extended to mixtures, and (2) the equations accurately model activity coefficients in high ionic strength solutions. By their nature, virial equations have well defined mixing rules, and a similar approach remains valid for Pitzer's equations. In the original model evaluations of systems up to 6 molal ionic strength, calculations are within experimental uncertainty [24]. One of the first applications to vapor-liquid equilibria is that of Edwards et al. [28] for systems up to 170 °C and ionic strengths to 6 molality. This effort employed an extended Pitzer activity model but neglected ternary interactions. Numerous works employing Pitzer's model have successfully applied the equations to systems ranging from 0.1 to over 20 molal ionic strength, with application to both activity modeling and vapor-liquid equilibrium [29-37].

In application of Pitzer's equations, a large number of binary ion-ion and molecule-ion parameters are presumably required in multi-solute systems, as the model takes into account the contributions of ion-molecule interactions, and ion-ion interactions. In practice, many of the parameters are unnecessary. For most single salts, only two parameters for 'pure' solutions, and one additional parameter for each additional electrolyte in a mixed system are necessary.

Another concern when applying the Pitzer equations is the availability of a consistent set of model parameters [38]. Fortunately, in addition to the compiled parameters from Pitzer, et al. [39], extensive efforts by Harvie, et al. [29, 40-54], and Kuhn, et al. [38, 55] are also available.

The ability of Pitzer's equations to model electrolyte mixtures across a broad range of ionic strength, its simplicity of use, and established mixing rules appear to outweigh the complications of unique parameterization and the semi-empirical formulation. Pitzer's equations find broad application in problems for natural systems and industrial processes [29-37]. Continued efforts to modify the model to alternate concentration bases [56] and to improve upon the original virial basis have also been recently attempted [57].

Hydration Theory

Based on the work of Stokes and Robinson [6], another group of models were developed by combining ion-ion interactions and ionic solvation in a chemical speciation approach.

Hydration models explain the deviation from the ideal mixtures as the result of ion-solvent hydration or solvation. Chemical hydration is pictured by the following reactions:

$$
\begin{aligned}
& MX \overset{H_2O}{\longleftrightarrow} M^+ + X^- \\
& M^+ + mH_2O \longleftrightarrow M^+ \cdot nH_2O \qquad\qquad (2.2\text{-}9) \\
& X^- + yH_2O \longleftrightarrow X^- \cdot yH_2O
\end{aligned}
$$

In these reactions, the undissociated electrolyte, MX, dissociates into, cations M^+ and anions X. The ions then 'react' forming hydrated compounds with a 'shell' of water molecules surrounding the charged specie. Hydration models are often described as a "chemical" theory of solutions.

The original solvation model, established by Stokes and Robinson [6, 58], was developed by combining a Debye-Hückel expression for long-range interionic forces with the ionic hydration concept. The correction to the Debye-Hückel model led to a simple hydration

model with two adjustable parameters: the hydration number in the solvent shell and the effective size of the solutes. The activity coefficients of the electrolytes can be represented accurately for strong electrolytes in dilute and moderately concentrated solutions up to 4 molality. However, the initial formulation by Stokes and Robinson included the assumption that the hydration number of an electrolyte is independent of concentration, limiting the model to dilute mixtures.

Extensions of the Stokes and Robinson model [6, 58], with modifications to correct the thermodynamic inconsistency arising from the assumption of fixed hydration spheres in the original model formulation [59-62], provide a framework for much research.

Experimental methods for estimating hydration numbers of ions have been pursued, including spectroscopic, transport, and thermo-chemical based methods [63]. However, these methods have produced widely different results. To define the contribution from any single ion, experimental data must also be 'split' into constituent ions by methods which are empirical at best.

Rapid development of modern computer technology has allowed computer simulation to play an increasingly important role in predicting properties that are hard to measure. Molecular simulations, primarily using Monte Carlo techniques, allow direct calculation of the contribution of each ion to hydration. In addition, simulations easily quantify forms of information, such as orientation behavior, which are difficult to obtain from experiments. Heinzinger [64] and Bopp [65] give a review of early molecular simulation efforts, while Ohtaki and Radnai [66] provide comprehensive review of the structure and dynamics of hydrated ions.

In the application of hydration models, Nesbitt [62] found that the hydration number parameter could be related to the ionic radius and standard entropy and are affected by the ion–dipole interaction. Lu and Maurer[67] proposed a hydration model based on the hydration number and calculated the properties for electrolyte mixtures. Researchers have found that the ionic hydration is one of the basic characteristics of electrolyte solutions.

Kawaguchi et al. [59, 60] described an extension of the Stokes and Robinson hydration equation by applying the Analytical Solutions of Groups (ASOG) model of Wilson and Deal [68] to account for the non-electrostatic contributions by assuming total hydration of ions. Nesbitt [62] proposed a correction for the the Stokes and Robinson hydration model based on the assumption that water molecules reside in two separate environments: the hydration shell and bulk solvent environment. This assumption allows the hydration number to decrease gradually in concentrated solution. The model can be extended to concentrations up to 5 molality using two parameters.

A similar hydration model developed by Ghosh and Patwardhan [61] shows accuracy in concentrations up to 20 molality for 150 electrolytes. The excess Gibbs free energy is expressed as the sum of ion-ion electrostatic contributions and ion-water contributions. Although there are no terms accounting for short-range ionic interactions, Ghosh and Patwardhan [61] suggested the hydration model as an alternative to the virial approach proposed by Pitzer. The model, based on a reference mixture (LiBr), involves only two empirical parameters related to the hydration number and the energy of hydration for each strong electrolyte. Unfortunately, the model has not been extended to multi-electrolyte solutions.

Although valid results are possible within this modeling framework, the principle shortcomings include a theoretically inconsistent description of the ion-ion interactions (long-range effects) in combination with the short-range interaction basis of the Debye-Hückel theory. The most practical drawback, however, is the difficulty in application of these models to multi-electrolyte systems in a self-consistent manner.

Models Based on Local Composition

The concept of relating the local composition of fluids to molecular characteristics and macroscopic thermodynamic properties was introduced for non-electrolyte mixtures by Wilson [69]. Local composition theory is the basis of the well-known Non-Random Two-Liquid (NRTL) [70] and Universal Quasi-Chemical (UNIQUAC) [71] equations. As local composition models derive from lattice theories of fluids and additional empirical interpretation, the approach is referred to as "physical" solution theory. Investigations using the concept of local composition and its relationship to molecular characteristics and macroscopic thermodynamic properties of mixtures have been made [69, 70, 72-80]. Although the original expressions of local composition theories are not directly suitable, they may be extended to electrolyte systems by application of a suitable solvation model [81].

Some authors have extended both the NRTL and UNIQUAC models to electrolytes. Cruz and Renon [82] have incorporated electrolytes into an NRTL model, and Ball, et al. [83] into a UNIQUAC model by developing extensions of the Debye-Hückel equation.

Cruz and Renon [82] expressed the excess Gibbs free energy as the sum of the contributions of long-range interionic forces and corrections for the short-range forces.

One of the deficiencies in the Debye-Hückel law is that the effect caused by the decrease of dielectric constant, *D*, with the increase of ionic concentration is neglected. Cruz and Renon expressed the long-range interaction as a Debye-Hückel term plus a Debye-McAulay term, as reported by Harned and Owen [84], taking into account the "salt effect" caused by a change in the dielectric constant with ionic concentration. The NRTL local composition model of Renon and Prausnitz [70] is introduced to account for the short-range forces. The NRTL model can represent the non-ideality of equilibrium properties in nonelectrolyte solutions and requires only binary adjustable parameters for extension to multicomponent systems. The model requires six adjustable parameters to represent single electrolytes, if partial dissociation is assumed. It also involves one additional adjustable parameter for each new ionic species.

The modified version by Ball et al. [83] used only two adjustable NRTL parameters to represent strong single electrolyte properties up to 6 molality, while no new adjustable parameters are needed for mixtures. This was achieved by introducing a new expression for the Debye-McAulay term to estimate the dielectric constant.

Using an approach similar to the Cruz and Renon [82] model, Chen et al. [85, 86] proposed the excess Gibbs free energy is the sum of two contributions: long-range interionic contributions and short-range contributions. In contrast to the Cruz and Renon method, Chen et al. made two basic assumptions: (l) the local composition of cations around a central cation is zero, and (2) the distribution of cations and anions around a central molecule leaves the net local ionic charges equal to zero. These assumptions enabled construction of a model with two binary energy parameters for each of the interactions associated with solvent-solvent pairs, solvent-salt pairs, and salt-salt pairs. In

mixed-solvent electrolyte systems, the long-range contribution due to the Pitzer-Debye-Hückel term was neglected, leaving only the local interaction term. The results obtained for isopropanol-water-LiCl and methanol-water-CaCl$_2$ systems are consistent with experimental data. However, this model required additional ternary mixture data to obtain the salt-salt energy parameters.

Chen et al. [86] modeled weak electrolyte systems by introducing the NRTL local composition concept. The highly concentrated NH$_3$-H$_2$S-H$_2$O system was examined at temperatures of 80 and 120°C. With more than 7 binary, temperature-dependent parameters, the fitting results had 9 percent average relative deviation in the partial pressure of ammonia. The reported results were less extensive than those of other authors and include no calculations for systems containing SO$_2$ or CO$_2$ [28, 87].

A more recent model by Lu and Maurer [67] combines solvation equilibrium between solvated and unsolvated ions with a Debye-Hückel expression and the UNIQUAC [71] model. The model requires five parameters: two binary interaction parameters between each cation and anion, and three solvation parameters per ion. The model correlates well for concentrated electrolytes from 3 to 29 molality. The model shows comparable results with other activity models suitable for extremely concentrated electrolyte solutions. The extension to mixed electrolytes requires no high-order parameters.

More recently, attempts to apply the concept of local composition have focused on extensions to the original lattice theory approach. Notable is the work of Lee et al. [79] which relates distribution functions from statistical thermodynamics and related potentials of mean force to the local composition model of Wilson [69]. Other work using computer simulation studies by Hoheisel and Kohler [80] and Nakanishi, et al. [88-

90] dispense with any reference to a particular theoretical model and provide data for molecules interacting under a Lennard-Jones potential, which then are used to test and improve LC models.

Models from Statistical Thermodynamics

All electrolyte solution models may be broadly classified into two methodologies, (1) those assuming discrete solute ions in the presence of a continuum solvent medium, and (2) those considering systems as mixtures of discrete solute and solvent molecules.

The continuum approach, also called the primitive model (PM), significantly simplifies the problem, and most theories, including those previously discussed, are based in this formalism. Considering both solute and solvent as discrete molecules is primarily limited to the domain of statistical thermodynamic theory and simulation methods. Here attention focuses on the resultant semi-empirical methods.

Planche and Renon [91] and Ball, et al. [92] began with a statistical thermodynamic expression for the interparticle potentials by introducing both long-range coulombic forces and short-range forces between all species. Employing Fourier transformations, analytical solutions of the radial distribution function based on the mean spherical approximation were performed. Subsequently, expressions for thermodynamic properties, such as Helmholtz energy and chemical potential, are derived, and an electrolyte equation of state is obtained by differentiation of the Helmholtz free energy based on fundamental thermodynamic relationships.

The model successfully correlated the osmotic coefficients of strong electrolytes up to 6 molality, with one adjustable parameter for each salt. The prediction of mixture

electrolytes requires no additional parameters. However, the only calculations reported were for osmotic coefficients of salts in water at 25 °C.

Similar work done by Copeman and Stein [93, 94] presented the contributions to Helmholtz free energy as an electrostatic term, a repulsive term, and an attractive term. The model was tested on 18 strong electrolytes at 25°C near atmosphere pressure. For highly concentrated systems, two binary parameters are needed.

Raatschen, et al. [95] expressed the Helmholtz free energy in terms of six contributions with three terms related to the presence of ions. Their work focused mainly on mixed solvent solutions such as the LiBr-methanol-water ternary system. The model requires three cation-anion binary parameters per electrolyte. However, Harvey and Prausnitz [96] point out that some of the expressions for ion contributions are not suitable for extension to supercritical components at high pressure, for example molecule-ion interaction terms.

Furst and Renon [97] developed a successful one-parameter Redlich-Kwong-Soave type equation of state from the Helmholtz free energy derived from mean spherical approximation. While the model agreed well with halide systems up to 6 molality, the extension to other nonhalide systems by assuming Pauling diameters for anions shows relatively large errors. A more recent work by Zuo, et al. [98] has attempted to extend Furst and Renon's equation of state to mixed solvent systems with some success.

Despite many promising beginnings, the current statistical thermodynamic models, or non-primitive models, are not yet robust enough to handle the range and variability of most electrolyte mixtures.

ACTIVITY MODEL SUMMARY

No single activity model provides a comprehensive basis for modeling electrolyte mixtures. Debye-Hückel Theory, as the limiting law is adequate for low ionic strength mixtures. Each subsequent modification or extension has benefits and drawbacks. The empirical extensions to Debye-Hückel have expanded the ionic strength range to perhaps as high as 5 molal, but no higher. The applications of local composition (LC) models suffer from concerns regarding pressure effects (not accounted for in the model framework) and require a very large experimental database for fitting of model parameters. Although molecular simulation investigations continue, with attempts to define hydration spheres, the most current statistical thermodynamics models built upon the simulated observations are not yet applicable to multicomponent mixtures. Of the virial models, Pitzer's model is the most robust but requires significant correlation efforts to construct a consistent set of model parameters. Pitzer's model finds widespread application and is able to handle mixed weak and strong electrolytes up to moderate ionic strengths. Many authors' works have contributed to the development of consistent model parameter sets. Numerous authors have also applied Pitzer's model to nearly every electrolyte mixture available experimentally, contributing to an abundant literature database.

Of the models reviewed, Pitzer's equations, with the large parameter database and applicability to mixtures of strong and/or weak electrolytes, provides the best framework for correcting an equation-of-state based approach to the electrolyte vapor liquid equilibria problem.

APPLIED METHODS IN ELECTROLYTE VAPOR-LIQUID EQUILIBRIA

While Debye-Hückel and the empirical extensions, the liquid phase activity models, Pitzer's model, and hydration theory, each focus primarily on accurate descriptions of liquid non-idealities in electrolyte mixtures, their application to vapor-liquid equilibrium problems was often a secondary consideration.

Edwards, et al. [16, 28] made a major contribution to development of the basic thermodynamic framework to correlate and predict the vapor-liquid equilibrium for volatile weak electrolyte solutions based on liquid phase activity models. Many researchers have focused on the improvement of liquid phase activity correlations, as these correlations are believed to be the major reason for the poor performance of models. Numerous applications have developed based on this framework, and combined with many of the activity models discussed, for modeling vapor liquid equilibria in electrolyte solutions.

Modifications to the Edward et al. basic approach have also been made, notably the applications of local composition (LC) models for solution of vapor-liquid, liquid-liquid, and solid-liquid equilibria problems [83, 99-103], as well as new implementations of local composition models combined with cubic equations of state, in the so-called $\gamma-\phi$ approach [104-106].

Other authors have developed electrolyte based equations of state beginning from well-known equations of state, from the perturbed hard chain equation of state, or from molecular dynamics theories of ionic systems [93, 95, 97, 107-113]. Electrolytes have also been incorporated into a class of equations of state based on association [59, 60, 114].

Empirical Methods

Rumpf and Maurer [115-123] have used a modified Pitzer equation to correlate experimental data. Excellent agreement was obtained with their measurements (for example, 1.6 % average relative errors in total pressure for CO_2-Salt-H_2O). The model also yields good agreement with data of Corti, et al. [124, 125]. The average deviation in total pressure is 14.2% at pressures less than 100 bar. Again, one has to face the problem of a large number of parameters possible in the Pitzer formalism, including ternary parameters. Furthermore, the Rumpf and Maurer approach is not applicable at high concentrations of weak electrolytes and pressures greater than 100 bars.

Another modeling effort by Wilson, et al. [126, 127] includes no expression for activity coefficients, but correlates the dissociation constants and Henry's constants as a function of composition and ionic strength. However, a large number of parameters, including quaternary parameters, are required for model correlation. The approach gives excellent agreement in systems of single strong electrolytes from dilute up to 6 molal concentrations. Wilson's model also shows some flexibility in terms of the ternary adjustable parameters. The third virial coefficient can be neglected at electrolyte concentration less than 2 molality. The equation remains subject to all the limitations of a virial equation. Moreover, it is not applicable to mixed solvent systems, because the parameters are unknown functions of solvent composition. The Wilson model has been developed extensively by regression of a large amount of binary and ternary experimental data.

Beutier and Renon [87] used the thermodynamic framework established by Edwards, et al. and modified the liquid activity equation to extend their model to higher electrolyte

concentrations. They presented a modified Pitzer equation by splitting the excess Gibbs free energy into three terms including additional molecule-molecule interactions. Unlike the method of Edwards, et al., ternary parameters are also included in the Pitzer activity coefficient equation. Generally the model provides similar agreement with experimental data as the model of Edwards, et al. [28].

Pawlikowski, et al. [128] revised the Edwards model by fitting ternary experimental data to obtain new interaction parameters. A computer program, TIDES, was developed by Pawlikowski [129] to correlate vapor-liquid equilibrium data for NH_3-CO_2-H_2O at 100 and 150 °C. Good results were obtained at 100°C for Pawlikowski's data (16% errors for CO_2 partial pressure and 13% errors for NH_3 partial pressure). However, the model correlation gives generally poorer agreement with other experimental results in ternary and quaternary systems (see Tables V and VI in Daumn, et al. [112]). The model involves a large number of parameters. For the CO_2-NH_3-H_2O ternary system, the model requires 14 ternary interaction parameters and 25 binary interaction parameters.

Electrolyte modified and electrolyte based equations of state

Less attention has been given to the extension of equations of state to electrolyte mixtures. The equation-of-state approach does not suffer the limitations of activity models at high pressure and temperature. Furthermore, it has the advantage of simple computational procedures with fewer adjustable parameters without sacrificing the ability to correlate the experimental data.

Approaches which combine an equation of state that successfully describes high-pressure phase equilibrium in non-aqueous systems with electrolyte effects have been proposed by

Daumn, et al. [112], Friedemann [130], and Jin and Donohue [109-111]. Several models have been developed by introducing a mixing rule combined with the activity coefficient models into a cubic equation of state [131-134]. However, none of these models account explicitly for the presence of ions.

Daumn, et al. [112] extended the perturbed-hard-chain equation of state [135], which applies successfully to polar mixtures at high pressure to aqueous weak electrolyte solutions. The model requires two temperature dependent parameters per binary system and two additional binary-pair parameters fitted from ternary systems. The prediction results were comparable with models of Edwards, et al. [28] and Wilson [126] for the quaternary CO_2-NH_3-H_2S-H_2O system. The average relative deviation in the partial pressures was approximately 30 % for all the models. The method fails at low pressure and at dilute concentrations, because the model neglects the dissociation of weak electrolytes.

Friedemann [130] applied the Soave-Redlich-Kwong equation of state to calculate the fugacity coefficients in the liquid phase. The major drawback in Friedemann's approach is that the activity coefficients for all species are assumed to be unity, whereas the nonideality in weak electrolyte systems results in activity coefficients deviating significantly from unity. The biggest advantage of the model is its simplicity and ability to predict multicomponent systems with few parameters from binary data reduction. The predictions are compared with the more complex Edwards, et al. [28] liquid activity models and Daumn, et al. [112] equation-of-state model for ternary NH_3-CO_2-H_2O and NH_3-H_2S-H_2O systems. The prediction results of Friedemann are approximately

127

equivalent with other complex model correlation results at high temperatures and pressures (see Tables IV and V in Friedemann, 1987).

Recently, a new equation of state based on perturbation theory was derived by Jin and Donohue [109-111]. The Helmholtz free energy contains up to ten terms taking into account molecule-molecule interactions, ion-ion interactions, and ion-molecule solvation effects. The equation of state requires one adjustable parameter per anion-cation pair. This model shows less than 6% average absolute deviations with experimental mean ionic activity coefficients at 25°C for single strong electrolytes up to 6 molality. The model was also used to predict vapor pressures of binary weak electrolyte mixtures. The model gave good agreement with the limited experimental data for aqueous CO_2, SO_2, and H_2S systems in moderate temperature and concentration ranges. Unfortunately, extension from binary to multicomponent systems is still not reported.

Mock, et al. [136] and Sander, et al. [99] developed models to calculate the phase equilibrium for multiple-solvent electrolyte solutions, but they do not include noncondensable gases. Jansson, et al. [137] have presented a detailed comparison for these two models. For noncondensable supercritical gases at high pressure, activity coefficient models cannot be used because there is no standard state for supercritical components.

REFERENCES

1. Anderson, G.M. and D.A. Crerar, *Thermodynamics in Geochemistry The Equilibrium Model*. 1993, New York: Oxford University Press. 588 pgs.

2. Prausnitz, J.M., R.N. Lichtenthaler, and E.G. de Azevedo, *Molecular Thermodynamics of Fluid-Phase Equilibria*. 3rd ed. 1999, Upper Saddle River, New Jersey: Prentice Hall. 860 pgs.

3. Debye, P. and E. Hückel *Zur Theorie der Elektrolyte.* Physiks Zeitshrift, 1923. 24: p. 185-206.

4. Stumm, W. and J.J. Morgan, *Aquatic Chemistry Chemical Equilibria and Rates in Natural Waters*. Third ed. 1996, New York: John Wiley & Sons, Inc. 1022 pgs.

5. Bethke, C.M., *Geochemical Reaction Modeling*. 1996, New York: Oxford University Press. 397 pgs.

6. Stokes, R.H. and R.A. Robinson, *Ionic Hydration and Activity in Electrolyte Solutions.* Journal of the American Chemical Society, 1948. 70: p. 1870-1878.

7. Loehe, J.R. and M.D. Donohue, *Recent Advances in Modeling Thermodynamic Properties of Aqueous Strong Electrolyte Systems.* AIChE Journal, 1997. 43(1): p. 180.

8. Helgeson, H.C., *Thermodynamics of hydrothermal systems at elevated temperatures.* American Journal of Science, 1969. 267: p. 729-804.

9. Helgeson, H.C. and D.H. Kirkham, *Theoretical prediction of the thermodynamic behavior of aqueous electrolytes at high pressures and temperatures: II. Debye-Huckel parameters for activity coefficients and relative partial-molal properties.* American Journal of Science, 1974. 274: p. 1199-1261.

10. Cogley, D.R. and J.N. Butler, *Automated Computation Methods*, in *IONIC EQUILIBRIUM: Solubility and pH Calculations*, John Wiley & Sons. p. 485-541.

11. Wolery, T.J., *Calculation of chemical equilibrium between aqueous solution and minerals: the EQ3/6 software package*. 1979, Lawrence Livermore Laboratory.

12.	Kharaka, Y.K., et al., *SOLMINEQ. 88: A Computer Program for Geochemical Modeling of Water-Rock Interactions*. 1988, U. S. Geological Survey: Menlo Park, California.

13.	Wolery, T.J., et al., *Current Status of the EQ3/6 Software Package for Geochemical Modeling*, in *Chemical Modeling of Aqqueous Systems II*, D.C. Melchior and R.L. Bassett, Editors. 1990, American Chemical Society: Washington, D.C.

14.	Bromley, L.A., *Approximate individual ion values for beta (or **b**) in extended Debye-Hueckel theory for uni-univalent aqueous solutions at 298.15 K*. Journal of Chemical Thermodynamics, 1972. 4: p. 669-673.

15.	Bromley, L.A., *Thermodynamic Properties of Strong Electrolytes in Aqueous Solutions*. AIChE Journal, 1973. 19(No. 2): p. 313-320.

16.	Edwards, T.J., et al., *Thermodynamics of Aqueous Solutions Containing Volatile Weak Electrolytes*. AIChE Journal, 1975. 21: p. 248-259.

17.	Meissner, H.P. and J.W. Tester, *Activity Coefficients of Strong Electrolytes in Aqueous Solutions*. Industrial Engineering Chemical Process Design and Development, 1972. 11(No. 1): p. 128-133.

18.	Meissner, H.P. and C.L. Kusik, *Actvity Coefficients of Strong Electrolytes in Multicomponent Aqueous Solutions*. AIChE Journal, 1972. 18(2): p. 294.

19.	Patwardhan, V.S. and A. Kumar, *A Unified Approach for Prediction of Thermodynamic Properties of Aqueous Mixed-Electrolyte Solutions Part I: Vapor Pressure and Heat of Vaporization*. AIChE, 1986. 32(9): p. 1419-1427.

20.	Patwardhan, V.S. and A. Kumar, *A Unified Approach for Prediction of Thermodynamic Properties of Aqueous Mixed-Electrolyte Solutions Part II: Volume, Thermal and Other Properties*. AIChE, 1986. 32: p. 1429-1438.

21.	Meissner, H.P. and C.L. Kusik, *Aqueous Solutions of Two or More Strong Electrolytes*. Industrial Engineering Chemistry and Process Design and Development, 1973. 12(2): p. 205.

22. Meissner, H.P., C.L. Kusik, and J.W. Tester, *Activity Coefficients of Strong Electrolytes in Aqueous Solution--Effect of Temperature.* AIChE Journal, 1972. 18(No. 3): p. 661-662.

23. Pitzer, K.S., *Thermodynamics of Electrolytes. I. Theoretical Basis and General Equations.* The Journal of Physical Chemistry, 1973. 77(2): p. 268-277.

24. Pitzer, K.S. and G. Mayorga, *Thermodynamics of Electrolytes. II. Activity and Osmotic Coefficients for Strong Electrolytes with One or Both Ions Univalent.* Journal of Physical Chemistry, 1973. 77(19): p. 2300.

25. Pitzer, K.S. and G. Mayorga, *Thermodynamics of Electrolytes III. Activity and Osmotic Coefficients for 2-2 Electrolytes.* Journal of Solution Chemistry, 1974. 3(No. 7): p. 539-547.

26. Pitzer, K.S. and J.J. Kim, *Thermodynamics of Electrolytes. IV. Activity and Osmotic Coefficients for Mixed Electrolytes.* Journal of th American Chemical Society, 1974. 96(18): p. 5701-5707.

27. Pitzer, K.S., *Thermodynamics of Electrolytes. V. Effects of Higher-Order Electrostatic Terms.* Journal of Solution Chemistry, 1975. 4(No. 3): p. 249-265.

28. Edwards, T.J., et al., *Vapor-Liquid Equilibria in Multicomponent Aqueous Solutions of Volatile Weak Electrolytes.* AIChE Journal, 1978. 24(6): p. 966.

29. Pitzer, K.S., *Characteristics of very concentrated aqueous solutions.* Physics and Chemistry of The Earth, 1981. 13-14: p. 249-272.

30. Reardon, E.J. and R.D. Beckie, *Modeling Chemical Equilibria of Acid Mine-Drainage: The $FeSO_4$-H_2SO_4-H_2O System.* Geochimica et Cosmochimica Acta, 1987. 51: p. 2355-2368.

31. Pabalan, R.T. and K.S. Pitzer, *Models for Aqueous Electrolyte Mixtures for Systems Extending from Dilute Solutions to Fused Salts*, in *Chemical Modeling of Aqueous Systems II*, D.C. Melchior and R.L. Bassett, Editors. 1990, American Chemical Society: Washington, D.C.

131

32.   He, S. and J.W. Morse, *Prediction of halite, gypsum, and anhydrite solubility in natural brines under subsurface conditions.* Computers & Geosciences, 1993. 19(1): p. 1-22.

33.   Kang, S.-P., M.-K. Chun, and H. Lee, *Phase equilibria of methane and carbon dioxide hydrates in the aqueous $MgCl_2$ solutions.* Fluid Phase Equilibria, 1998. 147: p. 229–238.

34.   Millero, F.J., *Marine solution chemistry and ionic interactions.* Marine Chemistry, 1990. 30: p. 205-229.

35.   Clegg, S.L. and P. Brimblecombe, *Solubility of Volatile Electrolytes in Multicomponent Solutions with Atmospheric Applications*, in *Chemical Modeling of Aqueous Systems II*, D.C. Melchior and R.L. Bassett, Editors. 1990, American Chemical Society: Washington, D.C.

36.   Millero, F.J., *The activity coefficients of non-electrolytes in seawater.* Marine Chemistry, 2000. 70: p. 5-22.

37.   Pierrot, D. and F.J. Millero, *The Apparent Molal Volume and Compressibility of Seawater Fit to the Pitzer Equations.* Journal of Solution Chemistry, 2000. 29(No. 8): p. 719-742.

38.   Kuhn, M., et al., *Modeling chemical brine-rock interaction in geothermal reservoirs.* 2002.

39.   Pitzer, K.S., *Activity Coefficients in Electrolyte Solutions.* Second ed. 1991, Boca Raton, Florida: CRC Press. 542 pgs.

40.   Marion, G.M. and R.E. Farren, *Mineral solubilities in the Na-K-Mg-Ca-Cl-SO_4 - H_2O system: A re-evaluation of the sulfate chemistry in the Spencer-Møller-Weare model.* Geochimica et Cosmochimica Acta, 1999. 63(9): p. 1305–1318.

41.   Eugster, H.P., C.E. Harvie, and J.H. Weare, *Mineral equilibria in a six-component seawater system, Na-K-Mg-Ca-SO_4-Cl-H_2O, at 25°C.* Geochimica et Cosmochimica Acta, 1980. 44: p. 1335-1347.

42. Harvie, C.E., H.P. Eugster, and J.H. Weare, *Mineral equilibria in the six-component seawater system, Na-K-Mg-Ca-SO$_4$-Cl-H$_2$O at 25°C. II: Compositions of the saturated solutions.* Geochimica et Cosmochimica Acta, 1982. 46: p. 1603-1618.

43. Harvie, C.E., N. Moller, and J.H. Weare, *The Prediction of Mineral Solubilities in Natural Waters: The Na-K-Mg-Ca-H-Cl-SO$_4$-OH-HCO$_3$-CO$_3$-CO$_2$-H$_2$O System to High Ionic Strengths at 25 C.* Geochimica et Cosmochimica Acta, 1984. 48: p. 723-751.

44. Moller, N. and J.H. Weare, *Prediction of Brine Process Chemistry from Theorectical Models.* Fluid Phase Equilibria, 1986. 30: p. 229-235.

45. Harvie, C.E., J.P. Greenberg, and J.H. Weare, *A chemical equilibrium algorithm for highly non-ideal multiphase systems: Free energy minimization.* Geochimica et Cosmochimica Acta, 1987. 51: p. 1045-1057.

46. Greenberg, J. and N. Moller, *The prediction of mineral solubilities in natural waters: A chemical equilibrium model for the Na-K-Ca-Cl-SO$_4$-H$_2$O system to high concentration from 0 to 250°C.* Geochimica et Cosmochimica Acta, 1989. 53: p. 2503-2518.

47. Duan, Z., et al., *The prediction of methane solubility in natural waters to high ionic strength from 0 to 250°C and from 0 to 1600 bar.* Geochimica et Cosmochimica Acta, 1992. 56: p. 1451-1460.

48. Duan, Z., N. Moller, and J.H. Weare, *Molecular dynamics equation of state for nonpolar geochemical fluids.* Geochimica et Cosmochimica Acta, 1995. 59(8, April): p. 1533-1538.

49. Duan, Z., N. Moller, and J.H. Weare, *A general equation of state for supercritical fluid mixtures and molecular dynamics simulation of mixture PVTX properties.* Geochimica et Cosmochimica Acta, 1996. 60(7): p. 1209-1216.

50. Duan, Z., N. Moller, and J.H. Weare, *Prediction of the solubility of H$_2$S in NaCl aqueous solution: an equation of state approach.* Chemical Geology, 1996. 130(1-2, 7 August): p. 15-20.

51.   Duan, Z., et al., *Prediction of boiling, scaling and formation conditions in geothermal reservoirs using computer programs tequil and geofluids.* Geothermics, 1996. 25(6, Dec): p. 663-678.

52.   Marion, G., M. and R.E. Farren, *Mineral Solubilities in the Na-K-Mg-Ca-Cl-SO-H$_2$O System: A re-evaluation of the Sulfate Chemistry in the Spencer-Moller - Weare Model.* Geochimica et Cosmochimica Acta, 1999. 63(No. 9): p. 1305-1318.

53.   Duan, Z., N. Moller, and J.H. Weare, *Accurate prediction of the thermodynamic properties of fluids in the system H$_2$O-CO$_2$-CH$_4$-N$_2$ up to 2000 K and 100 kbar from a corresponding states/one fluid equation of state.* Geochimica et Cosmochimica Acta, 2000. 64(6): p. 1069-1075.

54.   Duan, Z., N. Moller, and J.H. Weare, *Equation of state for the NaCl-H$_2$O-CO$_2$ system: prediction of phase equilibria and volumetric properties.* Geochimica et Cosmochimica Acta, 2000. 59(14): p. 2869-2882.

55.   Kuhn, M., *Issue Regarding the Constants included in "Modeling Brine Rock interaction in Geothermal Reservoirs"*, E.L. Maase, Editor. 2003.

56.   Rard, J.A. and A. M.Wijesinghe, *Conversion of parameters between different variants of Pitzer's ion-interaction model, both with and without ionic strength dependent higher-order terms.* The Journal of Chemical Thermodynamics, 2003. 35(3): p. 439-473.

57.   Krop, J., *New Approach to Simplify the Equation for the Excess Gibbs Free Energy of Aqueous Solutions of Electrolytes Applied to the Modelling of the NH$_3$-CO$_2$-H$_2$O Vapour-Liquid Equilibria.* Fluid Phase Equilibria, 1999. 163: p. 209-229.

58.   Stokes, R.H. and R.A. Robinson, *Solvation Equilibria in Very Concentrated Solutions.* Journal of Solution Chemistry, 1973. 2(2/3): p. 173-191.

59.   Kawaguchi, Y., et al., *Correlation for Activities of Water in Aqueous Electrolyte Solutions Using ASOG Model.* Journal of Chemical Engineering of Japan, 1981. 14(No. 3): p. 243-246.

60. Kawaguchi, Y., Y. Tashima, and Y. Arai, *Supplement to the Paper "Correlation for Activities of Water in Aqueous Electrolyte Solutions Using ASOG Model"*. Journal of Chemical Engineering of Japan, 1982. 15(No. 1): p. 62-63.

61. Ghosh, S. and V.S. Patwardhan, *Aqueous Solutions of Single Electrolytes: A Correlation Based on Ionic Hydration.* Chemical Engineering Science, 1990. 45(1): p. 79-87.

62. Nesbitt, H.W., *The Stokes and Robinson Hydration Theory: A Modification with Application to Concentrated Electrolyte Solutions.* Journal of Solution Chemistry, 1982. 11(6): p. 415.

63. Marcus, Y., *Ionic Radii in Aqueous Solutions.* Chemical RevieW, 1988. 88: p. 1475-1498.

64. Heinzinger, Pure & Applied Chemistry, 1985. 57: p. 1031.

65. Bopp, Pure & Applied Chemistry, 1987. 59: p. 1071.

66. Ohtaki, H. and T. Radnai, Chemical Reviews, 1993. 93: p. 1157.

67. Lu, X.-h. and G. Maurer, *Model for Describing Activity Coefficients in Mixed Electrolyte Aqueous Solutions.* AIChE Journal, 1993. 39(9): p. 1527.

68. Wilson, G.M. and C.H. Deal, *Activity Coefficients and Molecular Structure.* Industrial and Engineering Chemistry Fundamentals, 1962. 1(No. 1): p. 20-23.

69. Wilson, G.M., *Vapor-liquid equilibrium. XI. A new expression for the excess free energy of mixing.* J. Am. Chem. Sot., 1964. 86: p. 127-130.

70. Renon, H. and J.M. Prausnitz, *Local Compositions in Thermodynamic Excess Functions for Liquid Mixtures.* AIChE Journal, 1968. 14(1): p. 135.

71. Abrams, D.S. and J.M. Prausnitz, *Statistical Thermodynamics of Liquid Mixtures: A New Expression for the Excess Gibbs Energy of Partly or Completely Miscible Systems.* AIChE Journal, 1975. 21(1): p. 116-128.

72. McDermott, C. and N. Ashton, *Note on the Definition of Local Composition.* Fluid Phase Equilibria, 1977. 1: p. 33-35.

135

73.   Mollerup, J., *A Note on Excess Gibbs Energy Models, Equations of State and the Local Composition Concept.* Fluid Phase Equilibria, 1981. 7: p. 121-138.

74.   Kemeny, S. and P. Rasmussen, *A derivation of local composition expressions from partition functions.* Fluid Phase Equilibria, 1981. 7: p. 197-203.

75.   Whiting, W.B. and J.M. Prausnitz, *Equations of state for strongly nonideal fluid mixtures: application of local compositions toward density-dependent mixing rules.* Fluid Phase Equilibria, 1982. 9: p. 119-147.

76.   Mathias, P.M. and T.W. Copeman, *Extension of the Peng-Robinson Equation of State to Complex Mixtures: Evaluation of the Various Forms of the Local Composition Concept.* Fluid Phase Equilibria, 1983. 13: p. 91-108.

77.   Fischer, J., *Remarks on molecular approaches to liquid mixtures.* Fluid Phase Equilibria, 1983. 10: p. 1-7.

78.   Hu, Y., E.G. Azevedo, and J.M. Prausnitz, *The molecular basis for local compositions in liquid mixture models.* Fluid Phase Equilibria, 1983. 13: p. 351-360.

79.   Lee, L.L., T.H. Chung, and K.E. Starling, *A molecular theory for the thermodynamic behavior of polar mixtures. I. The statistical-mechanical local composition model.* Fluid Phase Equilibria, 1983. 12: p. 105-124.

80.   Hoheisel, C. and F. Kohler, *Local composition in liquid mixtures.* Fluid Phase Equilibria, 1984. 16: p. 13-24.

81.   Engels, H., *Phase Equilibria and phase Diagrams of Electrolytes*. Chemistry data series. Vol. 11. 1990, Frankfurt: DECHEMA. 130 pgs.

82.   Cruz, J.-L. and H. Renon, *A New Thermodynamic Representation of Binary Electrolyte Solutions Nonideality in the Whole Range of Concentrations.* AIChE Journal, 1978. 24(No. 5): p. 817-830.

83.   Ball, F.X., W. Furst, and H. Renon, *An NRTL Model for Representation and Prediction of Deviation for Ideality in Electrolyte Solutions Compared to the*

Models of Chen (1982) and Pitzer (1973). AIChE Journal, 1985. 31(No. 3): p. 392-399.

84.   Hamad, E.Z. and G.A. Mansoori, *A Fluctuation Solution Theory of Activity Coefficients: Phase Equilibria in Associating Molecular Solutions.* Journal of Physical Chemistry, 1990. 94: p. 3148-3152.

85.   Chen, C.-C., et al., *Local Composition Model for Excess Gibbs Energy of Electrolyte Systems.* AIChE Journal, 1982. 28(4): p. 588.

86.   Chen, C.-C. and L.B. Evans, *A Local Composition Model for the Excess Gibbs Energy of Aqueous Electrolyte Systems.* AIChE Journal, 1986. 32(3): p. 444.

87.   Beutier, D. and H. Renon, *Representation of NH_3-H_2S-H_2O, NH_3-CO_2-H_2O, and NH_3-SO_2-H_2O Vapor-Liquid Equilibria.* Industrial Engineering and Chemical Process Design Development, 1978. 17(No. 3): p. 220-230.

88.   Nakanishi, K. and K. Toukulio, *Molecular dynamics studies of Lennard-Jones liquid mixtures.* Journal of Chemical Physics, 1979. 70: p. 5848-5850.

89.   Nakanishi, K., et al., *Free energy of mixing, phase stability, and local composition in Lennard-Jones liquid mixtures.* Journal of Chemical Physics, 1982. 76(629-636).

90.   Nakanishi, K. and H. Tanaka, *Molecular dynamic studies on the local composition in Lennard-Jones liquid mixtures of nonspherical molecules.* Fluid Phase Equilibria, 1983. 13: p. 371-380.

91.   Planche, H. and H. Renon, *Mean Spherical Approximation Applied to a Simple but Nonprimitive Model of Interaction for Electrolyte Solutions and Polar Substances.* Journal of Physical Chemistry, 1981. 85: p. 3924-3929.

92.   Ball, F.-X., et al., *Representation of Deviation from Ideality in Concentrated Aqueous Solutions of Electrolytes Using a Mean Spherical Approximation Molecular Model.* AIChE Journal, 1985. 31(8): p. 1233.

93.   Copeman, T.W. and F.P. Stein, *A Perturbed Hard-Sphere Equation of State for Solutions Containing an Electrolyte.* Fluid Phase Equilibria, 1987. 35: p. 165-187.

94.   Copeman, T.W. and F.P. Stein, *An Explicit Non-Equal Diameter MSA Model for Electrolytes.* Fluid Phase Equilibria, 1986. 30: p. 237-245.

95.   Raatschen, W., A.H. Harvey, and J.M. Prausnitz, *Equations of State for Solutions of Electrolytes in Mixed Solvents.* Fluid Phase Equilibria, 1987. 38: p. 19-38.

96.   Harvey, A.M. and J.M. prausnitz, *Thermodynamics of High-pressure Aqueous Systems Containing Gases and Salts.* AIChE Journal, 1989. 35(4): p. 635.

97.   Furst, W. and H. Renon, *Representation of Excess Properties of Electrolyte Solutions Using a New Equation of State.* AIChE Journal, 1993. 39(2): p. 335-343.

98.   Zuo, Y.-X., D.D. Zhang, and W. Furst, *Extension of the electrolyte EOS of Fürst and Renon to mixed solvent electrolyte systems.* Fluid Phase Equilibria, 2000. 175: p. 285-310.

99.   Sander, B., A. Fredenslund, and P. Rasmussen, *Calculation of Vapour-Liquid Equilibria in Mixed Solvent/Salt Systems Using an Extended UNIQUAC Equation.* Chemical Engineering Science, 1986. 41(5): p. 1171-1183.

100.   Bernardis, M., G. Carvoli, and P. Deloge, NH_3-CO_2-H_2O *VLE Calculation Using an Extended UNIQUAC Equation.* AIChE Journal, 1989. 35(No. 2): p. 314-317.

101.   Kristensen, J.N. and P.L. Christensen, *A Combined Soave-Redlich-Kwong and NRTL Equation for Calculating the Distribution of Methanol Between Water and Hydrocarbon Phases.* Fluid Phase Equilibria, 1993. 82: p. 199-206.

102.   Abovsky, V., Y. Liu, and Watanasiri, *Representation of Nonideality in Concentrated Electrolyte Solutions Using the Electrolyte NRTL Model with Concentration-Dependent Parameters.* Fluid Phase Equilibria, 1998. 150-151: p. 277-286.

103.   Iliuta, M., K. Thomsen, and P. Rasmussen, *Extended UNIQUAC Model for Correlation and Prediction of Vapour-Liquid-Solid Equilibria in Aqueous Salt Systems Containing Non-Electrolytes. Part A. Methanol-Water-Salt Systems.* Chemical Engineering Science, 2000(55): p. 2673-2686.

104.   Tochigi, K., K. Kojima, and A.A. Fredenslund, *Prediction of Vapor-Liquid-Liquid Equilibria Using the UNIFAC, and GC-EOS Models.* Fluid Phase Equilibria, 1986. 25: p. 231-235.

105.   Krop, J., *New approach to simplify the equation for the excess Gibbs free energy of aqueous solutions of electrolytes applied to the modelling of the NH_3–CO_2 – H_2O vapour–liquid equilibria.* Fluid Phase Equilibira, 1999. 163: p. 209–229.

106.   Liu, Y., M. Wimby, and U. Gren, *An Activity-Coefficient Model for Electrolyte Systems.* Computers chem. Engng., 1989. 13(4/5): p. 405-410.

107.   Zuo, Y.-X. and W. Furst, *Use of an Electrolyte Equation of State for the Calculation of Vapor-Liquid Equilibria and Mean Activity Coefficients in Mixed Solvent Electrolyte Systems.* Fluid Phase Equilibria, 1998. 150-151: p. 267-275.

108.   Zuo, Y.-X. and W. Furst, *Prediction of Vapor Pressure for Nonaqueous Electrolyte Solutions Using an Electrolyte Equation of State.* Fluid Phase Equilibria, 1997. 138: p. 87-104.

109.   Jin, G. and M.D. Donohue, *An Equation of State for Electrolyte Solutions. 2. Single Volatile Weak Electrolytes in Water.* Industrial Engineering and Chemistry Reseach, 1988. 27: p. 1737-1743.

110.   Jin, G. and M.D. Donohue, *An Equation of State for Electrolyte Solutions. 1. Aqueous Systems Containing Strong Electrolytes.* Industrial Engineering and Chemistry Research, 1988. 27: p. 1073-1084.

111.   Jin, G. and M.D. Donohue, *An Equation of State for Electrolyte Solutions. 3. Aqueous Solutions Containing Multiple Salts.* Industrial Engineering and Chemistry Reseach, 1991. 30: p. 240-248.

112.   Daumn, K.J., et al., *An Equation of State Description of Weak Electrolyte VLE Behavior.* Fluid Phase Equilibria, 1986. 30: p. 197-212.

113.   Cherif, M., et al., *Representation of VLE and liquid phase composition with an electrolyte model: application to H_3PO_4–H_2O and H_2SO_4–H_2O.* Fluid Phase Equilibira, 2002. 194-197: p. 729–738.

114. Kontogeorgis, G.M., et al., *An Equation of State for Associating Fluids.* Ind. Eng. Chem. Res., 1996. 35(No. 11): p. 4310-4318.

115. Rumpf, B. and G. Maurer, *Solubilities of Hydrogen Cyanide and Sulfur Dioxide in Water at Temperatures from 293.15 to 413.15 K and Pressures up to 2.5 MPa.* Fluid Phase Equilibria, 1992. 81: p. 241-260.

116. Rumpf, B. and G. Maurer, *Solubility of Ammonia in Aqueous Solutions of Sodium Sulfate and Ammonium Sulfate at Temperatures from 333.15 K to 433.15 K and Pressures up to 3 MPa.* Ind. Eng. Chem. Res., 1993. 32: p. 1780-1789.

117. Rumpf, B. and G. Maurer, *An Experimental and Theoretical Investigation on the Solubility of Carbon Dioxide in Aqueous Solutions of Strong Electrolytes.* Ber. Bunsenges. Phys. Chem., 1993. 97(No. 1): p. 85-97.

118. Rumpf, B. and G. Maurer, *Solubility of sulfur dioxide in aqueous solutions of sodium-and ammonium sulfate at temperatures from 313.15 K to 393.15 K and pressures up to 3.5 MPa.* Fluid Phase Equilibria, 1993. 91: p. 113-131.

119. Rumpf, B., F. Weyrich, and G. Maurer, *Simultaneous Solubility of Ammonia and Sulfur Dioxide in Water at Temperatures from 313.15K to 373.15K and Pressures up to 2.2 MPa.* Fluid Phase Equilibria, 1993. 83: p. 253-260.

120. Rumpf, B., et al., *Solubility of Carbon Dioxide in Aqueous Solutions of Sodium Chloride: Experimental Results and Correlation.* Journal of Solution Chemistry, 1994. 23(No. 3): p. 431-448.

121. Rumpf, B. and G. Maurer, *Solubility of Ammonia in Aqueous Solutions of Phosphoric Acid: Model Development and Application.* Journal of Solution Chemistry, 1994. 23(No. 1.): p. 37-51.

122. Rumpf, B., J. Xia, and G. Maurer, *Solubility of Carbon Dioxide in Aqueous Solutions Containing Acetic Acid or Sodium Hydroxide in the Temperature Range from 313 to 433 K and at Total Pressures up to 10 MPa.* Ind. Eng. Chem. Res., 1998. 37: p. 2012-2019.

123. Rumpf, B., et al., *Simultaneous Solubility of Ammonia and Hydrogen Sulfide in Water at Temperatures from 313 K to 393 K.* Fluid Phase Equilibria, 1999. 158-160: p. 923-932.

124. Corti, H.R., et al., *Effect of a Dissolved Gas on the Solubility of an Electrolyte in Aqueous Solution.* 1990. 29: p. 1043-1050.

125. Corti, H.R., J.J. de Pablo, and J. Prausintz, *Phase equilibria for aqueous systems containing salts and carbon dioxide- application of Pitzer's theory for electrolyte solutions.* J. Phys. Chem., 1990. 94: p. 7876-7880.

126. Wilson, G.M., *A New Correlation of NH_3, CO_2 and H_2S Volatility Data From Aqueous Sour Water Systems.* API Publication 955, 1978.

127. Wilson, G.M. and E.W.Y. Wayne, *GPSWAT GPA Sour Water Equilibria Correlation and Computer Program.* 1990, Gas Processors Association: Tulsa.

128. Pawlikowski, E.M., J. Newman, and J.M. Prausnitz, *Phase Equilibria for Aqueous Solutions of Ammoia and Carbon Dioxide.* Industrial Engineering and Chemical Process Design and Development, 1982. 21: p. 764-770.

129. Pawlikowski, E.M., Ph.D. Dissertation, *Vapor-Liquid Equilibria of Volatile Weak Electrolytes in Aqueous Solutions*, Chemical Engineering, University of California - Berkeley, Berkeley, California, 1981.

130. Friedemann, J.D., Ph.D. Dissertation, *The Simulation of Vapor-Liquid Equilibria in Ionic Systems*, School of Chemical Engineering, Oklahoma State University, Stillwater, Oklahoma, 1987.

131. Huron, M.-J. and J. Vidal, *New Mixing Rules in Simple Equations of State for Representing Vapour-Liquid Equilibria of Strongly Non-Ideal Mixtures.* Fluid Phase Equilibria, 1979. 3: p. 255-271.

132. Michelsen, M.L., *A Modified Huron-Vidal Mixing Rule for Cubic Equations of State.* Fluid Phase Equilibria, 1990. 60: p. 213-219.

133. Wong, D.S.H. and S.I. Sandler, *A Theoretically Correct Mixing Rule for Cubic Equations of State.* AIChE Journal, 1992. 38(5): p. 671-680.

134. Wong, D.S.H., H. Orbey, and S.I. Sadler, *Equation of State Mixing Rule for Nonideal Mixtures Using Available Activity Coefficient Model Parameters and That Allows Extrapolation Over Large Ranges of Temperature and Pressure.* Industrial Engineering and Chemical Research, 1992. 31: p. 2033-2039.

135. Donohue, M.D. and J.M. Prausnitz, *Perturbed Hard Chain Theory for Fluid Mixtures: Thermodynamic Preoperties for Mixtures in Natural Gas and Petroleum Technology.* AIChE Journal, 1978. 24(5): p. 849.

136. Mock, B., L.B. Evans, and C.-C. Chen, *Thermodynamic Representation of Phase Equilibria of Mixed-Solvent Electrolyte Systems.* AIChE Journal, 1986. 32(10): p. 1655-1664.

137. Jansson, L.-J. and I.A. Furzer, *A Comparison of Thermodynamic Models for VLE Data in Electrolyte Systems.* AIChE Journal, 1989. 35(6): p. 1044-1048.

CHAPTER III

WEAK ELECTROLYTE VAPOR-LIQUID EQUILIBRIA WITH A CUBIC

EQUATION OF STATE

An approach developed by Friedemann [1], and extended by Chen, et al. [2] describes phase equilibrium in aqueous solutions containing weak electrolytes. The model framework is based on:

- Vapor-liquid equilibrium (VLE) of molecular species

- Chemical equilibrium in the liquid phase between dissociated (ionic) and undissociated (molecular) species

- Mass balance of electrolyte species in the liquid phase

- Bulk electroneutrality in the liquid phase

- Overall mass balance

As shown in Figure 39 the framework consists of two interdependent problems: molecular vapor-liquid equilibria and liquid phase chemical equilibria.
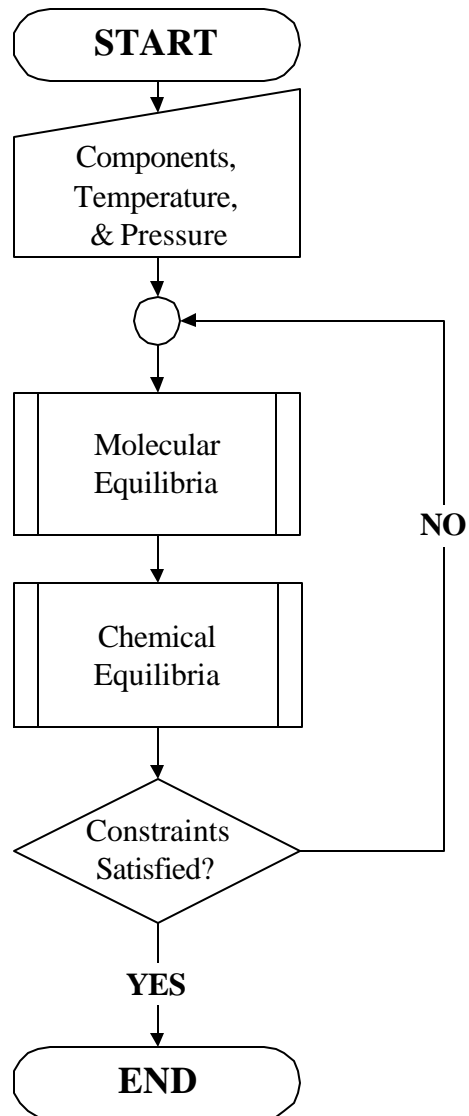
Figure 39. Phase and Chemical Equilibrium Calculations

Solution of the molecular vapor-liquid equilibrium is by application of an equation-of-state model applied to both vapor and liquid phases. The vapor-liquid equilibrium interacts with chemical equilibria by incorporating an extent of dissociation concept into the VLE calculations.

The extent of dissociation, (d_i), of reactive molecular species is defined by:

$$d_i = \frac{m_i}{M_i} \qquad (2.3\text{-}1)$$

144

where m_i is the actual (undissociated) concentration, and M_i is the apparent concentration (dissociated and undissociated) of molecular species in the aqueous phase. Corrected K_{VLE} values for dissociating species i are given by

$$K_{iVLE} = \frac{y_i}{x_i\, d_i} \qquad\qquad (2.3\text{-}2)$$

Phase equilibrium calculations continue with K_{VLE} values accurately reflecting concentrations of undissociated molecular species present in the liquid phase.

Molecular and chemical equilibria are executed in two loops. An inner, nested, loop for chemical equilibrium determines the extent of dissociation of reactive molecular species, and an outer vapor-liquid equilibrium calculation. The modified VLE calculation is outlined in Figure 40. The VLE loop solves for equality of fugacity for all molecular components in each phase as constrained by the molecular species mass balance.

In this work vapor-liquid equilibrium calculations are performed using the Soave-Redlich-Kwong equation of state [3, 4]. Chemical equilibria calculations are based on equations describing chemical dissociation constants [5-7], with Pitzer's ion-interaction model [8] describing aqueous species activities.
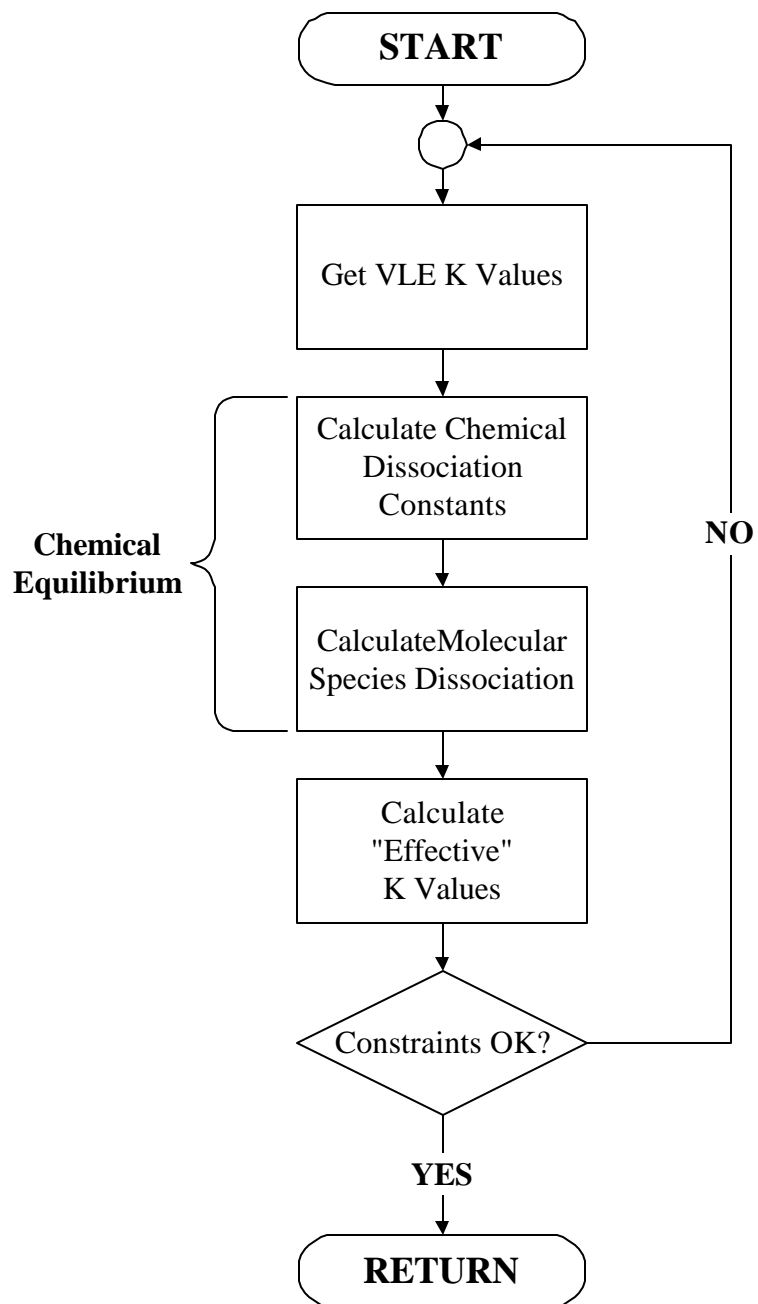
Figure 40. Chemical Equilibrium Modified VLE Loop

SOAVE-REDLICH-KWONG EQUATION OF STATE

The Soave-Redlich-Kwong (SRK) equation of state requires pure component critical temperatures, T_c, critical pressures, p_c, and accentric factors, ω. The values used in this work are those given by Reid et al. [9] and provided in the appendix. This work applies a modified SRK equation of state outlined by Graboski and Daubert [10, 11].

Fugacities from the SRK equation of state are expressed as

$$\ln \boldsymbol{f}_i = \frac{\sum x_j b_{ij}}{b}(Z-1) - \ln\left[Z\left(1-\frac{b}{\boldsymbol{n}}\right)\right]$$
$$+ \frac{a\boldsymbol{a}}{bRT}\left[\frac{\sum x_j b_{ij}}{b} - \frac{2}{a\boldsymbol{a}}\sum x_j (a\boldsymbol{a})_{ij}\right]\ln\left(1+\frac{b}{\boldsymbol{n}}\right) \qquad (2.3\text{-}3)$$

with the compressibility factor, Z, given by

$$Z^3 - Z^2 + \left(\frac{a\boldsymbol{a}P}{R^2T^2} - \frac{bP}{RT} - \left(\frac{bP}{RT}\right)^2\right)Z - \frac{a\boldsymbol{a}P}{R^2T^2}\frac{bP}{RT} = 0 \qquad (2.3\text{-}4)$$

where

$$a\boldsymbol{a} = \sum\sum x_i x_j (a\boldsymbol{a})_{ij} \qquad (2.3\text{-}5)$$

The mixing parameters, $(a\alpha)_{ij}$ and b_{ij} are given by

$$(a\boldsymbol{a})_{ij} = \left[(a\boldsymbol{a})_i (a\boldsymbol{a})_j\right]^{1/2}(1-C_{ij}) \qquad (2.3\text{-}6)$$

$$a_i = 0.42747\frac{R^2 T_{c_i}^2}{P_{c_i}} \qquad (2.3\text{-}7)$$

$$\boldsymbol{a}_i = \left[1 + \left(0.48508 + 1.5517\boldsymbol{v}_i - 0.15163\boldsymbol{v}_i^2\right)\left(1 - \sqrt{\frac{T}{T_{c_i}}}\right)\right]^2 \qquad (2.3\text{-}8)$$

147

$$b = \sum\sum x_i x_j b_{ij} \qquad (2.3\text{-}9)$$

$$b_{ij} = 0.5\left(b_i + b_j\right)\left(1 - D_{ij}\right) \qquad (2.3\text{-}10)$$

$$b_i = 0.08664 \frac{RT_{c_i}}{P_{c_i}} \qquad (2.3\text{-}11)$$

The C_{ij} term is an adjustable, empirically determined "binary interaction parameter" that characterizes the interactions between component i and component j. The parameter D_{ij} is a molecular volume interaction term recommended by Graboski and Daubert [10, 11].

VAPOR-LIQUID EQUILIBRIA ALGORITHM

Numerous algorithms for solution of vapor-liquid equilibrium problems by application of equation-of-state models are discussed in the literature. The method employed in this work is based on the Rachford-Rice formalism of the problem, solved with a Newton-Raphson iterative procedure [12]. This is the original and most widely accepted solution method and is well described in the literature [12-14].

CHEMICAL EQUILIBRIUM

Figure 41 shows an overview of the chemical equilibrium problem. The procedure requires initial estimates of component concentrations for both dissociated and undissociated species. Chemical dissociation constants and species activities are calculated. Iterations continue to update estimated species concentrations until a final equilibrium mixture composition satisfying the mass and the charge balance is obtained.
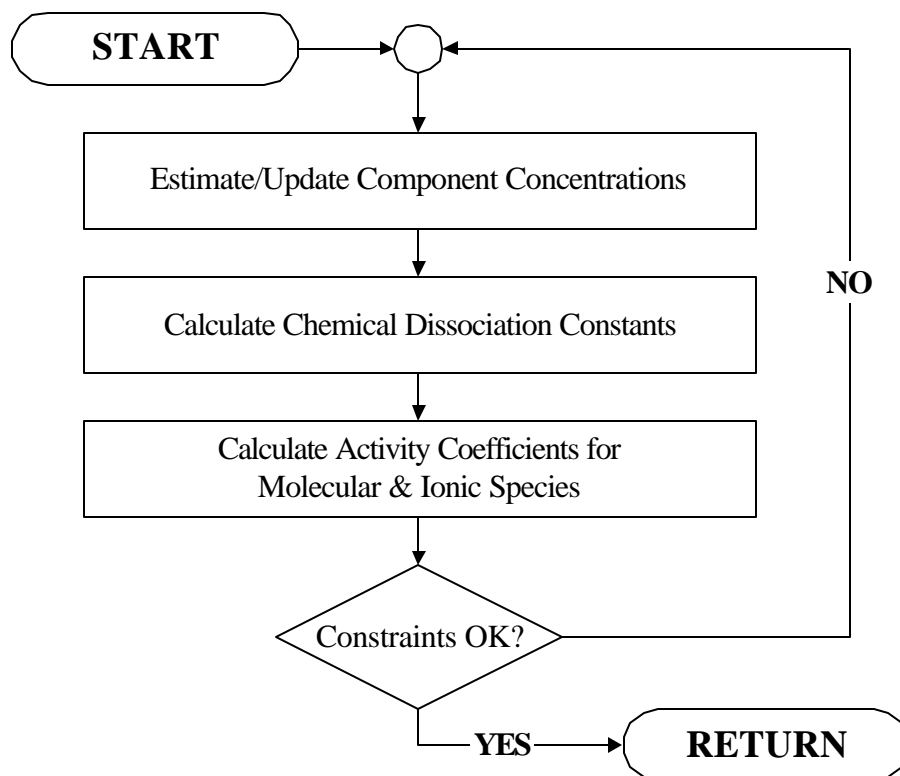
Figure 41. General Chemical Equilibrium Loop

Although the outer VLE loop employs mole fraction concentrations, the inner loop requires molal concentrations. Hence, a liquid phase mass basis is assumed, and liquid phase molecular species mole fractions are converted to molal equivalents. The equation-of-state molecular species activities are also on a mole fraction basis and must be converted to a molal basis. Finally, the mass balance constraint must be appropriately cast in either a stoichiometric basis or an atomic basis considering charged species.

ALGORITHMS FOR CHEMICAL EQUILIBRIA

There are numerous programs designed to compute chemical equilibrium for complex, multi-component mixtures. In general, these fall into three categories: those that use chemical equilibrium constants; those that use Gibbs free energy of each species and find

activities to minimize the free energy of the entire system; and those that follow reaction progress in steps toward a final equilibrium state [15]. Detailed examination of the various methods is not provided here. Reviews are available in the literature [16-20].

In this work two algorithms are applied: one using pH as a tare variable [1, 21], and a second, more generic, algorithm based on the suggestions of several authors [15, 22, 23]. Both algorithms employ chemical equilibrium constants as the basis for solution.

Bisection Algorithm: pH as a tare variable

Calculation of the chemical equilibria of a solution may proceed by use of pH as a tare variable. The algorithm is initialized with estimates for all component concentrations, from which the appropriate dissociation constants and species activities are determined. The pH, or hydrogen ion concentration, of the resultant mixture is then calculated. Electroneutrality serves as the algorithm closure test. Figure 42 provides a flowchart for the pH-based bisection algorithm.
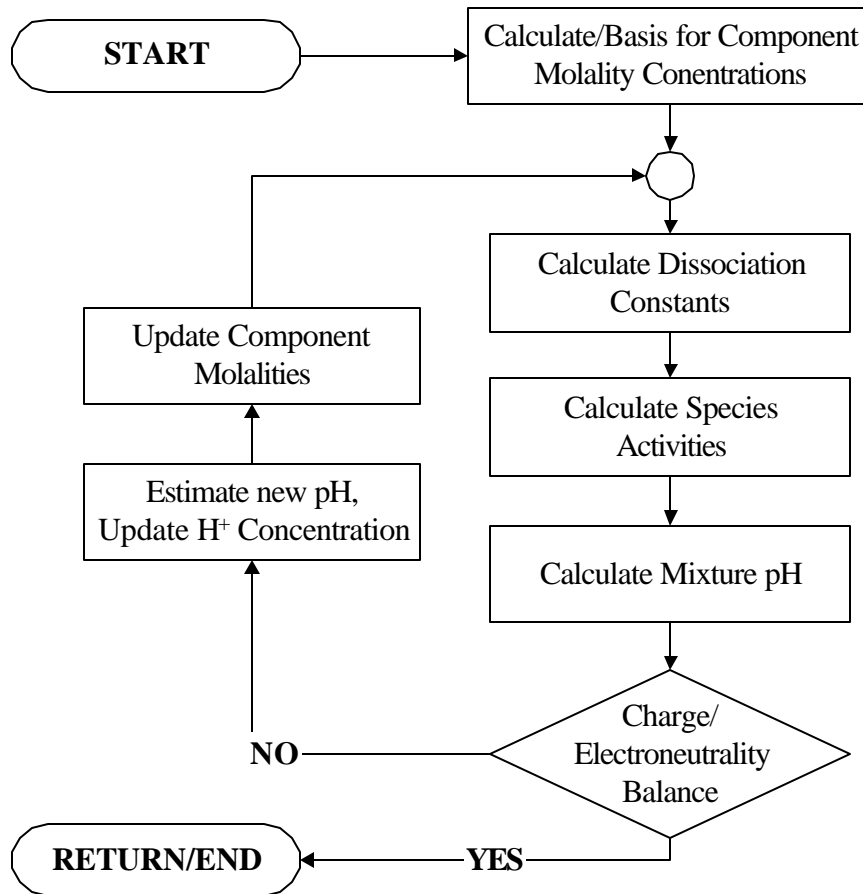
Figure 42. pH Based Chemical Equilibria Algorithm

The test condition for successful closure of the calculations is electroneutrality, or charge balance, condition. When a charge imbalance exists for a mixture, a new estimate of pH, and corresponding hydrogen ion concentration, is made. The pH of mixtures of interest occur in the common pH range, between 0 and 14.

As an example of the bisection algorithm, consider initial estimates of species concentrations resulting in the calculation of a pH of 6.5. If the charge balance for this mixture is negative, the next estimate for the mixture pH would be 10.25, calculated by bisecting the available pH range $(14.0 + 6.5)/2.0$. The hydrogen ion concentration and the new estimates for other mixture components concentrations are made. The

151

subsequent loop calculations could result in a positive charge balance, for which the new

pH value would be 8.375 (=[10.25 + 6.5]/2.0). If the charge imbalance remains negative,

the new pH would be 12.125. Iterations proceed by bisecting the pH range until the

mixture pH, and related component concentrations, satisfy the electroneutrality condition

within a preset tolerance (<1.0E-6).

The principle complication of the algorithm outlined is somewhat subtle and concerns the

procedure required to update component concentrations in each iteration. While the

hydrogen ion concentrations are directly specified by pH, the concentration of all other

components in a mixture must be related to the hydrogen ion concentration. All

components can be related to the hydrogen ion concentration, but each numerical

relationship is unique and must be coded into the program specifically for the species of

interest [1, 24]. The resulting program is limited to calculations of only the species and

reactions predetermined by the programmer.

General Chemical and Activity Algorithm

A more generic approach to the chemical equilibrium problem is possible by the

simultaneous use of the concentration and charge balance errors to estimate new

concentrations. The general algorithm is shown in Figure 43.

The general algorithm discussed below is based on the work of several authors [15, 19,

22, 23, 25] and variants of the method provide the basis for many of the computer

programs employed by commercial and government agencies for solution of chemical

equilibria problems in natural waters [26-43].

152
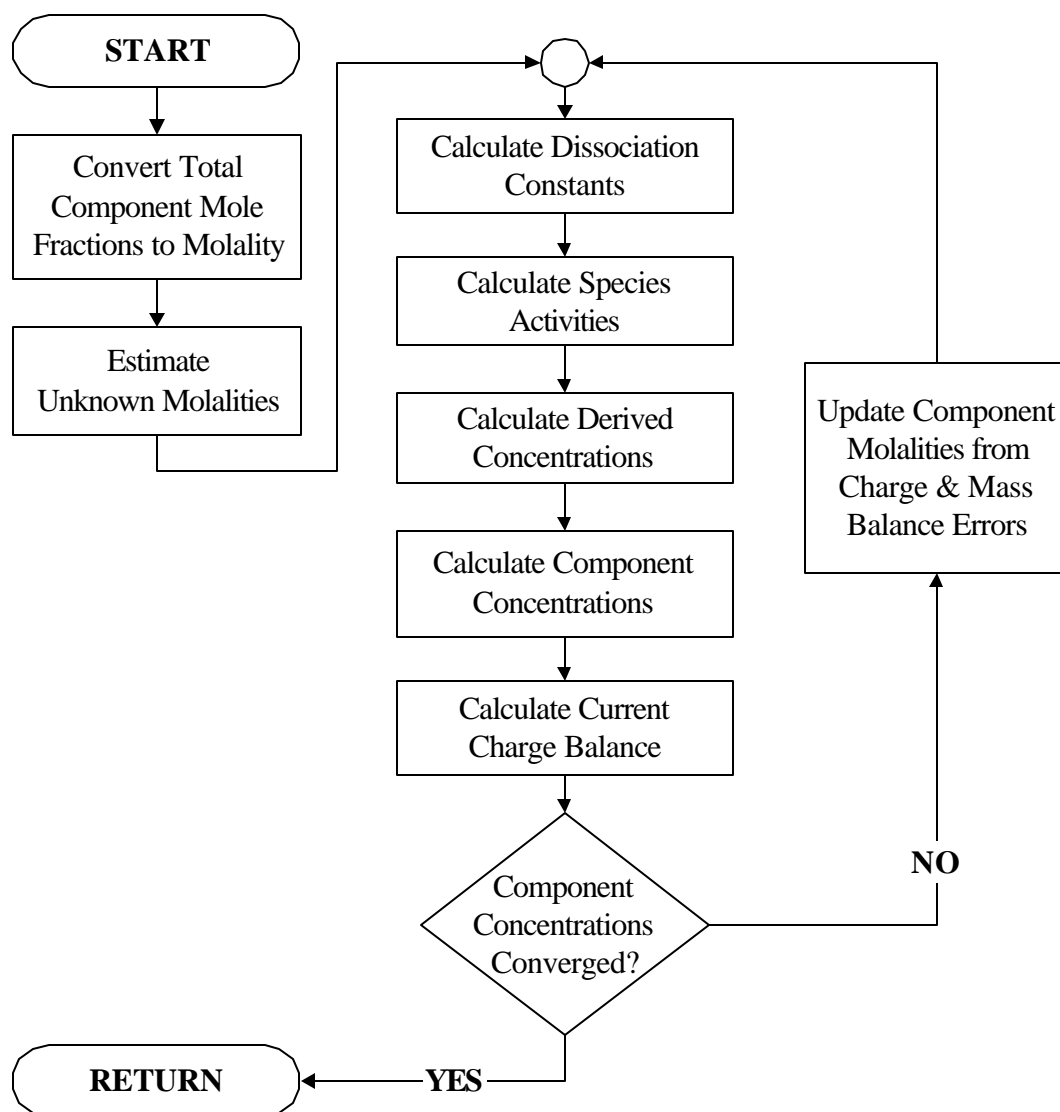
Figure 43. General Chemical Equilibria Algorithm

Consider a mixture of C molecular components, with N soluble and ionic chemical species. Chemical dissociation constants are available for M independent reactions relating some, or all, of the chemical species. Knowns include the total mass of molecular components and, for a given temperature, the dissociation constants for the independent reactions. The N unknowns include the concentrations of species derived from reactions. The number of constraints needed for solution of the system is equal to, N-M.

153

As an example, consider an aqueous mixture of two molecular species, CO_2 and H_2S. There are four independent reactions

$$CO_2 + H_2O \leftrightarrow H^+ + HCO_3^-$$ (2.3-12)

$$HCO_3^- \leftrightarrow H^+ + CO_3^{-2}$$ (2.3-13)

$$H_2S \leftrightarrow H^+ + HS^-$$ (2.3-14)

$$HS^- \leftrightarrow H^+ + S^{-2}$$ (2.3-15)

In these reactions, there are two soluble molecular species (CO_2, H_2S), and five derived ionic species (H^+, HCO_3^-, CO_3^{-2}, HS^-, S^{-2}). Three additional constraints (N-M =7-4= 3) are necessary to define the system. Electroneutrality and mass balance relations, in either stoichiometric or atomic form, provide the additional constraints.

There is one charge balance constraint (electroneutrality) given by

$$\Psi_1 = 0 = \sum_{i=1}^{N} z_i m_i$$ (2.3-16)

which is the sum over all species, i, of the product of valence, z_i, and molality, m_i. With the constraint provided by the charge balance, the number of mass balances necessary is equal to $(N$-$M)$-1.

The available mass balance relationships are represented by

$$\Psi_j = 0 = -M_e + \sum_{i=1}^{N} \mathbf{1}_{ei} m_i \qquad j = 2,3,\ldots,N-M; \ for \ e = j-1$$ (2.3-17)

where M_e is total known molal concentration of an elemental (or a basis) species. The total molal concentration is equal to the sum over all species, of the product of molality,

154

m_i, multiplied by a stoichiometric parameter, λ_i, which relates the contribution of each derived species to the overall elemental mass balance.

The M independent chemical equilibrium relationships are given by

$$K_k = \prod_{i=1}^{N} \left(m_i \, g_i \right)^{n_{ki}} \qquad k = 1, \ldots N \qquad (2.3\text{-}18)$$

where the stoichiometric coefficients of reactant species are negative, and those for product species are positive. Taking the logarithm of Equation (2.3-18) and reorganizing, Equations 2.2-16, 2.2-17, and 2.2-19 may be solved simultaneously by a Newton-Raphson iterative technique

$$\Psi_k = 0 = -\log K_k + \sum_{i=1}^{N} n_{ki} \log g_i + \sum_{i=1}^{N} n_{ki} \log m_i \quad \left(k = N - M + 1, \ldots, N \right) \qquad (2.3\text{-}19)$$

Newton-Raphson techniques require the partial derivates of each equation. These derivatives are,

$$\frac{\partial \Psi_1}{\partial m_i} = z_i \qquad \left(i = 1, \ldots, N \right) \qquad (2.3\text{-}20)$$

for the electroneutrality condition,

$$\frac{\partial \Psi_j}{\partial m_i} = I_{ei} \qquad \left(i = 1, \ldots, N; j = 2, \ldots, N - M \right) \qquad (2.3\text{-}21)$$

for each mass balance, and

$$\left(\frac{\partial \Psi}{\partial m_l} \right)_{m_i \neq m_l} = 0.43429 \left(\frac{n_{jl}}{m_l} \right) \quad \left(l = 1, \ldots, N; k = N - M + 1, \ldots, N \right) \qquad (2.3\text{-}22)$$

for the chemical equilibrium relationships. The constant 0.43429 arises as a consequence of converting logarithm to natural log functions prior to evaluating the derivatives.

The system of non-linear equations (represented by Equations 2.2-16, 2.2-17, and 2.2-19) is approximated by a linear system made up of these partial derivates,

$$
\begin{bmatrix}
z_1 & \cdots & z_N \\
\boldsymbol{l}_{1,l} & \cdots & \boldsymbol{l}_{1,N} \\
\vdots & & \vdots \\
\boldsymbol{l}_{N-M-1,l} & \cdots & \boldsymbol{l}_{N-M-1,N} \\
0.43429\left(\dfrac{\boldsymbol{n}_{1,l}}{m_l}\right) & & 0.43429\left(\dfrac{\boldsymbol{n}_{1,N}}{m_N}\right) \\
\vdots & & \vdots \\
0.43429\left(\dfrac{\boldsymbol{n}_{M,l}}{m_l}\right) & \cdots & 0.43429\left(\dfrac{\boldsymbol{n}_{M,N}}{m_N}\right)
\end{bmatrix}
\begin{bmatrix}
\boldsymbol{d}m_1 \\
\boldsymbol{d}m_2 \\
\vdots \\
\boldsymbol{d}m_{N-M} \\
\boldsymbol{d}m_{N-M+1} \\
\vdots \\
\boldsymbol{d}m_N
\end{bmatrix}
=
\begin{bmatrix}
-\Psi_1 \\
-\Psi_2 \\
\vdots \\
-\Psi_{N-M} \\
-\Psi_{N-M+1} \\
\vdots \\
-\Psi_N
\end{bmatrix}
\qquad (2.3\text{-}23)
$$

or

$$
\underline{\underline{\Psi}}'\left(N\times N\right)\cdot\underline{\boldsymbol{d}}\left(1\times N\right)=\underline{\Psi}\left(1\times N\right) \tag{2.3-24}
$$

in matrix notation.

An initial guess for concentrations of all N species, $m_{i,(0)}$ is made. These concentrations allow the calculation of the vector, $\underline{\Psi}\left(1\times N\right)$, from Equations 2.2-17 and 2.2-19, and determine the elements of the matrix $\underline{\underline{\Psi}}'\left(N\times N\right)$. Corrections to species concentrations $\underline{\boldsymbol{d}}\left(1\times N\right)$ (elements δm_i) are calculated from Equation 2.2-23.

These new estimates of concentrations are calculated as

$$
m_i^{(1)} = m_i^{(0)} + \boldsymbol{d}m_i \qquad \left(i = 1,\ldots,N\right) \tag{2.3-25}
$$

Iterations continue until the δm of all calculated components are less than a preset tolerance (1.0E-10).

This procedure is a more general approach to the chemical equilibria problem, but it does include pitfalls and complications. As with the previous pH tare method, water dissociation remains an assumed reaction and hydrogen and hydroxide ions are linked through the water dissociation constant, K_w. This is a common assumption in aqueous mixtures, but the complication inherent in this approach is that only one of the two species, hydrogen or hydroxide, may be part of the derived species basis. In most systems, the hydrogen ion is an appropriate derived species; other systems are more easily solved by inclusion of hydroxide as a derived species. The choice of hydrogen ion or hydroxide ion, selection of a set of independent reactions, and the choice of derived species in the reaction basis determines the effectiveness of the procedure.

In this work, for each mixture of interest, the reactions comprise independent sets and determine the derived species, thus the most appropriate reaction basis and derived species are predetermined. The one consideration required is the selection of hydroxide or hydrogen ion as derived specie. In most of the systems considered, the hydrogen ion is chosen as the derived species. The exceptions are most ammonia-water mixtures, particularly those with high mole fractions of ammonia, where the resultant aqueous solution is a strong base.

Solution of the chemical equilibrium problem requires descriptions of chemical equilibrium constants and activity coefficients. Chemical equilibria calculations are based on correlations describing chemical dissociation constants [5-7], with Pitzer's ion-interaction model [8] describing aqueous species activities.

CHEMICAL EQUILIBRIUM CONSTANTS

Published correlations by Maurer [153], Tsonopoulos, et al. [154], and Kawazuishi and Prausnitz [155], provide a quick method for calculating equilibrium constants as a function of temperature. The following correlation equations are used

$$pK_A = -\ln(K) = \frac{A}{T(K)} + B\ln(T(K)) + CT(K) + D \qquad (2.3\text{-}26)$$

$$pK_A = -\log_{10}(K) = \frac{A}{T(K)} + B\log_{10}(T(K)) + CT(K) + D \qquad (2.3\text{-}27)$$

with the coefficients for reactions of interest are summarized in Appendix E.

Prior to use the accuracy of these correlations were checked against literature sources. Millero [156] reported pK_1 values for the ionization of hydrogen sulfide (H_2S) at 25°C from 6.96 to 7.07. Although all three correlations return adequate values, 7.0033 [154] and 7.0225 [153, 155], at 25ºC, the correlation by Maurer [153] most accurately reflects the ionization constant over the entire temperature range of the experimental data reviewed [156]. Further evaluation with data given by Ellis, et al. [157] indicates that the correlation by Maurer [153] also more accurately characterizes HS^- ionization.

Similarly, based on data given by Ji, et al. [158-161] the carbamate (NH_2COO^-) reaction is found to be better represented by the correlation of Kawazuishi and Prausnitz [155].

Literature comparisons for sulfur dioxide (SO_2) reactions [139, 140, 162-164] and ammonia (NH_3) reactions [128, 155, 160, 165, 166] confirm the validity of the correlations for these reactions, and in all instances the best correlation is chosen for use.

SPECIES ACTIVITIES: MODELS AND CONVERSIONS

The chemical equilibrium problem requires activities of both soluble molecular and ionic components. The activities of molecular components are obtained from the equation of state, while ionic component activities are based on application of Pitzer's equations.

Molecular Component Activity Coefficients

The fundamental thermodynamic relation for activity coefficients, including the pressure-correction, or Poynting term [12], is given by

$$g_{i,x} = \frac{f_i^L(T,P)}{f_i^V(T,P)} \frac{P}{P_w} \exp\left[-\int_{P_w}^P \frac{u_i^{-\infty}}{RT} \, dP\right] \tag{2.3-28}$$

The relationships below are those necessary for conversion between mole fraction and molal compositions:

$$x_i = \frac{m_i}{\sum m_j} \tag{2.3-29}$$

$$g_w = x_w \, g_{w,x} \tag{2.3-30}$$

$$g_i = \left(\frac{55.6}{m_i} x_i\right) g_{i,x} \tag{2.3-31}$$

In these equations, $g_{i,x}$ is the activity coefficient of component i on the mole fraction scale; g_i is on a molal scale. For water, m_i is approximately 55.6 molal.

Electrolyte Activity Coefficients: Pitzer Equations

Pitzer's equations [44, 45] for the activity coefficients $\boldsymbol{g}_M$, $\boldsymbol{g}_X$ and $\boldsymbol{g}_N$ of cations, anions, and neutral species, respectively, are given by

$$
\begin{aligned}
\ln \boldsymbol{g}_M = {}& z_M^2 F + \sum_{a=1}^{N_a} m_a \left(2B_{Ma} + ZC_{Ma} \right) + \sum_{c=1}^{N_c} m_c \left(2\Phi_{Mc} + \sum_{a=1}^{N_a} m_a \boldsymbol{y}_{Mca} \right) \\
& + \sum_{a=1}^{N_a-1} \sum_{a'=a+1}^{N_a} m_a m_a \boldsymbol{y}_{a a'M} + \left| z_M \right| \sum_{c=1}^{N_c} \sum_{a=1}^{N_a} m_c m_a C_{ca} + \sum_{n=1}^{N_n} m_n \left(2\boldsymbol{I}_{nM} \right)
\end{aligned}
\tag{2.3-32}
$$

$$
\begin{aligned}
\ln \boldsymbol{g}_X = {}& z_X^2 F + \sum_{c=1}^{N_c} m_c \left(2B_{cX} + ZC_{cX} \right) + \sum_{a=1}^{N_a} m_a \left(2\Phi_{Xa} + \sum_{c=1}^{N_c} m_c \boldsymbol{y}_{Xac} \right) \\
& + \sum_{c=1}^{N_c-1} \sum_{c'=c+1}^{N_c} m_c m_c \boldsymbol{y}_{cc'X} + \left| z_X \right| \sum_{c=1}^{N_c} \sum_{a=1}^{N_a} m_c m_a C_{ca} + \sum_{n=1}^{N_n} m_n \left(2\boldsymbol{I}_{nX} \right)
\end{aligned}
\tag{2.3-33}
$$

$$
\ln \boldsymbol{g}_N = \sum_{c=1}^{N_c} m_c \left(2\boldsymbol{I}_{nc} \right) + \sum_{a=1}^{N_a} m_a \left(2\boldsymbol{I}_{na} \right)
\tag{2.3-34}
$$

The intermediate value in each of the equations, F, is related directly to the Debye-Hückel theory and given by

$$
\begin{aligned}
F = {}& -A^f \left(\frac{\sqrt{I}}{1+1.2\sqrt{I}} + \frac{2}{1.2} \ln \left(1 + 1.2\sqrt{I} \right) \right) \\
& + \sum_{c=1}^{N_c} \sum_{a=1}^{N_a} m_c m_a B'_{ca} + \sum_{c=1}^{N_c-1} \sum_{c'=c+1}^{N_c} m_c m_c \Phi'_{cc'} + \sum_{a=1}^{N_a-1} \sum_{a'=a+1}^{N_a} m_a m_a \Phi'_{aa'}
\end{aligned}
\tag{2.3-35}
$$

The osmotic coefficient, $\boldsymbol{f}$ is calculated as

$$\sum_i m_i (f-1) = 2 \left[\frac{-A^f I^{3/2}}{1+1.2\sqrt{I}} + \sum_{c=1}^{N_c} \sum_{a=1}^{N_a} m_c m_a \left(B_{ca}^f + ZC_{ca} \right) \right.$$

$$+ \sum_{c=1}^{N_c-1} \sum_{c'=c+1}^{N_c} m_c m_{c'} \left(\Phi_{cc'}^f + \sum_{a=1}^{N_a} m_a \Psi_{cc'a} \right)$$

$$+ \sum_{a=1}^{N_a-1} \sum_{a'=a+1}^{N_a} m_a m_{a'} \left(\Phi_{aa'}^f + \sum_{c=1}^{N_c} m_c \Psi_{aa'c} \right)$$

$$\left. + \sum_{n=1}^{N_n} \sum_{a=1}^{N_a} m_n m_a \boldsymbol{\lambda}_{na} + \sum_{n=1}^{N_n} \sum_{c=1}^{N_c} m_n m_c \boldsymbol{\lambda}_{nc} \right]$$

(2.3-36)

and the activity of water, a_w is given by

$$\ln a_w = -\frac{W}{1000} \left(\sum_i m_i \right) f$$

(2.3-37)

where $A^f = 2.303 (A/3)$. The Debye-Hückel parameter, A, is

$$A = -61.44534 \exp\left(\frac{T-273.15}{273.15} \right) + 2.864468 \left[\exp\left(\frac{T-273.15}{273.15} \right) \right]^2$$

$$+ 183.5379 \ln\left(\frac{T}{273.15} \right) - 0.6820223 (T - 273.15)$$

(2.3-38)

$$+ 0.0007875695 (T^2 - 273.15^2) + 58.95788 \left(\frac{273.15}{T} \right)$$

based on a correlation by Chen [46].

For each cation (M) - anion (X) pair, the second virial coefficients (B_{MX}, B'_{MX}, B_{MX}^f) are calculated from

$$B_{MX} = \boldsymbol{b}_{MX}^{(0)} + \boldsymbol{b}_{MX}^{(1)} \cdot g\left(\boldsymbol{a}_{MX} \sqrt{I} \right) + \boldsymbol{b}_{MX}^{(2)} \cdot g\left(12\sqrt{I} \right)$$

(2.3-39)

$$B'_{MX} = \boldsymbol{b}_{MX}^{(1)} \cdot g'\left(\boldsymbol{a}_{MX} \sqrt{I} \right) \Big/ I + \boldsymbol{b}_{MX}^{(2)} \cdot g'\left(12\sqrt{I} \right) \Big/ I$$

(2.3-40)

$$B_{MX}^f = B_{MX} + I \cdot B'_{MX}$$

(2.3-41)

In these equations, $b_{MX}^{(0)}, b_{MX}^{(1)}$ and $b_{MX}^{(2)}$ are constants determined from a fit of experimental data, I is the ionic strength of the solution, and the functions $g(x)$ and $g'(x)$ are evaluated as

$$g(x) = \frac{2\left[1-(1+x)e^{-x}\right]}{x^2} \tag{2.3-42}$$

and

$$g'(x) = -\frac{2\left[1-\left(1+x+\frac{x^2}{2}\right)e^{-x}\right]}{x^2} \tag{2.3-43}$$

For each cation-anion pair, the third virial coefficient C_{MX}, is

$$C_{MX} = \frac{C_{MX}^f}{2\sqrt{|z_M z_X|}} \tag{2.3-44}$$

where C_{MX}^f is a constant determined by a fit of experimental data.

For like charge interactions, the cation-cation and anion-anion second virial coefficients, represented by Φ_{ij}, Φ_{ij}', and Φ_{ij}^f, are defined as

$$\Phi_{ij} = q_{ij} + {}^E q_{ij}(I) \tag{2.3-45}$$

$$\Phi_{ij}' = {}^E q_{ij}'(I) \tag{2.3-46}$$

$$\Phi_{ij}^f = \Phi_{ij} + I\Phi_{ij}' \tag{2.3-47}$$

The ionic strength dependent functions, ${}^E q_{ij}(I)$ and ${}^E q_{ij}'(I)$, describe unsymmetrical mixing effects in terms of ionic charges and solvent properties [47, 48].

162

Pitzer Parameters

Implementation of the Pitzer model requires parameters based on ionic species interactions. For each cation-anion pair there are three second virial coefficient parameters, $\boldsymbol{b}_{MX}^{(0)}, \boldsymbol{b}_{MX}^{(1)}$, and $\boldsymbol{b}_{MX}^{(2)}$; the third virial coefficient parameter, C_{MX}^{f}; and a mixing parameter, $\boldsymbol{a}_{MX}$. Several additional parameters are also present in Pitzer's equations. The parameter $\boldsymbol{q}_{ij}$ incorporates influences of similarly charged ions, i.e. cation-cation or anion-anion interactions. The parameter Ψ_{ijk} represents a triplet interaction parameter describing cation-cation-anion, or anion-anion-cation interactions. A final parameter $\boldsymbol{l}_{ni}$ is available for incorporating neutral-ion specie interactions.

Pitzer model parameters for the species of interest are readily available from an extensive body of literature [17, 33, 37, 45, 49-51]. The values used in this work are provided in Appendix E.

COMPONENTS AND REACTIONS CONSIDERED

The molecular species included in this work are shown in Table 9. The list includes components which represent the principle pollutants in industrial wastewater streams from hydrocarbon processes [5, 6].

Table 9. Molecular Species

1	Water	H_2O
2	Ammonia	NH_3
3	Carbon Dioxide	CO_2
4	Hydrogen Sulfide	H_2S
5	Sulfur Dioxide	SO_2
6	Hydrogen Cyanide	HCN
7	Phenol	C_6H_5OH
8	Mercaptan	C_2H_5SH

The reactions and corresponding equilibrium relations considered for these species are given in Table 10. Although these are not the only possible reactions, they reflect the reactions believed to contribute to the primary electrolyte balance in aqueous mixtures with these molecular species [5, 6, 52].

Table 10. Chemical Reactions and Equilibrium Relations

Reaction	Equilibrium Relation
$H_2O \leftrightarrow H^+ + OH^-$	$K_1 = \dfrac{g_{H^+}[H^+] g_{OH^-}[OH^-]}{g_{H_2O}[H_2O]}$
$CO_2 + H_2O \leftrightarrow H^+ + HCO_3^-$	$K_2 = \dfrac{g_{H^+}[H^+] g_{HCO_3^-}[HCO_3^-]}{g_{CO_2}[CO_2] g_{H_2O}[H_2O]}$
$HCO_3^- \leftrightarrow H^+ + CO_3^{-2}$	$K_3 = \dfrac{g_{H^+}[H^+] g_{CO_3^{-2}}[CO_3^{-2}]}{g_{HCO_3^-}[HCO_3^-]}$
$H_2S \leftrightarrow H^+ + HS^-$	$K_4 = \dfrac{g_{H^+}[H^+] g_{HS^-}[HS^-]}{g_{H_2S}[H_2S]}$
$HS^- \leftrightarrow H^+ + S^{-2}$	$K_5 = \dfrac{g_{H^+}[H^+] g_{S^{-2}}[S^{-2}]}{g_{HS^-}[HS^-]}$
$SO_2 + H_2O \leftrightarrow H^+ + HSO_3^-$	$K_6 = \dfrac{g_{H^+}[H^+] g_{HSO_3^-}[HSO_3^-]}{g_{SO_2}[SO_2] g_{H_2O}[H_2O]}$
$HSO_3^- \leftrightarrow H^+ + SO_3^{-2}$	$K_7 = \dfrac{g_{H^+}[H^+] g_{SO_3^{-2}}[SO_3^{-2}]}{g_{HSO_3^-}[HSO_3^-]}$
$NH_3 + H_2O \leftrightarrow NH_4^+ + OH^-$	$K_8 = \dfrac{g_{NH^+}[NH^+] g_{OH^-}[OH^-]}{g_{NH_3}[NH_3] g_{H_2O}[H_2O]}$
$NH_3 + HCO_3^- \leftrightarrow NH_2COO^- + H_2O$	$K_9 = \dfrac{g_{NH_2COO^-}[NH_2COO^-] g_{H_2O}[H_2O]}{g_{NH_3}[NH_3] g_{HCO_3^-}[HCO_3^-]}$
$HCN \leftrightarrow H^+ + CN^-$	$K_{10} = \dfrac{g_{H^+}[H^+] g_{CN^-}[CN^-]}{g_{HCN}[HCN]}$
$C_6H_5OH \leftrightarrow H^+ + C_6H_5O^-$	$K_{11} = \dfrac{g_{H^+}[H^+] g_{C_6H_5O^-}[C_6H_5O^-]}{g_{C_6H_5OH}[C_6H_5OH]}$
$C_2H_5SH \leftrightarrow H^+ + C_2H_5S^-$	$K_{12} = \dfrac{g_{H^+}[H^+] g_{C_2H_5S^-}[C_2H_5S^-]}{g_{C_2H_5SH}[C_2H_5SH]}$

The cations and anions present in the reaction equilibrium relations are given in Table 11. Additional cations and anions appear in the tables to include the salts (strong electrolytes) from elements present in natural waters.

Table 11. Ionic Species

Cations		Anions	
Hydrogen	H^+	Hydroxide	OH^-
Ammonium	NH_4^+	Hydrogen Carbonate	HCO_3^-
Lithium	Li^+	Carbonate	CO_3^{2-}
Sodium	Na^+	Hydrogen Sulfide	HS^-
Potasium	K^+	Sulfide	S^{2-}
Magnesium	Mg^{2+}	Sulfite	HSO_3^-
Calcium	Ca^{2+}	Sulfate	SO_3^{2-}
Barium	Ba^{2+}	Carbamide	NH_2COO^-
Iron	Fe^{2+}	Cyanide	CN^-
		Phenyl	$C_6H_5O^-$
		Ethyl Sulfide	$C_2H_5S^-$
		Chloride	Cl^-
		Bromide	Br^-
		Sulfate	SO_4^{2-}

SUMMARY

A framework for the solution of vapor-liquid equilibria for aqueous electrolyte mixtures is outlined. An outer loop models molecular based vapor-liquid equilibria (VLE) with the Soave-Redlich-Kwong (SRK) cubic equation of state. The extent of dissociation of reactive liquid phase species is calculated in an inner loop modeling aqueous chemical equilibrium with chemical dissociation constants and the Pitzer activity coefficient model.

Solution of the inner loop chemical equilibrium problem is by either a pH-based bisection algorithm or a matrix-based Newton-Raphson method. The inner loop solution to the aqueous chemical equilibrium problem provides a more accurate description of the true aqueous molecular mole fractions for use in the outer VLE loop.

REFERENCES

1.   Friedemann, J.D., Ph.D. Dissertation, *The Simulation of Vapor-Liquid Equilibria in Ionic Systems*, School of Chemical Engineering, Oklahoma State University, Stillwater, Oklahoma, 1987.

2.   Chen, H., J. Wagner, and J.D. Friedemann. *Phase Equilibria in Aqueous Acid Gas Systems.* in *Seventy-Third GPA Annual Convention*. 1994. New Orleans, Louisiana.

3.   Soave, G., *Equilibrium Constants from a Modified Redlich-Kwong Equation of State.* Chemical Engineering Science, 1972. 27: p. 1197-1203.

4.   Soave, G., *20 Years of Redlich-Kwong Equation of State.* Fluid Phase Equilibria, 1993. 82: p. 345-359.

5.   Maurer, G., *Thermodynamics of Aqueous Systems with Industrial Application.* ACS Symposium Series, ed. S.A. Newman. Vol. 133. 1980: ACS pgs.

6.   Tsonopoulos, C., D.M. Coulson, and L.B. Inman, *Ionization Constants of Water Pollutants.* Journal of Chemical and Engineering Data, 1976. 21(No. 2): p. 190-193.

7.   Kawazuishi, K., Prausnitz, John M., *Correlation of Vapor-Liquid Equilibria for the System Ammonia-Carbon Dioxide-Water.* Ind. Eng. Chem. Res., 1987. 26: p. 1482-1485.

8.   Pitzer, K.S., *Theory: Ion Interaction Approach.* p. 157.

9.   Reid, R.C., J.M. Prausnitz, and B.E. Poling, *The Properties of Gases & Liquids.* Fourth ed. 1987, New York: McGraw-Hill, Inc. 741 pgs.

10.   Graboski, M.S. and T.E. Daubert, *A Modified Soave Equation of State for Phase Equilibrium Calculations. 1. Hydrocarbon Systems.* Industrial & Engineering Chemical Process Design and Development, 1978. 17: p. 86-91.

11.   Graboski, M.S. and T.E. Daubert, *A Modified Soave Equation of State for Phase Equilibrium Calculations. 2. Systems Containing CO_2, H_2S, N_2, and CO.*

Industrial & Engineering Chemical Process Design and Development, 1978. 17: p. 91-97.

12.   Prausnitz, J.M., R.N. Lichtenthaler, and E.G. de Azevedo, *Molecular Thermodynamics of Fluid-Phase Equilibria*. Second ed. 1986, Englewood Cliffs, New Jersey: PTR Prentice Hall. 600 pgs.

13.   Gundersen, T., *Numerical Aspects of the Implementation of Cubic Equations of State in Flash Calculation Routines*. Computers in Chemical Engineering, 1982. 6(3): p. 245-255.

14.   Nghiem, L.X., K. Aziz, and Y.K. Li, *A Robust Iterative Method for Flash Calculations Using the Soave-Redlich-Kwong or the Peng-Robinson Equation of State.* 1983: p. 521.

15.   Anderson, G.M. and D.A. Crerar, *Thermodynamics in Geochemistry The Equilibrium Model*. 1993, New York: Oxford University Press. 588 pgs.

16.   Nordstrom, D.K., et al., *A comparison of Computerized Chemical Models for Equilibrium Calculations in Aqueous Systems*, in *Chemical Modeling in Aqueous Systems*, E.A. Jenne, ed., Editor. 1979, American Chemical Society: Washingon, D.C.

17.   Wolery, T.J., *Calculation of chemical equilibrium between aqueous solution and minerals: the EQ3/6 software package*. 1979, Lawrence Livermore Laboratory.

18.   Smith, W.R. and R.W. Missen, *Strategies for Solving the Chemical Equilibrium Problem and an Efficient Microcomputer-Based Algorithm.* Canadian Journal of Chemical Engineering, 1988. 66(August): p. 591.

19.   Reed, M.H., *Calculation of multicomponent chemical equilibria and reaction processes in systems involving minerals, gases, and an aqueous phase.* Geochimica et Cosmochimica Acta, 1982. 46: p. 513-528.

20.   Nordstrom, D.K. and J.L. Munoz, *Geochemical Thermodynamics*. 1985, Menlo Park, CA: Benjamin/Cummings. 477 pgs.

21.   Chen, H. and J. Wagner. *Vapor-Liquid Equilibria of the Aqueous Solution of Weak Volatile Electrolytes*. in *Proceedings of the 73rd Annual GPA Convention*. 1994. New Orleans, Louisiana.

22.   Leung, V.W.-H., B.W. Darvell, and A.P.-C. Chan, *A Rapid Algorithm for Solution of the Equations of Multiple Equilibrium Systems -- Rameses*. Talania, 1988. 35(9): p. 713-718.

23.   Wada, S.-I. and H. Seki, *A Compact Computer Code for Ion Speciation in Aqueous Solutions Based on a Robust Algorithm*. Soil Sci. Plant Nutr., 1994. 40(1): p. 165-172.

24.   Lin, F., M.S., *Vapor-Liquid Equilibrium in Aqueous Solutions Containing Weak and Strong Electrolytes*, Chemical Engineering, Oklahoma State University, Stillwater, Oklahoma, 1994.

25.   Crerar, D.A., *A method for computing multicomponent chemical equilibria based on equilibrium constants*. Geochimica et Cosmochimica Acta, 1975. 39: p. 1375-1384.

26.   Fleming, G.W. and L.N. Plummer, *PHRQINPT-An Interactive Computer Program for Constructing Input Data Sets to the Geochemical Simulation Program PHREEQE*. 1983, U. S. Geological Survey.

27.   Brown, P.L., et al., *HARPHRQ: A geochemical speciation program based on PHREEQE*. 1991.

28.   Ball, J.W., E.A. Jenne, and D.K. Nordstrom, *WATEQ2-A Computerized Chemical Model for Trace and Major Elements Spciation and Mineral Equilibria of Natural Waters*, in *Chemical Modeling in Aqueous Systems*, E.A. Jenne, Editor. 1979, Americal Chemical Society: Washington, D.C. p. 815-835.

29.   Ball, J.W., E.A. Jenne, and M.W. Cantrell, *WATEQ3 - A geochemical model with uranium added*. 1981, US Geological Survey.

30. Ball, J.W., D.K. Nordstrom, and D.W. Zachmann, *WATEQ4F - A personal computer FORTRAN translation of the geochemical model WATEQ2 with revised data base*. 1987, US Geological Survey.

31. Ball, J.W. and D.K. Nordstrom, *WATEQ4FD-User's manual with revised thermodynamic database and test cases for calculating speciation of major, trace, and redox elements in natural waters*. 1991, U.S. Geological Survey.

32. Allison, J.D., D.S. Brown, and K.J. Novo-Gradae, *MINTEQA2/PRODEFA2, A Geochemical Assesment Model for Environmental Systems: Version 3.0 User's Manual*. 1991, Environmental Research Laboratory, Office of Research and Development, U.S. Environmental Protection Agency: Athens, GA. p. 1-115.

33. Kharaka, Y.K., et al., *SOLMINEQ. 88: A Computer Program for Geochemical Modeling of Water-Rock Interactions*. 1988, U. S. Geological Survey: Menlo Park, California.

34. Parkhurst, D.L., D.C. Thorstenson, and L.N. Plummer, *PHREEQE: a computer program for geochemical calculations*. 1980, US Geological Survey.

35. Parkhurst, D.L., *User's Guide to PHREEQCPHREEQC - A computer program for speciation, reaction path, advective-transport and inverse geochemical calculations*. 1995, US Geological Survey.

36. Parkhurst, D.L. and C.A.J. Appelo, *User's Guide to PHREEQC (Version 2) - A Computer Program for Speciation, Batch-Reaction, One-Dimensional Transport, and Inverse Geochemical Calculations*. 1999, U.S. Department of the Interior - U.S. Geological Survey: Denver, CO. p. 1-326.

37. Perkins, E.H., et al., *Geochemical Modeling of Water-Rock Interaction Using SOLMINEQ.88*, in *Chemical Modeling of Aqueous Systems II*, D.C. Melchior and R.L. Bassett, Editors. 1990, American Chemical Society: Washington, D.C.

38. Plummer, L.N., B.F. Jones, and A.H. Truesdell, *WATEQF: a FORTRAN IV version of WATEQ, a computer program for calculating chemical equilibria in natural waters*. 1976, US Geological Survey.

39.   Plummer, L.N. and D.L. Parkhurst, *Application of the Pitzer Equations to the PHREEQE Geochemical Model*, in *Chemical Modeling of Aqueous Systems II*, D.C. Melchior and R.L. Bassett, Editors. 1990, American Chemical Society: Washington, D.C.

40.   Plummer, L.N., et al., *A computer program incorporating Pitzer's equations for calculation of geochemical reactions in brines*. 1988, US Geological Survey.

41.   Rao, Y.K., *IECMQ: A Computer Program for Calculating Equilibrium-State in Aqueous Systems.* Marine Chemistry, 2000. 70: p. 61-78.

42.   Woolery, T.J., *EQ3/6, A Software Package for Geochemical Modeling of Aqueous Systems: Package Overview and Installation Guide (Version 7.0)*. 1992, Lawrence Livermore National Laboratory, University of California: Livermore, CA. p. 1-74.

43.   Woolery, T.J., *EQ3NR, A Computer Program for Geochemical Aqueous Speciation-Solubility Calculations: Theoretical Manual, User's Guide, and Related Documentation (Version 7.0)*. 1992, Lawrence Livermore National Laboratory, University of California: Livermore, CA. p. 1-262.

44.   Pitzer, K.S., *Thermodynamics of Electrolytes. I. Theoretical Basis and General Equations.* The Journal of Physical Chemistry, 1973. 77(2): p. 268-277.

45.   Pitzer, K.S., *Activity Coefficients in Electrolyte Solutions*. Second ed. 1991, Boca Raton, Florida: CRC Press. 542 pgs.

46.   Chen, C.-C., et al., *Local Composition Model for Excess Gibbs Energy of Electrolyte Systems.* AIChE Journal, 1982. 28(4): p. 588.

47.   Pitzer, K.S., *Theoretical Considerations of Solubility with Emphasis on Mixed Aqueous Electrolytes.* Pure & Applied Chemistry, 1986. 58(12): p. 1599-1610.

48.   Pitzer, K.S., *Thermodynamics of Electrolytes. V. Effects of Higher-Order Electrostatic Terms.* Journal of Solution Chemistry, 1975. 4(No. 3): p. 249-265.

49.   Siddiqi, M.A., J. Krissmann, and K. Lucas, *A new fibre optic-based technique for the spectrophotometric measurement of phase and chemical equilibria in aqueous*

solutions of volatile weak electrolytes. Fluid Phase Equilibira, 1997. 136: p. 185-195.

50. Millero, F.J., *The Thermodynamics and Kinetics of the Hydrogen Sulfide System in Natural Waters.* Marine Chemistry, 1996. 18: p. 121--147.

51. Kuhn, M., et al., *Modeling chemical brine-rock interaction in geothermal reservoirs.* 2002.

52. Wilson, G.M. and E.W.Y. Wayne, *GPSWAT GPA Sour Water Equilibria Correlation and Computer Program.* 1990, Gas Processors Association: Tulsa.

CHAPTER IV

MODEL APPLICATION

An approach developed by Friedemann [1], and extended by Chen, et al. [2] describes phase equilibrium in aqueous solutions containing weak electrolytes. Molecular and chemical equilibria are calculated in two loops. An inner, nested loop for chemical equilibrium determines the extent of dissociation of reactive molecular species, and an outer loop calculates vapor-liquid equilibrium. In this work vapor-liquid equilibrium calculations are performed using the Soave-Redlich-Kwong equation of state [3, 4]. Chemical equilibria are calculated from correlations describing chemical reaction dissociation constants [5-7] and Pitzer's ion-interaction model [8] to describe aqueous ionic species activities.

In this modeling approach, numerous fitting parameters are available broadly characterized as interactions between (1) between molecular species, (2) between ionic species, and (3) molecular and ionic species interactions. The principle goal in this study is an evaluation of the applicability of a common cubic equation of state, the Soave-Redlich-Kwong (SRK) equation of state, to model aqueous electrolyte mixtures. Only the binary interaction parameters (C_{ij} and D_{ij}) incorporated in the mixing rules for the cubic equation of state are employed as fitting parameters. Calculations could possibly be improved by the application of more complex mixing rules [9-14], but two aspects argue against the added complexity. As pointed out by Gerdes, et al. [15] errors in calculating phase equilibria are often larger than those in non-reacting systems due in part to larger

174

errors in the experimental data. Another complication includes the inherent limitations of cubic equations of state in modeling polar and strongly polar liquid phases. In order to construct a broadly applicable model, only the binary interaction parameters of the cubic equation of state are regressed for volatile electrolytes.

Determining appropriate binary interaction parameters requires reliable experimental vapor-liquid equilibrium data for these mixtures. These experimental datasets for parameter regressions are chosen from available literature, with consideration given to dataset accuracy as evaluated by other researchers, and, in this work, by comparison of the consistency of the available datasets.

The water - carbon dioxide (CO_2) system is perhaps the most thoroughly researched aqueous system with references far too numerous to list. In this work, the experimental data for the water - carbon dioxide (CO_2) regression calculations are based on the measurements of Takenouichi and Kennedy, Crovetto, and Carroll, et al. [16-19]. These datasets provide overlapping measurements covering a broad range of temperature, pressure, and composition.

The aqueous ammonia (NH_3) system is also widely researched. The experimental data of Muller, et al. is consistent with additional data from Gillespie who reviewed work published prior to 1985 [20, 21].

Water - hydrogen sulfide (H_2S) experimental data covering broad composition, temperature, and pressure ranges are from Lee and Mather [22].

The data of Rabe and Harris [23], as suggested by Goldberg and Parker [24] in their thermodynamic analysis, are combined with data from Rumpf and Maurer [25] to serve as the regression database for the water - sulfur dioxide (SO_2) binary.

Experimental data for the water - hydrogen cyanide (HCN) mixture system are from Rumpf and Maurer [25] and for the water - phenol (C_6H_5OH) binary from Onken [26].

The binary interaction parameters of the equation of state are fit by minimization of an objective function based on pressure

$$O = \sum_{i=1}^{NPTS} \left(\frac{P^{cal} - P^{\exp}}{P^{\exp}} \right)_i \qquad (2.4\text{-}1)$$

where, P is the total system pressure. In this objective function, the superscripts *exp* and *cal* refer to experimental and calculated values respectively. A FORTRAN subroutine for nonlinear least squares regression, MARQ [27], is incorporated into the primary program for this parameter regression.

Binary data fitting

The dissociation of a single molecular solute from weak electrolytes such as carbon dioxide, ammonia, etc. is relatively small in terms of the overall composition of any binary aqueous mixture. These chemical dissociations, particularly in the low and intermediate solute concentration range, do not appreciably affect the overall vapor-liquid equilibrium mass balance of the system considered. Binary system parameter regressions therefore act as indicators of the equation-of-state applicability to model the strong polar and associative effects present in electrolyte mixtures.

The summary of the regression calculations are given in Table 12. With experimental pressures commonly ranging over several orders of magnitude, there is no single method to quantify an average, or overall, "goodness of fit". Percentage errors tend to emphasize low-pressure results, while absolute deviations emphasize model deviations in high-pressure data. As shown, the model is able to predict the system pressure within 8% for any of the binary aqueous electrolyte mixtures. While the absolute average percent deviation and the bias of the error provide numerical quantifications, graphical examinations are useful in assessing the overall results.

The quality of the model fit for aqueous carbon dioxide mixtures is shown in Figure 44. Some of the experimental data available in the literature are reported in measurements of partial pressure of a system component or components [16, 17]. Available experimental carbon dioxide and water partial pressures from two references are shown in Figure 45. The experimental partial pressure data exhibit larger uncertainty than overall system pressure measurements. Due to the lower quality of experimental partial pressure data, as illustrated by Figure 45, all regression calculations are based on experimental total pressure.

Table 12 Binary Interaction Parameter Fitting

| Solute | Number of Data Points | Range of Experimental Data | | Pressure Error Measures | | | | | |
		T(K)	P (Bar)	%BIAS	AAPD	C_{ij}^{o}	C_{ij}^{1}	D_{ij}^{o}	D_{ij}^{1}
CO_2	279	273.15 - 623.15	1.540 - 3500	-1.1	1.2	0.429	-130	0.0	0.0
NH_3	73	313.15 - 588.7	1.538 - 217.8	-0.7	1.7	-0.003	0.00035	0.0	0.0
H_2S	325	283.2 - 453.2	1.548 - 66.7	-1.2	1.3	0.383	-88.70	0.0	0.0
SO_2	57	313.11 393.3	0.860 25.09	-4.1	4.4	-0.500	-157.6	0.0	0.0
C_6H_5OH	22	317.55 - 317.55	0.012 - 0.094	0.3	2.8	-0.003	-0.0018	-0.0005	0.0
HCN	49	313.13 - 413.14	0.269 - 4.844	-1.5	2.9	0.3274	32.16	0.5	0.0

Definitions of Error Measures:

$$\% Bias = \frac{100}{n} \sum_{n} \frac{P_{calc} - P_{Exp}}{P_{Exp}}$$

$$AAPD = \frac{100}{n} \sum_{n} \frac{|P_{calc} - P_{Exp}|}{P_{Exp}}$$
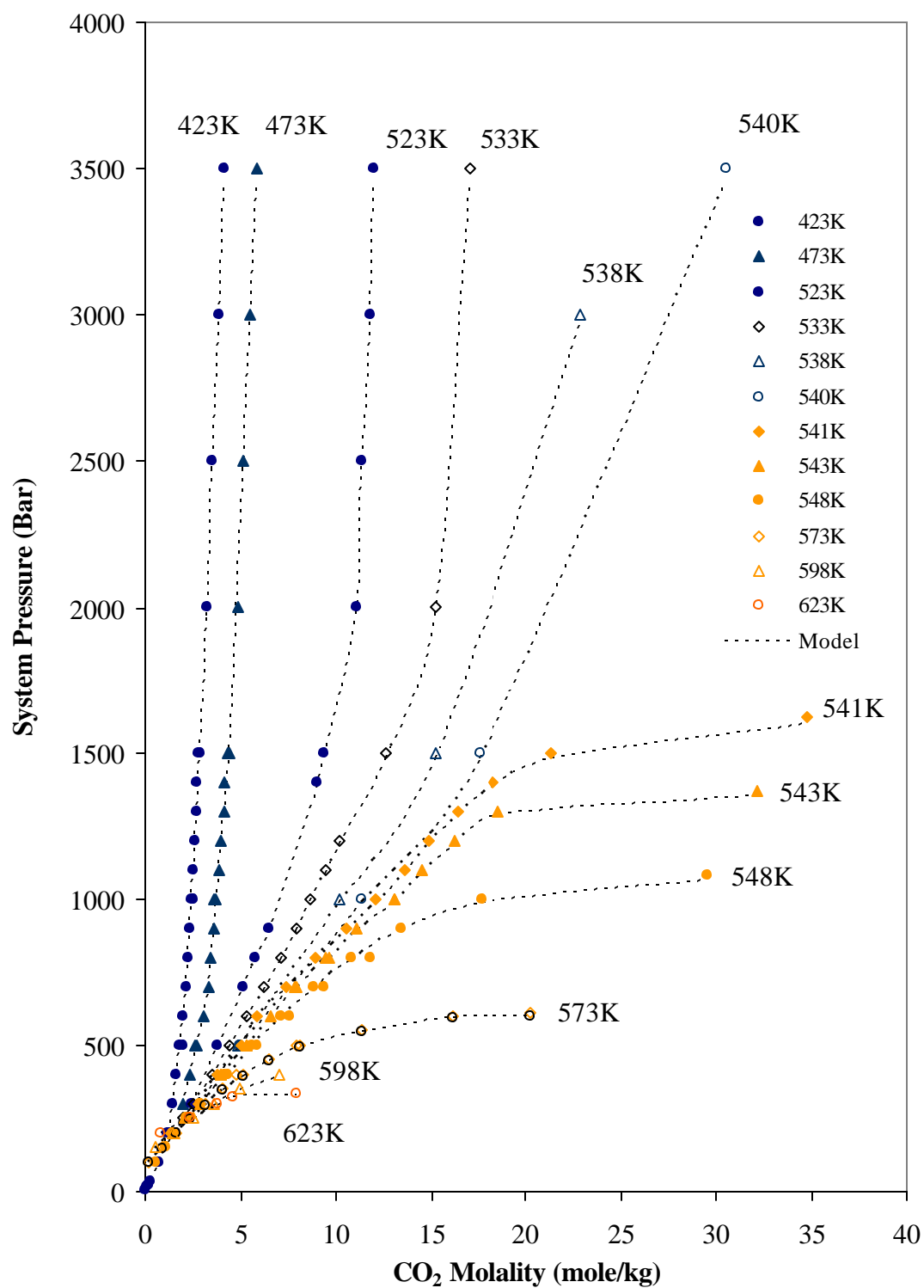
Figure 44. High Temperature Aqueous Carbon Dioxide
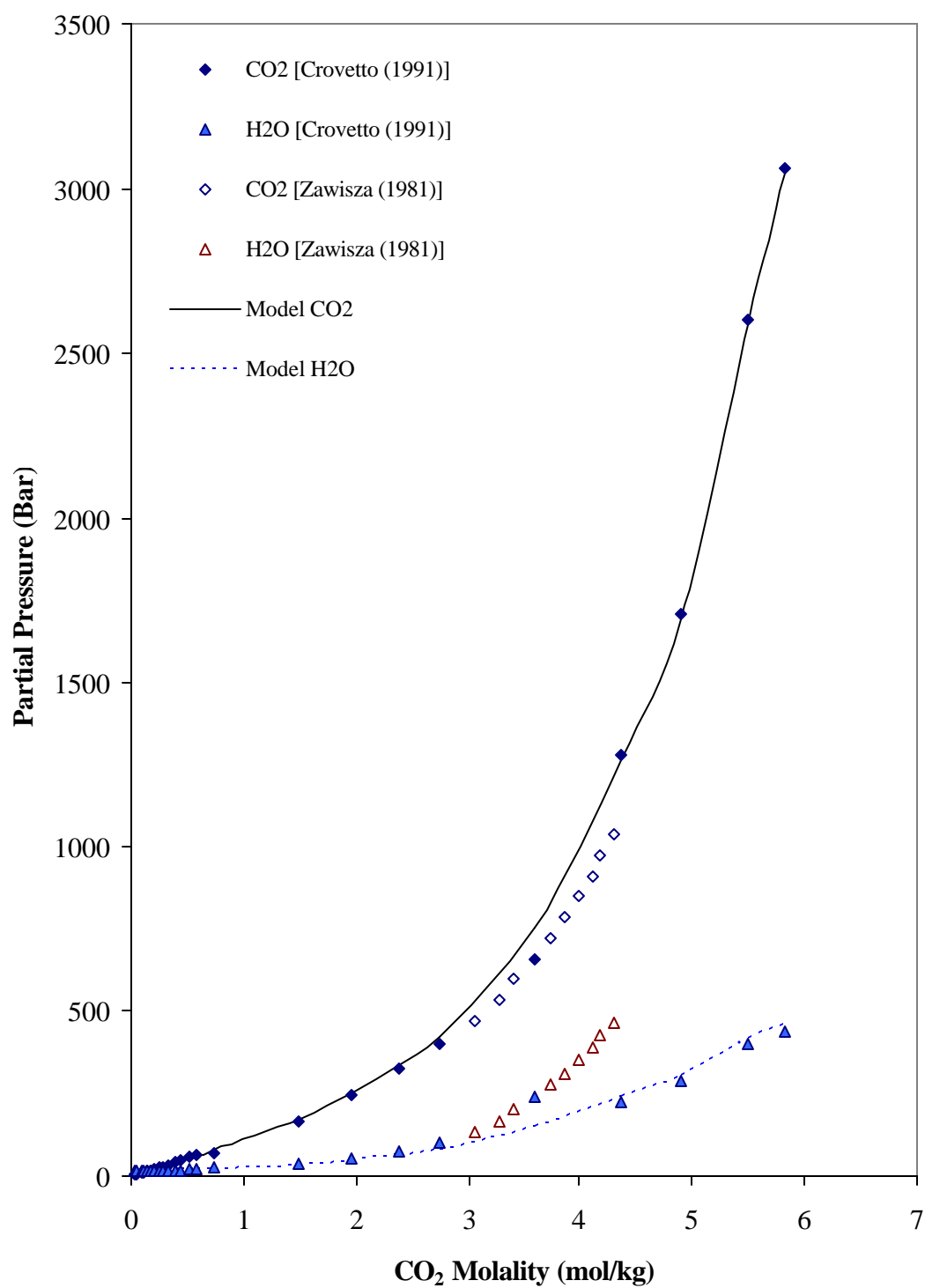
Figure 45. Carbon Dioxide and Water Partial Pressures at 473K

Qualities of fitting results for the sulfur dioxide - water system are shown in Figure 46 and results for the hydrogen sulfide - water system are shown in Figure 47. Model predictions compare favorably with the experimental data for both mixtures, without discernable deviations as a function of temperature, pressure, or concentration.

The model fits for the hydrogen cyanide - water system, shown in Figure 48, exhibit deviations as a function of concentration and temperature. At higher hydrogen cyanide concentrations, the model underpredicts experimental pressure. At low concentrations, the pressure calculation is slightly higher than experimental values. Model deviations also increases at lower temperatures. Overall, the deviation in the model is 2.9%, but model p`redictions do not accurately reflect experimental data. Additional experimental data for the hydrogen cyanide - water system is necessary to determine the source of the model error.

The quality of fit for ammonia - water systems is shown in Figure 49. The ammonia - water systems include points where ammonia concentrations are higher than the concentration range for which available Pitzer parameters were determined. Despite application of the Pitzer model to compositions outside these concentration ranges, model calculations compare favorably to the experimental data.

Additional results for the regression database and prediction comparisons of other weak electrolyte experimental data are available in Appendix H.
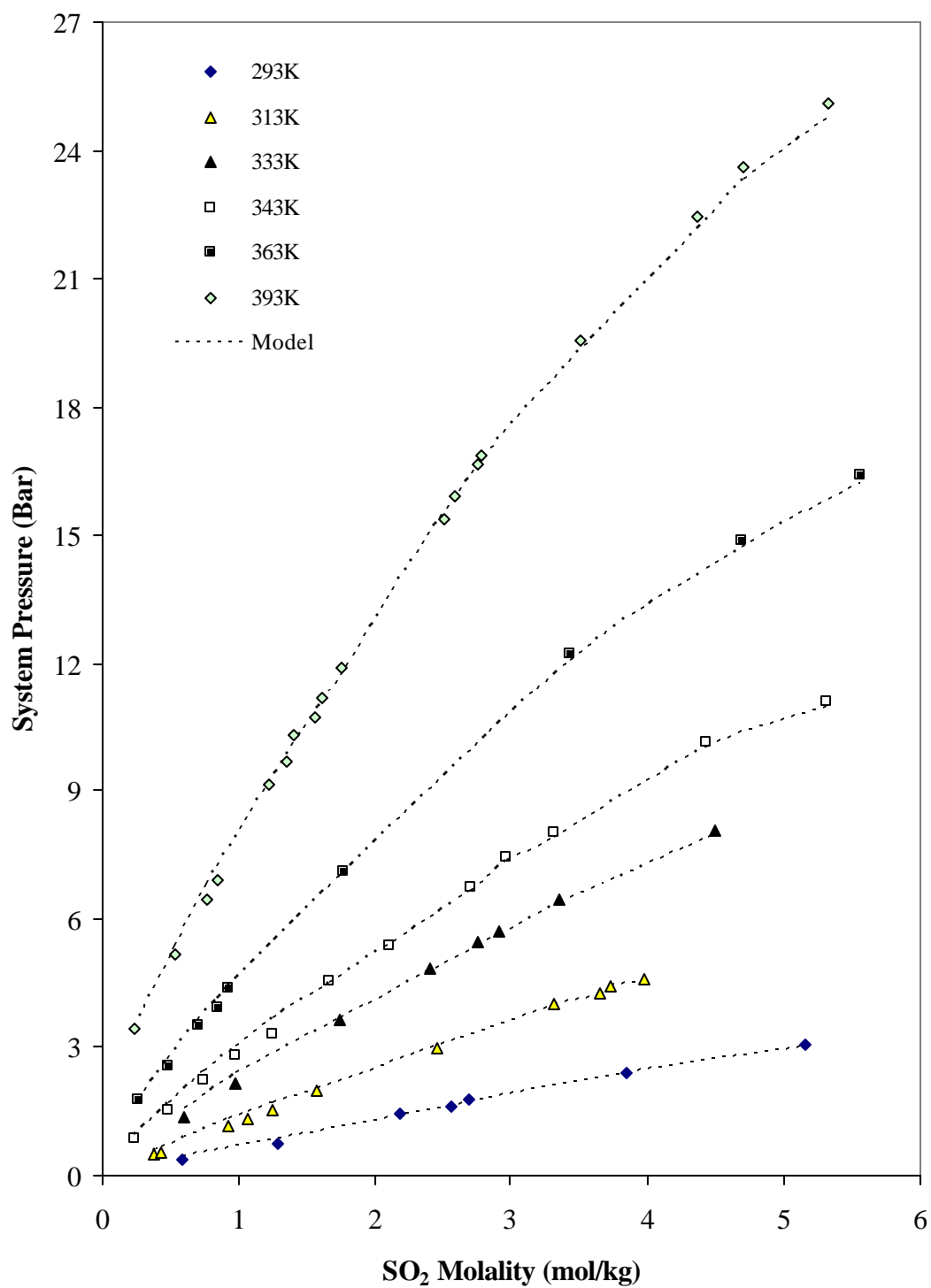
Figure 46. Aqueous Sulfur Dioxide

182
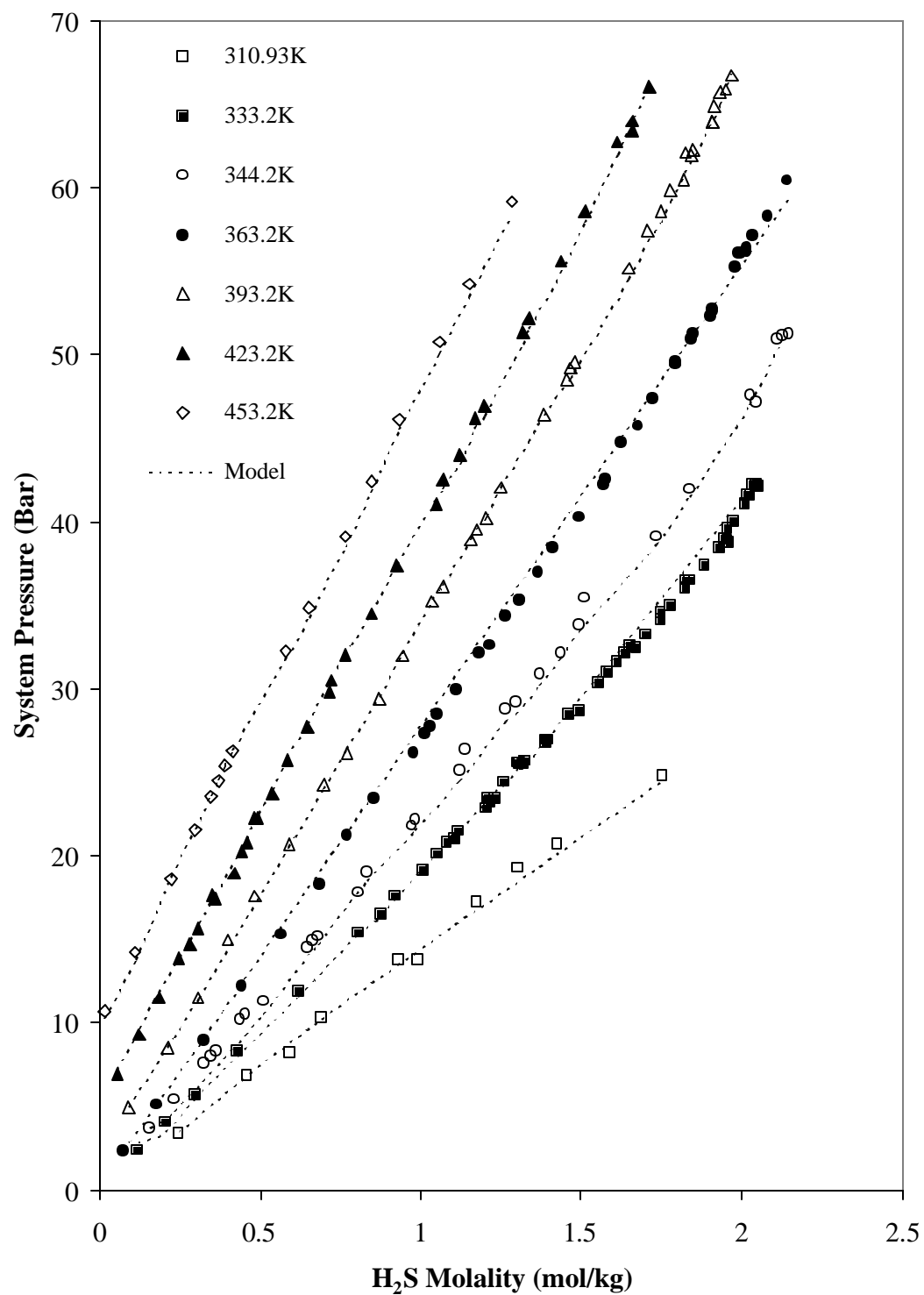
Figure 47. Aqueous Hydrogen Sulfide
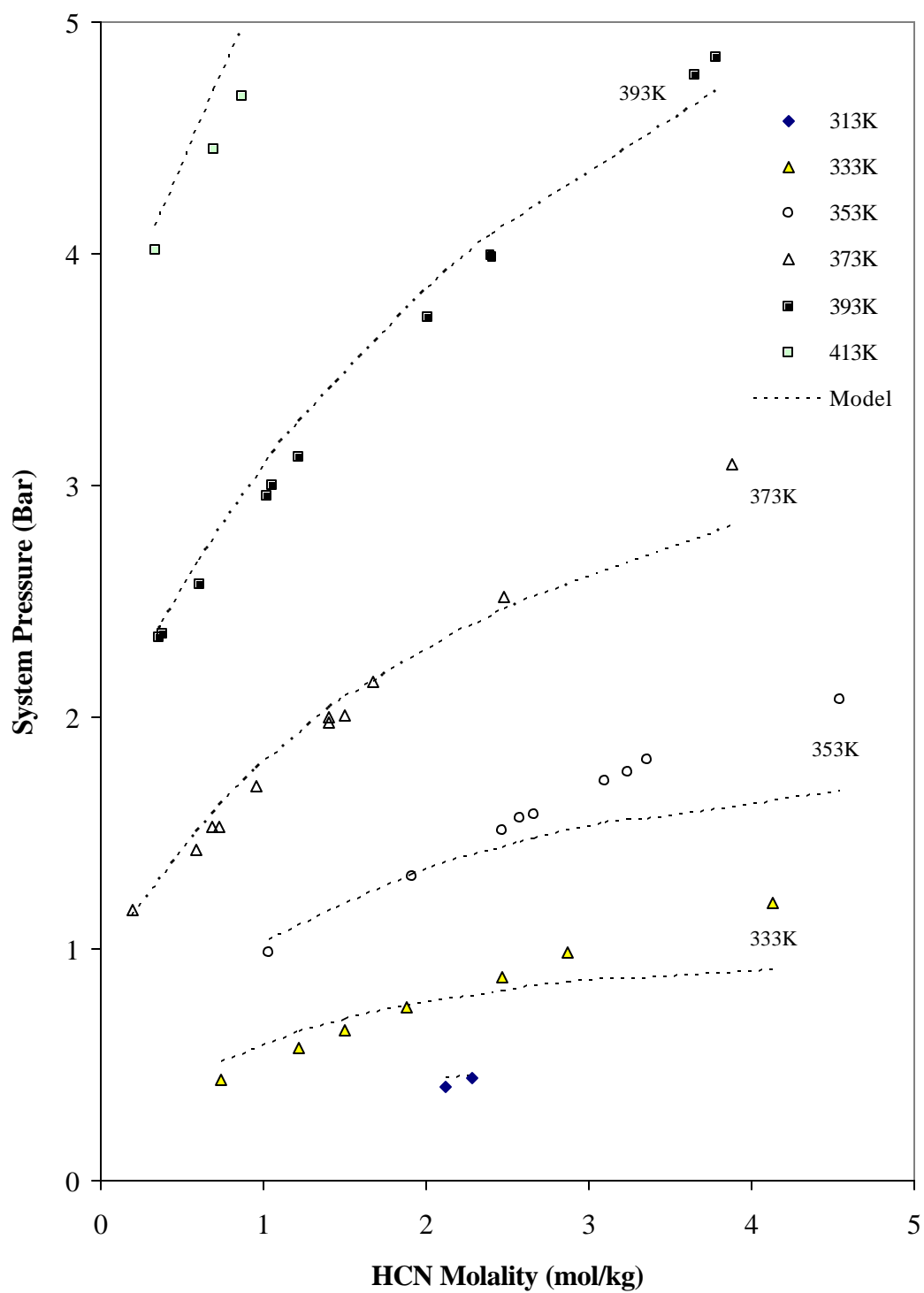
Figure 48. Aqueous Hydrogen Cyanide
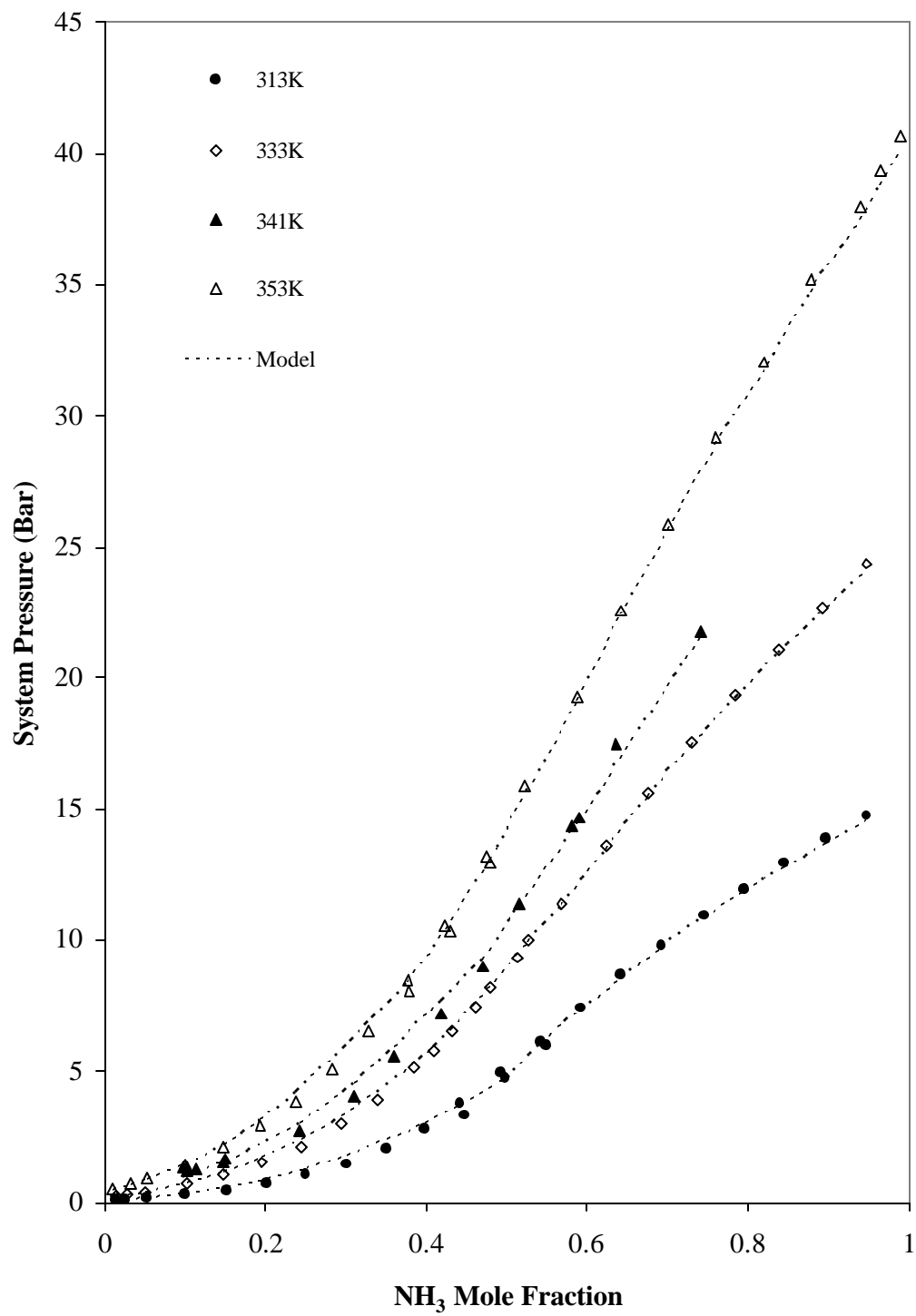
Figure 49. Aqueous Ammonia

185

WEAK ELECTROLYTE EQUILIBRIA IN AQUEOUS STRONG ELECTROLYTE MIXTURES

Ionic species dissociating from strong electrolytes, such as NaCl, have a significant influence on vapor-liquid equilibrium. The activity coefficient model in this work, Pitzer's equations, allows incorporation of strong electrolyte effects into the chemical equilibrium calculations. No additional modifications to the vapor-liquid equilibrium calculations, other than the previously regressed binary interaction coefficients, are required to incorporate salt effects on the vapor-liquid equilibrium calculation.

To evaluate the applicability of the model to these mixtures, numerous sources of experimental data for each of the weak electrolytes of interest in the presence of a strong electrolyte are examined. Table 13 provides a summary of carbon dioxide - salt mixture predictions.

Experimental data for aqueous carbon dioxide in aqueous sodium chloride (NaCl) mixtures from Nighswander, et al. [29], Rumpf, et al. [28], and Takenouchi and Kennedy [16] are predicted with deviations of less than 1.5 %.

Figure 50 provides an example of the salting out effect on carbon dioxide in 1.1 and 4.3 molal mixtures of NaCl with comparisons to the experimental data of Takenouchi and Kennedy [16]. Model predictions of the salting out effect of NaCl agree to 1% with experimental isotherms.

Data from Prutton and Savage [30] for calcium chloride ($CaCl_2$), including experimental data for the salt-free CO_2-H_2O binary, are accurately predicted by the model. Figure 51 shows model predictions at several molal concentrations of $CaCl_2$ for isotherms at 347 K.

The salting out effect on the aqueous carbon dioxide equilibria is well predicted by the model. The experimental data shown for the salt-free carbon dioxide - water mixture are also well represented by model predictions.

Table 13. CO_2 Equilibrium in Strong Electrolyte Mixtures

Salt (mol/kg)	# Pts	Range of Data T(K)	P (Bar)	Error Measures %BIAS	AAPD	Ref
NaCl						
4.0 - 6.0	50	313.1 - 433.0	6.02 - 96.4	-0.4%	0.9%	[28]
1.1 - 4.3	78	423.2 - 623.2	100.0 - 1400	-1.0%	1.0%	[29]
0.2 - 0.2	34	353.2 - 473.7	21.1 - 100.3	-1.5%	1.5%	[16]
$CaCl_2$						
0.0 - 3.9	156	348.7 - 394.2	15.2 - 885.6	-0.8%	0.9%	[30]
Na_2SO_4						
1.0 - 2.0	102	313.1 - 433.2	4.22 - 97.1	-0.3%	1.0%	[31]
0.21 - 2.21	26	288.2 - 308.2	1.013 - 1.013	-11.9%	11.9%	[33]
1.0 - 3.3	14	323.2 - 348.2	16.40 - 197.3	-1.2%	1.2%	[32]
$(NH_4)_2SO_4$						
2.0 - 4.0	80	313.1 - 433.1	5.18 - 98.7	-0.4%	1.1%	[31]
0.25 - 3.87	31	288.2 - 308.2	1.013 - 1.013	-10.9%	10.9%	[33]
Na_2SO_4 & $(NH_4)_2SO_4$						
1.0 + 1.0	35	313.2 - 433.2	5.04 - 96.7	-0.5%	1.0%	[31]
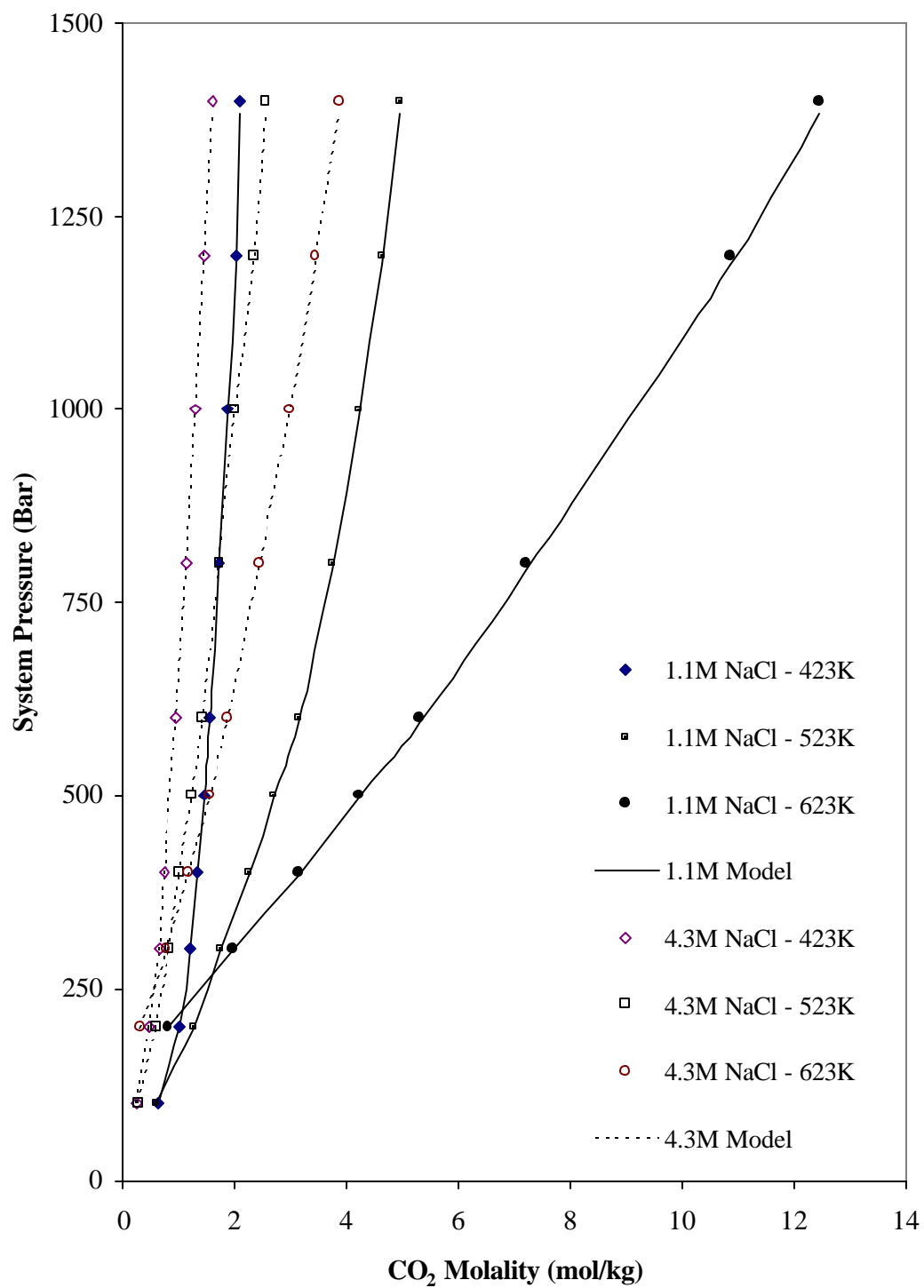
Figure 50. CO_2 in 1.1 molal and 4.3 molal Sodium Chloride (NaCl) Mixtures
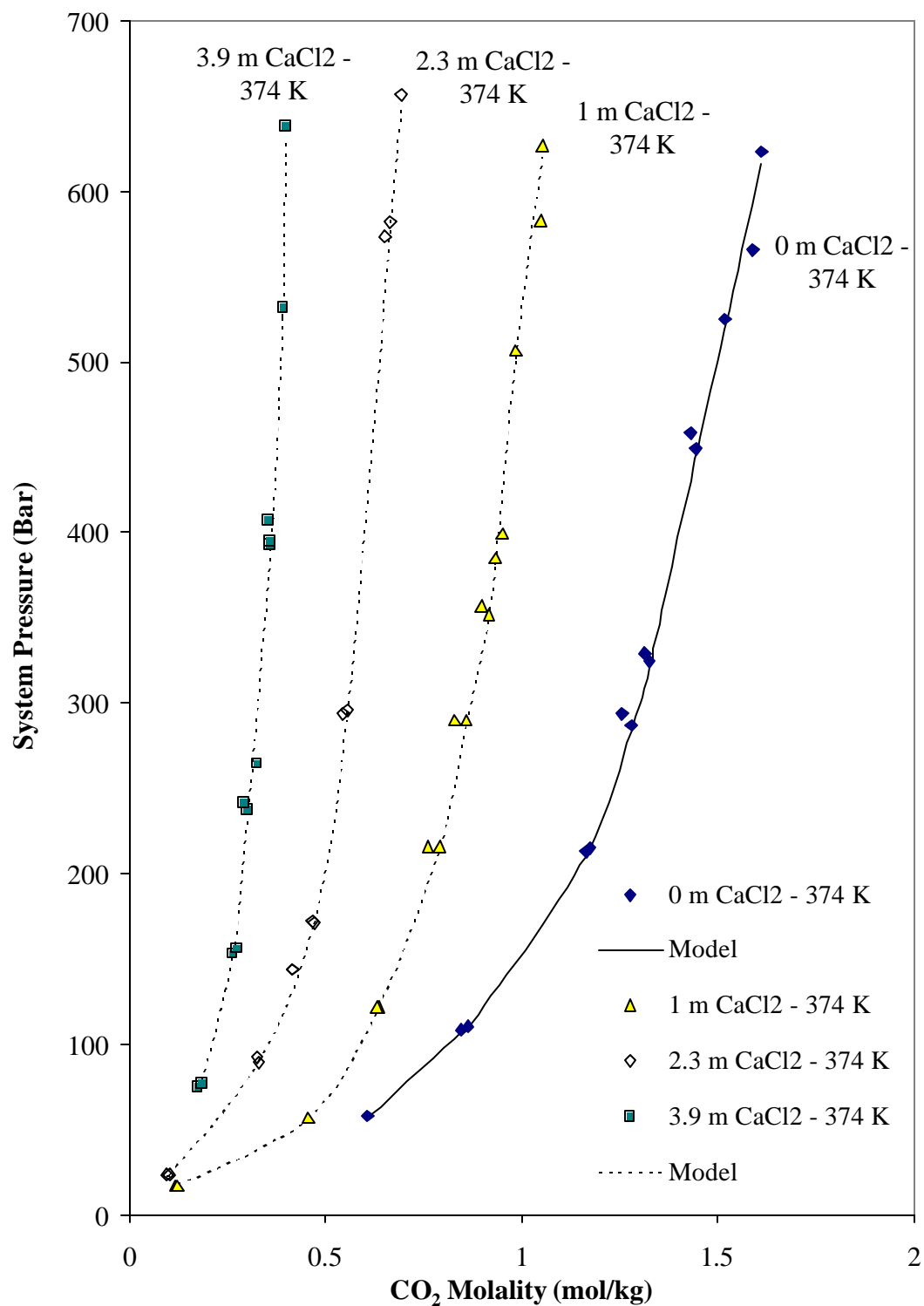
Figure 51. CO$_2$ in Aqueous Calcium Chloride (CaCl$_2$) Mixtures at 374 K

Three experimental data sources, Yasunishi and Fumitake [33], Corti, et al. [32], and Rumpf and Maurer [31] examine the effect of sodium sulfate (Na_2SO_4) and ammonium sulfate ((NH_4)$_2SO_4$) on aqueous carbon dioxide mixtures. Two of the experimental data sources are well predicted by the model. In Figure 52, predictions of the salting out effect of 1 and 2 molal sodium sulfate on aqueous carbon dioxide at three temperatures show good agreement with the experimental data of Runpf and Maurer [31].

The experimental data of Yasunishi and Fumitake [33] for aqueous ammonia in sodium sulfate (Na_2SO_4), ammonia sulfate ((NH_4)$_2SO_4$), and sulfate salt mixtures are reported for low-pressure (~1 bar) conditions. As discussed, using AAPD as a measure of goodness of fit deviation magnifies errors in the low-pressure range.

Predictions for carbon dioxide in a mixture of both sodium and ammonium sulfate are shown in Figure 53 and compared with data from Rumpf and Maurer [31].

Overall, the model accurately predicts experimental system pressure for aqueous carbon dioxide in mixtures of strong electrolytes (salts). Predictions for other volatile weak electrolytes in mixtures of strong electrolyte (salt) are given in Table 14. Pressure predictions for these systems are not as accurate as the carbon dioxide systems.
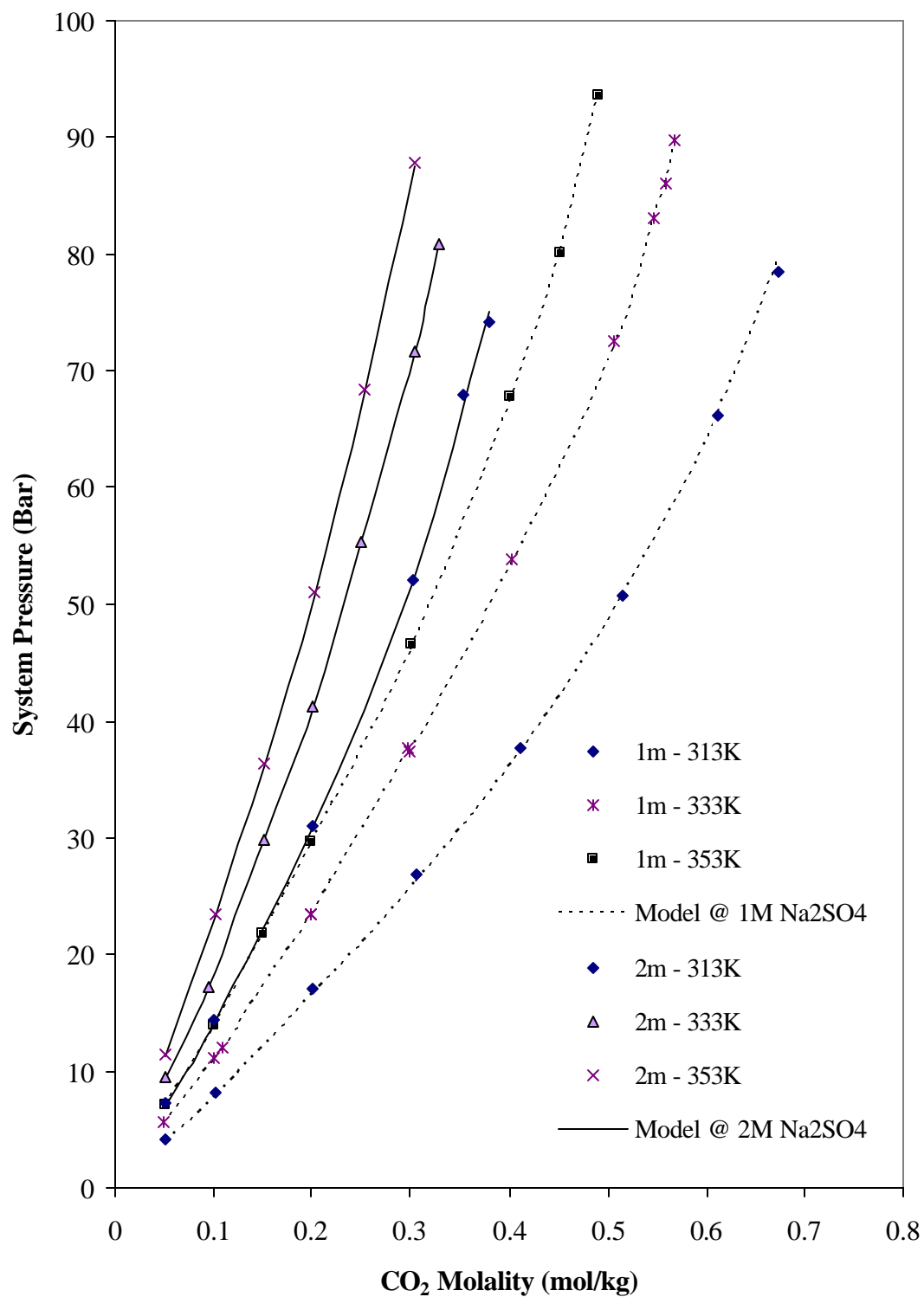
Figure 52. CO_2 in 1m and 2m Na_2SO_4 Mixtures

191
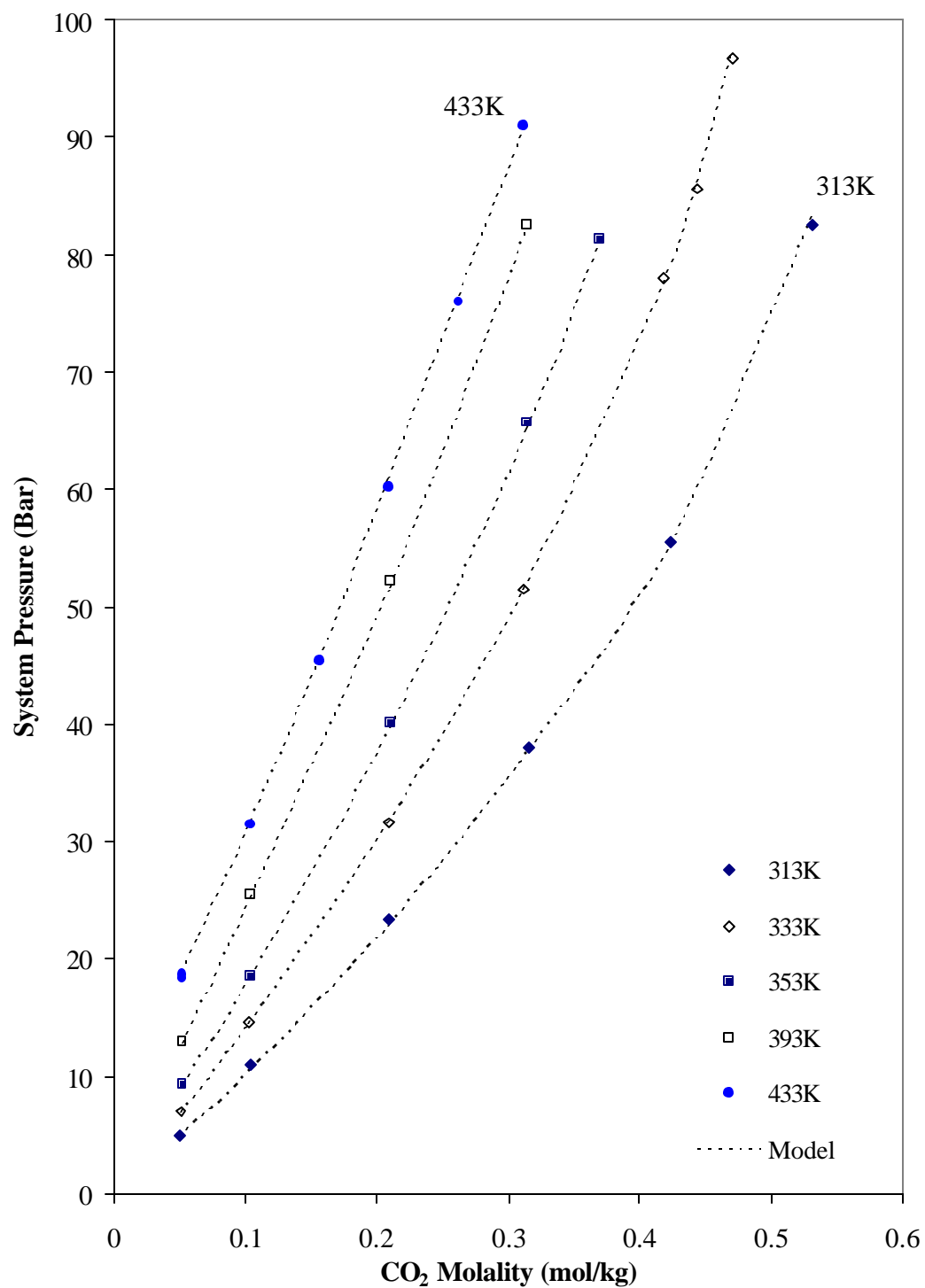
Figure 53. CO_2 in 1m Na_2SO_4 + 1m $(NH_4)_2SO_4$

Table 14. Average Errors for SO_2, H_2S, and NH_3 in strong electrolyte mixtures

Solute			Range of Data		Error Measures		
	Salt (M)	# Pts	T(K)	P (Bar)	%BIAS	AAPD	Ref
SO_2							
KCl							
	0.7 - 5.3	43	283.15 - 363.15	1.022 - 1.292	4.1%	5.2%	[35]
Na_2SO_4							
	0.5 - 1.0	65	312.82 - 393.18	0.111 - 32.82	9.3%	12.2%	[34]
	0.3 - 2.8	23	293.15 - 323.15	1.013 - 1.013	18.0%	18.9%	[35]
H_2S							
NaCl							
	1.0 - 5.0	238	296.15 - 369.65	1.013 - 1.013	-1.1%	4.4%	[36]
NH_3							
$(NH_4)_2SO_4$							
	0.4 - 0.4	33	298.95 - 319.65	0.224 - 0.889	-7.5%	10.7%	[37]
	2.0 - 3.9	49	333.07 - 433.25	0.518 - 26.72	-11.8%	11.9%	[38]
Na_2SO_4							
	1.0 - 1.0	49	333.13 - 413.2	0.440 - 11.68	-1.1%	1.1%	[38]

Sulfur dioxide (SO_2) and hydrogen sulfide (H_2S) are important acid gases, but dangerous to work with experimentally. Perhaps due to the health hazards less experimental work is available for these species in aqueous solutions.

Aqueous sulfur dioxide - salt mixtures are available from Rumpf and Maurer [34] and Hudson [35]. Figure 54 shows predictions for data from Rumpf and Maurer [34] in aqueous 1 molal sodium sulfate (Na_2SO_4) mixtures. The model predictions are good but not as accurate as the carbon dioxide systems previously examined. The model overpredicts pressure in low-pressure ranges. Similar behavior is found in the KCl salt predictions of the experimental data of Hudson [35]. The results for predictions of the KCl mixtures are better than expected given the experimental data are at or near one atmosphere.

The hydrogen sulfide - salt data are from Barrett, et al. [36]. Although these experimental data are at pressures near 1 atmosphere the prediction results are within 5 %.
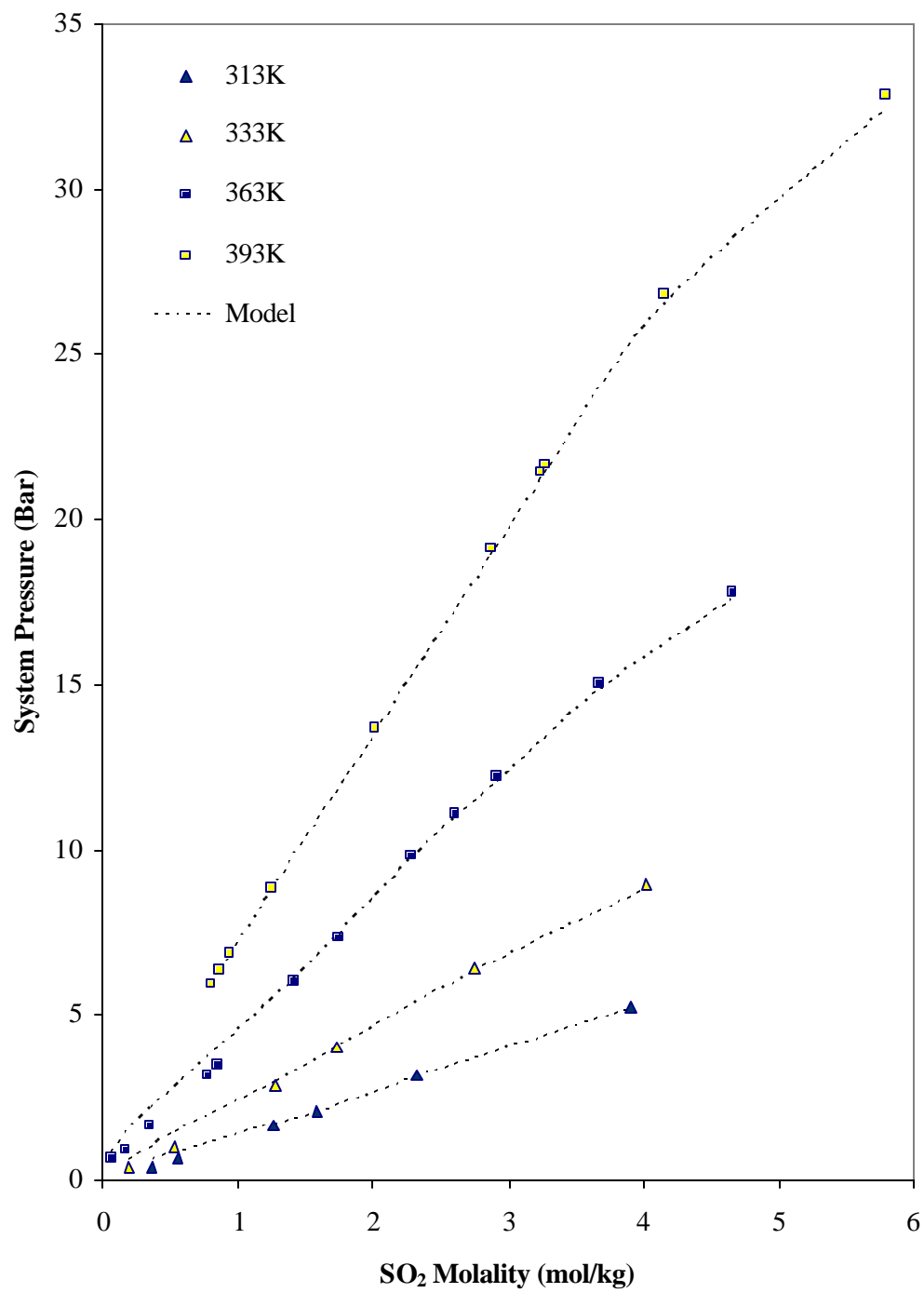
Figure 54. SO_2 in Aqueous 1m Na_2SO_4 Solutions

195

Two experimental sources for aqueous ammonia - salt mixtures are compared with model predictions. The experimental data of Perman [37] examined ammonia in sodium sulfate mixtures, and data from Rumpf and Maurer [38] examined ammonia in mixtures of sodium sulfate, ammonium sulfate, and sulfate salts.

The experimental data from Perman [37] are at less than atmospheric pressure, and show large absolute average deviations from model predictions. The corresponding large bias indicates the model consistently over predicts these data.

The experimental data from Rumpf and Maurer [38] cover broader pressure and temperature ranges. Figure 55 shows predictions for 1 molal sodium sulfate mixtures. As shown, predictions are in good agreement with the experimental data. Some model predictions for aqueous ammonia in 2 molal ammonium sulfate are shown Figure 56. The ammonium sulfate predictions show greater deviations from experimental data over the entire concentration range, while the trend of the model accurately reflects the experimental data. One source of the error in these predictions may arise from unconsidered chemical reactions that are possible in these systems. The equilibrium ammonium sulfate and ammonia species may not be accurately defined by the reactions currently considered in the model.

The model predicts carbon dioxide - salt mixtures very well. The accuracy of predictions for ammonia, hydrogen sulfide, and sulfur dioxide - salt mixtures are lower, but the overall trend of the model predictions is in agreement with experimental data. Additional model results are summarized along isotherms for specific salt concentrations in Appendix H.
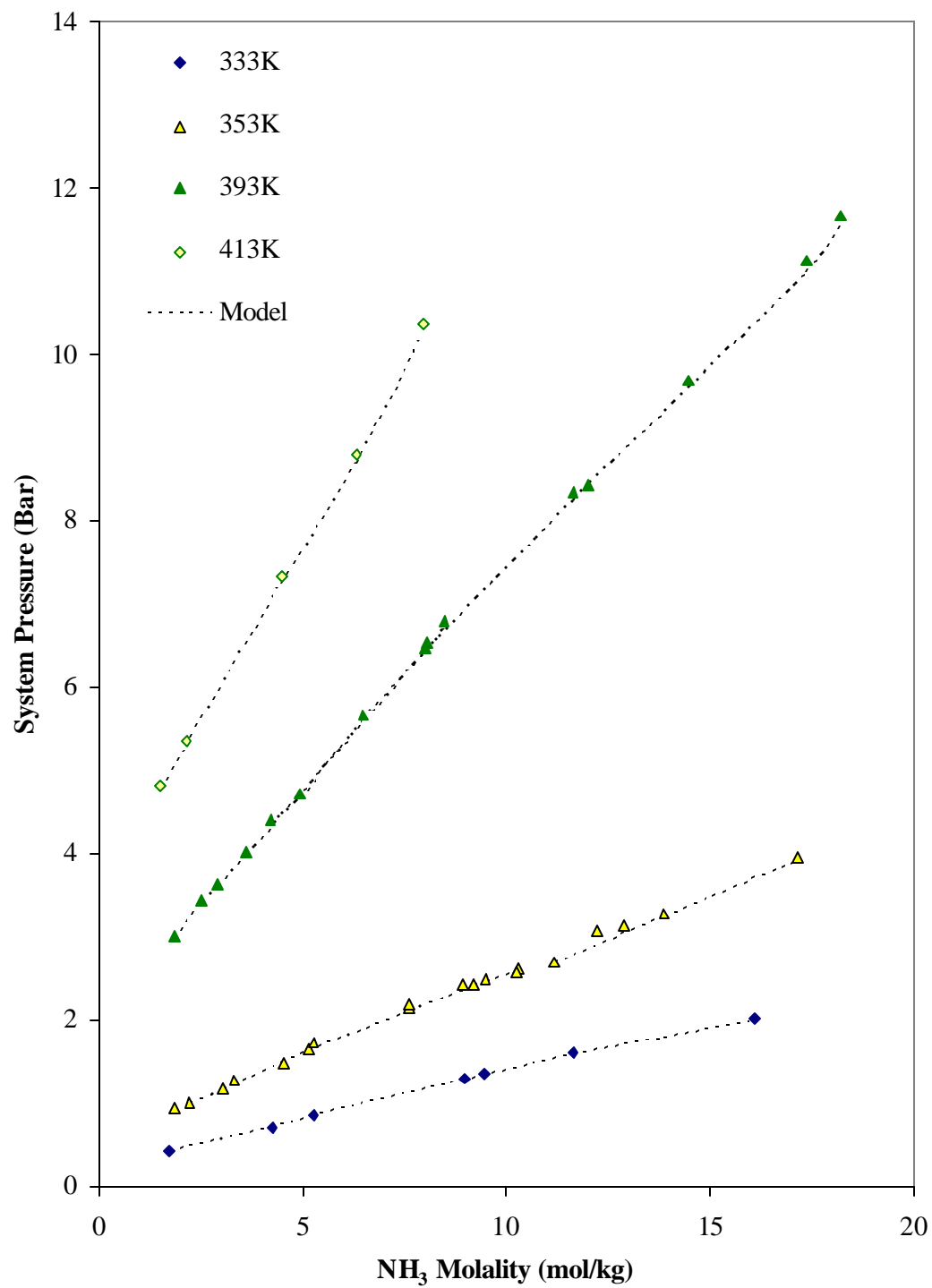
Figure 55. NH_3 in Aqueous 1m Na_2SO_4

197
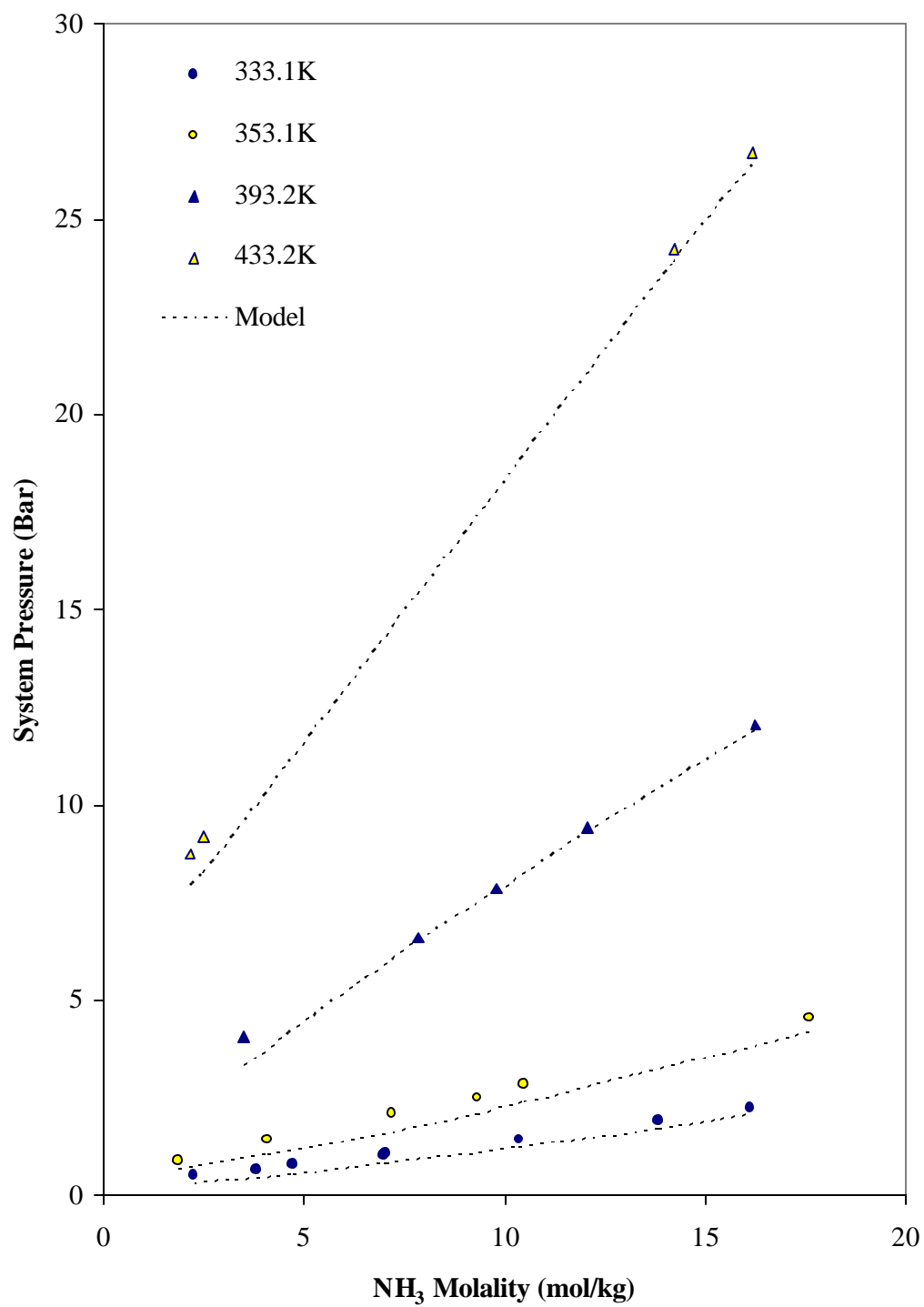
Figure 56. NH_3 in Aqueous 2m $(NH_4)_2SO_4$

198

AQUEOUS MULTICOMPONENT WEAK ELECTROLYTE MIXTURES

The application of the model to multicomponent weak electrolyte mixtures are predictive calculations using only parameters upon regressed from binary vapor-liquid equilibrium data. The results of predictions for mixtures of volatile weak electrolytes are given in Table 15.

Table 15. Multicomponent Volatile Aqueous Weak Electrolytes

	Molalities (mol/kg)	Pts	Range of Data T(K)	P (Bar)	Error %BIAS	AAPD	Ref
NH_3	0.1 - 26.0	948	293.2 - 533.2	0.03 - 158.5	5.6%	8.5%	[38-44]
CO_2	0.0 - 13.3						
NH_3	0.67 - 10.9	81	293.2 - 383.2	0.04 - 4.46	-12.8%	26.1%	[40, 42]
H_2S	0.27 - 5.20						[45-47]
NH_3	3.19 - 6.09	61	313.1 - 373.2	0.21 - 20.47	-6.3%	13.4%	[48]
SO_2	0.43 - 10.53						
NH_3	1.06 - 13.3	14	366.5 - 533.2	1.15 - 199.9	-1.8%	5.5%	[42]
CO_2	0.14 - 3.12						
H_2S	0.28 - 3.05						

Numerous experimental studies of the ammonia - carbon dioxide - water system have been published [39-46]. Table 16 provides a summary of the data sources examined in this work. Of the 948 data points examined, agreement between the studies is reasonably good with the exception of the experimental data of Pexton and Badger [39] and Badger [40].

Table 16. Aqueous Ammonia - Carbon Dioxide Mixtures

Range of Data		Molalities		Error				
T(K)	P (Bar)	(mol/kg)		Measure	Pts	%BIAS	AAPD	REF
333.15 - 393.15	0.78 - 70.27	NH_3	0.5 - 16.5	P_{TOT}	541	2.3%	4.4%	[46]
		CO_2	0.2 - 13.0	$ppNH_3$	350	4.4%	6.1%	
				$ppCO_2$	505	-0.2%	7.3%	
373.15 - 473.15	1.92 - 88.10	NH_3	2.4 - 26.0	P_{TOT}	254	-0.2%	3.1%	[17]
		CO_2	0.2 - 13.3	$ppNH_3$	254	1.1%	3.0%	
				$ppCO_2$	254	-1.1%	3.0%	
293.15 - 333.15	0.97 - 1.51	NH_3	0.1 - 2.0	P_{TOT}	55	-2.5%	6.2%	[42]
		CO_2	0.0 - 1.3					
293.15 - 313.15	0.03 - 0.92	NH_3	0.1 - 2.0	P_{TOT}	74	57.6%	60.0%	[40,41]
		CO_2	0.0 - 1.9					
373.15 - 423.15	2.23 - 34.70	NH_3	2.6 - 9.6	P_{TOT}	18	2.0%	3.0%	[45]
		CO_2	0.3 - 5.4	$ppNH_3$	18	2.7%	3.0%	
				$ppCO_2$	18	-2.7%	3.0%	
422.04 - 533.15	8.27 - 158.54	NH_3	1.2 - 2.4	P_{TOT}	6	-2.6%	2.6%	[44]
		CO_2	0.2 - 1.2	$ppNH_3$	6	-1.3%	1.7%	
				$ppCO_2$	6	-1.3%	1.7%	

The experimental pressure for the data of Pexton and Badger [39] and Badger [40] are below atmospheric pressure where larger deviations are expected. These deviations are significantly larger than model deviations in predictions for the low-pressure data of van Krevlen [42]. The reasons for the larger than expected deviations in the Pexton and Badger [39] and Badger [40] data are unknown.

System pressure predictions and experimental data from Goppert and Maurer [46] for the 393 K isotherms at various aqueous ammonia concentrations are shown in Figure 57. These predictions are good overall, but increasingly larger deviations appear as ammonia concentration increases. Model predictions shown in Figure 58 are for 8 molal NH_3 at 393 K for data from Mueller, et al. [45]. These results include comparison of experimental partial pressures to model predictions for ammonia and carbon dioxide. Deviation of model predictions increase, with the model overpredicting partial pressure, as carbon dioxide concentration increases. Figure 59 presents predictions for experimental data of Muller [45] at the highest ammonia concentration measured experimentally.

Additional predictions for experimental data from Pawlikowski [44], and Owens, et al. [43] show similar results, with model deviation increasing as the ammonia concentration increases. Overall, the predictions of the experimental data are quite good. Additional results, given along isotherms are provided in Appendix H.
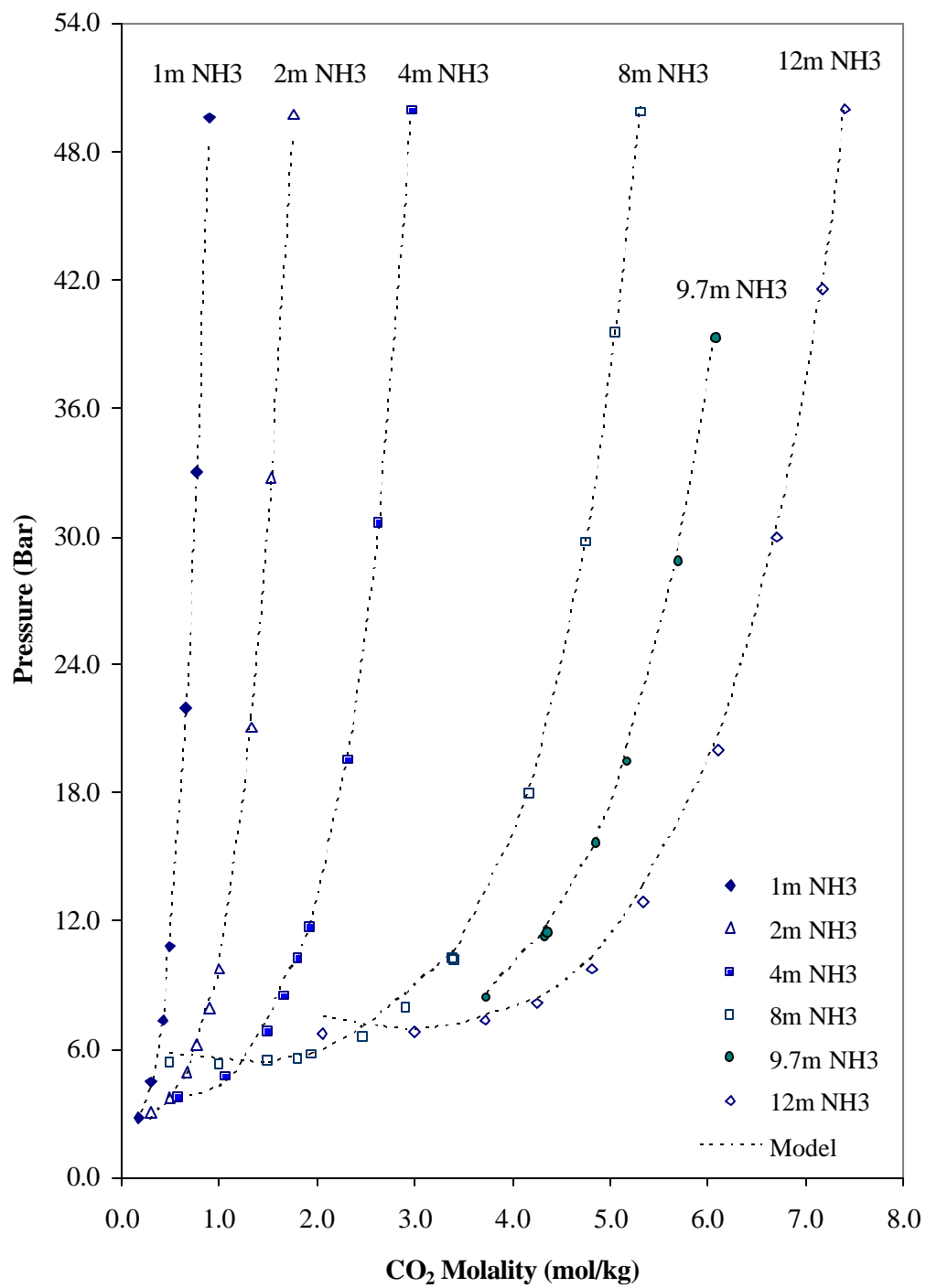
Figure 57. CO_2-NH_3 at 393K at various aqueous NH_3 concentrations
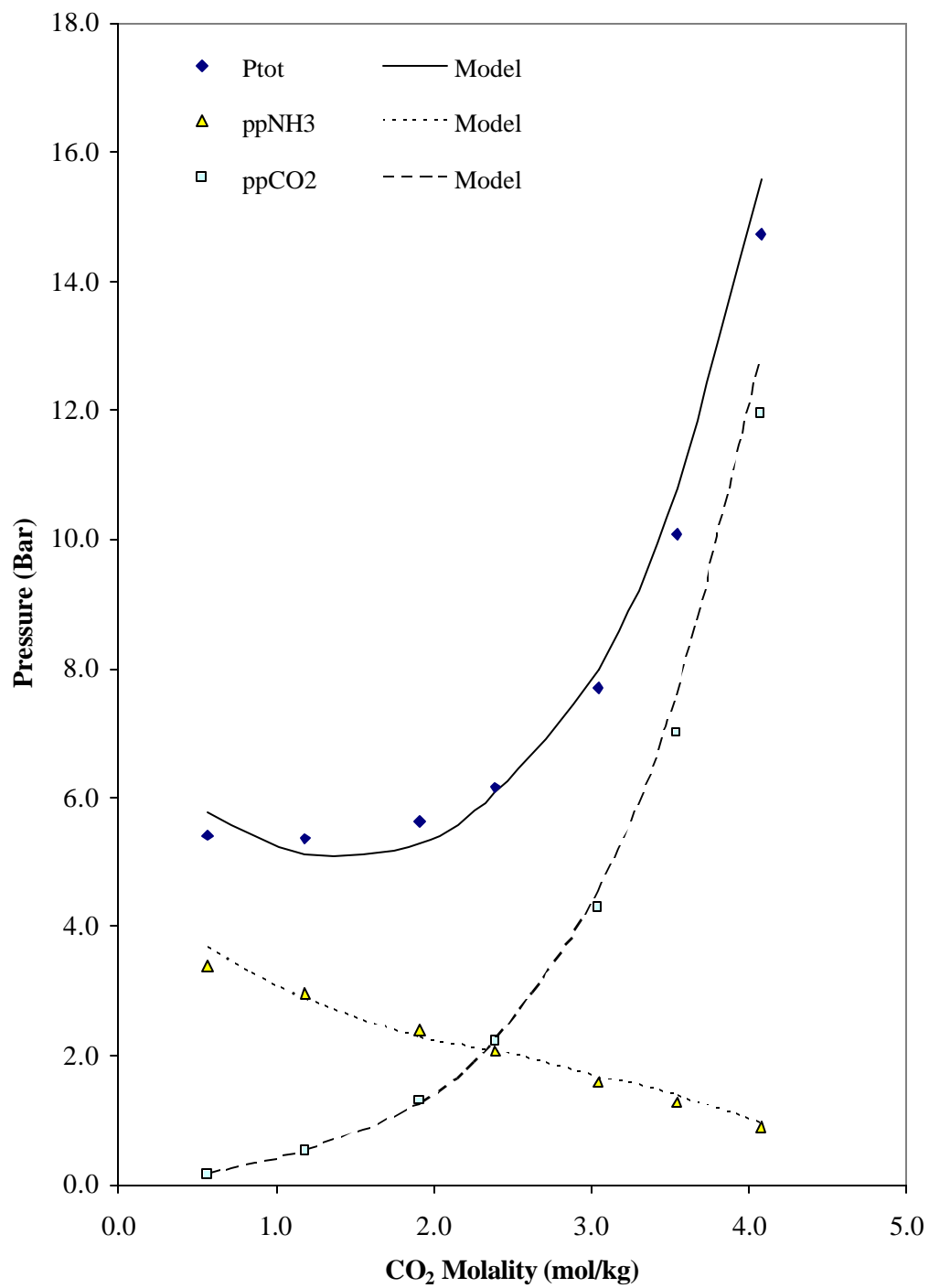
Figure 58. CO_2-NH_3 at 393K in 8 molal aqueous NH_3
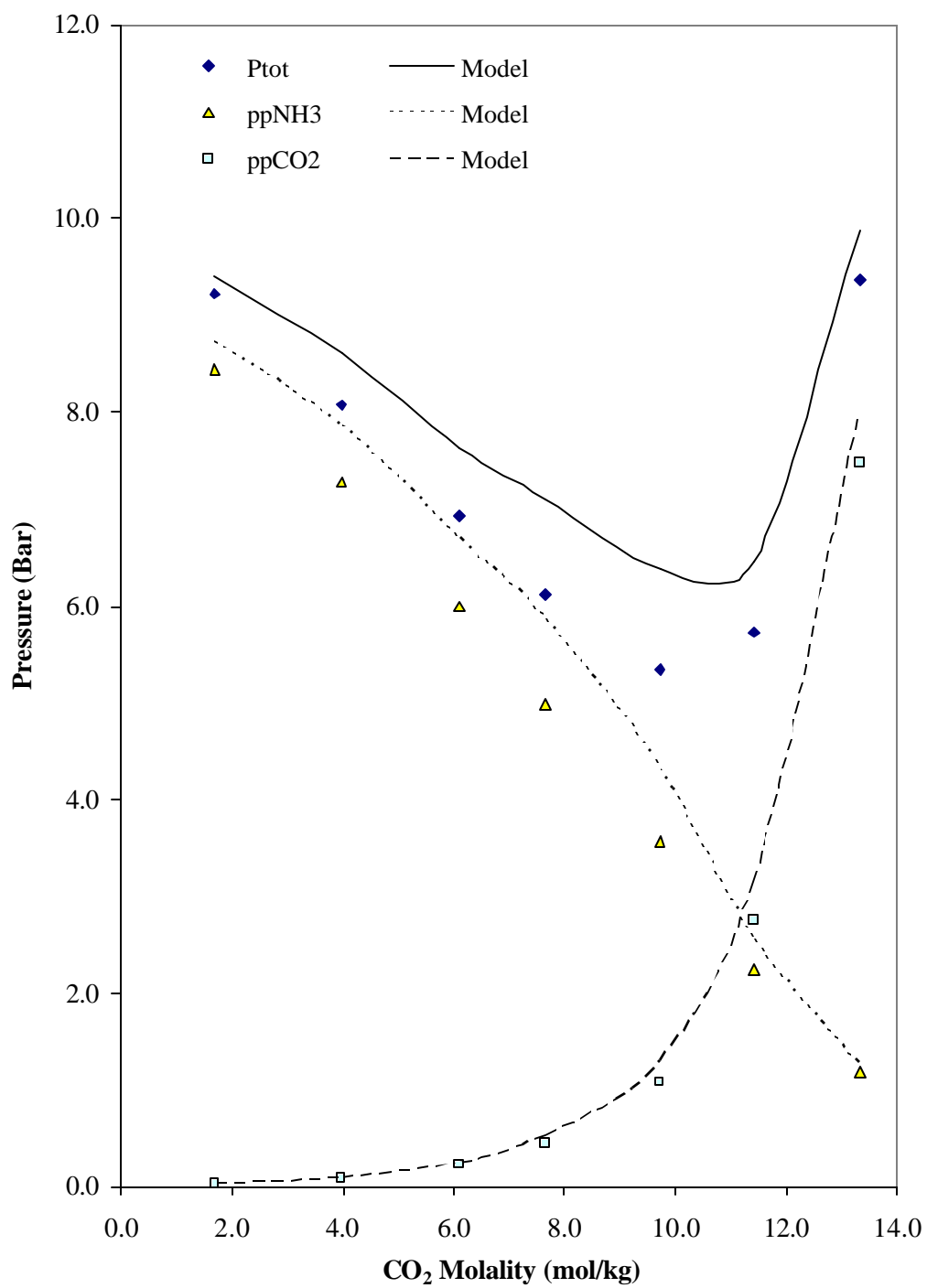
Figure 59. CO_2-NH_3 at 373K in 25 molal aqueous NH_3

Experimental data for the ammonia - hydrogen sulfide system are available from van Krevlen [41], Owens, et al. [43], Wilson [47], and Miles and Wilson [48]. Nearly all of the available data are for lower experimental pressures and have correspondingly higher prediction errors.

Experimental data for ammonia - sulfur dioxide are from Rumpf and Maurer [49]. The experimental data and model predictions at the 3.2 and 6.1 molal ammonia concentrations are shown in Figure 60. The model predictions follow the salting-in and salting-out effects of aqueous ammonia and sulfur dioxide concentrations along these 353 K isotherms. Although the model appears to perform well for the data points in Figure 60, in general, for both low sulfur dioxide concentrations and at lower pressures the model predictions exhibits significant mismatch from experimental data.

The experimental data for ammonia - carbon dioxide - hydrogen sulfide system are from Owens, et al. [43]. Pressures for this ternary system are predicted within 6% over the temperature and pressure ranges considered.
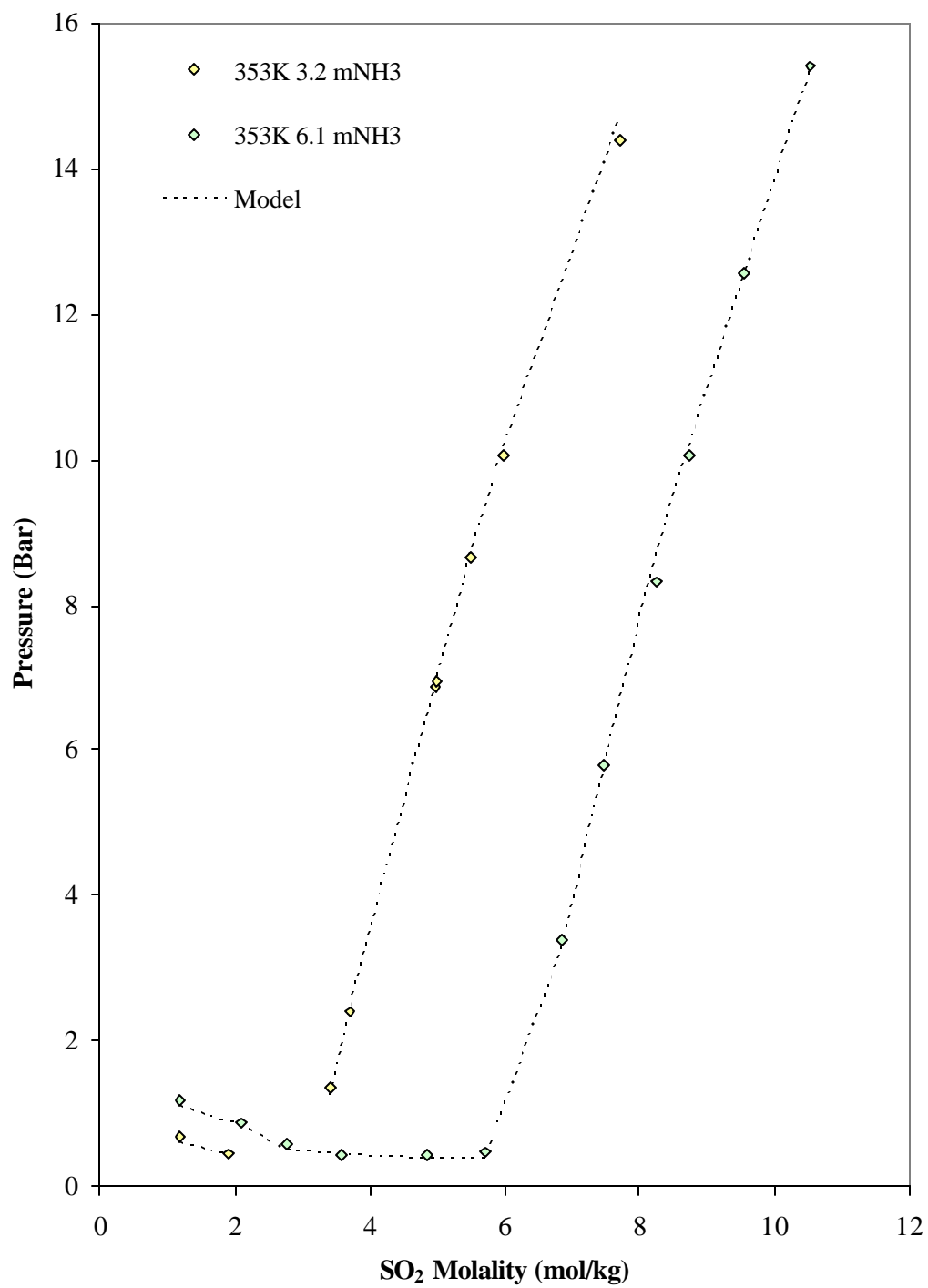
Figure 60. SO_2-NH_3 at 353K in 3.2 and 6.1 molal NH_3

SUMMARY

Modeling of aqueous electrolyte mixtures is accomplished using the Soave-Redlich-Kwong equation of state by incorporating corrections based on a chemical equilibrium - activity coefficient model. A regression of the binary interaction parameters (C_{ij} and D_{ij}), in the mixing rule for the cubic equation of state allows the cubic equation of state to provide accurate agreement with experimental data for volatile weak electrolyte - water mixtures to within 4.5 % AAD.

The incorporation of non-volatile strong electrolytes, or salts, into the model requires no additional parameters. Model predictions of weak electrolyte - salt systems compare favorably to experimental data.

Weak electrolyte mixtures are predicted without additional fitting parameters. Predictions for ammonia - carbon dioxide mixtures are accurately represented over a broad range of temperature, pressure, and concentration. Additional predictions of other weak electrolyte mixtures vary in quality and further examination of these systems is desirable.

REFERENCES

1.   Friedemann, J.D., Ph.D. Dissertation, *The Simulation of Vapor-Liquid Equilibria in Ionic Systems*, School of Chemical Engineering, Oklahoma State University, Stillwater, Oklahoma, 1987.

2.   Chen, H., J. Wagner, and J.D. Friedemann. *Phase Equilibria in Aqueous Acid Gas Systems.* in *Seventy-Third GPA Annual Convention*. 1994. New Orleans, Louisiana.

3.   Soave, G., *Equilibrium Constants from a Modified Redlich-Kwong Equation of State*. Chemical Engineering Science, 1972. 27: p. 1197-1203.

4.   Soave, G., *20 Years of Redlich-Kwong Equation of State.* Fluid Phase Equilibria, 1993. 82: p. 345-359.

5.   Maurer, G., *Thermodynamics of Aqueous Systems with Industrial Application*. ACS Symposium Series, ed. S.A. Newman. Vol. 133. 1980: ACS pgs.

6.   Tsonopoulos, C., D.M. Coulson, and L.B. Inman, *Ionization Constants of Water Pollutants.* Journal of Chemical and Engineering Data, 1976. 21(No. 2): p. 190-193.

7.   Kawazuishi, K., Prausnitz, John M., *Correlation of Vapor-Liquid Equilibria for the System Ammonia-Carbon Dioxide-Water.* Ind. Eng. Chem. Res., 1987. 26: p. 1482-1485.

8.   Pitzer, K.S., *Theory: Ion Interaction Approach*. p. 157.

9.   Yoon, J.-H., Chun, Moon-Kyoon, Hong, Won-Hi, Lee Huen, *High-Pressure Phase Equilibria for Carbon Dioxide-Methanol-Water System: Experimental Data and Critical Evaluation of Mixing Rules.* Industrial Engineering and Chemical Research, 1993. 32: p. 2881-2887.

10.   Voros, N.G. and D.P. Tassios, *Vapor-Liquid Equilibria in Nonpolar/Weakly Polar Systems with Different Types of Mixing Rules.* Fluid Phase Equilibria, 1993. 91: p. 1-29.

11. Knudsen, K., E.H. Stenby, and A. Fredenslund, *A Comprehensive Comparison of Mixing Rules for Calculation of Phase Equilbria in Complex Systems.* Fluid Phase Equilibria, 1993. 82: p. 361-368.

12. Wong, D.S.H., H. Orbey, and S.I. Sadler, *Equation of State Mixing Rule for Nonideal Mixtures Using Available Activity Coefficient Model Parameters and That Allows Extrapolation Over Large Ranges of Temperature and Pressure.* Industrial Engineering and Chemical Research, 1992. 31: p. 2033-2039.

13. Wong, D.S.H. and S.I. Sandler, *A Theoretically Correct Mixing Rule for Cubic Equations of State.* AIChE Journal, 1992. 38(5): p. 671-680.

14. Michelsen, M.L., *A Modified Huron-Vidal Mixing Rule for Cubic Equations of State.* Fluid Phase Equilibria, 1990. 60: p. 213-219.

15. Gerdes, K., J.E. Johnson, and G.M. Wilson. *Application of GPSWAT to Sour Water Systems, Design and Engineering Problems.* in *68th Annual GPA Convention.* 1989. San Antonio, Texas.

16. Takenouchi, S. and G.C. Kennedy, *The Solubility of Carbon Dioxide in NaCl Solutions at High Pressure Temperatures and Pressures.* American Journal of Science, 1965. 263(May): p. 445-454.

17. Zawisza, A. and B. Malesinska, Journal of Chemical and Engineering Data, 1981. 26: p. 388-391.

18. Carroll, J.J., J.D. Slupsky, and A.E. Mather, *The Solubility of Carbon Dioxide in Water at Low Pressure.* Journal of Physical and Chemical Reference Data, 1991. 20(6): p. 1201-1209.

19. Crovetto, R., *Evaluation of Solubility Data of the System CO_2–H_2O from 273 K to the Critical Point of Water.* Journal of Physical and Chemical Reference Data, 1991. 20(3): p. 575-589.

20. Gillespie, P.C., W.V. Wilding, and G.M. Wilson, *Vapor-Liquid Equilibrium Measurements on the Ammonia-Water System from 313K to 589K.* 1985, Gas Processors Association: Tulsa.

21. Gillespie, P.C., W.V. Wilding, and G.M. Wilson, *Vapor-Liquid Equilibrium Measurements on the Ammonia-Water System From 313 K to 589 K.* AIChE Symposium Series: Phase Equilibrium Measurements (DIPPR), 1983. 83(No. 256): p. 97-127.

22. Lee, J.I. and A.E. Mather, Ber. Bunsenges. Phys. Chem., 1977. 8: p. 1021-1023.

23. Rabe, A.E. and J.F. Harris, *Vapor-Liquid-Equilibrium Data for the Binary System, Sulfur Dioxide and Water.* Journal of Chemical and Engineering Data, 1963. 8: p. 333-336.

24. Goldberg, R.N. and V.B. Parker, J. Res. NBS, 1985. 90: p. 341-358.

25. Rumpf, B. and G. Maurer, *Solubilities of Hydrogen Cyanide and Sulfur Dioxide in Water at Temperatures from 293.15 to 413.15 K and Pressures up to 2.5 MPa.* Fluid Phase Equilibria, 1992. 81: p. 241-260.

26. Onken, U., J. Ghmeling, and W. Arlt, *Vapor-Liquid Equilibrium Data Collection, Aqueous-Organic Systems*, ed. D. Bekrens and R. Eckermann. Vol. Vol 1, Part Ia. 1981: DECEMA pgs.

27. Chandler, J.P., *MARQ Documentation and Revisions*. 1984, Oklahoma State University: Stillwater, OK.

28. Rumpf, B., et al., *Solubility of Carbon Dioxide in Aqueous Solutions of Sodium Chloride: Experimental Results and Correlation.* Journal of Solution Chemistry, 1994. 23(No. 3): p. 431-448.

29. Nighswander, J.A., N. Kalogerakis, and A.K. Mehrotra, *Solubilities of Carbon Dioxide in Water and 1 wt % NaCl Solution at Pressures up to 10 MPa and Temperatures from 80 to 200 C.* J. Chem. Eng. Data, 1989. 34: p. 355-360.

30. Prutton, C.F. and R.L. Savage, *The Solubility of Carbon Dioxide in Calcium Chloride-Water Solutions at 75, 100, 120 and High Pressures.* Am. Chem. Soc. J., 1945. 67: p. 1550-1554.

31. Rumpf, B. and G. Maurer, *An Experimental and Theoretical Investigation on the Solubility of Carbon Dioxide in Aqueous Solutions of Strong Electrolytes.* Ber. Bunsenges. Phys. Chem., 1993. 97(No. 1): p. 85-97.

32. Corti, H.R., et al., *Effect of a Dissolved Gas on the Solubility of an Electrolyte in Aqueous Solution.* 1990. 29: p. 1043-1050.

33. Yasunishi, A. and Y. Fumitake, *Solubility of Carbon Dioxide in Aqueous Electrolyte Solutions.* Journal of Chemical and Engineering Data, 1979. 24(No. 1): p. 11-14.

34. Rumpf, B. and G. Maurer, *Solubility of sulfur dioxide in aqueous solutions of sodium-and ammonium sulfate at temperatures from 313.15 K to 393.15 K and pressures up to 3.5 MPa.* Fluid Phase Equilibria, 1993. 91: p. 113-131.

35. Hudson, J., *CLXXXIII.--The Solubility of Sulphur Dioxide in Water and in Aqueous Solutions of Potassium Chloride and Sodium Sulphate*, Imperial College: London. p. 1332-1347.

36. Barrett, T.J., G.M. Anderson, and J. Lugowski, *The solubility of hydrogen sulphide in 0-5 m NaCl solutions at 25-95 C and one atmosphere.* Geochimica et Cosmochimica Acta, 1988. 52: p. 807-811.

37. Perman, E.P., *LXXXII.--Influence of Sodium Sulphate on the Vapour Pressure of Aqueous Ammonia Solution.* J. Chem. Soc., 1901. 79: p. 725-729.

38. Rumpf, B. and G. Maurer, *Solubility of Ammonia in Aqueous Solutions of Sodium Sulfate and Ammonium Sulfate at Temperatures from 333.15 K to 433.15 K and Pressures up to 3 MPa.* Ind. Eng. Chem. Res., 1993. 32: p. 1780-1789.

39. Pexton, S. and E.H.M. Badger, Chem. Soc. Ind., 1938. 57: p. 106-113.

40. Badger, E.H.M. and D.S. Wilson, Chem. Soc. Ind., 1947. 66: p. 84.

41. Van Krevelen, D.W., P.J. Hoftijzer, and F.J. Huntjens, *Composition and Vapour Pressures of Aqueous Solutions of Ammonia, Carbon Dioxide and Hydrogen Sulphide.* Recueil, 1949. 68: p. 191-216.

42.   Otsuka, E., S. Yoshimura, and M. Yakabe, Kogyo Kagaku Zasshi, 1960. 62(1214).

43.   Owens, J.L., J.R. Cunningham, and G.M. Wilson, *Vapor-Liquid Equilibria for Sour Water Systems at High Pressure*. 1983, Gas Processors Association: Tulsa.

44.   Pawlikowski, E.M., J. Newman, and J.M. Prausnitz, *Phase Equilibria for Aqueous Solutions of Ammoia and Carbon Dioxide*. Industrial Engineering and Chemical Process Design and Development, 1982. 21: p. 764-770.

45.   Mueller, G., E. Bender, and G. Maurer, *Das Dampf-Fluessigkeitsfleichgewicht des ternaeren Systems Ammoniak-Kohlendioxid-Wasser bei hohen Wassergehalten im Bereich zwischen 373 und 473 Kelvin.* Ber. Bunsenges. Phys. Chem., 1988. 92: p. 148-160.

46.   Goppert, U. and G. Maurer, *Vapor-Liquid Equilibria in Aqueous Solutions of Ammonia and Carbon Dioxide at Temperatures between 333 and 393 K and Pressures up to 7 MPa.* Fluid Phase Equilibria, 1988. 41: p. 153-185.

47.   Wilson, G.M., *A New Correlation of NH_3, CO_2 and H_2S Volatility Data From Aqueous Sour Water Systems.* API Publication 955, 1978.

48.   Miles, D.H. and G.M. Wilson, *Vapor Liquid Equilibrium Data for Design of Sour Water Strippers*. 1975, Brigham Young University: Provo, UT.

49.   Rumpf, B., F. Weyrich, and G. Maurer, *Simultaneous Solubility of Ammonia and Sulfur Dioxide in Water at Temperatures from 313.15K to 373.15K and Pressures up to 2.2 MPa.* Fluid Phase Equilibria, 1993. 83: p. 253-260.

APPENDICES

APPENDIX A

GPA DATABASE OVERVIEW

Tables

Table A1. Summary of database records by data type.

Category	No. of Data Sets	Percentage of Total Sets	No. of Data Points	Percentage of Total Points
Dew and Bubble Point	25	2.8	1,099	2.2
Vapor-Liquid-Equilibrium	412	43.6	16,103	35.2
Vapor-Liquid-Liquid/Solid	93	9.8	4,553	10.0
Hydrate Equilibrium	125	13.2	2,083	4.6
Enthalpy Departure	195	20.6	18,662	40.8
Enthalpy of Solution	12	1.3	1,890	4.1
Amine Solutions	82	8.7	1,456	3.2

Table A2. Temperature and pressure ranges by data type.

Category	Temperature (^{o}F)		Pressure (psia)	
	Minimum	Maximum	Minimum	Maximum
Dew/Bubble	-250	400	12.44	8,000
Enthalpy Departure	-280	900	14.70	9,427
Enthalpy of Solution	60	1,000	60.00	1,000
Hydrate	-297	122	0.02	57,580
Vapor Liquid-Equilibrium	-431	870	0.0005	60,003
Vapor-Liquid-Liquid/Solid	-301	44	$0^{(1)}$	13,683
Amine	25	248	$0^{(1)}$	1,583
Note: (1) Pressure is not always reported for all data; set to zero for search purposes.				

Table A3. Number of data sets/systems by data type and number of components.

Category	Number of Components										
	1	2	3	4	5	6	7	8	9	10	13
Dew/Bubble		860	81	20		29				14	4	
Enthalpy Departure	3,058	13,890	1,611	80							13	8
Enthalpy of Solution			1,885									
Hydrate		681	972	162	64	55	87	26	36			
Vapor-Liquid Equilibrium		13,240	2,624	9	19	43	63	37	68			
Vapor-Liquid-Liquid/Solid		681	3,528	278	25	26	11	4				
Amine Solutions		53	1,163	236								

Table A4. Enthalpy departure data for pure components.

System Components		L	LLV	LV	LVV	V	No. Pts
N_2	Nitrogen	7				48	55
H_2S	Hydrogen Sulfide				2	59	61
CH_4	Methane	14				25	39
C_2H_6	Ethane	41				28	69
C_3H_8	Propane	40				21	61
C_5H_{10}	Cis-2-Pentene	49	19	27	17	193	305
C_6H_6	Benzene	108	10	14	4	239	375
C_5H_{12}	n-Pentane	141	1	14	4	249	409
C_6H_{12}	Cyclohexane	128	5	8	5	176	322
C_7H_8	Toluene	107				38	145
C_7H_{14}	Methylcyclohexane	122				46	168
C_7H_{16}	n-Heptane	105				52	157
C_8H_{10}	Ethylbenzene	33				12	45
C_8H_{16}	Ethylcyclohexane	21					21
C_8H_{18}	Isooctane	18					18
C_8H_{18}	n-Octane	154	3	8		81	246
$C_{10}H_{12}$	1,2,3,4-Tetrahydronapthalene	70	20	58	2	34	184
$C_{10}H_{18}$	Cis-Decalin	34	10	6	2	30	82
$C_{10}H_{18}$	Trans-Decalin	120	4	14	17	33	188
$C_{16}H_{34}$	n-Hexadecane	81	1	5	1	20	108
	Totals	1,393	73	154	54	1,384	3,058

Table A5. Enthalpy departure data for binary systems.

System Components		L	LLV	LV	LVV	V	NPTS
CH_4, C_3H_8	Methane, Propane	1140		337		902	2379
CH_4, C_4H_{10}	Methane, Isobutene	2					2
CH_4, C_7H_{14}	Methane, Methylcyclohexane	68		3		36	107
CH_4, C_7H_{16}	Methane, n-Heptane	111		136		158	405
CH_4, C_7H_8	Methane, Toluene	40		62		33	135
CH_4, CO_2	Methane, Carbon Dioxide				4	183	187
CH_4, CO_2	Methane, Carbon Dioxide			8		40	48
CH_4, H_2S	Methane, Hydrogen Sulfide					81	81
CH_4, H_2S	Methane, Hydrogen Sulfide	6		17		25	48
CH_4, N_2	Methane, Nitrogen	7		95		369	471
CH_4, H_2	Methane, Hydrogen			13		82	95
C_2H_6, C_3H_8	Ethane, Propane	134		42		88	264
C_2H_6, H_2S	Ethane, Hydrogen Sulfide	25		4		18	47
C_3H_8, C_5H_{12}	Propane, Isopentane	14		20		21	55
C_3H_8, C_6H_6	Propane, Benzene	19		11		9	39
C_5H_{12}, $C_{10}H_{12}$	Isopentane, 1,2,3,4-Tetrahydronapthalene	80		192		152	424
C_5H_{12}, $C_{10}H_{12}$	n-Pentane, 1,2,3,4-Tetrahydronapthalene	210		414		292	916
C_5H_{12}, $C_{10}H_{18}$	n-Pentane, Trans-Decalin	285		536		252	1073
C_5H_{12}, $C_{16}H_{34}$	n-Pentane, n-Hexadecane	168		363		65	596
C_5H_{12}, C_5H_{10}	n-Pentane, Cis-2-Pentene	43		12		116	171
C_5H_{12}, C_6H_{12}	n-Pentane, Cyclohexane	364	17	100	34	760	1275
C_5H_{12}, C_6H_6	n-Pentane, Benzene	272	23	165	36	899	1395
C_5H_{12}, C_8H_{18}	n-Pentane, n-Octane	201	6	91	17	284	599
C_5H_{12}, CO_2	n-Pentane, Carbon Dioxide	25	3	14		28	70
C_8H_{18}, C_6H_6	n-Octane, Benzene	555		261	2	535	1353
C_8H_{10}, C_8H_{18}	n-Octane, Ethylbenzene	4		1		10	15
$C_{16}H_{34}$, C_6H_6	n-Hexadecane, Benzene	338	1	453		230	1022
C_7H_{14}, H_2S	Methylcyclohexane, Hydrogen Sulfide			20	3	63	86
H_2S, CO_2	Carbon Dioxide, Hydrogen Sulfide			5		79	84
H_2S, CO_2	Carbon Dioxide, Hydrogen Sulfide			25	2	94	121
CO_2, N_2	Carbon Dioxide, Nitrogen			1	6	184	191
H_2, CO	Carbon Monoxide, Hydrogen					136	136
	Totals	4,111	50	3,401	104	6,224	13,890

217

Table A6. Enthalpy departure data for multicomponent systems.

System Components		L	LLV	LV	LVV	V	No. Pts
CH_4, C_2H_6, C_3H_8	Methane, Ethane, Propane	159		76		36	271
CH_4, C_2H_6, CO_2	Carbon Dioxide, Methane, Ethane	5		5		38	48
CH_4, C_2H_6, H_2S	Hydrogen Sulfide, Methane, Ethane	12		9		27	48
C_5H_{12}, C_6H_{12}, C_6H_6	n-Pentane, Cyclohexane, Benzene	226	12	199	5	423	865
C_8H_{18}, $C_{10}H_{12}$, C_6H_6	Benzene, n-Octane, 1,2,3,4-Tetrahydronapthalene	171		135	1	72	379
CH_4, C_7H_{14}, C_7H_8, H_2S	Methane, Methylcyclohexane, Toluene, Hydrogen Sulfide			14	5	61	80
CH_4, C_2H_6, C_3H_8, C_4H_{10}, C_3H_6, COS, H_2O, H_2S, CO_2, N_2	Methane, Ethane, Propane, n-Butane, Propene, Carbonyl Sulfide, Carbon Dioxide, Water, Nitrogen, Hydrogen Sulfide					13	13
CH_4, C_2H_6, C_3H_8, i-C_4H_{10}, n-C_4H_{10}, i-C_5H_{12}, n-C_5H_{12}, C_3H_6, H_2O, H_2, CO_2, N_2, He	Methane, Ethane, Propane, Isobutane, n-Butane, Isopentane, n-Pentane, Propene, Water, Hydrogen, Carbon Dioxide, Nitrogen, Helium					8	8
	Totals	573	12	438	11	678	1,712

Table A7. Enthalpy of solution data.

System Components[1]		10	20	30	40	50	60	100	No. Pts
		Weight Percent Loading							
$C_4H_{11}NO_2$, CO_2	Diethanolamine, Carbon Dioxide		155	164		174			493
$C_4H_{11}NO_2$, H_2S	Diethanolamine, Hydrogen Sulfide		109	138		157			404
$C_4H_{11}NO_2$, CO_2	Diglycolamine, Carbon Dioxide	4	7		16		10		37
$C_5H_{13}NO_2$, CO_2	Methyldiethanolamine, Carbon Dioxide		161		223		183		567
$C_5H_{13}NO_2$, H_2S	Methyldiethanolamine, Hydrogen Sulfide		117	162		104		1	384
	Totals	4	549	464	239	435	193	1	1,885

Table Notes:
(1) Water is a component in each system shown

Table A8. Pure and binary amine systems summarized by weight percent loading.

System Components [1]		Weight Percent Loading															
		0	0.5	1	2 [2]	5	10	17	20 [3]	23 [4]	26	30	35 [5]	40	50	60	No. Pts
Carbon Dioxide	CO_2	1															1
Hydrogen Sulfide	H_2S	1															1
Nitrogen	N_2	1															1
Carbon Dioxide, Monoethanolamine	CO_2				1				1			1					3
Carbon Dioxide, Diethanolamine	$C_4H_{11}NO_2$, CO_2		1		1			2	4		1	1	3		2		15
Carbon Dioxide, Diglycolamine	$C_4H_{11}NO_2$, CO_2								1					1		1	3
Carbon Dioxide, Methyldiethanolamine	$C_5H_{13}NO_2$, CO_2			1	1				1	4					3		10
Hydrogen Sulfide, Monoethanolamine	H_2S				1				1			1					3
Hydrogen Sulfide, Diethanolamine	$C_4H_{11}NO_2$, H_2S								3			1	2		3		9
Hydrogen Sulfide, Diglycolamine	$C_4H_{11}NO_2$, H_2S													1		1	2
Hydrogen Sulfide, Methyldiethanolamine	$C_5H_{13}NO_2$, H_2S			1					1	1					1		4
Nitrogen, Diethanolamine	$C_4H_{11}NO_2$, N_2							1									1
Table Notes:	Totals	3	1	2	4	0	0	3	12	5	1	4	5	2	9	2	53
(1) Water is a component in each system shown																	
(2) Data is from precentages of 2 and 2.5 measured in normality																	
(3) Includes data at percentages between 20 and 20.4																	
(4) Includes data at percentages between 23 and 23.1																	
(5) Includes data at percentages between 34 and 35.1																	

Table A9. Multicomponent amine systems summarized by weight percent loading.

System Components[1]		Weight Percent Loading															
		0	0.5	1	2[2]	5	10	17	20[3]	23[4]	26	30	35[5]	40	50	60	No. Pts
Hydrogen Sulfide, Carbon Dioxide, Diethanolamine	$C_4H_{11}NO_2$, H_2S, CO_2								6								6
Hydrogen Sulfide, Carbon Dioxide, Methyldiethanolamine	$C_5H_{13}NO_2$, H_2S, CO_2									6					4		10
Carbon Dioxide, Methyldiethanolamine, Phenol	$C_5H_{13}NO_2$, C_6H_6O, CO_2			1		1							2				4
Hydrogen Sulfide, Methyldiethanolamine, Phenol	$C_5H_{13}NO_2$, C_6H_6O, H_2S			1	1	1							3				6
Carbon Dioxide, Diethanolamine, Methyldiethanolamine,	$C_5H_{13}NO_2$, $C_4H_{11}NO_2$, CO_2					2	1						3				6
Hydrogen Sulfide, Diethanolamine, Methyldiethanolamine	$C_5H_{13}NO_2$, $C_4H_{11}NO_2$, H_2S					1	1						2				4
Hydrogen Sulfide, Diethanolamine, Carbon Dioxide, Methyldiethanolamine	$C_5H_{13}NO_2$, $C_4H_{11}NO_2$, H_2S, CO_2					1	1						2				4
Totals		0	0	2	1	6	3	0	6	6	0	0	12	0	4	0	40

Notes:

(1) Water is a component in each system shown

(2) Data is from precentages of 2 and 2.5 measured in normality

(3) Includes data at percentages between 20 and 20.4

(4) Includes data at percentages between 23 and 23.1

(5) Includes data at percentages between 34 and 35.1

Table A10. Criteria used to identify records requiring further evaluation.

Criterion	Description
1	Data-entry errors not noted by inspection.
2	Data points exhibiting deviations in calculated enthalpy departure values that are greater than twice the root-mean-squared error (RMSE for the entire data set. Near critical data points are given special attention.
3	Data points showing an abrupt change in the sign of the deviation.
4	Datapoints exhibiting gross systematic errors; these are identified by comparing the deviations among reported data sets for the same system at identical or similar conditions.

Table A11. Dew-point and bubble-point data summarized by components.

Component	Data Sets	Data Pts	Temperature ($^\circ$F)		Pressure (psia)	
			Minimum	Maximum	Minimum	Maximum
Carbon Dioxide	11	381	-184	400.4	61.00	2,675
Ethane	8	77	-250	250	12.44	2,675
Hydrogen	1	14	98.8	199.9	1,000.00	8,000
Hydrogen Sulfide	5	70	-100	400.4	61.00	1,820
Methane	22	982	-250	400.4	12.44	7,070
n-Butane	7	220	-200.01	250	12.44	2,675
n-Heptane	2	57	-150	40	19.80	3,272
n-Hexane	3	132	-150	250	19.90	2,675
n-Octane	2	18	-150	250	530.00	2,675
n-Pentane	8	188	-200	250	12.44	2,675
Nitrogen	11	78	-250	250	12.44	2,675
Propane	8	68	-250	250	12.44	8,000
Toluene	1	85	-120	40	50.00	7,070
Water	2	14	-459.67	400.4	0.00	536

Table A12. Dew-point and bubble-point data summarized by number of components.

Number of Components	Number of Systems	Dew	Bubble	Critical	Triple	Totals
2	9	663	147	37	13	860
3	4	47	34	0	0	81
4	2	13	6	1	0	20
6+	1	14	28	5	0	47
	Totals	737	215	43	13	1,008

Table A13. Dew-point and bubble-point data summarized by composition.

System Components		Dew	Bubble	Critical	Triple
CH_4, C_4H_{10}	Methane, n-Butane	173			
CH_4, C_5H_{12}	Methane, n-Pentane	118	23		
CH_4, C_6H_{14}	Methane, n-Hexane	108		6	
CH_4, C_7H_{16}	Methane, n-Heptane	50		3	
CH_4, C_7H_8	Methane, Toluene	24	59	2	
CH_4, CO_2	Methane, Carbon Dioxide	178	65	12	13
CO_2, N_2	Carbon Dioxide, Nitrogen	7			
H_2, C_3H_8	Hydrogen, Propane			14	
H_2S, N_2	Hydrogen Sulfide, Nitrogen	5			
CH_4, C_2H_6, CO_2	Methane, Ethane, Carbon Dioxide	10	13		
CH_4, CO_2, H_2S	Methane, Carbon Dioxide, Hydrogen Sulfide	25	21		
CH_4, CO_2, N_2	Methane, Carbon Dioxide, Nitrogen	6			
CH_4, H_2S, N_2	Methane, Hydrogen Sulfide, Nitrogen	6			
CH_4, C_2H_6, C_3H_8, N_2	Methane, Ethane, Propane, Nitrogen			6	1
CH_4, CO_2, H_2S, H_2O	Methane, Carbon Dioxide, Hydrogen Sulfide, Water	13			
CH_4, C_2H_6, C_3H_8, C_4H_{10}, C_5H_{12}, N_2	Methane, Ethane, Propane, n-Butane, n-Pentane, Nitrogen	7	19	3	
CH_4, C_2H_6, C_3H_8, C_4H_{10}, C_5H_{12}, C_6H_{14}, C_8H_{18}, CO_2, N_2	Methane, Ethane, Propane, n-Butane, n-Pentane, n-Hexane, n-Octane, Carbon Dioxide, Nitrogen	7	6	1	
CH_4, C_2H_6, C_3H_8, C_4H_{10}, C_5H_{12}, C_6H_{14}, C_7H_{16}, C_8H_{18}, CO_2, N_2	Methane, Ethane, Propane, n-Butane, n-Pentane, n-Hexane, n-Heptane, n-Octane, Carbon Dioxide, Nitrogen			3	1
	Totals	737	215	43	13

Table A14. VLE data sets summarized by number of components.

Number of Components	Number of Systems	Type of Data		
		Undetermined	Raw	Smooth
2	334	67	230	37
3	60	9	45	6
4+	18	10	8	0
Totals	412	86	283	43

Table A15. VLE data points summarized by number of components.

Number of Components	Number of Points	Outside Critical Region	Critical Region	Critical Point
2	13,240	12,321	68	851
3	2,624	2,620	4	
4+	239	239		
Totals	16,103	15,180	72	851

Table A16. Vapor-liquid-liquid and vapor-liquid-solid equilibrium data.

Number of Components	Number of Systems	SLV	SLLV	LLV	SL=LV	L=LV	LL=V	L=L=V	SLL=V	Total
2	27	476	8	161	2	4	30			681
3	23	241	346	2028	23	391	427	26	46	3528
4	8	98	8	146			26			278
5+	9	164	8	146			26			344
Totals		881	362	2335	25	395	483	26	46	4553

Note: The = sign indicates a critical point. For example, L=L-V is the tricritical point.

Table A17. Hydrate data.

Number of Components[1]	Number of Systems	Number of Data Sets			Number of Data Points
		Total	Uninhibited	Inhibited	
2	17	58	58	0	681
3	21	38	29	9	968
4	5	9	4	5	162
5+	16	18	15	3	268
	Totals	123	106	17	2,079

Notes:
(1) Component totals include water and inhibitors

APPENDIX B

GPA DATABASE RELATIONAL STRUCTURE

In the relational database model, data are divided into groups based on similar features of each particular group, which make the grouping an efficient description set.

Data Set and Data Point Levels

While the data types are unique, certain thermodynamic variables are repeated within each type. In what may be considered a super-set, all data are characterized by reference information, i.e., by the original reference source of the data (book or journal) and the authors of the article. Figure B1 shows the relationships between references and authors, and Table B1 and Table B2 describe the corresponding fields in the database.
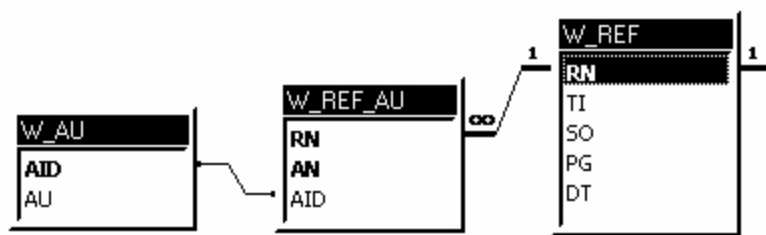
Figure B1. Reference information table.

Table B1 contains all the information for a given reference.

Table B1. References Table Relationships.

RN	Literature reference number – Indexing Field.
TI	Reference title.
SO	Reference source.
PG	Volume and page details for the reference.
DT	Year of publication.

Table B2 is the many-to-one relation between the W_REF and W_AU, linking the authors to each reference.

Table B2. W_REF_AU: Index to author for references.

RN	Literature reference number.
AN	Author number for the reference.
AID	Used for Author identification.

Finally, the table W_AU described in Table B3 provides the authors names based on an author index value.

Table B3. W_AU: Author names table.

AID	Index Used for Author identification.
AU	Author's Name

The data set table described in Table B4 is the primary table used in most search and descriptive operations. This table has a many-to-one relationship with the reference table W_REF, as a reference may be a source of multiple data sets.

Table B4. DS: Summary data set table.

DSN	Data Set Number - Database Primary Key for Data Set.
RN	Literature reference number.
DT	Index identifying the data type.
NC	Number of components in the mixture.
NDP	Total number of data points in the data set.
TMIN	Minimum temperature (Rankine) for the data set.
TMAX	Maximum temperature (Rankine) for the data set.
PMIN	Minimum pressure (psia) for the data set.
PMAX	Maximum pressure (psia) for the data set.
EID	Editing Privilege Code for the Data Set
DCK	Yes/No indicating Data Set Checked Against Original Reference

The components present in the systems also represent what may be considered supplemental information for pure components in the database. Physical properties and

225

other thermophysical constants, while not strictly necessary, are also contained in the database, in three tables all linked by an index table (Figure B2). A fourth table, WpropA contains API-44 constants [14] for calculating absolute enthalpies from the enthalpy departure data in the database.
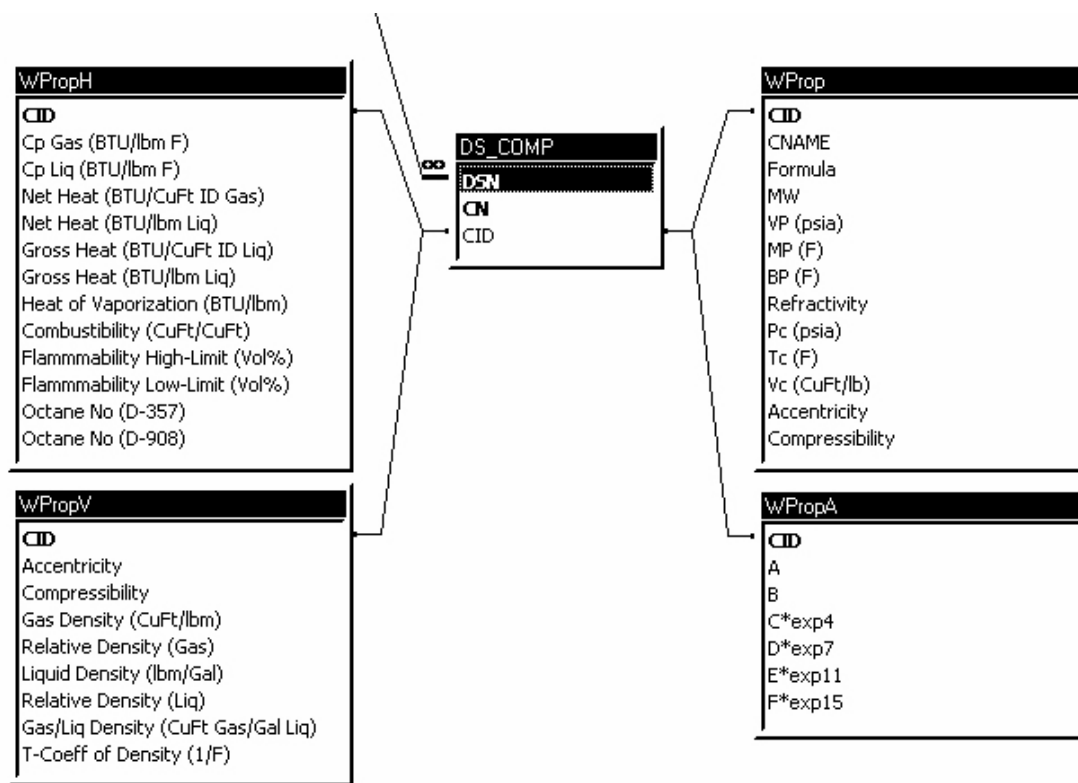
Figure B2. Component Properties Tables Relationships.

Enthalpy Data

Enthalpy Departure Data

The structure of the Enthalpy Departure data type differs from other database data structures. Both the data point and data set level information are directly connected to the data set summary table (Table B4) in one-to-many relationships. This is shown in Figure B3 below.
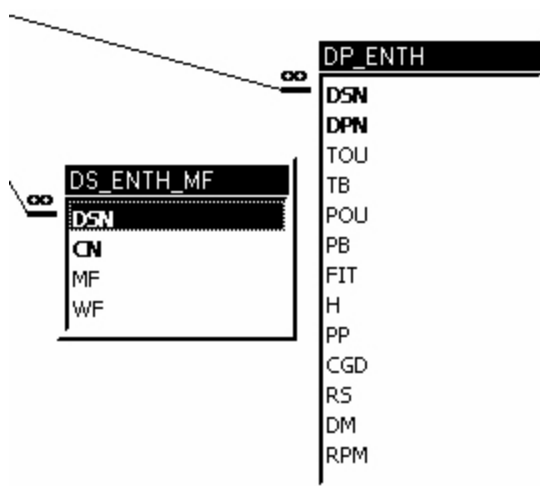
Figure B3. Enthalpy Departure Table Relationships.

The composition records are at the data set level in DS_ENTH_MF (Table B5).

Table B5. DS_ENTH_MF: Enthalpy Departure data set table.	
DSN	Data Set Number - Database Primary Key for Data Set.
CN	Component number in the mixture.
MF	Mole fraction of the component in the mixture.
WF	Weight Fraction of the component in the mixture.

The DP_ENTH table (

Table B6) includes temperature, pressure, and the departure method used to convert the

measurements (Lenoir, 1973).

Table B6. DP_ENTH: Enthalpy Depature data point table.	
DSN	Data Set Number - Database Primary Key for Data Set.
DPN	Data Point Number - Database Primary Key for Data Points.
TOU	Temperature for this data point based on original Reference units.
TB	Temperature for data point in Database reference unit: Rankine
POU	Pressure for this data point based on original Reference units.
PB	Pressure for data point in Database reference unit: psia
FIT	Estimated normalized accuracy of this data point.
H	Departure from ideal gas state at 0 K and 0 psia in (BTU/lb.).
PP	Phase code of the mixture.
CGD	# Indicates that enthalpy depature or phase was changed.
RS	R = Raw, S = Smooth, ? = Unevaluated.
DM	Departure method used.
RPM	Reliablity Index for Associated System Memo Table

Enthalpy of Solution Data

Enthalpy of Solution data are stored in four related tables: one at the data set level and three at the data point level (Figure B4). A feature of this data type is that in any particular case only one of the two final tables, based either on case "A" or case "B," are relevant to the data set. No data set has entries in all tables.
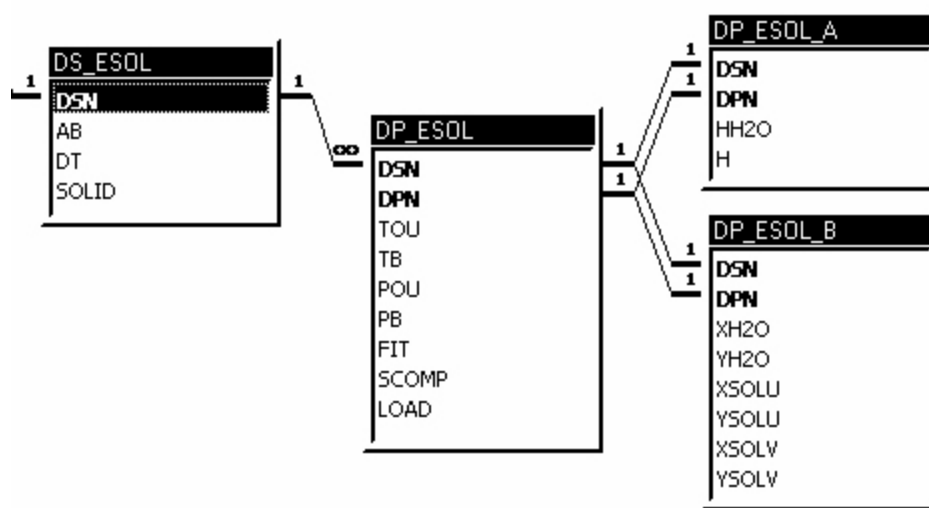
Figure B4. Enthalpy of Solution Table Relationships.

The DS_ESOL table, at the data set level, contains identifying criteria determining which of the subsequent data point level tables.

Table B7. DS_ESOL: Enthalpy of Solution data set table.

DSN	Data Set Number - Database Primary Key for Data Set.
DPN	Data Point Number - Database Primary Key for Data Points.
TOU	Temperature for this data point based on original Reference units.
TB	Temperature for data point in Database reference unit: Rankine
POU	Pressure for this data point based on original Reference units.
PB	Pressure for data point in Database reference unit: psia
FIT	Estimated normalized accuracy of this data point.
H	Departure from ideal gas state at 0 K and 0 psia in (BTU/lb.).
PP	Phase code of the mixture.
CGD	# Indicates that enthalpy depature or phase was changed.
RS	R = Raw, S = Smooth, ? = Unevaluated.
DM	Departure method used.
RPM	Reliablity Index for Associated System Memo Table

The DP_ESOL table contains data for the fields given in Table B8 and is present for each data set.

Table B8. DP_ESOL: Enthalpy of Solution data point table.

DSN	Data Set Number - Database Primary Key for Data Set.
DPN	Data Point Number - Database Primary Key for Data Points.
TOU	Temperature for this data point based on original Reference units.
TB	Temperature for data point in Database reference unit: Rankine
POU	Pressure for this data point based on original Reference units.
PB	Pressure for data point in Database reference unit: psia
FIT	Estimated normalized accuracy of this data point.
SCOMP	Weight percent in water of solvent.
LOAD	Loading (mol solute/ mole H2O free solvent).

The table DP_ESOL_A () contains enthalpy of solution data, and the DP_ESOL_B table (Table B9) contains phase composition records. Only one of these tables is used for each data set.

Table B9. DP_ESOL_A: Enthalpy of Solution data point table with enthalpy of solution.

DSN	Data Set Number - Database Primary Key for Data Set.
DPN	Data Point Number - Database Primary Key for Data Points.
HH2O	Enthalpy of solution (BTU / lb. of H20 free solvent).
H	Enthalpy of solution (BTU / lb. solvent).

Table B10. DP_ESOL_B: Enthalpy of Solution data point table with mole fractions.

DSN	Data Set Number - Database Primary Key for Data Set.
DPN	Data Point Number - Database Primary Key for Data Points.
XH2O	Liquid mole fraction of H2O.
YH2O	Vapor mole fraction of H2O.
XSOLU	Liquid mole fraction of solute.
YSOLU	Vapor mole fraction of solute.
XSOLV	Liquid mole fraction of solvent.
YSOLV	Vapor mole fraction of solvent.

Amine Data

Four tables characterize the amine data type (Figure B5) with one at the data set, and three at the data point level.
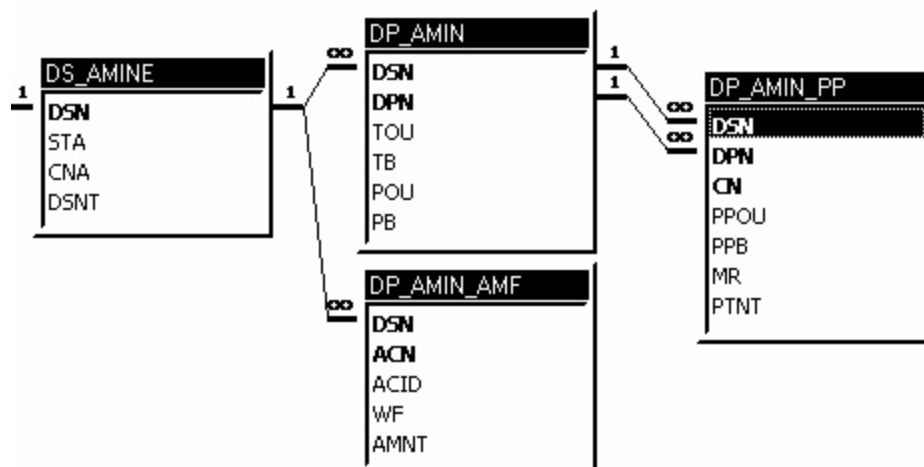
Figure B5. Amine Table Relationships.

The DS_AMINE table (Table B11) contains a field for data set notes. This field is included to account for the differences in amine data sets (such as amine composition being given in normality) without having to create another data structure.

Table B11. DS_AMINE: Amine data set table.

DSN	Data Set Number - Database Primary Key for Data Set.
STA	Yes/No.
CAN	Number of Amines in the system.
DSNT	Extra Data Set Notes.

The DP_AMIN_AMF table contains the composition of the unloaded amine solvent.

Table B12. DP_AMIN: Amine data point table.

DSN	Data Set Number - Database Primary Key for Data Set.
DPN	Data Point Number - Database Primary Key for Data Points.
TOU	Temperature for this data point based on original Reference units.
TB	Temperature for data point in Database reference unit: Rankine
POU	Pressure for this data point based on original Reference units.
PB	Pressure for data point in Database reference unit: psia

The DP_AMIN_AMF table contains the composition of the unloaded amine solvent.

Table B13. DP_AMIN_AMP: Amine data point table with amine weight fraction.

DSN	Data Set Number - Database Primary Key for Data Set.
CAN	Amine Component Number.
ACID	Amine Component Index.
WF	Weight Fraction.
AMNT	Amine Note.

230

Table B14. DP_AMIN_PP: Amine data point table with partial pressure

DSN	Data Set Number - Database Primary Key for Data Set.
DPN	Data Point Number - Database Primary Key for Data Points.
CN	Compnent Number.
PPOU	Partial Pressure in original reference units.
PPB	Partial Pressure in database base units: psia.
MR	Molar Ratio.
PTNT	PTNT

Phase Equilibrium Data

Dew-Point and Bubble-Point Data

Three tables, shown in Figure B6, form the relational database structure for the Dew/Bubble category of data.
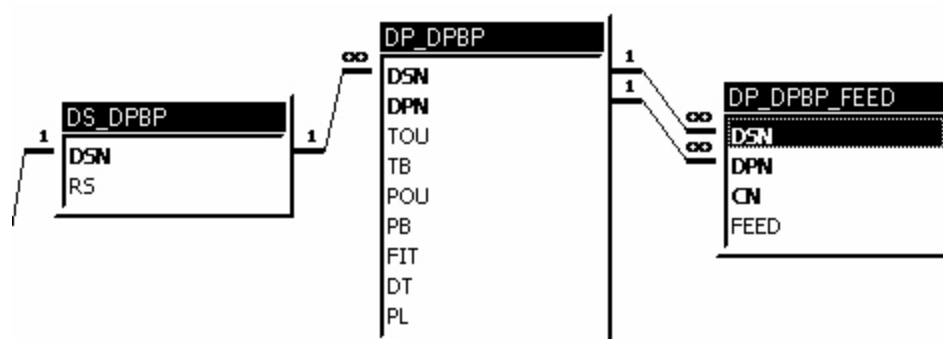
Figure B6. Dew/Bubble Data Table Relationships.

One of these tables, DS_DPBP is at the data-set level; the fields are described in Table B15. This table has a one-to-one relationship with the Table B4 described in the "Data Set and Data Point Levels" section of this report.

Table B15. DS_DPBP: Dew/Bubble data set table.

DSN	Data Set Number - Database Primary Key for Data Set.
RS	R = Raw, S = Smooth, or ? = Unevaluated.

The DP_DPBP and DP_DPBP_FEED tables are data point level tables. The DP_DPBP table (Table B16) contains the data point properties temperature, pressure, etc. This table

is related to the data set level table by a many-to-one relationship, e.g., one data set contains multiple data points.

Table B16. DP_DPBP: Dew/Bubble data point table.

DSN	Data Set Number - Database Primary Key for Data Set.
DPN	Data Point Number - Database Primary Key for Data Points.
TOU	Temperature for this data point based on original Reference units.
TB	Temperature for data point in Database reference unit: Rankine
POU	Pressure for this data point based on original Reference units.
PB	Pressure for data point in Database reference unit: psia
FIT	Estimated normalized accuracy of this data point.
DT	DP = Dew Point, BP = Bubble Point.
PL	Percent liquid.

Table B17. DP_DPBP_FEED: Dew/Bubble data point table with mole fraction.

DSN	Data Set Number - Database Primary Key for Data Set.
DPN	Data Point Number - Database Primary Key for Data Points.
CN	Component number in the mixture.
FEED	Feed mole fraction for this mixture.

Vapor-Liquid Equilibrium (VLE) Data

The Vapor-Liquid Equilibrium, or VLE, data type are represented by three tables as shown in Figure B7: one table at the data set level and two at the data point level.
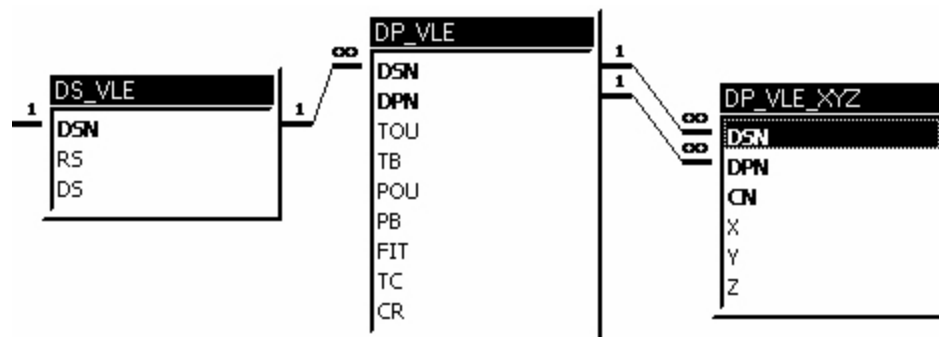
Figure B7. Vapor-Liquid Equilibria Table Relationships.

The DS_VLE table (Table B18) and contains data set level information pertinent to the vapor liquid equilibrium data type.

232

Table B18.	DS_VLE: Vapor-Liquid Equilibria data set table.
DSN	Data Set Number - Database Primary Key for Data Set.
RS	R = Raw, S = Smooth, or ? = Unevaluated.
DS	G = Gas Processors Association, K = Knapp (Berlin Data Book).

The DP_VLE table (Table B19) contains the temperature and pressure records at the data point level. The DP_VLE_XYZ table (Table B20) contains liquid, vapor, and composition information for the vapor liquid equilibrium data points.

Table B19.	DP_VLE: Vapor-Liquid Equilibria data point table.
DSN	Data Set Number - Database Primary Key for Data Set.
DPN	Data Point Number - Database Primary Key for Data Points.
TOU	Temperature for this data point based on original Reference units.
TB	Temperature for data point in Database reference unit: Rankine
POU	Pressure for this data point based on original Reference units.
PB	Pressure for data point in Database reference unit: psia
FIT	Data Point fit
TC	Thermodynamic Consistency
CR	Critical Point or Condition of Point

Table B20.	DP_VLE_XYZ: Vapor-Liquid Equilibria data point table with mole fractions.
DSN	Data Set Number - Database Primary Key for Data Set.
DPN	Data Point Number - Database Primary Key for Data Points.
CN	Component number in the mixture.
X	Liquid mole fraction of the component in the mixture.
Y	Vapor mole fraction of the component in the mixture,
Z	Feed mole fraction of the component in the mixture.

Vapor-Liquid-Liquid/Solid Data (VLLSE) Data

This category of data includes vapor-liquid-liquid, vapor-liquid-solid, and liquid-liquid-solid equilibrium data points. In keeping with the abbreviations used in the database program this is shortened to VLS, referring to combinations of these phases that do not fall into either the Dew/Bubble or Vapor-Liquid equilibrium (VLE) categories.

233

This data category is similar to both the Dew/Bubble and VLE types and is structured into three tables: one at the data set level and two at the data point level. These three tables and the relationships and fields of data used are shown in Figure B8.
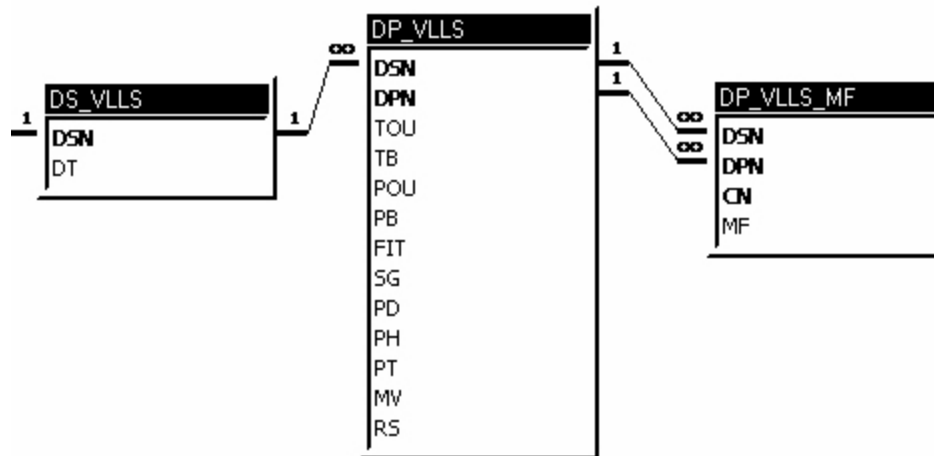
Figure B8. Vapor-Liquid-Liquid-Solid Table Relationships

The DS_VLLS table contains data set level information for the VLLSE data type.

Table B 21 DS_VLLS: Vapor-Liquid-Liquid-Solid data set table.

DSN	Data Set Number - Database Primary Key for Data Set.
DT	Vapor-Liquid-Liquid or Vapor Liquid Solid Equilibria.

At the data point level, the DP_VLLS table (Table B 22) contains temperature, pressure and phase designation entries.

234

Table B 22 DP_VLLS: Vapor-Liquid-Liquid-Solid data point table.

DSN	Data Set Number - Database Primary Key for Data Set.
DPN	Data Point Number - Database Primary Key for Data Points.
TOU	Temperature for this data point based on original Reference units.
TB	Temperature for data point in Database reference unit: Rankine
POU	Pressure for this data point based on original Reference units.
PB	Pressure for data point in Database reference unit: psia
FIT	Estimated normalized accuracy of this data point.
SG	Sub group identification.
PD	Phase designation.
PH	Phase being analyzed.
PT	Phase type.
MV	Molar volume (ml / gram-mole).
RS	R = Raw, S = Smoothed, "Blank" = Unevaluated.

The DP_VLLS_MF table (Table B 23) contains the mole fraction information. The DP_VLLS table is related by a one-to-many relationship with records in DP_VLLS_MF, where each record in DP_VLLS has multiple components associated with it.

Table B 23 DP_VLLS_MF: Vapor-Liquid-Liquid-Solid data point table with mole fractions.

DSN	Data Set Number - Database Primary Key for Data Set.
DPN	Data Point Number - Database Primary Key for Data Points.
CN	Component number in the mixture.
MF	Mole fraction of the component in the mixture.

Hydrate Data

Hydrate data falls into two categories: inhibited and uninhibited. Hydrate data are divided into five total tables.
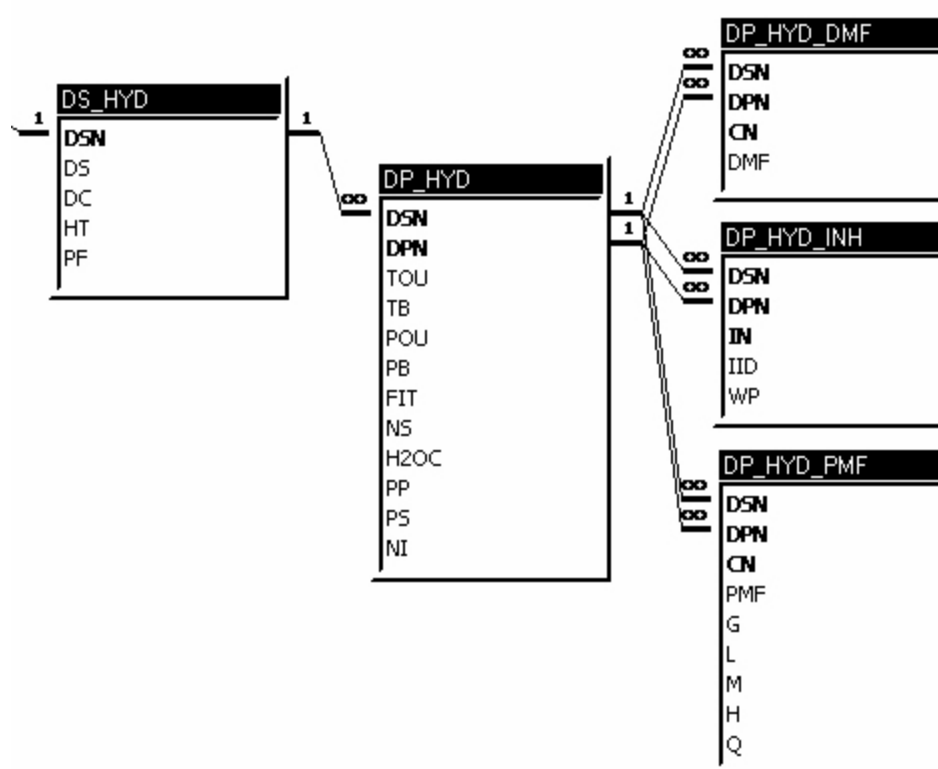
Figure B9. Hydrate Table Relationships.

DS_HYD (Table B9) at the data set level, defines each hydrate data set in the database. This table also characterizes each data set as inhibited or uninhibited and indicates whether phase mole fraction data exist for the set.

Table B 24 DS_HYD: Hydrate data set table.

DSN	Data Set Number - Database Primary Key for Data Set.
DS	G = GPA, L = Literature data.
DC	UH = Uninhibited, IH = Inhibited Hydrate.
HT	Yes/No; If True, Inhibited System
PF	Yes/No; If True, Phase Mole Fraction Data (PMF) Exists

There are two principal tables at the data point level: DP_HYD (Table B 25) contains temperature, pressure, and other data point records, and DP_HYD_DMF (Table B 26) contains the mole fraction data based on a dry basis.

Table B 25 DP_HYD: Hydrate data point table.

DSN	Data Set Number - Database Primary Key for Data Set.
DPN	Data Point Number - Database Primary Key for Data Points.
TOU	Temperature for this data point based on original Reference units.
TB	Temperature for data point in Database reference unit: Rankine
POU	Pressure for this data point based on original Reference units.
PB	Pressure for data point in Database reference unit: psia
FIT	Estimated normalized accuracy of this data point.
NS	Total number of T, P states in set.
H2OC	H2O content for this data point.
PP	Phases present at this data point.
PS	Phase being measured.
NI	Number of inhibitors present for this data set.

Table B 26 DP_HYD_DMF: Hydrate data point table with dry mole fractions.

DSN	Data Set Number - Database Primary Key for Data Set.
DPN	Data Point Number - Database Primary Key for Data Points.
CN	Component number in the mixture.
DMF	Dry mole fraction of the component in the mixture.

Two additional tables DP_HYD_INH (Table B 27) and DP_HYD_PMF (Table B 28) complete the hydrate data structure. Not every hydrate data set will include records in these tables. From DS_HYD the existence of records in DS_HYD_IN is determined by the value of the HT field for the data set, e.g., where true the hydrate data includes an inhibitor such as methanol.

Table B 27 DP_HYD_INH: Hydrate data point table for inhibitors.

DSN	Data Set Number - Database Primary Key for Data Set.
DPN	Data Point Number - Database Primary Key for Data Points.
IN	Inhibitor number in the hydrate.
IID	Used for identifying the inhibitor.
WP	Weight percent of the inhibitor.

Similarly, if the value of PT in DS_HYD is true, then DP_HYD_PMF contains mole fraction data for the data set.

Table B 28 DP_HYD_PMF: Hydrate data point table for phase mole fractions.

DSN	Data Set Number - Database Primary Key for Data Set.
DPN	Data Point Number - Database Primary Key for Data Points.
CN	Component number in the mixture.
PMF	Phase mole fractions of the components in the system.
G	Phase mole fractions of the components in the system.
L	Phase mole fractions of the components in the system.
M	Phase mole fractions of the components in the system.
H	Phase mole fractions of the components in the system.
Q	Phase mole fractions of the components in the system.

APPENDIX C

DATABASE TABLES AND FIELD DESCRIPTIONS

The DC_COMP table is the link in a many-to-many relationship between the DS table and the various W_PROP tables. It stores information on the components present in each data set.

Table C1. DC_COMP: Component index table for data sets.

DSN	Data Set Number - Database Primary Key for Data Set.
CN	Component number in the mixture.
CID	Used for component identification.

The DT table contains descriptive information for the categories of data present in the database.

Table C2. DT: Data type constants.

DT	Identifies Data Type
DTD	Description of the data type.
DTP	Bitmap Picture Representative of the data type
DTSP	Small Picture
DTLI	Large Icon (as Bitmap)
DTSI	Small Icon (as Bitmap)

The WDSN table contains the original reference unit information and other notes for each data set.

Table C3. WDSN: Data set notes and unit codes.

DSN	Data Set Number, Used as a primary key for data sets.
TU	Original reference units for Temperature
PU	Original reference units for Pressure
HU	Original reference units for Enthalpy
COMMENT	Note to users about this data set
NOTE	System administrator notes about this data set

The WENTH table contains a list of notes regarding the identification enthalpy points as outliers.

Table C 4. WENTH: Enthalpy departure set notes.

NTE	Enthalpy note type
ENOTE	Enthalpy Note text

The WPROP, WpropA, WpropH, and WpropV contain thermodynamic and physical constants for pure components from Table 23-2 of the GPSA Engineering Databook [10].

Table C 5. WPROP: Basic physical properties.

CID	Index used for component identification
CNAME	Chemical name of the component
Formula	Chemical Formula
MW	Molecular Weight in grams per mole
VP (psia)	Vapor Pressure in pounds per square inch
MP (F)	Melting Point in Fahrenheit
BP (F)	Boiling Point in Fahrenheit
Refractivity	Refractive Index
Pc (psia)	Critical Pressure in pounds per square inch
Tc (F)	Critical Temperature in Fahrenheit
Vc (CuFt/lb)	Critical Volume in cubic feet per pound
Accentricity	Accentric Factor, usually denoted by Greek omega
Compressibility	Compressibility Factor, usually denoted by Z

Table C 6. WpropA: API-44 constants for absolute enthalpy calculations.

CID	Index used for component identification
A	API-44 Constant for Enthalpy and Entropy Equations
B	API-44 Constant for Enthalpy and Entropy Equations
C*exp4	API-44 Constant for Enthalpy and Entropy Equations
D*exp7	API-44 Constant for Enthalpy and Entropy Equations
E*exp11	API-44 Constant for Enthalpy and Entropy Equations
F*exp15	API-44 Constant for Enthalpy and Entropy Equations

Table C7. WpropH: Physical property constants related to energy.

CID	Index used for component identification
Cp Gas (BTU/lbm F)	Gas Heat Capacity in BTUs per pound-mass Fahrenheit
Cp Liq (BTU/lbm F)	Liquid Heat Capacity in BTUs per pound-mass Fahrenheit
Net Heat (BTU/CuFt ID Gas)	Gas Net Heating Value in BTUs per cubic foot if Ideal
Net Heat (BTU/lbm Liq)	Liquid Net Heating Value in BTUs per pound-mass
Gross Heat (BTU/CuFt ID	Gas Gross Heat Value in BTUs per cubic foot if Ideal
Gross Heat (BTU/lbm Liq)	Liquid Gross Heat Value in BTUs per pound-mass
Heat of Vaporization (BTU/lbm)	Heat of Vaporization in BTUs per pound-mass
Combustibility (CuFt/CuFt)	Combustibility ?? cubic foot per cubic foot ??
Flammability High-Limit (Vol%)	High Flammability limit by percent volume
Flammability Low-Limit (Vol%)	Low Flammability limit by percent volume
Octane No (D-357)	Octane number standard D-357
Octane No (D-908)	Octane number standard D-908

Table C8. WpropV: Physical property constants related to volume.

CID	Index Key
Accentricity	Accentricity
Compressibility	Compressibility
Gas Density (CuFt/lbm)	Gas Density (CuFt/lbm)
Relative Density (Gas)	Relative Density (Gas)
Liquid Density (lbm/Gal)	Liquid Density (lbm/Gal)
Relative Density (Liq)	Relative Density (Liq)
Gas/Liq Density (CuFt Gas/Gal Liq)	Gas/Liq Density (CuFt Gas/Gal Liq)
T-Coeff of Density (1/F)	T-Coeff of Density (1/F)

Table C 9. List of Database Data Tables.

Table	Description
W_REF	Primary Table - Reference Information
W_REF_AU	Authors Index Links for References
W_AU	Authors Names By Index
DS	Data Set Main Summary Information
DS_COMP	Component Index Links for Data Sets
WDSN	Units Index Links for Data Sets
DT	Data Type Names and Information
DS_DPBP	Data Set Table for Dew-Bubble Data Type
DP_DPBP	Data Point Table for Dew-Bubble Data Type
DP_DPBP_FEED	Data Point Table for Dew-Bubble Data Type - Mole Fractions in Feed
DS_VLE	Data Set Table for Vapor-Liquid Equilibria Data Type
DP_VLE	Data Point Table for Vapor-Liquid Equilibria Data Type
DP_VLE_XYZ	Data Point Table for Vapor-Liquid Equilibria Data Type - Mole Fractions Measured
DS_VLLS	Data Set Table for Vapor-Liquid-Solid Data Type
DP_VLLS	Data Point Table for Vapor-Liquid-Solid Data Type
DP_VLLS_MF	Data Point Table for Vapor-Liquid-Solid Data Type - Mole Fractions
DS_HYD	Data Set Table for Hydrate Data Type
DP_HYD	Data Point Table for Hydrate Data Type
DP_HYD_DMF	Data Point Table for Hydrate Data Type - Dry Mole Fractions in Feed
DP_HYD_INH	Hydrate Inhibitor Information
DP_HYD_PMF	Hydrate Measured Phase Mole Fractions
DS_ENTH_MF	Data Set Table for Enthalpy Departure Data Type
DP_ENTH	Enthalpy Data Set Information
DS_ESOL	Data Set Table for Enthalpy Of Solution Data Type
DP_ESOL	Data Point Table for Enthalpy Of Solution Data Type
DP_ESOL_A	Data Point Table for Enthalpy Of Solution Data Type - Type A
DP_ESOL_B	Data Point Table for Enthalpy Of Solution Data Type - Type B
DS_AMINE	Data Set Table for Amine Data Type
DP_AMIN	Data Point Table for Amine Data Type
DP_AMIN_PP	Partial Pressure Data
DP_AMIN_AMF	Amine Weight Fraction Information
WPROP	Properties Table – Primary Data
WPropA	Properties Table - Enthalpy Calculation Constants
WPropV	Properties Table - Volumetric
WPropH	Properties Table - Heat Data
Wunit	Units Conversion Information and Unit Names
WART	Artwork Data
WARTM	Artwork Data
WENTH	Enthalpy Data Point Notes Table

APPENDIX D

ENTHALPY EVALUATION INFORMATION

Table D 1. Pure Fluid Critical Properties Used in Evaluations

No.	Compound	Formula	Molecular Weight	Pressure (psia)	Temperature (F)	Accentric Factor, ?
1	Methane	CH_4	16.043	666.4	-116.67	0.0104
2	Ethane	C_2H_6	30.070	706.5	89.92	0.0979
3	Propane	C_3H_8	44.097	616.0	206.06	0.1522
4	i-Butane	C_4H_{10}	58.123	527.9	274.46	0.1852
5	n-Butane	C_4H_{10}	58.123	550.6	305.62	0.1995
6	i-Pentane	C_5H_{12}	72.150	490.4	369.10	0.2280
7	n-Pentane	C_5H_{12}	72.150	488.6	385.80	0.2514
8	n-Heptane	C_7H_{16}	100.204	396.8	512.70	0.3494
9	n-Octane	C_8H_{18}	114.231	360.7	564.22	0.3977
10	i-Octane	C_8H_{18}	114.231	372.4	519.46	0.3035
11	n-Hexadecane	$C_{16}H_{34}$	226.448	205.7	830.93	0.7420
12	Cyclohexane	C_6H_{12}	84.161	590.8	536.60	0.2096
13	Methylcyclohexane	C_7H_{14}	98.188	503.5	570.27	0.2358
14	Ethylcyclohexane	C_8H_{16}	112.216	438.4	636.50	0.2430
15	Propene	C_3H_6	42.081	668.6	197.17	0.1356
16	cis-2-Pentene	C_5H_{10}	70.135	529.05	397.13	0.2400
17	Benzene	C_6H_6	78.114	710.4	552.22	0.2093
18	Toluene	C_7H_8	92.141	595.5	605.57	0.2633
19	Ethylbenzene	C_8H_{10}	106.167	523.0	654.29	0.3027
20	Tetralin	$C_{10}H_{12}$	132.206	509.9	834.50	0.3030
21	cis-Decalin	$C_{10}H_{18}$	138.254	455.6	804.30	0.2300
22	trans-Decalin	$C_{10}H_{18}$	138.254	455.6	782.30	0.2700
23	Carbon Monoxide	CO	28.010	507.5	-220.43	0.0484
24	Carbon Dioxide	CO_2	44.010	1,071.0	87.91	0.2667
25	Hydrogen Sulfide	H_2S	34.080	1,300.0	212.45	0.0948
26	Sulfur Dioxide	SO_2	64.060	1,143.0	315.80	0.2548
27	Carbonyl Sulfide	COS	60.070	852.37	215.33	0.0990
28	Hydrogen	H_2	2.0159	188.1	-399.90	-0.2202
29	Nitrogen	N_2	28.0134	439.1	-232.51	0.0372
30	Water	H_2O	18.0153	3,198.8	705.16	0.3443
31	Helium	He	4.0026	32.99	-450.31	0.0000

Table D 2. GPA Enthalpy References

#364 Yarborough, L., Edmister, W.C., Calorimetric Determination of the Isothermal Pressure Effect on the Enthalpy of the Propane-Benzene Systems, AIChE Journal, 11,492, 1965

#370 Bhirud, V.L., Powers, J.E., Thermodynamic Properties of a 5 Mole Percent Propane in Methane Mixture, Report to the NGPA, , Aug 1969

#458 Storvic, T.S., Smith,J.M., Thermodynamic Properties of Polar Substances: Enthalpy of Hydrocarbon-Alcohol Systems, J. Chem. Eng., 5,133, 1960

#556 Yorizane, M., Yoshimura, S., Masuoka, H., Vapor Liquid Equilibrium at High Pressure (N(2) - CO(2) System), Kagaku Kogaku, 34 (9), 953, 1970

#558 Gonikberg, M.G., Fastowsky, W.G., Gurwitsch, J.G., The Solubility of Gases in Liquids at Low Temperatures and High Pressures. I. The Solubility of Hydrogen in Liquid Nitrogen at Temperatures of 79.0-109.0 Degrees K and Pressures Up to 190 Atm, Acta Physicochim. URSS, 11 (6), 865, 1939

#573 Dillard, D.D., Edmister, W.C., Erbar, J.H., Robinson, R.L., Jr., Calorimetric Determination of the Isothermal Effect of Pressure on the Enthalpy of Methane and Two Methane Propane Mixtures, AIChE Journal, 14,923, 1968

#574 Furtado, A.W., Katz, D.L., Powers, J.E., Paper presented at 159th National ACS meeting, , , Feb 1970

#578 Jones, M.L., Jr., Mage, D.T., Faulkner, R.C., Katz, D.L., Measurement of the Thermodynamic Properties of gases at Low Temperature and High Pressure-Methane, Chem. Eng. Prog. Sym. Series, 59 (44) 52-60, 1963

#579 Lenoir, J.M., A Program of Experimental Measurement of Enthalpies of Binary Hydrocarbon Mixtures above 100 deg. F., and in the Critical Region, Proceedings of API, 47, 640-652, 1967

#580 Lenoir, J.M., Hayworth, K.E., Hipkin, H.G., Some Measurements and Predictons of Enthalpy of Hydrocarbon Mixtures, Proceedings of API, 50, 212, 1970

#581 Lenoir, J.M., Hayworth, K.E., Hipkin, H.G., Enthalpy Measurements for Hydrocarbon Mixtures, Proceedings of API, 51,405, 1971

#582 Lenoir, J.M., Hayworth, K.E., Hipkin, H.G., Enthalpies of Decalin and Trans-Decalin and n-Pentane Mixtures, J. of Chem. Eng. Data, 16,129, 1971

#583 Lenoir, J.M., Hipkin, H.G., Enthalpies of Mixtures of n-Hexadecane and n-Pentane, J. of Chem. Eng. Data, 15,368, 1970

#584 Lenoir, J.M., Kuravila, G.K., Hipkin, H.G., Measured Enthalpies of Binary Mixtures of Hydrocarbons with Pentane, Proceedings of API, 49,89, 1969

#585 Lenoir, J.M., Robinson, D.R., Hipkin, H.G., Flow Calorimeter and Measurement of the Enthalpy of n-Pentane, J. Chem. Eng. Data, 15,23, 1970

.

Table D 2. GPA Enthalpy References (Cont'd)

#586 Lenoir, J.M., Robinson, D.R., Hipkin, H.G., Enthalpies of Mixtures of n-Octane and n-Pentane, J. Chem. Eng. Data, 15,26, 1970

#587 Mage, D.T., Jones, M.L., Jr., Katz, D.L., Roebuck, J.R., Experimental Enthalpies for Nitrogen, Chem. Eng. Prog. Sym. Series, 59 (44), 61, 1963

#588 Mather, A.E., The Direct Determination of the Enthalpy of Fluids Under Pressure, Phd Thesis U. Michigan, , 1967

#590 Yesavage, V.F., The Measurement and Prediction of the Enthalpy of Fluid Mixtures Under Pressure, Phd Thesis U. Michigan, , 1968

#591 Starling, K.E., Johnson, D.W., Colver, C.P., Evaluations of Eight Enthalpy Correlations, NGPA Research Report, RR-4, 1971

#592 Starling, K.E., 1971-1972 Enthalpy Correlation Evaluation Study, NGPA Research Report, RR-8, 1972

#663 Lenoir, J.M., Robinson, D.R., Hipkin, H.G., Measurement of the Enthalpy of Pentane, Octane, and Pentane-Octane Mixtures, Proceedings of API, 48, 346-396, 1968

#665 Lenoir, J.M. Private Communication, Univ. of Southern Cal. Los Angeles, 1972

#666 Eakin, B., Wilson, G.M., DeVaney, W., Enthalpies of Methane-Seven Carbon Systems, NGPA Research Report, RR-6, 1972

#667 Cochran, G.A., Lenoir, J.M., GPA Experimental Values Referred to Two Base Levels, GPA Research Report, RR-11, 1974

#670 Eakin, B., DeVaney, W., Enthalpies of Hydrogen Sulfide-Methane-Ethane Systems, NGPA Research Report, RR-9, 1973

#671 Furtado, A.W.   The Measurement and Prediction of Thermal Properties of Selected Mixtures of Methane, Ethane, and Propane, Technical Report, Project 345330 Division of Research Development and Administration, , 27030

#672 Peterson, J.M., Wilson, G.M., Enthalpy and Phase Boundary Measurements on Carbon Dioxide and Mixtures of Carbon Dioxide with Methane, Ethane and Hydrogen Sulfide, NGPA Project 731, RR-12, Mar 25 1974

#673 Berryman, J.M., DeVaney, W., Eakin, B., Baily, N.L., Enthalpy Measurements on Synthetic Gas Systems: Hydrogen-Methane, Hydrogen-Carbon Monoxide, GPA Research Report, RR-37, 1979

#674 Scheloske, J.J., Hall, K.R., Eubank, P.T., Holste, J.C., Experimental Densities and Enthalpies for Water-Natural Gas Systems, GPA Research Report, RR-53, 1981

#675 Lenoir, J.M., Hayworth, K.E., Hipkin, H.G., Enthalpies of Tetralin and Mixtures of Tetralin and n-Pentane, J. Chem. Eng. Data, 15, 474, 1970

#676 Cediel, L.E., Eubank, P.T., Holste, J.C., Hall, K.R., Experimental Enthalpies for Pure Toluene and Pure Methylcyclohexane, GPA Research Report, RR-63, 1982

#677   Lenoir, J.M., Kuravila, G.K., Hipkin, H.G., Enthalpies of Cyclohexane and Mixtures of n-Pentane and Cyclohexane, J. Chem. Eng. Data, 16, 271, 1971

#678   Lenoir, J.M., Rebert, C.J., Hipkin, H.G., Enthalpies of Cis-2-Pentane and a Mixture with n-Pentane, J. Chem. Eng. Data, 16, 401, 1971

#679   Lenoir, J.M., Hayworth, K.E., Hipkin, H.G., Enthalpies of Benzene with n-Octane, J. Chem. Eng. Data, 16, 280, 1971

#680   Lenoir, J.M., Hayworth, K.E., Hipkin, H.G., Enthalpies of Mixtures of Benzene and Cyclohexane, J. Chem. Eng. Data, 16, 285, 1971

#681   Lenoir, J.M., Hipkin, H.G., Measured Enthalpies for Mixtures of Benzene and Hexadecane, J. Chem. Eng. Data, 17, 319, 1972

#682   Hayworth, K.E., Lenoir, J.M., Hipkin, H.G., Enthalpies of Mixtures of Benzene and Hexadecane, J. Chem. Eng. Data, 16,276, 1971

#683   Lenoir, J.M., Bal, M., Hipkin, H.G., Enthalpies of Ternary System Pentane-Cyclohexane-Benzene, J. Chem. Eng. Data, 17, 461, 1972

#684   Lenoir, J.M., Hipkin, H.G., Enthalpies of Two Ternary Mixtures of Benzene-Octane-Tetralin, J. Chem. Eng. Data, 17, 461, 1972

#685   Cunningham, J.R., Enthalpy and Phase Boundary Measurements--Equal Molar Mixtures of n-Pentane with Carbon Dioxide and Hydrogen Sulfide, GPA Research Report, RR-103, 1986

#686   Bailey, D.M., Eubank, P.T., Hall, K.R., Holste, J.C., Marsh, K. M., Liu, C.H., Thermodynamic Properties of Pure Hydrogen Sulfide with Methane, Carbon Dioxide, Methylcyclohexane and Toluene, GPA Research Report, RR-107, 1987

#687   Eubank, P.T., Hall, K.R., Holste, J.C., Johnson, M.G., Experimental Enthalpies of Pentanes-plus Fractions, GPA Research Report, RR-121, 1989

#688   Bailey, D.M., Esker, G.J., Holste, J.C., Hall, K.R., Eubank, P.T., Marsh, K. M., Rogers, W.J., Properties of Carbon Dioxide Mixtures with Nitrogen and Methane, GPA Research Report, RR-122, 1989

#689   Christensen, S.P., Christensen, J.J., Izatt, R.M., Enthalpies of Solution CO2 in Aqueous Diglycolamine Solutions, GPA Research Report, RR-85, 1985

#690   Merkley, K.E., Christensen, J.J., Izatt, R.M., Enthlapies of Solution CO2 in Aqueous Methyldiethanolamine Solutions, GPA Research Report, RR-102, 1986

#691   Helton, R., Christensen, J.J., Izatt, R.M., Enthalpies of Solution CO2 in Aqueous Diethanolamine Solutions, GPA Research Report, RR-108, 1987

#692   Van Dam, R., Christensen, J.J., Izatt, R.M., Oscarson, J.L., Enthalpies of H2S in Aqueous Diethnolamine Solutions, GPA Research Report, RR-114, 1988

#693   Oscarson, J.L., Izatt, R.M., Enthalpies of Solution H2S in Aqueous Methyldiethanolamine Solutions, GPA Research Report, RR-127, 1990

APPENDIX E

PURE COMPONENT ENTHALPY EVALUATION SUMMARIES

Table E 1. Component Summary by Phase

COMPONENT	PHASE	REF	RMSE	AAD	%AAD	BIAS	Temp Tmin	Temp Tmax	Press Pmin	Press Pmax	Max Dev Low	Max Dev High	NPTS
benzene	L	581	5.5	5.0	4.5	5.0	155.8	549.9	20	800	0.3	8.3	43
		584	3.2	2.6	2.2	2.4	200.8	542.5	200	1,400	-1.5	7.0	21
		679	4.6	3.7	3.6	3.6	380.0	552.0	200	1,400	-0.7	9.0	44
	Subtotal		4.8	4.0	3.7	4.0	155.8	552.0	20	1,400	-1.5	9.0	108
	V	581	4.3	2.2	16.1	1.7	238.4	589.2	20	750	-4.0	20.8	31
		584	6.5	3.0	6.4	1.7	445.9	696.5	100	1,400	-4.0	29.4	46
		679	8.0	3.6	5.9	2.8	400.0	700.0	200	1,400	-4.9	30.4	162
	Subtotal		7.3	3.3	7.3	2.5	238.4	700.0	20	1,400	-4.9	30.4	239
	L-L-V	581	36.3	24.0	56.7	-14.8	502.0	551.5	500	714	-72.6	8.0	10
	L-V-V	581	3.9	3.3	24.2	2.8	313.4	552.4	70	708	-0.9	6.8	4
	Total		8.9	4.1	7.8	2.4	155.8	700.0	20	1,400	-72.6	30.4	361
cis-2-pentene	L	581	3.6	3.1	3.1	2.4	348.7	395.5	400	1,400	-2.2	7.5	15
		678	3.2	2.5	2.4	2.1	330.0	395.0	300	1,400	-2.2	7.4	34
	Subtotal		3.3	2.7	2.6	2.2	330.0	395.5	300	1,400	-2.2	7.5	49
	V	581	6.0	4.0	15.3	1.0	159.8	545.9	20	1,400	-5.3	20.7	107
		678	8.7	4.3	8.2	1.9	330.0	440.0	200	1,400	-4.0	57.6	86
	Subtotal		7.3	4.1	12.2	1.4	159.8	545.9	20	1,400	-5.3	57.6	193
	L-L-V	581	4.1	3.7	3.7	3.7	335.7	391.6	350	600	1.1	7.6	19
	L-V-V	581	5.1	3.6	6.8	-3.1	365.7	401.0	400	540	-15.0	3.1	16
		678	5.6	5.6	11.0	-5.6	390.0	390.0	500	500	-5.6	-5.6	1
	Subtotal		5.1	3.7	7.1	-3.2	365.7	401.0	400	540	-15.0	3.1	17
	Total		6.5	3.8	9.6	1.4	159.8	545.9	20	1,400	-15.0	57.6	278

Table E 1. Component Summary by Phase (Cont'd)

COMPONENT	PHASE	REF	RMSE	AAD	%AAD	BIAS	Temp Tmin	Tmax	Press Pmin	Pmax	Max Dev Low	High	NPTS
cis-decalin	L	580	9.0	7.8	5.9	7.8	149.0	474.9	25	1,400	1.4	15.8	20
		582	6.7	6.5	5.8	6.5	460.0	600.0	40	1,400	4.0	9.9	14
	Subtotal		8.1	7.3	5.9	7.3	149.0	600.0	25	1,400	1.4	15.8	34
	V	580	3.9	3.6	609.4	-3.6	450.5	595.9	25	100	-6.5	-0.6	16
		582	3.7	2.8	38.5	2.8	460.0	600.0	25	100	0.5	8.8	14
	Subtotal		3.8	3.2	343.0	-0.6	450.5	600.0	25	100	-6.5	8.8	30
	L-L-V	580	1.2	0.9	0.9	0.3	494.1	592.4	70	1,400	-2.6	2.0	10
	L-V-V	580	6.7	6.5	60.2	6.5	432.4	574.9	25	100	4.8	8.2	2
	Total		6.1	4.8	139.7	3.2	149.0	600.0	25	1,400	-6.5	15.8	76
cyclohexane	L	584	3.0	2.1	1.7	1.2	117.0	531.1	15	1,400	-4.7	10.7	69
		677	3.0	2.2	2.0	0.6	300.0	540.0	100	1,400	-3.0	9.3	59
	Subtotal		3.0	2.1	1.9	0.9	117.0	540.0	15	1,400	-4.7	10.7	128
	V	584	5.2	3.6	130.5	1.1	194.5	689.0	15	1,400	-12.4	23.6	69
		677	5.1	2.9	10.0	2.7	340.0	680.0	100	1,400	-1.4	24.8	107
	Subtotal		5.1	3.2	57.2	2.0	194.5	689.0	15	1,400	-12.4	24.8	176
	L-L-V	584	6.5	5.0	5.1	4.7	391.3	548.2	200	800	-0.7	9.9	5
	L-V-V	584	4.6	4.0	18.8	4.0	320.8	515.4	100	500	2.8	8.3	5
	Total		4.4	2.8	33.2	1.7	117.0	689.0	15	1,400	-12.4	24.8	314
ethane	L	592	2.6	1.8	0.9	1.7	-240.0	80.0	200	2,000	-0.7	5.6	41
	V	592	8.4	3.9	6.1	2.1	40.0	280.0	200	2,000	-2.8	32.3	28
	Total		5.7	2.7	3.0	1.9	-240.0	280.0	200	2,000	-2.8	32.3	69
ethylbenzene	L	687	2.1	1.5	1.1	0.6	170.4	530.4	290	2,900	-2.1	5.2	33
	V	687	0.9	0.8	71.9	-0.8	350.4	485.4	22	80	-1.3	-0.4	12
	Total		1.9	1.3	19.9	0.2	170.4	530.4	22	2,900	-2.1	5.2	45

Table E1. Component Summary by Phase (Cont'd)

COMPONENT	PHASE	REF	RMSE	AAD	%AAD	BIAS	Temp		Press		Max Dev		NPTS
							Tmin	Tmax	Pmin	Pmax	Low	High	
ethylcyclohexane	L	687	9.2	8.1	6.8	8.1	224.4	584.4	290	1,450	3.4	19.8	21
hydrogen sulfide	V	686	4.9	2.2	5.3	1.1	80.3	440.3	145	4,351	-2.3	19.9	59
	L-V-V	686	4.1	3.5	9.4	3.5	80.3	170.3	306	866	1.4	5.6	2
	Total		4.9	2.3	5.5	1.1	80.3	440.3	145	4,351	-2.3	19.9	61
iso-octane	L	687	1.8	1.6	1.6	-1.0	188.4	476.4	290	1,450	-2.0	4.0	18
methane	L	578	1.8	1.4	0.7	0.0	-250.0	-150.0	250	2,000	-2.3	4.4	14
	V	573	3.9	3.7	14.4	-3.7	150.0	150.0	500	2,000	-5.0	-2.0	4
		578	12.3	5.9	8.5	2.9	-150.0	50.0	250	2,000	-3.8	46.3	21
	Subtotal		11.4	5.5	9.4	1.8	-150.0	150.0	250	2,000	-5.0	46.3	25
	Total		9.2	4.0	6.3	1.2	-250.0	150.0	250	2,000	-5.0	46.3	39
methylcyclohexane	L	375	6.7	6.7	6.6	-6.7	464.0	464.0	1,365	1,365	-6.7	-6.7	1
		592	8.6	8.4	6.1	8.4	50.0	550.0	50	2,500	4.5	12.2	86
		675	4.1	4.1	3.2	-4.1	212.0	248.0	1,365	1,365	-4.3	-3.9	2
		676	1.9	1.5	1.3	-0.8	176.0	464.0	115	1,365	-5.6	1.9	33
	Subtotal		7.3	6.4	4.8	5.5	50.0	550.0	50	2,500	-6.7	12.2	122
	V	592	8.4	7.1	31.9	7.1	350.0	650.0	50	2,500	0.5	18.9	31
		676	4.1	3.8	60.4	3.8	212.0	464.0	17	100	2.3	7.7	15
	Subtotal		7.3	6.0	41.2	6.0	212.0	650.0	17	2,500	0.5	18.9	46
	Total		7.3	6.3	14.7	5.7	50.0	650.0	17	2,500	-6.7	18.9	168

Table E1. Component Summary by Phase (Cont'd)

COMPONENT	PHASE	REF	RMSE	AAD	%AAD	BIAS	Temp Tmin	Tmax	Press Pmin	Pmax	Max Dev Low	High	NPTS
n-heptane	L	556	5.8	5.7	4.2	5.7	50.0	500.0	50	2,500	4.0	8.5	78
		666	11.3	11.1	6.2	11.1	-100.0	0.0	50	2,500	8.5	14.5	27
	Subtotal		7.6	7.1	4.8	7.1	-100.0	500.0	50	2,500	4.0	14.5	105
	V	556	6.2	5.0	24.5	5.0	300.0	600.0	50	2,500	0.3	15.0	28
		665	1.8	1.6	99.6	-1.0	361.8	589.3	50	100	-3.1	2.9	24
	Subtotal		4.7	3.4	59.1	2.2	300.0	600.0	50	2,500	-3.1	15.0	52
	Total		6.8	5.9	22.8	5.5	-100.0	600.0	50	2,500	-3.1	15.0	157
n-hexadecane	L	583	1.7	1.2	1.2	0.5	400.0	640.0	25	1,400	-4.8	4.3	53
		584	6.3	4.4	3.8	3.8	199.5	628.0	25	1,400	-3.7	21.2	28
	Subtotal		4.0	2.3	2.1	1.7	199.5	640.0	25	1,400	-4.8	21.2	81
	V	583	4.7	4.4	54.8	4.4	610.0	660.0	25	40	2.2	7.0	13
		584	4.3	4.1	52.2	4.1	602.5	657.0	25	40	2.4	6.6	6
	Subtotal		4.6	4.3	54.0	4.3	602.5	660.0	25	40	2.2	7.0	19
	L-L-V	584	1.6	1.6	1.8	-1.6	595.1	595.1	1,400	1,400	-1.6	-1.6	1
	L-V-V	584	14.0	14.0	78.3	14.0	619.2	619.2	32	32	14.0	14.0	1
	Total		4.3	2.8	12.5	2.2	199.5	660.0	25	1,400	-4.8	21.2	102
nitrogen	L	587	1.0	0.8	1.3	0.5	-250.0	-250.0	500	3,000	-0.8	1.8	7
	V	587	2.9	1.7	10.3	-0.3	-250.0	50.0	200	3,000	-1.8	12.3	48
	Total		2.8	1.6	9.2	-0.2	-250.0	50.0	200	3,000	-1.8	12.3	55

Table E1. Component Summary by Phase (Cont'd)

COMPONENT	PHASE	REF	RMSE	AAD	%AAD	BIAS	Temp Tmin	Tmax	Press Pmin	Pmax	Max Dev Low	High	NPTS
n-octane	L	586	1.9	1.3	1.3	0.8	75.0	560.0	200	1,400	-1.3	5.8	90
		663	2.9	2.2	2.2	1.5	150.8	565.4	15	1,400	-4.2	8.3	64
	Subtotal		2.3	1.7	1.7	1.1	75.0	565.4	15	1,400	-4.2	8.3	154
	V	586	6.4	5.0	11.3	5.0	500.0	600.0	200	1,400	0.5	18.4	39
		663	7.4	5.7	17.7	5.7	397.7	600.3	15	1,400	-0.2	19.7	42
	Subtotal		7.0	5.4	14.6	5.4	397.7	600.3	15	1,400	-0.2	19.7	81
	L-L-V	586	6.0	6.0	7.4	6.0	560.0	560.0	400	400	6.0	6.0	1
		663	2.7	2.7	2.1	-2.7	254.0	254.1	15	15	-2.8	-2.6	2
	Subtotal		4.1	3.8	3.9	0.2	254.0	560.0	15	400	-2.8	6.0	3
	Total		4.5	3.0	6.1	2.5	75.0	600.3	15	1,400	-4.2	19.7	238
n-pentane	L	458	5.3	4.1	3.7	4.0	250.0	400.0	200	700	-0.1	10.0	13
		585	1.6	1.2	1.0	1.1	75.0	380.0	200	1,400	-1.0	5.7	71
		663	4.3	3.4	3.0	3.4	95.9	406.0	15	1,400	0.0	10.4	57
	Subtotal		3.4	2.4	2.1	2.3	75.0	406.0	15	1,400	-1.0	10.4	141
	V	458	6.9	3.6	9.3	2.5	250.0	500.0	100	1,100	-2.1	29.5	35
		585	8.3	3.8	6.7	3.3	300.0	700.0	200	1,400	-3.0	36.7	124
		663	3.9	2.6	14.2	1.9	211.3	691.5	15	1,400	-5.2	14.5	90
	Subtotal		6.8	3.3	9.8	2.7	211.3	700.0	15	1,400	-5.2	36.7	249
	L-L-V	663	8.6	8.6	9.4	8.6	381.7	381.7	489	489	8.6	8.6	1
	L-V-V	663	2.8	2.6	13.2	2.6	295.0	299.6	200	200	1.0	3.3	4
	Total		5.8	3.0	7.0	2.6	75.0	700.0	15	1,400	-5.2	36.7	395

Table E 1. Component Summary by Phase (Cont'd)

COMPONENT	PHASE	REF	RMSE	AAD	%AAD	BIAS	Temp Tmin	Temp Tmax	Press Pmin	Press Pmax	Max Dev Low	Max Dev High	NPTS
propane	L	364	10.5	10.5	8.4	10.5	200.0	200.0	750	750	-2.9	18.0	1
		590	5.5	4.2	2.1	4.1	-250.0	200.0	500	2,000	-1.6	21.5	39
	Subtotal		5.7	4.3	2.3	4.3	-250.0	200.0	500	2,000	-2.9	21.5	40
	V	364	5.7	3.2	9.8	1.0	200.0	400.0	200	1,000	-2.9	18.0	11
		590	9.2	6.0	7.9	5.1	200.0	300.0	250	2,000	-1.6	21.5	10
	Subtotal		7.6	4.6	8.9	3.0	200.0	400.0	200	2,000	-2.9	21.5	21
	Total		6.4	4.4	4.5	3.8	-250.0	400.0	200	2,000	-2.9	21.5	61
tetrahydronaphthalene	L	580	6.1	4.5	3.1	2.3	102.1	653.6	25	1,400	-5.9	15.3	42
		675	1.2	1.1	0.9	0.3	480.0	660.0	40	1,400	-2.5	1.7	28
	Subtotal		4.8	3.1	2.2	1.5	102.1	660.0	25	1,400	-5.9	15.3	70
	V	580	3.0	3.0	1,479.6	-3.0	499.2	499.2	40	40	-3.0	-3.0	1
		675	1.5	1.3	23.9	1.3	480.0	660.0	25	150	0.1	3.3	33
	Subtotal		1.6	1.3	66.7	1.2	480.0	660.0	25	150	-3.0	3.3	34
	L-L-V	580	4.7	4.3	3.9	-4.3	495.3	677.3	70	1,400	-7.1	-1.0	20
	L-V-V	580	6.3	5.7	51.9	5.7	498.9	626.8	40	100	3.0	8.5	2
	Total		4.2	2.9	20.7	0.5	102.1	677.3	25	1,400	-7.1	15.3	126
toluene	L	592	3.7	3.3	2.3	-1.1	50.0	500.0	50	2,500	-5.5	5.2	77
		676	2.3	1.9	1.3	-0.2	140.0	464.0	215	1,365	-5.9	2.9	30
	Subtotal		3.4	2.9	2.0	-0.8	50.0	500.0	50	2,500	-5.9	5.2	107
	V	592	2.2	1.9	152.6	-1.3	350.0	650.0	50	2,500	-3.3	4.8	25
		676	2.9	2.6	56.0	2.6	212.0	446.0	17	45	0.7	4.5	13
	Subtotal		2.5	2.1	119.6	0.1	212.0	650.0	17	2,500	-3.3	4.8	38
	Total		3.1	2.7	32.8	-0.6	50.0	650.0	17	2,500	-5.9	5.2	145

Table E 2. Class Summary by Phase

CLASS	Phase	RMSE	AAD	%AAD	Bias	Temp Min	Temp Max	Press Min	Press Max	Max Dev Min	Max Dev Max	Npts
HETEROGENEOUS	L	1.0	0.8	1.3	0.5	-250.0	-250.0	500	3,000	-0.8	1.8	7
	V	4.1	2.0	7.6	0.5	-250.0	440.3	145	4,351	-2.3	19.9	107
	LVV	4.1	3.5	9.4	3.5	80.3	170.3	306	866	1.4	5.6	2
Total		4.0	2.0	7.2	0.5	-250.0	440.3	145	4,351	-2.3	19.9	116
HYDROCARBONS	L	4.7	3.5	2.8	2.3	-250.0	660.0	15	2,900	-12.4	21.2	1,386
	V	6.6	3.7	34.8	2.4	-150.0	700.0	15	2,500	-12.4	57.6	1,276
	LLV	14.1	6.6	10.9	-2.1	254.0	677.3	15	1,400	-72.6	9.9	73
	LVV	7.6	6.2	34.4	3.9	295.0	626.8	20	708	-15.0	14.6	52
Total		6.1	3.7	18.2	2.3	-250.0	700.0	15	2,900	-72.6	57.6	2,787

CLASS	Phase	RMSE	AAD	%AAD	Bias	Temp Min	Temp Max	Press Min	Press Max	Max Dev Min	Max Dev Max	Npts
Paraffins (s)	L	4.4	3.1	2.3	2.8	-250.0	640.0	15	2,500	-4.8	21.2	576
	V	7.0	3.9	17.5	3.1	-150.0	700.0	15	2,500	-5.2	46.3	475
	LLV	5.0	4.3	4.6	1.5	254.0	595.1	15	1,400	-2.8	8.6	5
	LVV	6.7	4.9	26.2	4.9	295.0	619.2	32	200	1.0	14.0	5
Total		5.8	3.5	9.3	2.9	-250.0	700.0	15	2,500	-5.2	46.3	1,061
Paraffins (b)	L	1.8	1.6	1.6	-1.0	188.4	476.4	290	1,450	-2.0	4.0	18
Olefins (b)	L	3.3	2.7	2.6	2.2	330.0	395.5	300	1,400	-2.2	7.5	49
	V	7.3	4.1	12.2	1.4	159.8	545.9	20	1,400	-5.3	57.6	193
	LLV	4.1	3.7	3.7	3.7	335.7	391.6	350	600	1.1	7.6	19
	LVV	5.1	3.7	7.1	-3.2	365.7	401.0	400	540	-15.0	3.1	17

Table E2. Class Summary by Phase (Cont'd)

CLASS	Phase	RMSE	AAD	%AAD	Bias	Temp Min	Temp Max	Press Min	Press Max	Max Dev Min	Max Dev Max	Npts
Napthenes	L	5.6	4.2	3.4	2.3	50.0	660.0	15	2,500	-12.4	19.8	495
	V	5.1	3.5	83.2	2.4	194.5	689.0	15	2,500	-12.4	24.8	319
	LLV	4.7	3.7	3.5	-2.2	391.3	677.3	20	1,400	-9.4	9.9	39
	LVV	9.3	8.5	55.4	8.5	320.8	626.8	20	500	2.8	14.6	26
Total		5.5	4.1	33.9	2.4	50.0	689.0	15	2,500	-12.4	24.8	879
Aromatics	L	3.9	3.2	2.6	1.4	50.0	552.0	20	2,900	-5.9	9.0	248
	V	6.7	3.1	24.8	2.0	212.0	700.0	17	2,500	-4.9	30.4	289
	LLV	36.3	24.0	56.7	-14.8	502.0	551.5	500	714	-72.6	8.0	10
	LVV	3.9	3.3	24.2	2.8	313.4	552.4	70	708	-0.9	6.8	4
Total		7.4	3.5	15.4	1.5	50.0	700.0	17	2,900	-72.6	30.4	551
RINGS	L	5.1	3.9	3.1	2.0	50.0	660.0	15	2,900	-12.4	19.8	743
	V	5.9	3.3	55.4	2.2	194.5	700.0	15	2,500	-12.4	30.4	608
	LLV	16.9	7.9	14.4	-4.8	391.3	677.3	20	1,400	-72.6	9.9	49
	LVV	8.7	7.8	51.2	7.7	313.4	626.8	20	708	-0.9	14.6	30
Total		6.3	3.8	26.8	2.0	50.0	700.0	15	2,900	-72.6	30.4	1,430

Title: Table E 3. Class Summary by Phase - Group Totals

Page number 257 on left side (rotated).Table E 3. Class Summary by Phase - Group Totals

CLASS		RMSE	AAD	%AAD	Bias	Temp Min	Temp Max	Press Min	Press Max	Max Dev Min	Max Dev Max	Npts
HETEROGENEOUS		4.0	2.0	7.2	0.5	-250.0	440.3	145	4,351	-2.3	19.9	116
HYDROCARBONS		6.1	3.7	18.2	2.3	-250.0	700.0	15	2,900	-72.6	57.6	2,787
Paraffins (s)		5.8	3.5	9.3	2.9	-250.0	700.0	15	2,500	-5.2	46.3	1,061
Paraffins (b)		1.8	1.6	1.6	-1.0	188.4	476.4	290	1,450	-2.0	4.0	18
Olefins (b)		6.5	3.8	9.6	1.4	159.8	545.9	20	1,400	-15.0	57.6	278
BRANCHED	Subtotal	6.3	3.7	9.1	1.3	159.8	545.9	20	1,450	-15.0	57.6	296
PARAFFINS	Subtotal	5.7	3.5	9.1	2.9	-250.0	700.0	15	2,500	-5.2	46.3	1,079
Napthenes		5.5	4.1	33.9	2.4	50.0	689.0	15	2,500	-12.4	24.8	879
Aromatics		7.4	3.5	15.4	1.5	50.0	700.0	17	2,900	-72.6	30.4	551
RINGS	Subtotal	6.3	3.8	26.8	2.0	50.0	700.0	15	2,900	-72.6	30.4	1,430
Total All Components		6.0	3.6	17.8	2.2	-250.0	700.0	15	4,351	-72.6	57.6	2,903

APPENDIX F

BINARY COMPONENT ENTHALPY EVALUATION SUMMARIES

Table F 1. Benzene - Hexadecane Enthalpy Summary

Components	Phase	x_1	x_2	REF	RMSE	AAD	%AAD	BIAS	T (°F) min	T (°F) max	P (psia) min	P (psia) max	Max Dev min	Max Dev max	NPTS
benzene (1)	L	0.419	0.581	580	10.9	10.6	8.1	10.6	148	589	20	1,400	5.9	15.8	40
n-hexadecane (2)				682	2.5	2.3	2.2	2.1	440	600	150	1,400	-1.6	4.4	19
				Subtotal	9.1	7.9	6.2	7.8	148	600	20	1,400	-1.6	15.8	59
		0.670	0.330	580	14.2	14.0	10.3	14.0	152	592	20	1,400	7.5	18.2	46
				682	6.3	3.8	3.9	-0.3	440	600	200	1,400	-18.9	4.4	20
				Subtotal	12.4	10.9	8.3	9.6	152	600	20	1,400	-18.9	18.2	66
		0.814	0.186	580	14.1	14.0	9.8	14.0	151	593	20	1,400	9.2	17.6	39
				682	4.2	3.9	3.7	3.9	420	600	300	1,400	1.9	7.7	25
				Subtotal	11.3	10.0	7.4	10.0	151	600	20	1,400	1.9	17.6	64
		0.920	0.800	580	11.1	11.0	7.5	11.0	151	565	20	1,400	7.0	14.1	43
				682	5.2	3.9	3.6	3.8	400	600	300	1,400	-1.3	15.8	22
				Subtotal	9.5	8.6	6.2	8.6	151	600	20	1,400	-1.3	15.8	65
		0.963	0.037	580	7.8	7.5	5.4	7.5	150	590	20	1,400	3.6	17.9	57
				682	4.0	3.1	2.7	2.3	360	560	200	1,400	-4.7	10.3	26
				Subtotal	6.8	6.1	4.6	5.9	150	590	20	1,400	-4.7	17.9	83
	Totals				9.9	8.6	6.4	8.3	148	600	20	1,400	-18.9	18.2	337

Table F 1. Benzene - Hexadecane Enthalpy Summary (Cont'd)

Components	Phase	x_1	x_2	REF	RMSE	AAD	%AAD	BIAS	T (°F) min	max	P (psia) min	max	Max Dev min	max	NPTS
benzene (1)	V	0.419	0.581	580	6.5	6.3	69.2	6.3	539	602	20	40	4.9	9.5	7
n-hexadecane (2)		0.670	0.330	580	10.3	10.2	81.2	10.2	496	594	20	70	8.2	12.8	9
		0.814	0.186	580	10.6	10.5	76.0	10.5	475	595	20	150	7.7	14.1	17
				682	1.3	1.2	14.6	1.2	580	600	100	150	0.6	1.8	3
				Subtotal	9.8	9.1	66.8	9.1	475	600	20	150	0.6	14.1	20
		0.920	0.080	580	8.7	8.2	58.1	8.2	384	595	20	500	3.5	17.9	55
				682	2.4	1.7	361.1	0.8	520	600	100	400	-4.9	5.4	14
				Subtotal	7.8	6.9	119.6	6.7	384	600	20	500	-4.9	17.9	69
		0.963	0.037	580	8.1	7.1	48.2	7.0	312	593	20	600	-1.4	17.5	84
				682	3.6	2.3	13.9	1.7	440	600	100	1,400	-1.8	11.4	40
				Subtotal	7.0	5.5	37.2	5.3	312	600	20	1,400	-1.8	17.5	124
	Totals				7.7	6.5	67.3	6.3	312	602	20	1,400	-4.9	17.9	229
	L-L-V	0.963	0.037	682	3.4	3.4	2.5	-3.4	360	360	150	150	-3.4	-3.4	1
benzene (1) n-hexadecane (2)	TOTAL				9.0	7.7	31.0	7.4	148	602	20	1,400	-18.9	18.2	567

Table F 2. Benzene - Octane Enthalpy Summary

Components	Phase	x_1	x_2	REF	RMSE	AAD	%AAD	BIAS	T (°F) min	T (°F) max	P (psia) min	P (psia) max	Max Dev min	Max Dev max	NPTS
benzene (1)	L	0.271	0.729	581	3.7	2.8	2.8	2.8	158	566	20	1,400	-0.2	11.0	76
n-octane (2)				679	2.3	1.3	1.3	0.7	380	540	200	1,400	-1.2	8.7	20
				Subtotal	3.4	2.5	2.5	2.3	158	566	20	1,400	-1.2	11.0	96
		0.446	0.554	581	5.4	4.4	4.1	4.4	159	556	20	1,400	0.3	14.4	106
				679	3.1	2.4	2.4	1.0	380	540	200	1,400	-2.7	8.4	26
				Subtotal	5.0	4.0	3.8	3.7	159	556	20	1,400	-2.7	14.4	132
		0.676	0.324	581	6.3	5.7	4.9	5.6	152	548	20	1,400	-3.5	14.3	80
				679	2.9	2.3	2.2	1.3	380	540	200	1,400	-1.9	8.4	23
				Subtotal	5.8	4.9	4.3	4.6	152	548	20	1,400	-3.5	14.3	103
		0.771	0.229	581	6.7	6.0	5.6	6.0	369	556	200	1,400	1.3	12.3	33
				679	3.3	2.3	2.2	1.7	380	540	200	1,400	-1.9	10.3	23
				Subtotal	5.5	4.5	4.2	4.3	369	556	200	1,400	-1.9	12.3	56
		0.857	0.143	581	6.6	5.7	4.9	5.7	179	559	20	1,400	-0.9	16.6	75
				679	3.0	2.2	2.0	1.8	380	540	200	1,400	-1.2	6.5	22
				Subtotal	5.9	4.9	4.3	4.8	179	559	20	1,400	-1.2	16.6	97
		0.930	0.070	581	5.7	5.2	4.6	5.2	367	556	200	1,400	1.5	10.7	52
				679	2.3	1.6	1.4	1.4	380	540	300	1,400	-0.6	6.5	19
				Subtotal	5.0	4.2	3.8	4.1	367	556	200	1,400	-0.6	10.7	71
	Totals				5.2	4.1	3.8	4.0	152	566	20	1,400	-3.5	16.6	555

Table F 2. Benzene - Octane Enthalpy Summary (Cont'd)

Components	Phase	x_1	x_2	REF	RMSE	AAD	%AAD	BIAS	T (°F) min	T (°F) max	P (psia) min	P (psia) max	Max Dev min	Max Dev max	NPTS
benzene (1)	V	0.271	0.729	581	8.9	6.7	28.1	6.6	282	599	20	1,400	-1.0	22.8	67
n-octane (2)				679	6.3	3.5	7.8	3.4	480	600	200	1,400	-0.4	23.6	23
				Subtotal	8.3	5.9	22.9	5.8	282	600	20	1,400	-1.0	23.6	90
		0.446	0.554	581	7.0	6.1	36.3	6.1	279	598	20	1,400	2.0	21.4	50
				679	7.9	5.0	8.3	4.9	460	600	200	1,400	-0.7	22.4	39
				Subtotal	7.4	5.6	24.0	5.6	279	600	20	1,400	-0.7	22.4	89
		0.676	0.324	581	6.8	5.1	31.2	5.1	299	600	20	1,400	0.2	22.4	49
				679	4.5	3.0	8.1	0.9	440	600	200	1,400	-4.1	16.0	40
				Subtotal	5.9	4.2	20.8	3.2	299	600	20	1,400	-4.1	22.4	89
		0.771	0.229	581	8.4	5.4	15.8	4.9	477	597	20	1,400	-2.7	22.5	34
				679	4.4	2.5	6.5	0.7	420	600	200	1,400	-5.0	22.1	42
				Subtotal	6.5	3.8	10.6	2.6	420	600	20	1,400	-5.0	22.5	76
		0.857	0.143	581	4.4	3.7	25.6	3.5	239	597	20	1,400	-3.2	11.6	56
				679	5.5	3.3	9.3	1.5	420	600	200	1,400	-4.3	22.1	47
				Subtotal	4.9	3.5	18.1	2.6	239	600	20	1,400	-4.3	22.1	103
		0.930	0.070	581	3.7	2.8	8.6	2.1	403	597	200	1,400	-3.4	12.2	39
				679	18.2	5.5	9.5	3.9	380	600	200	1,400	-3.0	120.6	49
				Subtotal	13.8	4.3	9.1	3.1	380	600	200	1,400	-3.4	120.6	88
	Totals				8.3	4.5	17.8	3.8	239	600	20	1,400	-5.0	120.6	535

Table F 2. Benzene - Octane Enthalpy Summary (Cont'd)

Components	Phase	x_1	x_2	REF	RMSE	AAD	%AAD	BIAS	T (°F) min	T (°F) max	P (psia) min	P (psia) max	Max Dev min	Max Dev max	NPTS
benzene (1)															
n-octane (2)	L-V-V	0.771	0.229	581	1.3	1.3	2.4	0.3	554	558	600	600	-0.9	1.6	2
	TOTAL				6.9	4.3	10.6	3.9	152	600	20	1,400	-5.0	120.6	1,092

Table F 3. Benzene - Pentane Enthalpy Summary

Components	Phase	x_1	x_2	REF	RMSE	AAD	%AAD	BIAS	T (°F) min	T (°F) max	P (psia) min	P (psia) max	Max Dev min	Max Dev max	NPTS
benzene (1)	L	0.199	0.801	581	5.1	5.1	5.4	5.1	404	411	528	560	3.4	6.3	5
n-pentane (2)				584	2.5	1.9	1.9	1.2	152	439	50	1,400	-2.2	5.5	32
				681	2.1	1.8	1.6	-0.6	300	400	300	1,400	-3.6	2.5	17
				Subtotal	2.7	2.2	2.1	1.0	152	439	50	1,400	-3.6	6.3	54
		0.406	0.594	584	4.0	3.4	2.9	2.1	153	470	200	1,400	-4.4	8.4	37
				681	2.6	2.2	2.0	-1.1	300	440	200	1,400	-5.3	3.8	24
				Subtotal	3.5	2.9	2.5	0.8	153	470	200	1,400	-5.3	8.4	61
		0.600	0.400	581	3.4	3.1	3.1	3.1	364	479	300	660	0.3	4.7	12
				584	2.4	1.9	1.6	0.8	150	487	25	1,400	-8.6	3.9	46
				681	2.4	1.9	1.7	-0.5	320	480	200	1,400	-5.6	4.7	35
				Subtotal	2.5	2.1	1.9	0.6	150	487	25	1,400	-8.6	4.7	93
		0.814	0.186	581	4.3	4.2	4.1	4.2	460	510	500	700	3.1	5.0	10
				584	4.5	2.4	1.8	-1.2	152	522	15	1,400	-17.6	3.6	18
				681	2.6	1.9	1.7	0.0	360	515	300	1,400	-8.4	5.1	36
				Subtotal	3.5	2.4	2.1	0.3	152	522	15	1,400	-17.6	5.1	64
	Totals				3.1	2.3	2.1	0.7	150	522	15	1,400	-17.6	8.4	272

Table F 3. Benzene - Pentane Enthalpy Summary (Cont'd)

Components	Phase	x_1	x_2	REF	RMSE	AAD	%AAD	BIAS	T (°F) min	T (°F) max	P (psia) min	P (psia) max	Max Dev min	Max Dev max	NPTS
benzene (1)	V	0.199	0.801	581	4.6	3.8	5.8	1.7	332	443	200	700	-2.8	9.0	7
n-pentane (2)				584	6.9	4.5	28.2	3.0	193	693	25	1,400	-5.8	33.0	88
				681	7.6	4.4	11.8	1.1	320	680	200	1,400	-4.7	34.3	129
				Subtotal	7.2	4.4	18.1	1.9	193	693	25	1,400	-5.8	34.3	224
		0.406	0.594	581	7.6	6.9	8.4	6.9	460	478	700	700	2.6	10.4	4
				584	6.0	4.8	27.2	4.7	206	694	25	1,400	-1.2	17.1	60
				681	7.3	4.5	14.5	0.7	340	700	200	1,400	-7.2	35.6	161
				Subtotal	7.0	4.7	17.7	1.9	206	700	25	1,400	-7.2	35.6	225
		0.600	0.400	581	3.4	2.4	10.9	0.2	364	594	40	1,400	-5.5	13.0	45
				584	7.5	5.6	22.9	1.8	195	695	25	1,400	-19.5	22.0	52
				681	6.2	4.0	13.6	0.0	360	700	200	1,400	-6.8	26.9	151
				Subtotal	6.1	4.0	15.1	0.4	195	700	25	1,400	-19.5	26.9	248
		0.814	0.186	581	0.4	0.3	0.9	-0.3	508	510	560	560	-0.5	-0.2	2
				584	4.8	3.4	24.0	0.3	198	694	15	1,400	-6.1	21.7	57
				681	7.1	3.9	9.9	1.2	380	700	200	1,400	-5.5	33.1	143
				Subtotal	6.5	3.7	13.8	0.9	198	700	15	1,400	-6.1	33.1	202
	Totals				6.7	4.2	16.2	1.3	193	700	15	1,400	-19.5	35.6	899

Table F 3. Benzene - Pentane Enthalpy Summary (Cont'd)

Components	Phase	x_1	x_2	REF	RMSE	AAD	%AAD	BIAS	T (°F) min	max	P (psia) min	max	Max Dev min	max	NPTS
benzene (1)	L-L-V	0.199	0.801	581	7.7	7.7	8.4	7.7	410	410	528	528	7.7	7.7	1
n-pentane (2)				584	5.2	4.8	5.1	4.8	364	425	400	600	1.4	7.5	5
				Subtotal	5.7	5.3	5.7	5.3	364	425	400	600	1.4	7.7	6
		0.406	0.594	581	4.2	4.2	4.4	4.2	431	441	560	575	3.0	5.1	4
				584	45.8	27.3	110.6	-21.1	333	467	200	660	-106.8	8.5	10
				Subtotal	38.8	20.7	80.3	-13.9	333	467	200	660	-106.8	8.5	14
		0.600	0.400	581	1.5	1.3	1.2	0.3	375	438	300	500	-1.5	2.0	3
				584	1.7	1.6	1.3	-1.6	327	415	200	400	-2.1	-1.0	2
				Subtotal	1.5	1.4	1.2	-0.4	327	438	200	500	-2.1	2.0	5
		0.814	0.186	581	4.6	3.9	4.0	2.9	439	517	400	700	-2.0	7.2	4
	Totals				27.1	11.9	40.7	-5.3	327	517	200	700	-106.8	8.5	29
	L-V-V	0.199	0.801	581	1.4	1.2	4.2	-0.4	313	425	200	528	-2.5	1.7	6
				584	2.6	2.2	7.1	-2.2	385	421	300	500	-4.2	-0.3	4
				Subtotal	1.9	1.6	5.4	-1.1	313	425	200	528	-4.2	1.7	10
		0.406	0.594	581	4.3	3.1	6.4	3.1	441	450	500	575	1.0	7.3	3
		0.600	0.400	581	1.1	0.8	2.1	0.7	411	476	300	580	-0.2	2.3	7
				584	1.8	1.4	4.2	1.0	414	465	300	500	-0.4	2.5	2
				Subtotal	1.3	0.9	2.6	0.7	411	476	300	580	-0.4	2.5	9
		0.814	0.186	581	1.9	1.6	5.4	1.6	428	513	300	600	0.4	3.5	8
	Totals				2.1	1.5	4.7	0.6	313	513	200	600	-4.2	7.3	30
	TOTAL				7.2	3.9	13.4	1.0	150	700	15	1,400	-106.8	35.6	1,230

Table F 4. Benzene - Propane Enthalpy Summary

Components	Phase	x_1	x_2	REF	RMSE	AAD	%AAD	BIAS	T (°F) min	T (°F) max	P (psia) min	P (psia) max	Max Dev min	Max Dev max	NPTS
benzene (1)	L	0.203	0.797	364	6.0	4.7	3.9	4.7	200	300	500	1,000	1.9	10.1	3
propane (2)		0.502	0.498	364	3.4	2.8	2.3	1.8	200	400	500	1,000	-3.3	5.4	7
		0.748	0.252	364	4.5	4.0	2.7	3.0	200	400	200	1,000	-2.8	7.2	9
	Totals				4.4	3.7	2.7	2.8	200	400	200	1,000	-3.3	10.1	19
	V	0.203	0.797	364	2.9	2.3	10.2	2.3	300	400	200	1,000	0.2	5.1	5
		0.502	0.498	364	1.1	0.9	8.3	0.9	300	400	165	200	0.3	1.6	2
		0.748	0.252	364	4.8	3.7	16.7	3.7	400	400	200	300	0.7	6.7	2
	Totals				3.2	2.3	11.2	2.3	300	400	165	1,000	0.2	6.7	9
	TOTAL				4.1	3.2	5.4	2.6	200	400	165	1,000	-3.3	10.1	28

Table F 5. Carbon Dioxide - Hydrogen Sulfide Enthalpy Summary

Components	Phase	x_1	x_2	REF	RMSE	AAD	%AAD	BIAS	T (°F) min	T (°F) max	P (psia) min	P (psia) max	Max Dev min	Max Dev max	NPTS
carbon dioxide (1)	V	0.082	0.915	686	6.8	4.5	8.8	4.5	215	440	145	9,428	0.3	19.7	94
hydrogen sulfide (2)		0.514	0.486	686	6.6	5.1	16.2	-3.4	125	440	145	8,702	-13.8	15.9	79
					6.7	4.8	12.2	0.9	125	440	145	9,428	-13.8	19.7	173
	L-V-V	0.082	0.915	686	2.7	2.7	6.6	2.7	260	260	1,015	1,160	2.4	3.0	2
	Totals				6.7	4.7	12.1	0.9	125	440	145	9,428	-13.8	19.7	175

Table F 6. Carbon Monoxide - Hydrogen Enthalpy Summary

Components	Phase	x_1	x_2	REF	RMSE	AAD	%AAD	BIAS	T (°F) min	max	P (psia) min	max	Max Dev min	max	NPTS
carbon monoxide (1)	V	0.250	0.750	673	16.6	10.4	253.9	-10.4	-250	900	20	2,500	-57.9	0.0	70
hydrogen (2)		0.500	0.500	673	22.9	13.8	659.8	-13.8	-250	800	20	2,500	-74.3	0.0	66
	Totals				19.9	12.0	450.9	-12.0	-250	900	20	2,500	-74.3	0.0	136

Table F 7. Ethane - Hydrogen Sulfide Enthalpy Summary

Components	Phase	x_1	x_2	REF	RMSE	AAD	%AAD	BIAS	T (°F) min	max	P (psia) min	max	Max Dev min	max	NPTS
ethane (1)	L	0.500	0.500	670	6.4	5.1	3.0	-4.7	-120	150	20	2,000	-12.5	1.2	25
hydrogen sulfide (2)	V	0.500	0.500	670	1.8	1.2	26.2	-1.1	-80	200	20	500	-4.8	0.6	18
	TOTAL				5.0	3.5	12.7	-3.2	-120	200	20	2,000	-12.5	1.2	43

Table F 8. Ethane - Propane Enthalpy Summary

Components	Phase	x_1	x_2	REF	RMSE	AAD	%AAD	BIAS	T (°F) min	T (°F) max	P (psia) min	P (psia) max	Max Dev min	Max Dev max	NPTS
ethane (1)	L	0.237	0.763	592	8.6	7.2	3.6	5.2	-240	120	250	2,000	-10.7	15.5	18
propane (2)				671	11.5	9.3	5.9	-0.8	-280	147	250	2,000	-25.5	18.1	42
				Subtotal	10.7	8.7	5.2	1.0	-280	147	250	2,000	-25.5	18.1	60
		0.502	0.498	592	3.4	2.4	1.4	2.4	-240	160	250	2,000	-0.2	8.8	18
				671	5.2	3.9	2.3	3.8	-280	180	250	2,000	-0.4	10.6	30
				Subtotal	4.6	3.3	2.0	3.3	-280	180	250	2,000	-0.4	10.6	48
		0.724	0.276	592	32.2	14.4	10.1	12.3	-240	160	500	1,000	-3.0	104.2	12
				671	6.6	3.7	2.4	1.5	-280	140	500	1,000	-2.9	22.2	14
				Subtotal	22.4	8.7	5.9	6.5	-280	160	500	1,000	-3.0	104.2	26
	Totals				12.5	6.8	4.2	2.9	-280	180	250	2,000	-25.5	104.2	134
	V	0.237	0.763	592	8.3	6.7	17.7	-0.1	80	240	250	2,000	-13.0	18.3	12
				671	19.5	15.6	37.5	-15.6	100	280	250	2,000	-3.3	-42.6	25
				Subtotal	16.7	12.7	31.1	-10.6	80	280	250	2,000	-42.6	18.3	37
		0.502	0.498	592	3.6	2.0	3.5	1.5	120	240	250	2,000	-1.5	10.5	10
				671	5.6	2.9	8.4	-1.2	90	300	250	2,000	-18.6	2.9	18
				Subtotal	5.0	2.6	6.6	-0.2	90	300	250	2,000	-18.6	10.5	28
		0.724	0.276	592	22.5	18.4	23.5	18.4	160	240	500	2,000	6.1	45.7	6
				671	14.1	12.7	20.5	12.7	155	300	500	2,000	5.6	33.9	17
				Subtotal	16.7	14.1	21.3	14.1	155	300	500	2,000	5.6	45.7	23
	Totals				14.1	9.9	20.7	-0.8	80	300	250	2,000	-42.6	45.7	88
	TOTAL				13.1	8.0	10.8	1.4	-280	300	250	2,000	-42.6	104.2	222

Table F 9. Ethylbenzene - Octane Enthalpy Summary

Components	Phase	x_1	x_2	REF	RMSE	AAD	%AAD	BIAS	T (°F) min	T (°F) max	P (psia) min	P (psia) max	Max Dev min	Max Dev max	NPTS
ethylbenzene (1)	L	0.271	0.729	679	2.2	2.2	2.3	-2.2	500	540	700	800	-2.0	-2.6	4
n-octane (2)	V	0.271	0.729	679	10.2	7.1	11.8	-7.1	560	600	500	800	-2.0	-22.4	10
	TOTAL				8.7	5.7	9.1	-5.7	500	600	500	800	-2.0	-22.4	14

Table F 10. Isopentane - Tetrahydronapthalene Enthalpy Summary

Components	Phase	x_1	x_2	REF	RMSE	AAD	%AAD	BIAS	T (°F) min	T (°F) max	P (psia) min	P (psia) max	Max Dev min	Max Dev max	NPTS
isopentane (1)	L	0.197	0.803	675	2.4	2.2	2.0	-0.4	480	660	150	1,400	-4.3	3.6	35
tetrahydronaphthalene (2)		0.399	0.601	675	3.5	3.3	3.2	3.3	540	660	1,000	1,400	1.2	5.3	12
		0.893	0.107	675	7.6	7.4	7.2	7.4	340	640	300	1,400	4.6	12.9	32
	Totals				5.3	4.5	4.3	3.4	340	660	150	1,400	-4.3	12.9	79
	V	0.197	0.803	675	16.6	7.0	37.6	7.0	500	660	40	150	0.9	70.0	21
		0.399	0.601	675	3.1	2.6	28.3	2.6	500	640	70	150	0.6	4.8	7
		0.588	0.412	675	3.0	2.4	31.4	2.4	460	640	25	300	0.2	6.1	23
		0.795	0.205	675	2.0	1.4	12.2	1.4	480	640	40	600	-0.3	5.5	29
		0.893	0.107	675	3.6	2.8	20.3	2.8	340	640	40	1,000	0.4	10.6	72
	Totals				6.8	3.1	23.2	3.0	340	660	25	1,000	-0.3	70.0	152
	TOTAL				6.4	3.5	16.7	3.2	340	660	25	1,400	-4.3	70.0	231

Table F 11. Methane - Carbon Dioxide Enthalpy Summary

Components	Phase	x_1	x_2	REF	RMSE	AAD	%AAD	BIAS	T (°F) min	max	P (psia) min	max	Max Dev min	max	NPTS
methane (1)	V	0.476	0.524	688	7.9	5.9	14.8	-5.8	-64	116	73	7,252	-17.8	1.4	183
carbon dioxide (2)		0.500	0.500	667	5.3	4.5	37.8	-4.5	-50	300	100	2,000	-0.6	-12.0	40
Totals					7.5	5.7	18.9	-5.6	-64	300	73	7,252	-17.8	1.4	223
L-V-V	0.476	0.524	688		25.1	13.3	32.7	-12.8	-64	-10	206	843	-50.2	1.1	4
TOTAL					8.1	5.8	19.2	-5.7	-64	300	73	7,252	-50.2	1.4	227

Table F 12. Methane - Hydrogen Enthalpy Summary

Components	Phase	x_1	x_2	REF	RMSE	AAD	%AAD	BIAS	T (°F) min	max	P (psia) min	max	Max Dev min	max	NPTS
methane (1)															
hydrogen (2)	V	0.500	0.500	673	3.9	2.7	148.3	-2.7	-250	900	20	2,500	-10.7	0.4	82

Table F 13. Methane - Isobutene Enthalpy Summary

Components	Phase	x_1	x_2	REF	RMSE	AAD	%AAD	BIAS	T (°F) min	max	P (psia) min	max	Max Dev min	max	NPTS
methane (1)															
isobutene (2)	L	0.883	0.117	670	6.9	6.9	3.0	6.9	-270	-270	250	250	6.9	6.9	1

Table F 14. Methane - Hydrogen Sulfide Enthalpy Summary

Components	Phase	x_1	x_2	REF	RMSE	AAD	%AAD	BIAS	T (°F) min	max	P (psia) min	max	Max Dev min	max	NPTS
methane (1)	L	0.500	0.500	670	7.4	7.2	4.0	-7.2	-110	0	1,000	2,000	-11.0	-5.2	6
hydrogen sulfide (2)	V	0.493	0.507	686	12.8	10.9	44.5	-10.9	80	440	145	5,076	-0.9	-29.4	81
		0.500	0.500	670	5.8	2.8	18.3	-2.7	-80	200	20	2,000	-23.2	0.5	25
	Totals				11.6	9.0	38.3	-8.9	-80	440	20	5,076	-29.4	0.5	106
	TOTAL				11.4	8.9	36.5	-8.8	-110	440	20	5,076	-29.4	0.5	112

Table F 15. Methane - Methylcyclohexane Enthalpy Summary

Components	Phase	x_1	x_2	REF	RMSE	AAD	%AAD	BIAS	T (°F) min	max	P (psia) min	max	Max Dev min	max	NPTS
methane (1)	L	0.500	0.500	592	12.2	12.2	7.8	12.2	50	50	2,500	2,500	12.2	12.2	1
methylcyclohexane (2)				667	13.9	8.0	6.0	-1.8	-100	250	50	2,500	-19.5	91.5	67
				Subtotal	13.9	8.0	6.0	-1.6	-100	250	50	2,500	-19.5	91.5	68
	V	0.500	0.500	592	4.1	3.5	34.2	2.6	300	600	50	2,500	-3.1	7.6	35
				667	6.1	6.1	69.3	6.1	250	250	50	50	6.1	6.1	1
				Subtotal	4.1	3.6	35.1	2.7	250	600	50	2,500	-3.1	7.6	36
	TOTAL				11.5	6.5	16.1	-0.1	-100	600	50	2,500	-19.5	91.5	104

Table F 16. Methane - Heptane Enthalpy Summary

Components	Phase	x_1	x_2	REF	RMSE	AAD	%AAD	BIAS	T (°F) min	max	P (psia) min	max	Max Dev min	max	NPTS
methane (1)	L	0.249	0.751	592	2.3	2.0	1.7	-1.5	50	500	800	2,500	-4.2	1.8	23
n-heptane (2)				667	5.7	4.3	3.0	-0.7	-100	400	50	2,500	-18.9	17.7	67
				Subtotal	5.1	3.7	2.7	-0.9	-100	500	50	2,500	-18.9	17.7	90
		0.491	0.509	592	1.5	1.1	0.8	1.1	50	200	2,500	2,500	-0.1	2.4	4
				667	7.1	6.9	4.0	6.9	-100	0	600	2,500	4.4	8.7	11
				Subtotal	6.1	5.4	3.1	5.4	-100	200	600	2,500	-0.1	8.7	15
		0.951	0.049	592	1.2	1.2	2.1	-1.2	200	200	2,500	2,500	-1.2	-1.2	1
				667	8.8	8.7	5.5	8.7	-100	0	1,000	2,500	7.0	10.4	5
				Subtotal	8.0	7.4	4.9	7.0	-100	200	1,000	2,500	-1.2	10.4	6
	Totals				5.4	4.1	2.9	0.4	-100	500	50	2,500	-18.9	17.7	111
	V	0.249	0.751	592	4.2	3.8	152.6	-3.7	300	600	50	2,500	-7.5	0.5	35
		0.491	0.509	592	3.3	2.3	21.3	1.4	300	600	50	2,500	-4.6	10.3	39
				667	11.6	10.5	35.5	10.5	250	450	50	2,500	6.2	18.3	5
				Subtotal	5.0	3.3	22.9	2.4	250	600	50	2,500	-4.6	18.3	44
		0.951	0.049	592	1.6	1.1	16.0	0.2	150	600	50	2,500	-3.4	7.5	79
	Totals				3.5	2.3	48.2	-0.1	150	600	50	2,500	-7.5	18.3	158
	TOTAL				4.4	3.1	29.5	0.1	-100	600	50	2,500	-18.9	18.3	269

Table F 17. Methane - Nitrogen Enthalpy Summary

Components	Phase	x_1	x_2	REF	RMSE	AAD	%AAD	BIAS	T (°F) min	max	P (psia) min	max	Max Dev min	max	NPTS
methane (1)	L	0.566	0.434	591	2.2	2.2	1.8	-2.2	-250	-200	250	2,000	-1.0	-2.6	7
nitrogen (2)	V	0.566	0.434	591	6.6	3.5	13.7	0.6	-250	250	250	2,000	-3.1	27.0	47
				666	1.1	1.1	20.7	-1.1	180	180	500	500	-1.1	-1.1	1
				667	3.7	2.5	13.9	-1.0	-150	300	250	2,000	-3.2	23.4	321
				Subtotal	4.1	2.6	13.9	-0.8	-250	300	250	2,000	-3.2	27.0	369
	TOTAL				4.1	2.6	13.6	-0.9	-250	300	250	2,000	-3.2	27.0	376

Table F 18. Methane - Toluene Enthalpy Summary

Components	Phase	x_1	x_2	REF	RMSE	AAD	%AAD	BIAS	T (°F) min	max	P (psia) min	max	Max Dev min	max	NPTS
methane (1)	L	0.500	0.500	592	7.8	7.8	4.6	7.8	50	50	2,500	2,500	7.8	7.8	1
toluene (2)				667	37.8	29.9	32.3	29.9	-100	500	100	2,500	1.7	90.1	39
				Subtotal	37.4	29.3	31.6	29.3	-100	500	100	2,500	1.7	90.1	40
	V	0.500	0.500	592	1.1	0.9	18.4	0.4	300	600	50	2,500	-1.3	3.2	33
	TOTAL				27.7	16.4	25.6	16.2	-100	600	50	2,500	-1.3	90.1	73

Table F 19. Methane - Propane Enthalpy Summary

Components	Phase	x_1	x_2	REF	RMSE	AAD	%AAD	BIAS	T (°F) min	T (°F) max	P (psia) min	P (psia) max	Max Dev min	Max Dev max	NPTS
methane (1)	L	0.234	0.766	370	4.5	3.3	1.6	3.2	-280	180	250	2,000	-0.8	9.8	282
propane (2)				590	4.8	3.7	1.8	3.6	-250	150	250	2,000	-0.6	8.9	40
				Subtotal	4.5	3.3	1.6	3.2	-280	180	250	2,000	-0.8	9.8	322
		0.494	0.506	370	4.4	3.6	1.8	3.6	-280	130	250	2,000	0.4	8.8	223
				590	4.2	3.5	1.8	3.5	-250	100	250	2,000	0.5	7.6	29
				Subtotal	4.3	3.6	1.8	3.6	-280	130	250	2,000	0.4	8.8	252
		0.720	0.280	370	2.6	2.0	1.0	2.0	-280	70	250	2,000	-0.7	5.9	183
				588	2.6	2.1	1.1	2.1	-250	50	250	2,000	0.4	5.0	27
				Subtotal	2.6	2.1	1.0	2.0	-280	70	250	2,000	-0.7	5.9	210
		0.883	0.117	370	1.9	1.6	0.9	1.4	-280	20	250	2,000	-1.5	4.7	167
				588	2.1	1.8	0.9	1.6	-250	0	250	2,000	-1.2	4.2	23
				Subtotal	2.0	1.6	0.9	1.4	-280	20	250	2,000	-1.5	4.7	190
		0.948	0.052	370	1.5	1.2	0.7	-0.3	-280	-40	250	2,000	-2.4	4.3	158
				591	1.5	1.4	0.7	-1.4	-250	-200	250	2,000	-0.6	-2.3	7
				666	1.4	1.4	0.7	-1.4	-220	-220	400	400	-1.4	-1.4	1
				Subtotal	1.5	1.3	0.7	-0.4	-280	-40	250	2,000	-2.4	4.3	166
	Totals				3.5	2.6	1.3	2.3	-280	180	250	2,000	-2.4	9.8	1,140

Table F 19. Methane - Propane Enthalpy Summary (Cont'd)

Components	Phase	x_1	x_2	REF	RMSE	AAD	%AAD	BIAS	T (°F) min	T (°F) max	P (psia) min	P (psia) max	Max Dev min	Max Dev max	NPTS
methane (1)	V	0.234	0.766	370	1.7	1.3	3.6	-0.5	110	300	250	2,000	-2.8	8.6	89
propane (2)				590	2.5	1.5	4.2	0.6	100	250	250	2,000	-1.6	8.0	13
				Subtotal	1.8	1.3	3.7	-0.4	100	300	250	2,000	-2.8	8.6	102
		0.494	0.506	370	1.0	0.9	3.1	-0.4	70	300	250	2,000	-2.4	1.8	120
				590	1.2	0.9	2.6	0.1	100	250	250	2,000	-1.3	3.5	16
				Subtotal	1.1	0.9	3.0	-0.4	70	300	250	2,000	-2.4	3.5	136
		0.720	0.280	368	1.6	1.6	2.3	-1.6	160	160	2,000	2,000	-1.6	-1.6	1
				370	2.5	2.1	7.7	-2.1	30	300	250	2,000	-5.1	0.7	153
				558	3.4	3.2	11.1	-3.2	250	250	500	2,000	-4.3	-1.8	4
				588	1.6	1.3	5.4	-1.2	50	250	250	2,000	-3.4	0.3	17
				Subtotal	2.5	2.1	7.6	-2.1	30	300	250	2,000	-5.1	0.7	175
		0.874	0.126	573	4.0	3.8	12.4	-3.8	90	200	500	2,000	-1.8	-6.2	12
		0.883	0.117	370	3.2	3.0	12.5	-3.0	-20	300	250	2,000	-4.7	1.5	184
				558	3.2	3.0	14.0	-3.0	150	250	250	2,000	-4.6	-0.9	15
				588	2.2	2.0	7.9	-2.0	0	120	250	2,000	-3.6	0.2	14
				Subtotal	3.2	2.9	12.3	-2.9	-20	300	250	2,000	-4.7	1.5	213
		0.948	0.052	370	2.8	2.3	21.2	-2.3	-260	300	15	2,000	-5.2	0.7	247
				591	3.1	3.0	17.1	-3.0	250	250	500	1,500	-4.0	-1.7	3
				680	3.4	3.2	9.4	-3.2	40	70	500	1,500	-4.4	-1.9	2
				Subtotal	2.9	2.4	21.0	-2.3	-260	300	15	2,000	-5.2	0.7	252
		0.949	0.051	573	5.3	4.8	16.4	-4.8	90	200	500	2,000	-9.1	-1.4	12
	Totals				2.6	2.2	11.5	-1.9	-260	300	15	2,000	-9.1	8.6	902
	TOTAL				3.1	2.4	5.8	0.4	-280	300	15	2,000	-9.1	9.8	2,042

276

Table F 20. Propane - Isopentane Enthalpy Summary

Components	Phase	x_1	x_2	REF	RMSE	AAD	%AAD	BIAS	T (°F) min	T (°F) max	P (psia) min	P (psia) max	Max Dev min	Max Dev max	NPTS
propane (1)															
iso-pentane (2)	L	0.430	0.570	579	5.2	4.3	4.0	-3.4	164	313	600	700	-9.5	2.0	14

Table F 21. Methylcyclohexane - Hydrogen Sulfide Enthalpy Summary

Components	Phase	x_1	x_2	REF	RMSE	AAD	%AAD	BIAS	T (°F) min	T (°F) max	P (psia) min	P (psia) max	Max Dev min	Max Dev max	NPTS
methylcyclohexane (1)	V	0.107	0.893	686	12.5	10.4	27.2	-6.9	170	440	145	6,527	-26.7	15.2	63
hydrogen sulfide (2)	L-V-V	0.107	0.893	686	14.2	13.5	43.7	-13.5	260	260	725	1,015	-8.5	-19.4	3
	TOTAL				12.6	10.6	28.0	-7.2	170	440	145	6,527	-26.7	15.2	66

Table F 22. Pentane - Carbon Dioxide Enthalpy Summary

Components	Phase	x_1	x_2	REF	RMSE	AAD	%AAD	BIAS	T (°F) min	T (°F) max	P (psia) min	P (psia) max	Max Dev min	Max Dev max	NPTS
n-pentane (1)	L	0.500	0.500	685	13.3	13.0	9.8	-13.0	-50	250	100	2,000	-8.7	-18.1	25
carbon dioxide (2)	V	0.500	0.500	685	6.9	3.8	26.8	-1.5	100	400	20	2,000	-8.9	30.5	28
	L-L-V	0.500	0.500	685	10.7	10.6	10.2	-10.6	150	250	1,200	1,600	-9.5	-11.9	3
	TOTAL				10.4	8.3	18.4	-7.1	-50	400	20	2,000	-18.1	30.5	56

Table F 23. Pentane - Tetrahydronapthalene Enthalpy Summary

Components	Phase	x_1	x_2	REF	RMSE	AAD	%AAD	BIAS	T (°F) min	T (°F) max	P (psia) min	P (psia) max	Max Dev min	Max Dev max	NPTS
n-pentane (1)	L	0.197	0.803	580	7.2	5.9	3.9	5.6	101	675	25	1,400	-2.9	12.9	45
tetrahydronaphthalene (2)		0.399	0.601	580	6.1	5.4	3.7	5.4	148	638	25	1,400	0.4	10.0	27
		0.588	0.412	580	6.2	5.8	4.2	5.8	123	616	25	1,400	1.9	9.5	38
		0.795	0.205	580	4.4	4.2	3.2	4.2	120	599	25	1,400	0.6	6.9	49
		0.893	0.107	580	3.2	3.0	2.3	2.6	120	549	25	1,400	-4.5	5.9	46
	Totals				5.5	4.8	3.4	4.6	101	675	25	1,400	-4.5	12.9	205
	V	0.197	0.803	580	44.3	27.3	63.9	27.3	401	696	25	200	0.5	111.5	56
		0.399	0.601	580	6.1	5.1	53.0	5.1	427	677	25	200	1.3	13.4	39
		0.588	0.412	580	7.3	7.1	60.7	7.1	386	636	25	300	3.7	13.0	36
		0.795	0.205	580	5.3	5.0	43.0	4.9	356	640	25	800	-3.4	11.2	75
		0.893	0.107	580	8.6	5.8	39.0	5.6	200	638	25	600	-1.9	41.8	86
	Totals				20.4	9.8	49.3	9.7	200	696	25	800	-3.4	111.5	292
	TOTAL				16.1	7.7	30.4	7.6	101	696	25	1,400	-4.5	111.5	497

Table F 24. Pentane - cis-2-Pentene Enthalpy Summary

Components	Phase	x_1	x_2	REF	RMSE	AAD	%AAD	BIAS	T (°F) min	T (°F) max	P (psia) min	P (psia) max	Max Dev min	Max Dev max	NPTS
n-pentane (1)	L	0.502	0.498	581	5.3	5.0	4.7	5.0	331	390	350	1,400	-0.3	7.8	20
cis-2-pentene (2)				678	3.3	2.3	2.2	2.1	350	390	400	1,400	-1.8	7.5	23
				Subtotal	4.4	3.5	3.3	3.4	331	390	350	1,400	-1.8	7.8	43
	V	0.502	0.498	581	9.2	5.3	8.1	4.7	349	450	20	1,400	-2.9	30.6	51
				678	5.2	2.8	4.8	1.4	350	440	300	1,400	-2.3	24.8	65
				Subtotal	7.2	3.9	6.3	2.9	349	450	20	1,400	-2.9	30.6	116
	TOTAL				6.6	3.8	5.5	3.0	331	450	20	1,400	-2.9	30.6	159

Table F 25. Pentane - Cyclohexane Enthalpy Summary

Components	Phase	x_1	x_2	REF	RMSE	AAD	%AAD	BIAS	T (°F) min	T (°F) max	P (psia) min	P (psia) max	Max Dev min	Max Dev max	NPTS
n-pentane (1)	L	0.197	0.803	580	3.0	2.4	2.2	2.4	318	467	150	500	1.1	4.9	3
cyclohexane (2)				584	3.5	3.1	2.4	3.0	123	521	15	1,400	-0.7	9.5	63
				677	2.9	2.3	2.1	0.4	360	500	200	1,400	-3.3	8.4	31
				Subtotal	3.3	2.8	2.3	2.2	123	521	15	1,400	-3.3	9.5	97
		0.385	0.615	580	3.7	3.5	2.7	3.5	291	376	150	300	1.9	6.1	6
				584	1.9	1.6	1.2	1.0	120	488	100	1,400	-3.2	3.7	50
				677	1.7	1.4	1.2	-0.3	300	480	150	1,400	-4.2	3.5	40
				Subtotal	2.0	1.6	1.3	0.6	120	488	100	1,400	-4.2	6.1	96
		0.612	0.388	580	3.0	3.0	2.3	3.0	271	316	150	200	1.9	3.8	6
				584	3.3	3.0	2.3	2.1	127	447	200	1,400	-5.1	6.5	44
				677	2.7	2.0	1.8	1.0	280	440	150	1,400	-4.4	8.9	39
				Subtotal	3.1	2.6	2.1	1.7	127	447	150	1,400	-5.1	8.9	89
		0.793	0.207	580	3.4	3.0	2.4	3.0	262	418	150	1,400	0.4	5.2	6
				584	3.6	3.1	2.5	3.1	141	429	200	1,400	0.3	8.5	38
				677	2.9	2.1	1.9	1.7	260	400	150	1,400	-2.1	9.1	38
				Subtotal	3.3	2.6	2.2	2.5	141	429	150	1,400	-2.1	9.1	82
	Totals				2.9	2.4	2.0	1.7	120	521	15	1,400	-5.1	9.5	364

Table F 25. Pentane - Cyclohexane Enthalpy Summary (Cont'd)

Components	Phase	x_1	x_2	REF	RMSE	AAD	%AAD	BIAS	T (°F)		P (psia)		Max Dev		NPTS
									min	max	min	max	min	max	
n-pentane (1)	V	0.197	0.803	580	3.8	3.8	25.7	3.8	356	365	150	150	2.9	4.6	2
cyclohexane (2)				584	6.9	6.2	45.1	5.9	220	696	15	1,400	-4.3	18.0	53
				677	4.5	2.3	7.7	1.9	360	680	100	1,400	-3.0	25.8	115
				Subtotal	5.4	3.5	19.6	3.1	220	696	15	1,400	-4.3	25.8	170
		0.385	0.615	580	3.3	3.3	23.6	3.3	352	352	150	150	3.3	3.3	1
				584	3.9	3.1	37.4	-2.2	296	705	100	1,400	-7.4	10.5	48
				677	4.7	2.7	11.2	-0.5	340	680	100	1,400	-15.0	23.4	118
				Subtotal	4.4	2.9	18.8	-1.0	296	705	100	1,400	-15.0	23.4	167
		0.612	0.388	580	3.9	3.7	22.2	3.7	322	355	150	200	1.8	4.6	4
				584	4.1	2.4	20.5	1.1	299	704	100	1,400	-4.0	23.4	58
				673	0.3	0.3	2.7	0.3	440	440	200	200	0.3	0.3	1
				677	5.6	2.9	126.0	-0.1	320	680	100	1,400	-14.4	29.3	127
				Subtotal	5.1	2.8	91.0	0.3	299	704	100	1,400	-14.4	29.3	190
		0.793	0.207	580	2.7	2.5	11.0	2.5	298	431	150	500	0.8	4.5	8
				584	3.8	2.5	49.7	-0.4	197	707	25	1,400	-6.7	21.1	85
				677	6.8	3.4	12.4	0.7	300	680	100	1,400	-11.3	41.5	140
				Subtotal	5.8	3.0	25.9	0.3	197	707	25	1,400	-11.3	41.5	233
	Totals				5.3	3.0	39.2	0.7	197	707	15	1,400	-15.0	41.5	760

Table F 25. Pentane - Cyclohexane Enthalpy Summary (Cont'd)

Components	Phase	x_1	x_2	REF	RMSE	AAD	%AAD	BIAS	T (°F) min	T (°F) max	P (psia) min	P (psia) max	Max Dev min	Max Dev max	NPTS
n-pentane (1)	L-L-V	0.197	0.803	580	3.6	3.3	3.1	3.3	360	471	200	500	1.0	4.5	3
cyclohexane (2)				584	9.0	7.5	6.8	7.5	348	475	200	500	2.5	12.5	2
				Subtotal	6.4	5.0	4.6	5.0	348	475	200	500	1.0	12.5	5
		0.385	0.615	580	7.0	6.9	6.7	6.9	385	456	300	500	4.7	7.9	3
				584	2.5	2.0	2.1	0.8	340	475	200	600	-1.0	4.2	3
				Subtotal	5.3	4.4	4.4	3.8	340	475	200	600	-1.0	7.9	6
		0.612	0.388	580	8.1	8.1	7.3	8.1	393	393	400	400	8.1	8.1	1
				584	4.8	3.9	3.5	3.9	390	418	400	600	1.0	6.7	2
				Subtotal	6.1	5.3	4.8	5.3	390	418	400	600	1.0	8.1	3
		0.793	0.207	580	5.9	5.7	5.2	5.7	346	376	300	400	4.3	7.2	2
				584	8.9	8.9	8.3	8.9	380	380	400	400	8.9	8.9	1
				Subtotal	7.1	6.8	6.2	6.8	346	380	300	400	4.3	8.9	3
	Totals				6.1	5.1	4.8	4.9	340	475	200	600	-1.0	12.5	17

Table F 25. Pentane - Cyclohexane Enthalpy Summary (Cont'd)

Components	Phase	x_1	x_2	REF	RMSE	AAD	%AAD	BIAS	T (°F)		P (psia)		Max Dev		NPTS
									min	max	min	max	min	max	
n-pentane (1)	L-V-V	0.197	0.803	580	5.4	5.4	32.8	5.4	350	350	150	150	5.4	5.4	1
cyclohexane (2)				584	8.4	8.2	29.1	8.2	338	526	100	600	6.3	11.0	6
				Subtotal	8.0	7.8	29.6	7.8	338	526	100	600	5.4	11.0	7
		0.385	0.615	580	3.5	3.3	17.6	3.3	334	450	150	400	1.8	4.4	7
				584	0.8	0.7	1.7	-0.7	485	499	500	600	-0.9	-0.6	2
				Subtotal	3.1	2.8	14.0	2.4	334	499	150	600	-0.9	4.4	9
		0.612	0.388	580	3.8	3.7	18.1	3.7	314	400	150	300	2.8	5.1	3
				584	2.4	2.1	8.5	2.1	340	449	200	400	1.1	3.1	2
				677	0.5	0.4	0.8	0.4	380	440	300	500	0.1	0.6	2
				Subtotal	2.8	2.3	10.4	2.3	314	449	150	500	0.1	5.1	7
		0.793	0.207	580	3.6	3.3	12.4	3.3	289	425	150	500	2.0	6.4	8
				584	7.0	5.7	35.4	5.7	172	429	25	500	2.3	11.5	3
				Subtotal	4.8	4.0	18.6	4.0	172	429	25	500	2.0	11.5	11
	Totals				5.0	4.1	18.0	4.0	172	526	25	600	-0.9	11.5	34
	TOTAL				4.7	2.9	26.6	1.2	120	707	15	1,400	-15.0	41.5	1,175

Table F 26. Pentane - Hexadecane Enthalpy Summary

Components	Phase	x_1	x_2	REF	RMSE	AAD	%AAD	BIAS	T (°F) min	max	P (psia) min	max	Max Dev min	max	NPTS
n-pentane (1)	L	0.167	0.833	583	2.8	2.7	2.5	2.7	400	600	1,400	1,400	1.4	4.3	11
hexadecane (2)				584	4.5	3.8	3.1	3.1	199	597	25	1,400	-3.4	9.0	17
				Subtotal	3.9	3.3	2.9	3.0	199	600	25	1,400	-3.4	9.0	28
		0.386	0.614	583	3.0	2.6	2.8	0.9	400	620	200	1,400	-7.5	4.4	26
				584	4.3	3.4	2.9	3.3	179	618	40	1,400	-0.9	7.8	13
				Subtotal	3.5	2.9	2.8	1.7	179	620	40	1,400	-7.5	7.8	39
		0.587	0.413	583	2.7	2.4	2.5	1.7	400	600	400	1,400	-4.2	4.2	32
				584	5.1	4.7	3.7	4.2	200	596	70	1,400	-2.3	7.0	8
				Subtotal	3.3	2.9	2.7	2.2	200	600	70	1,400	-4.2	7.0	40
		0.794	0.206	583	2.3	2.2	2.3	2.2	400	620	400	1,400	-0.3	3.5	35
				584	3.7	3.3	2.9	3.2	117	625	25	1,400	-0.6	7.4	25
				Subtotal	2.9	2.6	2.5	2.6	117	625	25	1,400	-0.6	7.4	60
	Totals				3.3	2.9	2.7	2.3	117	625	25	1,400	-7.5	9.0	167

Table F 26. Pentane - Hexadecane Enthalpy Summary (Cont'd)

Components	Phase	x_1	x_2	REF	RMSE	AAD	%AAD	BIAS	T (°F) min	T (°F) max	P (psia) min	P (psia) max	Max Dev min	Max Dev max	NPTS
n-pentane (1)	V	0.167	0.833	583	2.9	2.9	52.3	2.9	600	620	25	25	2.6	3.1	2
hexadecane (2)		0.386	0.614	583	2.7	2.6	48.4	2.6	560	620	25	40	1.7	4.0	6
				584	3.6	3.2	49.7	3.2	561	619	25	40	0.9	7.1	10
				Subtotal	3.3	3.0	49.2	3.0	560	620	25	40	0.9	7.1	16
		0.587	0.413	583	1.5	1.3	31.1	1.3	540	620	25	70	0.3	2.2	9
				584	2.2	2.0	40.0	2.0	537	617	25	70	0.3	3.4	7
				Subtotal	1.8	1.6	35.0	1.6	537	620	25	70	0.3	3.4	16
		0.794	0.206	583	10.2	2.7	23.1	2.1	400	620	25	100	-1.0	43.2	18
				584	1.9	1.6	213.8	-0.4	480	618	25	100	-2.6	4.1	13
				Subtotal	7.9	2.3	103.0	1.0	400	620	25	100	-2.6	43.2	31
	Totals				5.8	2.3	71.5	1.7	400	620	25	100	-2.6	43.2	65
	TOTAL				4.2	2.7	22.0	2.2	117	625	25	1,400	-7.5	43.2	232

Table F 27. Pentane - Octane Enthalpy Summary

Components	Phase	x_1	x_2	REF	RMSE	AAD	%AAD	BIAS	T (°F) min	T (°F) max	P (psia) min	P (psia) max	Max Dev min	Max Dev max	NPTS
n-pentane (1)	L	0.218	0.782	663	2.5	2.0	2.0	1.3	75	550	200	1,400	-2.9	6.2	66
n-octane (2)		0.392	0.608	663	3.1	2.6	2.4	2.3	75	540	200	1,400	-2.7	6.7	52
		0.597	0.403	663	3.5	2.9	2.7	2.9	75	523	200	1,400	-0.3	7.4	51
		0.809	0.191	663	1.2	0.9	0.8	0.6	75	441	1,400	1,400	-1.7	2.7	10
	Totals				2.9	2.3	2.2	2.0	75	550	200	1,400	-2.9	7.4	179
	V	0.218	0.782	663	6.0	4.1	125.6	3.7	75	605	15	1,400	-4.0	33.9	80
		0.392	0.608	663	7.6	5.8	19.7	5.7	400	602	15	1,400	-1.5	23.3	61
		0.597	0.403	663	7.5	5.5	11.1	5.2	440	605	200	1,400	-2.9	25.3	69
		0.809	0.191	663	8.6	4.6	10.3	4.5	75	606	200	1,400	-1.9	57.8	74
	Totals				7.4	4.9	45.0	4.7	75	606	15	1,400	-4.0	57.8	284
	L-L-V	0.218	0.782	663	2.3	2.3	2.7	2.3	509	509	432	432	2.3	2.3	1
		0.392	0.608	663	2.5	2.5	2.7	2.5	479	479	500	500	2.5	2.5	1
		0.597	0.403	663	8.0	8.0	8.5	8.0	451	460	500	500	7.3	8.6	2
		0.809	0.191	663	4.6	4.5	3.6	4.5	297	299	200	200	3.4	5.6	2
	Totals				5.5	5.0	4.9	5.0	297	509	200	500	2.3	8.6	6
	L-V-V	0.218	0.782	663	2.9	2.9	5.9	2.9	542	542	400	400	2.9	2.9	1
		0.392	0.608	663	8.8	8.2	20.4	8.2	483	522	200	500	4.6	12.6	3
		0.597	0.403	663	5.0	4.5	13.4	4.5	471	501	200	500	2.2	8.3	6
		0.809	0.191	663	1.7	1.6	5.5	0.9	373	482	200	600	-1.6	3.0	7
	Totals				4.9	3.9	10.9	3.6	373	542	200	600	-1.6	12.6	17
	TOTAL				6.1	3.9	27.6	3.7	75	606	15	1,400	-4.0	57.8	486

Table F 28. Pentane - trans-Decalin Enthalpy Summary

Components	Phase	x_1	x_2	REF	RMSE	AAD	%AAD	BIAS	T (°F) min	max	P (psia) min	max	Max Dev min	max	NPTS
n-pentane (1)	L	0.322	0.678	580	5.6	5.4	4.5	5.4	150	597	20	1,400	1.2	9.8	48
trans-decalin (2)				582	3.2	2.9	3.1	-2.9	460	600	300	1,400	-0.5	-5.7	36
				Subtotal	4.7	4.3	3.9	1.8	150	600	20	1,400	-5.7	9.8	84
		0.561	0.439	580	4.9	4.6	3.9	4.6	149	598	40	1,400	2.7	9.1	40
				582	3.1	1.8	1.7	0.7	460	600	400	1,400	-2.1	8.6	23
				Subtotal	4.3	3.6	3.1	3.2	149	600	40	1,400	-2.1	9.1	63
		0.725	0.275	580	4.0	3.2	2.5	3.2	119	598	30	1,400	0.2	14.2	42
				582	1.9	1.8	2.3	-1.6	460	600	600	1,400	-2.8	1.8	18
				Subtotal	3.5	2.8	2.5	1.7	119	600	30	1,400	-2.8	14.2	60
		0.884	0.116	580	3.0	2.9	2.3	2.7	100	598	20	1,400	-3.1	5.2	38
				582	2.1	1.6	2.2	0.9	400	600	500	1,400	-1.8	4.9	38
				Subtotal	2.6	2.2	2.2	1.8	100	600	20	1,400	-3.1	5.2	76
	Totals				3.9	3.3	3.0	2.1	100	600	20	1,400	-5.7	14.2	283

Table F 28. Pentane - trans-Decalin Enthalpy Summary (Cont'd)

Components	Phase	x_1	x_2	REF	RMSE	AAD	%AAD	BIAS	T (°F)		P (psia)		Max Dev		NPTS
									min	max	min	max	min	max	
n-pentane (1)	V	0.322	0.678	580	7.1	7.0	65.3	7.0	383	598	20	200	3.8	10.2	28
trans-decalin (2)				582	1.7	1.3	26.8	-1.2	460	600	20	200	-3.2	0.7	17
				Subtotal	5.7	4.8	50.8	3.9	383	600	20	200	-3.2	10.2	45
		0.561	0.439	580	7.6	7.5	55.8	7.5	371	599	20	300	5.7	10.4	23
				582	1.1	0.9	13.0	-0.8	460	600	70	300	-2.7	0.4	18
				Subtotal	5.7	4.6	37.0	3.8	371	600	20	300	-2.7	10.4	41
		0.725	0.275	580	4.8	4.5	33.0	4.5	339	597	30	700	1.8	10.6	46
				582	1.5	1.4	20.7	-1.4	460	600	40	500	-0.2	-3.0	32
				Subtotal	3.8	3.2	28.0	2.1	339	600	30	700	-3.0	10.6	78
		0.884	0.116	580	3.3	3.0	28.3	2.9	280	598	20	800	-1.4	6.8	46
				582	0.9	0.5	5.6	0.0	400	600	40	500	-2.4	3.9	42
				Subtotal	2.4	1.8	17.4	1.5	280	600	20	800	-2.4	6.8	88
	Totals				4.2	3.2	29.8	2.5	280	600	20	800	-3.2	10.6	252
	TOTAL				4.0	3.3	15.6	2.3	100	600	20	1,400	-5.7	14.2	535

APPENDIX G

MODEL PARAMETERS: CRITICAL CONSTANTS, DISSOCIATION

COEFFICIENTS AND PITZER MODEL COEFFICIENTS

Table G 1. Critical Constants

Component		T_c (K)	P_c (atm)	Accentric Factor
Water	H_2O	647.3	221.2	0.344
Ammonia	NH_3	405.5	113.5	0.250
Carbon Dioxide	CO_2	304.1	73.8	0.239
Hydrogen Sulfide	H_2S	373.2	89.4	0.081
Sulfur Dioxide	SO_2	430.8	78.8	0.256
Hydrogen Cyanide	HCN	456.7	53.9	0.388
Phenol	C_6H_5OH	694.2	61.3	0.438
Mercaptan	CH_3SH	470.0	72.3	0.153
Carbon Monoxide	CO	132.9	35.0	0.066
Nitrogen	N_2	126.2	33.9	0.039
Methane	CH_4	190.4	46.0	0.011
Hydrogen	H_2	33.2	13.0	-0.218

Table G 2. Chemical Equilibrium Correlation Coefficients

Reaction	EQ#	A	B	C	D	T(°C) Range	Ref
$H_2O = H^+ + OH^-$	2	5839.5	22.4773	0.000	-61.2062	0-225	[11]
	1	-13445.9	-22.4773	0.000	140.932		[12]
$NH_3 + H_2O = NH_4^+ + OH^-$	2	4390.82	23.9744	-0.0160935	-60.0072	0-225	[11]
	1	-3335.7	1.4971	-0.0370566	2.76		[12]
	1	-5914.082	-15.06399	-0.01100801	97.97152	0-175	[13]
$CO_2 + H_2O = H^+ + HCO_3^-$	1	-12092.1	-36.7816	0.000	235.482		[12]
	1	-7726.01	-14.50613	-0.0279842	102.2755	0-225	[13]
$H_2S = H^+ + HS^-$	2	5643.83	33.5471	0	-94.9363	0-150	[11]
	1	-12995.4	-33.5471	0.000	218.5989		[12]
	1	-18034.72	-78.07186	0.0919824	461.7162	0-275	[13]
$SO_2 + H_2O = H^+ + HSO_3^-$	1	-3768	-20.0000	0.000	122.53		[12]
	1	26404.29	160.3981	-0.2752224	-924.6255	0-175	[13]
$HCO_3^- = H^+ + CO_3^{-2}$	1	-12431.7	-35.4819	0.000	220.067		[12]
	1	-9137.258	-18.11192	-0.02245619	116.7371	0-225	[13]
$HS^- = H^+ + S^{-2}$	1	-7211.2	0.000	0.000	-7.489		[12]
[11] assumes K_{HS} ~ $0.018 * K_{H2O}$	1	-406.0035	33.88898	-0.05411082	-214.5592	0-225	[13]
$HSO_3^- = H^+ + SO_3^{-2}$	1	1333.4	0.000	0.000	-21.274		[12]
	1	-5421.93	-4.689868	-0.0498769	43.13158	0-175	[13]
$NH_3 + HCO_3^- = NH_2COO^- + H_2O$	1	2895.65	0.000	0.000	-8.5994		[12]
	1	604.1164	-4.017263	0.005039095	20.15214	0-175	[13]
$HCN = H^+ + CN^-$	2	4319.290	0.000	0.022	-11.691	10-150	[11], [12]
$C_6H_5OH = H^+ + C_6H_5O^-$	2	5068.190	27.726	0.000	-75.625	25-150	[11], [12]
	2	2896.140	12.123	0.000	-29.114	25-150	[11], [12]

Correlation Equations for Dissociation Constants as a function of Temperature (K)

Published correlations by Tsonopoulos, et al. [11], Maurer [12], and Kawazuishi and Prausnitz [13], provide a quick method for calculating equilibrium constants as a function of temperature. The following correlation equations are used

#1: $$pK_A = -\ln(K) = \frac{A}{T(K)} + B\ln(T(K)) + CT(K) + D$$

#2: $$pK_A = -\log_{10}(K) = \frac{A}{T(K)} + B\log_{10}(T(K)) + CT(K) + D$$

Correlation Equations for Pitzer Constants as a function of Temperature (K)

$$P(T(K)) = C_1 + C_2\left(\frac{1}{T(K)} - \frac{1}{273.15}\right) + C_3\ln\left(\frac{T(K)}{273.15}\right)$$
$$+ C_4(T(K) - 273.15) + C_5\left((T(K))^2 - 273.15^2\right)$$

Table G 3. Beta(0)

	C_1	C_2	C_3	C_4	C_5	REF
Ba-Cl	0.290748	-1.34E+03	-5.30E+00	6.38E-04	4.61E-06	10
Ca-Cl	0.305320	-2.18E+04	-1.85E+02	5.23E-01	-2.46E-04	1
Ca-HCO$_3$	0.182545	-5.77E+05	-5.66E+03	1.84E+01	-9.99E-03	8
Ca-OH	-0.174700	0	0	0	0	7
Ca-SO$_4$	0.015000	0	0	0	0	1
H-Cl	0.177500	0	0	0	0	7
H-SO$_4$	0.029800	0	0	0	0	7
K-Cl	0.048080	-7.58E+02	-4.71E+00	1.01E-02	-3.76E-06	1
K-CO$_3$	0.128800	1.41E-05	3.73E-09	1.10E-03	-7.11E-15	8
K-HCO$_3$	-0.010702	-7.03E-04	-4.71E-06	1.00E-03	-1.07E-14	8
K-OH	0.129800	0	0	0	0	7
K-SO$_4$	0.055536	-1.42E+03	-6.75E+00	8.27E-03	-2.52E-13	1
Mg-Cl	0.351088	2.38E-06	4.66E-09	-9.32E-04	5.94E-07	3
Mg-HCO$_3$	-0.009313	-2.73E+05	-2.61E+03	8.25E+00	-4.34E-03	8
Mg-SO$_4$	0.215092	-5.47E+03	-4.23E+01	1.07E-01	-4.29E-05	3
Na-Cl	0.075359	-2.37E+03	-1.79E+01	4.67E-02	-2.08E-05	1
Na-CO$_3$	0.036205	1.11E+03	1.12E+01	-2.33E-02	4.28E-13	8
Na-HCO$_3$	0.028002	6.83E+02	6.90E+00	-1.45E-02	2.64E-13	8
Na-OH	0.091900	6.59E+03	6.14E+01	-1.86E-01	9.20E-05	4
Na-SO$_4$	0.018693	-1.97E+04	-1.60E+02	4.37E-01	-1.99E-04	1

Table G 4. Beta(1)

	C_1	C_2	C_3	C_4	C_5	REF
Ba-Cl	1.25002	4.37E+03	1.59E+01	3.22E-03	-6.77E-06	10
Ca-Cl	1.70813	-1.72E-05	2.98E-08	-1.54E-02	3.18E-05	1
Ca-HCO$_3$	0.30004	2.65E+04	1.83E+02	-3.73E-01	8.97E-05	8
Ca-OH	-0.23030	0	0	0	0	7
Ca-SO$_4$	3.00000	0	0	0	0	1
H-Cl	0.29450	0	0	0	0	5
K-Cl	0.21803	-6594.5	-53.9	0.1477	0	1
K-CO$_3$	1.43300	1.18E-03	5.96E-08	4.36E-03	2.84E-14	8
K-HCO$_3$	0.04780	9.32E-04	6.16E-06	1.10E-03	-1.78E-14	8
K-OH	0.32000	0	0	0	0	7
K-SO$_4$	0.79639	2067.1	0	0	0	1
Mg-Cl	1.65119	-2.29E-05	1.49E-08	-1.09E-02	2.60E-05	3
Mg-HCO$_3$	0.80474	3.20E+06	2.99E+04	-9.28E+01	4.78E-02	8
Mg-SO$_4$	3.36625	-5.78E+03	3.43E-07	-1.48E-01	1.58E-04	3
Na-Cl	0.27703	-4.81E+03	-3.92E+01	1.07E-01	-4.71E-05	1
Na-CO$_3$	1.51207	4.41E+03	4.46E+01	-9.99E-02	1.73E-12	8
Na-HCO$_3$	0.04401	1.13E+03	1.14E+01	-2.45E-02	4.39E-13	8
Na-OH	0.25300	-1.03E+04	-8.60E+01	2.39E-01	-1.08E-04	4
Na-SO$_4$	1.09940	-1.52E+04	-1.13E+02	2.87E-01	-1.25E-04	1

Table G 5. Beta(2)

	C_1	C_2	C_3	C_4	C_5	REF
Ca-OH	-5.72E+00	0	0	0	0	7
Ca-SO$_4$	-1.00E+01	-1.53E-03	-9.54E-07	4.00E-01	1.82E-12	3
Mg-SO$_4$	-3.28E+01	-9.98E+05	-1.10E+04	4.18E+01	-2.73E-02	3

Table G 6. C-Phi

	C_1	C_2	C_3	C_4	C_5	REF
Ba-Cl	-0.03047	1.141E+03	8.094E+00	-1.866E-02	7.034E-06	10
Ca-Cl	0.00234	1.955E+03	1.656E+01	-4.689E-02	2.205E-05	1
H-Cl	0.00080	0	0	0	0	7
H-SO$_4$	0.04380	0	0	0	0	7
K-Cl	-0.00079	9.127E+01	5.865E-01	-1.298E-03	4.957E-07	1
K-CO$_3$	0.00050	0	0	0	0	8
K-HCO$_3$	-0.00800	0	0	0	0	7
K-OH	0.00410	0	0	0	0	7
Mg-Cl	0.00651	4.023E-07	1.164E-09	-2.499E-04	2.418E-07	3
Mg-SO$_4$	0.02792	1.647E+03	1.388E+01	-3.901E-02	1.783E-05	3
Na-Cl	0.00141	3.511E+02	2.742E+00	-7.337E-03	3.318E-06	1
Na-CO$_3$	0.00520	0	0	0	0	8
Na-OH	0.00361	-3.584E+02	-3.430E+00	1.045E-02	-5.161E-06	4
Na-SO$_4$	0.00630	-3.895E+02	-5.663E+00	2.122E-02	-1.195E-05	1

Table G 7. Theta for Anion- Anion

	C_1	C_2	C_3	C_4	C_5	REF
CO_3-Cl	-2.00E-02	0	0	0	0	7
CO_3-HCO_3	-4.00E-02	0	0	0	0	7
CO_3-OH	1.00E-01	0	0	0	0	7
CO_3-SO_4	2.00E-02	0	0	0	0	7
HCO_3-Cl	3.00E-02	0	0	0	0	7
HCO_3-SO_4	1.00E-02	0	0	0	0	7
OH-Cl	-5.00E-02	0	0	0	0	3
OH-SO_4	-1.30E-02	0	0	0	0	3
SO_4-Cl	7.00E-02	0	0	0	0	1

Table G 8. Theta for Cation - Cation

	C_1	C_2	C_3	C_4	C_5	REF
Ca-K	1.16E-01	0	0	0	0	1
Ca-Mg	7.00E-03	0	0	0	0	7
Ca-Na	5.00E-02	0	0	0	0	1
H-Ca	9.20E-02	0	0	0	0	7
H-K	5.00E-03	0	0	0	0	7
H-Mg	1.00E-01	0	0	0	0	7
H-Na	3.60E-02	0	0	0	0	7
Mg-Na	7.00E-02	0	0	0	0	3
Na-K	-3.20E-03	1.40E+01	-2.33E-10	1.36E-12	-2.22E-16	1

Table G 9. Cation - Cation - Anion

	C_1	C_2	C_3	C_4	C_5	REF
Ca-H-Cl	-0.0150	0	0	0	0	7
Ca-Mg-Cl	-0.0120	0	0	0	0	7
Ca-Mg-SO$_4$	0.0240	0	0	0	0	7
K-Ca-Cl	-0.0432	0	0	0	0	1
K-H-Cl	-0.0110	0	0	0	0	7
K-H-SO	0.1970	0	0	0	0	7
K-Mg-Cl	-0.0264	0	0	0	0	3, 7
K-Mg-SO$_4$	-0.0480	0	0	0	0	7
Mg-H-Cl	-0.0110	0	0	0	0	7
Mg-H-SO$_4$	-0.0178	0	0	0	0	7
Na-Ca-Cl	-0.0030	0	0	0	0	1
Na-Ca-SO$_4$	-0.0120	0	0	0	0	1
Na-H-Cl	-0.0040	0	0	0	0	7
Na-K-Cl	-0.0037	0	0	0	0	1
Na-K-HCO$_3$	-0.0030	0	0	0	0	7
Na-K-SO$_4$	0.0073	0	0	0	0	1
Na-Mg-Cl	-0.0149	0	0	0	0	3, 7
Na-Mg-SO$_4$	-0.0150	0	0	0	0	7

Table G 10. Anion - Anion - Cation

	C_1	C_2	C_3	C_4	C_5	REF
Cl-SO$_4$-K	-0.0016	0	0	0	0	1
Cl-OH-K	-0.0060	0	0	0	0	7
Cl-HCO$_3$-Mg	-0.0960	0	0	0	0	7
SO$_4$-OH-Na	-0.0126	0	0	0	0	3, 7
SO$_4$-HCO$_3$-Mg	-0.0161	0	0	0	0	7
OH-CO$_3$-Na	-0.0170	0	0	0	0	7
HCO$_3$-CO$_3$-K	0.0120	0	0	0	0	7
Cl-SO$_4$-Ca	-0.0180	0	0	0	0	1
Cl-OH-Ca	-0.0250	0	0	0	0	7
Cl-CO$_3$-Na	0.0085	0	0	0	0	7
SO$_4$-OH-K	-0.0500	0	0	0	0	7
SO$_4$-CO$_3$-Na	-0.0050	0	0	0	0	7
OH-CO$_3$-K	-0.0100	0	0	0	0	7
Cl-SO$_4$-Na	-0.0091	0	0	0	0	1
Cl-SO$_4$-Mg	-0.0080	0	0	0	0	3
Cl-OH-Na	-0.0091	0	0	0	0	3, 7
Cl-HCO$_3$-Na	-0.0150	0	0	0	0	7
Cl-CO$_3$-K	0.0040	0	0	0	0	7
SO$_4$-HCO$_3$-Na	-0.0050	0	0	0	0	7
SO$_4$-CO$_3$-K	-0.0090	0	0	0	0	7

REFERENCES

1. Greenberg, J. and N. Moller, The prediction of mineral solubilities in natural waters: A chemical equilibrium model for the Na-K-Ca-Cl-SO$_4$-H$_2$O system to high concentration from 0 to 250°C. Geochimica et Cosmochimica Acta, 1989. 53: p. 2503-2518.

2. Spencer, C.F., T.E. Daubert, and R.P. Danner, A Critical Review of Correlations for the Critical Properties of Defined Mixtures. AIChE Journal, 1973. 19(3): p. 521-527.

3. Pabalan, R.T. and K.S. Pitzer, Thermodynamics of concentrated electrolyte mixtures and prediction of solubilities high temperatures in Na-K-Mg-Cl-SO$_4$-OH-H$_2$O. Geochimica et Cosmochimica Acta, 1987. 51: p. 2429-2443.

4. Pabalan, R.T. and K.S. Pitzer, Thermodynamics of NaOH(aq) in hydrothermal solutions. Geochimica et Cosmochimica Acta, 1987. 51: p. 829–837.

5. Holmes, H. F., Baes, C. F. B. Jr., and Mesmer, R. E. (1987): The enthalpy of dilution of HCl(aq) to 648 K and 40 MPa: Thermodynamic properties. J. Chem. Thermodyn., 19, 863-890.

6. Holmes, H.,F. and Mesmer, R. E. (1992): Isopiestic studies of H$_2$SO$_4$(aq) at elevated temperatures - Thermodynamic properties. J. Chem. thermodynamics, 24, 317-328.

7. Harvie, C. E., Moller, N., and Weare, J. H. (1984): The prediction of mineral solubilities in natural waters: The Na-K-Mg-Ca-H-Cl-SO$_4$-OH-HCO$_3$-CO$_3$-CO$_2$-H$_2$O system to high ionic strengths at 25°C. Geochim. Cosmochim. Acta, 48, 723-751.

8. He, S. and Morse, J. W. (1993): The carbonic acid system and calcite solubility in aqueous Na-K-Ca-Mg-Cl-SO$_4$ solutions from 0-90°C. Geochim. Cosmochim. Acta, 57, 3533-3554.

9. Azaroual, M., Fouillac, C., and Matray, J. M. (1997): Solubility of silica polymorphs in electrolyte solutions, I. Activity coefficients of aqueous silica from 25° to 250°C, Pitzer's parameterisation. Chemical Geology, 140, 155-165.

10. Monnin, C. (1999): A thermodynamic model for the solubility of barite and celestite in electrolyte solutions and seawater to 200°C and to 1 kbar. Chemical Geology, 127, 141-159.

11. Tsonopoulos, C., D.M. Coulson, and L.B. Inman, *Ionization Constants of Water Pollutants.* Journal of Chemical and Engineering Data, 1976. 21(No. 2): p. 190-193.

12. Maurer, G., *Thermodynamics of Aqueous Systems with Industrial Application.* ACS Symposium Series, ed. S.A. Newman. Vol. 133. 1980: ACS pgs.

13. Kawazuishi, K. and J.M. Prausnitz, *Correlation of Vapor-Liquid Equilibria for the System Ammonia-Carbon Dioxide-Water.* Industrial Engineering and Chemical Research, 1987. 26: p. 1482-1485.

APPENDIX H

ADDITIONAL MODEL RESULTS

Table H 1. All Carbon Dioxide

T (K)	P (Bar)	CO_2 (mol/kg)		NPTS	BIAS	AAD
273.2 - 623.2	0.77 - 3500.0	0.0 - 41.9	P_{TOT}	1006	1.4%	3.8%
			$ppCO_2$	298	18.8%	22.0%
			ppH_2O	298	-10.4%	28.1%

Table H 2. Carbon Dioxide Sorted By Reference Source [1-3]

T (K)	P (Bar)	CO_2 (mol/kg)	NPTS	BIAS	AAD	REF
273.2 - 473.2	1.54 - 709.3	0.0 - 1.8	116	4.1%	6.1%	[C2]
288.7 - 623.2	3.25 - 3500.0	0.0 - 41.9	298	4.1%	5.9%	[C3]
352.8 - 471.2	20.40 - 102.1	0.1 - 0.9	33	6.0%	8.3%	[3]
423.2 - 623.2	100.0 - 1399.9	0.2 - 17.1	39	0.5%	1.7%	[2]
273.2 - 285.6	5.14 - 30.8	0.2 - 1.5	12	-0.5%	3.2%	[C6]
274.2 - 288.2	0.77 - 22.1	0.0 - 1.0	54	-2.7%	6.0%	[C7]
293.2 - 333.2	24.82 - 119.3	0.3 - 1.2	34	-0.3%	0.5%	[C8]
293.2 - 308.2	25.67 - 77.0	0.5 - 1.2	20	-0.6%	0.6%	[C9]
293.2 - 303.2	4.92 - 29.8	0.2 - 0.9	10	-1.3%	3.4%	[C10]
288.8 - 366.5	6.99 - 205.4	0.1 - 1.5	16	-2.9%	2.9%	[C11]
273.2 - 288.2	5.14 - 53.4	0.2 - 1.7	18	-0.7%	2.6%	[C12]
273.2 - 298.2	10.26 - 46.2	0.5 - 1.5	12	0.9%	2.4%	[C13]
277.1 - 283.2	20.26 - 42.6	0.9 - 1.5	9	-0.9%	0.9%	[C14]
281.2 - 281.2	33.44 - 33.4	0.2 - 0.2	1	1.8%	1.8%	[C15]
278.0 - 293.0	65.25 - 298.8	1.4 - 2.0	24	-0.6%	0.7%	[C16]
323.2 - 373.2	101.32 - 810.6	0.8 - 2.0	9	-1.0%	1.0%	[C17]
283.2 - 343.2	10.13 - 162.1	0.1 - 1.4	23	-0.8%	1.5%	[C18]
298.3 - 298.6	21.99 - 77.9	0.7 - 1.4	9	-0.5%	0.6%	[C19]
273.2 - 373.2	10.98 - 95.7	0.2 - 1.5	80	-0.7%	1.4%	[C20]
298.2 - 348.2	50.21 - 50.2	0.6 - 1.3	11	-1.1%	1.1%	[C21]
298.2 - 373.2	50.21 - 50.2	0.4 - 1.3	7	-1.5%	1.5%	[C22]
285.2 - 373.2	25.67 - 718.7	0.2 - 1.8	71	-0.9%	1.0%	[C23]
283.2 - 303.2	1.02 - 20.5	0.0 - 0.9	15	-2.7%	3.9%	[C24]
303.2 - 353.2	8.94 - 39.5	0.1 - 1.0	13	0.1%	2.3%	[C25]
323.2 - 373.2	4.94 - 46.2	0.1 - 0.4	9	-2.0%	2.2%	[C26]
373.2 - 373.2	3.29 - 23.4	0.0 - 0.2	7	2.9%	2.9%	[C27]
288.2 - 298.2	61.61 - 246.4	1.4 - 1.8	27	-0.6%	0.6%	[C28]
323.2 - 353.1	41.04 - 143.0	0.4 - 1.2	29	-0.9%	0.9%	[C29]

Table H 3 Carbon Dioxide data sources from Diamond, et al. [1]

[C2] Caroll, et al. (1991) [13] Zawisza, A. and B. Malesinska, Journal of Chemical and Engineering Data, 1981

[C3] Crovetto (1991)

[3] Nighswander, JA; J. Chem. Eng. Data., 1989,34,355-360, co2+h2o

[2] Takenouchi, 1940

[C6] S.V. Wroblewski, Ann. Phys. Chem. 18 (1883) 290–308.

[C7] G.K. Anderson, J. Chem. Eng. Data 47 (2002) 219–222.

[C8] W. Sander, Z. Phys. Chem., Stoechiom. Verwandtschaftsl. 78 (1912) 513–549.

[C9] R. Vilcu, I. Gainar, Revue Romaine de Chimie 12 (1967) 181–189.

[C10] I.R. Kritschewsky, N.M. Shaworonkoff, V.A. Aepelbaum, Z. Phys. Chem. A 175 (1935) 232–238.

[C11] P.C. Gillespie, G.M. Wilson, Vapor–liquid and liquid–liquid equilibria: water–methane, water–carbon dioxide, water–hydrogen sulfide, water–n-pentane, water–methane–n-pentane, Gas Processors Association, Tulsa, Research Report RR48,

[C12] O. Hähnel, Centr. Min. Geol. 25 (1920) 25–32.

[C13] P.B. Stewart, P. Munjal, J. Chem. Eng. Data 15 (1970) 67–71.

[C14] P. Servio, P. Englezos, Fluid Phase Equilib. 190 (2001) 127–134.

[C15] S.D. Cramer, The solubility of methane, carbon dioxide, and oxygen in brines from 0 to 300 ?C, US Bureau of Mines Report of Investigations, vol. 8706, 1982.

[C16] H. Teng, A. Yamasaki, M.-K. Chun, H. Lee, J. Chem. Thermodyn. 29 (1997) 1301–1310.

[C17] R.A. Shagiakhmetov, A.A. Tarzimanov, Deposited Document SPSTL 200 khp—D 81—1982 (1981).

[C18] P.M. Oleinik, Neftepromyslovoe Delo, vol. 8, p. 7 (in Russian), cited in [30].

[C19] S.O. Yang, I.M. Yang, Y.S. Kim, C.S. Lee, Fluid Phase Equilib. 175 (2000) 75–89.

[C20] Y.D. Zel'vinskii, Zhurn. Khim. Prom. 14 (1937) 1250–1257 (in Russian).

[C21] S.D. Malinin, N.I. Savelyeva, Geochem. Int. 9 (1972) 410–418.

[C22] S.D. Malinin, N.A. Kurovskaya, Geochem. Int. 12 (1975) 199–201.

[C23] R. Wiebe, V.L. Gaddy, J. Am. Chem. Soc. 62 (1940) 815–817.
R. Wiebe, V.L. Gaddy, J. Am. Chem. Soc. 61 (1939) 315–318.

[C24] E. Bartholomé, H. Friz, Chem. Ing. Tech. 28 (1956) 706–708.

[C25] J. Matous, J. Sobr, J.P. Novak, J. Pick, Collect. Czech. Chem. Commun. 34 (1969) 3982–3985.

[C26] A. Zawisza, B. Malesinska, J. Chem. Eng. Data 26 (1981) 388–391.

[C27] G. Müller, E. Bender, G. Maurer, Ber. Bunsenges. Phys. Chem. 92 (1988) 148–160.

[C28] M.B. King, A. Mubarak, J.D. Kim, T.R. Bott, J. Supercritical Fluids 5 (1992) 296–302.

[C29] A. Bamberger, G. Sieder, G. Maurer, J. Supercritical Fluids 17 (2000) 97–110.

SO$_2$ SUMMARY RESULTS

Table H 4. Sulfur Dioxide Data [4-6]

T (K)	P (Bar)	SO$_2$ (mol/kg)	Pts	BIAS	AAPD	REF
293.1 - 393.3	0.4 - 25.1	0.2 - 5.6	66	1.9%	5.6%	[4]
283.2 - 363.2	1.0 - 1.3	0.3 - 2.4	42	-7.1%	18.3%	[5]
273.0 - 300.2	0.6 - 3.4	1.4 - 4.7	25	-1.4%	1.4%	[6]

Table H 5. Sulfur Dioxide Data – Isotherms [4]

T (K)	P (Bar)	SO$_2$ (mol/kg)	Pts	BIAS	AAPD
293.1 - 293.2	0.4 - 3.1	0.6 - 5.2	7	-0.4%	12.4%
313.1 - 313.3	0.5 - 4.6	0.4 - 4.0	11	6.6%	9.2%
333.2 - 333.2	1.4 - 8.1	0.6 - 4.5	9	3.1%	5.6%
343.1 - 343.2	0.9 - 11.1	0.2 - 5.3	12	3.3%	4.7%
363.2 - 363.2	1.8 - 16.4	0.3 - 5.6	9	1.4%	2.4%
393.1 - 393.3	3.4 - 25.1	0.2 - 5.3	18	-1.3%	3.0%

H$_2$S SUMMARY RESULTS

Table H 6. All Hydrogen Sulfide Data Points [7]

T (K)	P (Bar)	H$_2$S (mol/kg)		Pts	BIAS	AAPD
273.2 - 588.7	0.4 - 206.8	0.02 - 10.47	P$_{TOT}$	492	-1.4%	3.0%
			pp H$_2$S	167	-14.7%	19.9%
			pp H$_2$O	162	97.9%	116.9%

Table H 7. Hydrogen Sulfide Total Pressure Data [7]

T (K)	P (Bar)	H$_2$S (mol/kg)	Pts	BIAS	AAPD
283.2 - 453.2	1.5 - 66.7	0.02 - 2.28	325	-1.2%	1.3%

Table H 8. Hydrogen Sulfide Total Pressure Data – Isotherms [7]

T (K)	P (Bar)	H_2S (mol/kg)	Pts	BIAS	AAPD
283	1.5 - 3.6	0.23 - 0.50	9	0.1%	2.3%
293	1.7 - 13.6	0.18 - 1.44	16	-2.5%	2.5%
303	2.1 - 22.7	0.18 - 1.89	28	-1.3%	1.3%
313	4.7 - 25.6	0.35 - 1.71	31	-1.2%	1.2%
323	7.2 - 28.9	0.44 - 1.61	30	-1.2%	1.2%
333	2.4 - 42.2	0.12 - 2.05	54	-1.2%	1.2%
344	3.7 - 51.3	0.16 - 2.15	30	-1.2%	1.2%
363	2.4 - 65.7	0.07 - 2.28	43	-1.2%	1.2%
393	5.0 - 66.7	0.09 - 1.97	34	-1.2%	1.2%
423	6.9 - 66.0	0.06 - 1.71	34	-1.0%	1.3%
453	10.7 - 59.2	0.02 - 1.28	16	-0.7%	1.0%

Table H 9. Hydrogen Sulfide Partial Pressure Data [7]

T (K)	P (Bar)	H_2S (mol/kg)		Pts	BIAS	AAPD
273.2 - 588.7	0.4 - 206.8	0.03 - 10.47	P_{TOT}	167	-1.8%	6.4%
			pp H_2S	167	-14.7%	19.9%
			pp H_2O	162	97.9%	116.9%

Table H 10. Hydrogen Sulfide Partial Pressure Data – Isotherms [7]

T (K)	P (Bar)	H_2S (mol/kg)		Pts	BIAS	AAPD
273	0.5 - 0.8	0.11 - 0.17	P_{TOT}	3	34.3%	34.3%
			pp H_2S	3	36.7%	36.7%
			pp H_2O	3	-29.3%	29.3%
278	0.4 - 1.6	0.06 - 0.27	P_{TOT}	8	20.6%	20.9%
			pp H_2S	8	23.5%	23.5%
			pp H_2O	8	-36.5%	36.5%
283	0.4 - 2.8	0.06 - 0.41	P_{TOT}	10	8.6%	9.6%
			pp H_2S	10	10.7%	10.7%
			pp H_2O	10	-24.7%	24.7%
288	0.4 - 3.0	0.06 - 0.39	P_{TOT}	9	1.2%	2.0%
			pp H_2S	9	3.1%	3.1%
			pp H_2O	9	-22.5%	22.5%
293	0.5 - 3.3	0.06 - 0.36	P_{TOT}	10	-3.6%	3.6%
			pp H_2S	10	-1.9%	2.3%
			pp H_2O	10	-17.5%	17.5%
298	0.5 - 3.5	0.05 - 0.35	P_{TOT}	15	-10.0%	10.0%
			pp H_2S	15	-8.3%	8.4%
			pp H_2O	15	-19.0%	19.0%
303	0.6 - 3.7	0.05 - 0.32	P_{TOT}	9	-8.8%	8.8%
			pp H_2S	9	-7.4%	7.4%
			pp H_2O	9	-10.5%	10.9%
311	3.4 - 24.8	0.25 - 1.75	P_{TOT}	10	-1.3%	1.3%
			pp H_2S	10	-0.1%	0.1%
			pp H_2O	6	9.6%	9.6%
313	0.5 - 4.1	0.03 - 0.30	P_{TOT}	9	-16.1%	16.1%
			pp H_2S	9	-15.6%	15.6%
			pp H_2O	9	-4.5%	18.6%
323	0.6 - 4.5	0.03 - 0.27	P_{TOT}	9	-16.2%	16.2%
			pp H_2S	9	-17.6%	17.6%
			pp H_2O	9	10.6%	26.8%

Table H 10. Hydrogen Sulfide Partial Pressure Data - Isotherms (Cont'd) [7]

T (K)	P (Bar)	H_2S (mol/kg)		Pts	BIAS	AAPD
333	0.9 - 4.9	0.04 - 0.23	P_{TOT}	6	-6.8%	6.8%
			pp H_2S	6	-9.7%	9.7%
			pp H_2O	6	38.9%	43.8%
344	6.9 - 48.2	0.28 - 2.10	P_{TOT}	9	-1.2%	1.2%
			pp H_2S	9	-1.6%	1.6%
			pp H_2O	9	64.0%	64.0%
366	8.3 - 74.4	0.27 - 2.39	P_{TOT}	5	-1.2%	1.2%
			pp H_2S	5	-5.2%	5.2%
			pp H_2O	4	114.4%	114.4%
378	13.8 - 206.8	0.43 - 10.47	P_{TOT}	13	-0.9%	0.9%
			pp H_2S	13	-7.3%	7.3%
			pp H_2O	13	171.5%	171.5%
411	13.8 - 206.8	0.32 - 6.91	P_{TOT}	13	-0.2%	1.1%
			pp H_2S	13	-39.7%	39.7%
			pp H_2O	13	483.3%	483.3%
422	31.0 - 206.8	0.73 - 4.22	P_{TOT}	3	-0.5%	0.6%
			pp H_2S	3	-68.6%	68.6%
			pp H_2O	3	634.9%	634.9%
444	13.8 - 206.8	0.16 - 6.34	P_{TOT}	13	-0.6%	0.7%
			pp H_2S	13	-57.0%	57.0%
			pp H_2O	13	349.5%	349.5%
478	31.0 - 206.8	0.36 - 5.98	P_{TOT}	6	-0.6%	0.7%
			pp H_2S	6	-55.3%	55.3%
			pp H_2O	6	170.3%	170.3%
533	55.1 - 206.8	0.25 - 5.76	P_{TOT}	3	-1.1%	1.1%
			pp H_2S	3	-58.1%	58.1%
			pp H_2O	3	52.2%	52.2%
589	137.9 - 206.8	0.57 - 4.36	P_{TOT}	4	-1.0%	1.0%
			pp H_2S	4	-52.9%	52.9%
			pp H_2O	4	18.3%	18.3%

Table H 11. Phenol System Pressure Data [8]

T(K)	P (Bar)	C_6H_5OH (mol/kg)	Pts	BIAS	AAPD
317.55	0.012 - 0.094	0.3 - 1053.2	13	-1.0%	2.8%

Table H 12. Hydrogen Cyanide System Pressure Data [9]

T(K)	P (Bar)	HCN (mol/kg)	Pts	BIAS	AAPD
313.13 - 413.14	0.3 - 4.8	0.2 - 6.6	49	-1.7%	8.1%

Table H 13. Hydrogen Cyanide System Pressure Data - Isotherms [9]

T(K)	P (Bar)	HCN (mol/kg)	Pts	BIAS	AAPD
313	0.3 - 0.8	1.1 - 5.8	6	-8.2%	20.6%
333	0.4 - 1.2	0.7 - 4.1	7	-0.9%	11.9%
353	1.0 - 2.1	1.0 - 4.5	10	-6.9%	8.1%
373	1.2 - 3.9	0.2 - 6.6	12	0.0%	4.7%
393	2.3 - 4.8	0.4 - 3.8	11	2.3%	3.3%
413	4.0 - 4.7	0.3 - 0.9	3	4.8%	4.8%

NH$_3$ SUMMARY RESULTS

Table H 14. Ammonia in Regression Calculations [10]

T (K)	P (Bar)	NH$_3$		NPTS	BIAS	AAD
313.2 - 588.7	1.5 - 217.8	0.008 - 0.929	P_{TOT}	74	-0.5%	1.9%
			ppNH$_3$	74	-3.0%	5.6%
			ppH$_2$O	72	1.9%	6.4%

Table H 15. Ammonia in Regression Calculations [10] - Isotherms

T (K)	P (Bar)	NH$_3$		NPTS	BIAS	AAD
313.15	1.5 - 14.1	0.293 - 0.885	P$_{TOT}$	6	-0.7%	4.1%
			ppNH$_3$	6	0.8%	3.6%
			ppH$_2$O	6	11.8%	17.1%
333.15	3.1 - 23.8	0.295 - 0.906	P$_{TOT}$	6	-0.9%	3.5%
			ppNH$_3$	6	0.5%	2.9%
			ppH$_2$O	6	1.6%	4.6%
353.15	5.8 - 38.1	0.310 - 0.929	P$_{TOT}$	9	-0.6%	2.7%
			ppNH$_3$	9	0.8%	1.8%
			ppH$_2$O	9	-0.3%	1.8%
394.3	3.1 - 54.5	0.044 - 0.683	P$_{TOT}$	5	-0.3%	3.1%
			ppNH$_3$	5	1.0%	3.5%
			ppH$_2$O	5	-1.2%	1.6%
405.9	4.3 - 96.2	0.045 - 0.920	P$_{TOT}$	6	-0.5%	1.3%
			ppNH$_3$	6	2.1%	2.4%
			ppH$_2$O	6	-4.6%	4.7%
449.8	12.5 - 171.9	0.047 - 0.892	P$_{TOT}$	10	0.4%	1.0%
			ppNH$_3$	10	0.5%	2.8%
			ppH$_2$O	9	-3.2%	14.0%
519.3	37.8 - 217.8	0.011 - 0.658	P$_{TOT}$	20	-0.2%	1.0%
			ppNH$_3$	20	-4.3%	4.3%
			ppH$_2$O	20	5.4%	5.5%
588.7	107.8 - 206.8	0.008 - 0.317	P$_{TOT}$	12	-1.3%	1.3%
			ppNH$_3$	12	-14.2%	17.8%
			ppH$_2$O	11	1.4%	3.6%

Table H 16. Ammonia Predictions [10]

T (K)	P (Bar)	NH$_3$		NPTS	BIAS	AAD
313.2 - 588.7	0.1 - 217.8	0.008 - 0.989	P$_{TOT}$	219	-0.9%	3.3%
			ppNH$_3$	219	-0.6%	4.6%
			ppH$_2$O	215	-0.2%	6.3%

Table H 17. Ammonia Predictions [10] - Isotherms

T (K)	P (Bar)	NH₃		NPTS	BIAS	AAD
313.15	0.1 - 14.8	0.016 - 0.949	P_{TOT}	30	0.2%	7.8%
			$ppNH_3$	30	3.1%	7.4%
			ppH_2O	30	3.1%	11.7%
333.15	0.3 - 24.4	0.016 - 0.947	P_{TOT}	30	-1.0%	5.3%
			$ppNH_3$	30	0.9%	5.0%
			ppH_2O	30	1.0%	6.1%
353.15	0.6 - 40.7	0.011 - 0.989	P_{TOT}	35	-0.7%	3.6%
			$ppNH_3$	35	1.2%	3.2%
			ppH_2O	35	0.0%	5.2%
394.3	2.3 - 92.0	0.009 - 0.987	P_{TOT}	31	-1.5%	2.5%
			$ppNH_3$	31	-0.8%	3.1%
			ppH_2O	31	-4.9%	5.1%
405.9	3.1 - 110.2	0.010 - 0.983	P_{TOT}	32	-0.9%	1.2%
			$ppNH_3$	32	1.0%	1.6%
			ppH_2O	30	-4.5%	4.8%
449.8	9.6 - 171.9	0.010 - 0.892	P_{TOT}	29	-1.5%	2.2%
			$ppNH_3$	29	-1.9%	3.0%
			ppH_2O	28	-0.5%	6.9%
519.3	37.8 - 217.8	0.011 - 0.658	P_{TOT}	20	-0.2%	1.0%
			$ppNH_3$	20	-4.3%	4.3%
			ppH_2O	20	5.4%	5.5%
588.7	107.8 - 206.8	0.008 - 0.317	P_{TOT}	12	-1.3%	1.3%
			$ppNH_3$	12	-14.2%	17.8%
			ppH_2O	11	1.4%	3.6%

Table H 18. Ammonia Predictions [10]

T (K)	P (Bar)	NH₃		NPTS	BIAS	AAD
303.2 - 422.8	0.2 - 138.5	0.011 - 0.993	P_{TOT}	186	-3.7%	5.7%
			$ppNH_3$	174	5.0%	8.4%
			ppH_2O	186	-26.0%	27.3%

Table H 19. Ammonia Predictions [10] - Temperature Ranges

T (K)	P (Bar)	NH_3		NPTS	BIAS	AAD
303.2 - 309.0	0.2 - 12.3	0.034 - 0.909	P_{TOT}	14	-20.1%	21.1%
			$ppNH_3$	13	-13.3%	15.8%
			ppH_2O	14	-50.1%	50.1%
339.5 - 344.8	0.9 - 28.8	0.062 - 0.956	P_{TOT}	22	-3.6%	8.8%
			$ppNH_3$	22	5.2%	8.1%
			ppH_2O	22	-28.9%	29.6%
359.5 - 359.8	1.2 - 45.2	0.037 - 0.971	P_{TOT}	19	-2.0%	4.6%
			$ppNH_3$	19	13.9%	14.5%
			ppH_2O	19	-32.3%	32.3%
372.2 - 377.2	1.2 - 52.4	0.014 - 0.766	P_{TOT}	34	-3.7%	5.4%
			$ppNH_3$	28	4.0%	4.6%
			ppH_2O	34	-25.5%	25.9%
381.5 - 382.3	1.8 - 67.5	0.017 - 0.946	P_{TOT}	30	-1.8%	3.4%
			$ppNH_3$	30	10.3%	10.6%
			ppH_2O	30	-17.1%	17.1%
399.0 - 405.8	3.6 - 111.9	0.011 - 0.993	P_{TOT}	30	-1.5%	3.7%
			$ppNH_3$	25	1.0%	4.9%
			ppH_2O	30	-26.1%	29.7%
411.2 - 412.3	4.3 - 124.7	0.023 - 0.972	P_{TOT}	20	-2.0%	2.7%
			$ppNH_3$	20	6.5%	6.8%
			ppH_2O	20	-21.3%	21.3%
421.7 - 422.8	5.6 - 138.5	0.019 - 0.936	P_{TOT}	17	-0.8%	2.3%
			$ppNH_3$	17	5.7%	5.8%
			ppH_2O	17	-17.8%	24.1%

Table H 20. Ammonia Predictions [10]

T (K)	P (Bar)	NH_3		NPTS	BIAS	AAD
446.1 - 618.8	11.1 - 225.2	0.008 - 0.883	P_{TOT}	168	-1.4%	2.1%
			$ppNH_3$	132	0.1%	6.2%
			ppH_2O	168	-8.8%	15.2%

Table H 21. Ammonia Predictions [10] - Temperature Ranges

T (K)	P (Bar)	NH$_3$		NPTS	BIAS	AAD
446.1 - 453.1	11.1 - 160.5	0.017 - 0.883	P$_{TOT}$	28	-0.3%	2.5%
			ppNH$_3$	20	-2.6%	4.8%
			ppH$_2$O	28	-24.1%	29.5%
480.7 - 484.7	20.4 - 190.0	0.014 - 0.748	P$_{TOT}$	44	-2.2%	2.8%
			ppNH$_3$	35	-0.2%	3.5%
			ppH$_2$O	44	-10.1%	21.4%
503.1 - 503.1	40.6 - 71.7	0.076 - 0.238	P$_{TOT}$	5	-0.2%	1.4%
			ppNH$_3$	2	-6.3%	6.3%
			ppH$_2$O	5	-22.1%	28.7%
523.9 - 527.1	42.5 - 214.2	0.016 - 0.570	P$_{TOT}$	33	-2.0%	2.5%
			ppNH$_3$	29	0.4%	3.1%
			ppH$_2$O	33	-5.0%	10.9%
577.8 - 583.8	98.2 - 223.9	0.017 - 0.387	P$_{TOT}$	23	-1.5%	1.6%
			ppNH$_3$	21	5.2%	8.5%
			ppH$_2$O	23	-2.2%	4.5%
607.8 - 618.8	143.2 - 225.2	0.008 - 0.244	P$_{TOT}$	35	-0.8%	1.0%
			ppNH$_3$	25	-1.6%	12.6%
			ppH$_2$O	35	-1.2%	5.1%

MODEL PREDICTIONS IN SALT MIXTURES

Table H 22. Carbon Dioxide in Aqueous NaCl Mixtures [11]

T(K)	NaCl (mol/kg)	CO_2 (mol/kg)	P (Bar)	Pts	Bias	AAPD	REF
423	1.1	0.62 - 2.10	100 - 1400	10	-1.0%	1.0%	[11]
473	1.1	0.62 - 2.90	100 - 1400	10	-0.9%	0.9%	
523	1.1	0.59 - 4.95	100 - 1400	10	-1.0%	1.0%	
573	1.1	0.22 - 8.19	100 - 1400	10	-1.0%	1.0%	
623	1.1	0.80 - 12.46	200 - 1400	9	-1.1%	1.1%	
				49	-1.0%	1.0%	
423	4.3	0.26 - 1.59	100 - 1400	10	-0.9%	0.9%	[11]
523	4.3	0.29 - 2.54	100 - 1400	10	-1.1%	1.1%	
623	4.3	0.32 - 3.87	200 - 1400	9	-1.2%	1.2%	
				29	-1.1%	1.1%	
				78	-1.0%	1.0%	[11]

Table H 23. Carbon Dioxide in Aqueous NaCl Mixtures [12]

T(K)	NaCl (mol/kg)	CO_2 (mol/kg)	P (Bar)	Pts	Bias	AAPD	REF
313	4	0.09 - 0.51	9.11 - 69.17	5	-0.7%	1.1%	[12]
333	4	0.05 - 0.49	6.25 - 96.42	9	-0.4%	1.2%	
353	4	0.05 - 0.43	8.17 - 96.37	7	-0.6%	0.7%	
393	4	0.05 - 0.34	12.04 - 93.28	5	-0.4%	0.9%	
413	4	0.05 - 0.31	13.93 - 86.71	4	0.0%	1.1%	
433	4	0.05 - 0.30	16.62 - 90.48	4	0.7%	0.8%	
				34	-0.3%	1.0%	
313	6	0.05 - 0.42	6.02 - 84.27	6	-0.6%	1.2%	[12]
333	6	0.05 - 0.36	8.20 - 86.70	5	-0.5%	0.7%	
353	6	0.05 - 0.32	9.97 - 90.44	5	-0.8%	0.8%	
				16	-0.6%	0.9%	
				50	-0.4%	0.9%	[12]

Table H 24. Carbon Dioxide in Aqueous NaCl Mixtures [3]

T(K)	NaCl (mol/kg)	CO_2 (mol/kg)	P (Bar)	Pts	Bias	AAPD	REF
353	0.2	0.41 - 0.87	40.4 - 99.4	8	-1.2%	1.2%	[3]
393	0.2	0.16 - 0.78	21.1 - 100.3	10	-2.0%	2.0%	
433	0.2	0.16 - 0.77	21.5 - 99.7	9	-1.2%	1.2%	
473	0.2	0.26 - 0.74	41.2 - 99.3	7	-1.6%	1.6%	
				34	-1.5%	1.5%	

Table H 25. Carbon Dioxide in Aqueous $CaCl_2$ Mixtures [13]

T(K)	$CaCl_2$ (mol/kg)	CO_2 (mol/kg)	P (Bar)	Pts	Bias	AAPD	REF
374	0	0.61 - 1.61	57.76 - 623.15	14	-1.1%	1.1%	[13]
393	0	0.21 - 1.72	23.30 - 703.20	12	-1.2%	1.2%	
				26	-1.2%	1.2%	
349	1	0.14 - 1.09	16.21 - 628.21	12	-0.8%	0.8%	[13]
374	1	0.12 - 1.05	17.23 - 626.19	16	-0.9%	0.9%	
393-4	1	0.15 - 1.25	21.28 - 885.58	27	-0.8%	0.8%	
				55	-0.8%	0.8%	
349	2.3	0.12 - 0.66	22.29 - 607.95	12	-0.5%	0.7%	[13]
374	2.3	0.09 - 0.69	23.30 - 656.59	13	-0.6%	0.8%	
394	2.3	0.09 - 0.66	25.33 - 667.73	14	-0.7%	0.9%	
				39	-0.6%	0.8%	
349	3.9	0.05 - 0.39	15.20 - 633.28	13	-0.7%	0.7%	[13]
374	3.9	0.17 - 0.40	74.98 - 638.35	12	-0.5%	0.9%	
394	3.9	0.17 - 0.41	84.10 - 673.81	11	-0.7%	0.8%	
				36	-0.6%	0.8%	
				130	-0.7%	0.8%	[13]

Table H 26. Carbon Dioxide in Aqueous Na_2SO_4 Mixtures [14]

T(K)	Na_2SO_4 (mol/kg)	CO_2 (mol/kg)	P (Bar)	Pts	Bias	AAPD	REF
313	1	0.05 - 0.67	4.2 - 78.5	8	-1.7%	2.2%	[14]
323	1	0.05 - 0.60	5.1 - 83.2	9	-0.3%	1.8%	
333	1	0.05 - 0.57	5.6 - 89.8	12	-0.7%	0.7%	
353	1	0.05 - 0.49	7.2 - 93.6	9	-0.5%	0.8%	
393	1	0.05 - 0.43	10.2 - 93.7	9	-0.4%	0.7%	
413	1	0.05 - 0.43	12.1 - 97.1	8	0.2%	0.8%	
433	1	0.05 - 0.40	15.7 - 90.5	8	0.8%	0.9%	
				63	-0.4%	1.1%	
313	2	0.05 - 0.38	7.3 - 74.2	6	-1.1%	1.7%	[14]
333	2	0.05 - 0.33	9.5 - 80.8	7	-0.4%	0.5%	
353	2	0.05 - 0.30	11.4 - 87.8	6	-0.7%	0.7%	
393	2	0.05 - 0.28	14.9 - 88.6	7	-0.4%	0.7%	
413	2	0.05 - 0.28	16.6 - 90.9	6	0.1%	0.8%	
433	2	0.05 - 0.28	19.0 - 91.9	7	0.9%	1.1%	
				39	-0.3%	0.9%	[14]
				102	-0.3%	1.0%	[14]

Table H 27. Carbon Dioxide in Aqueous Na_2SO_4 Mixtures [15]

T(K)	Na_2SO_4 (mol/kg)	CO_2 (mol/kg)	P (Bar)	Pts	Bias	AAPD	REF
323	2	0.33 - 0.35	95.6 - 145.1	2	-1.2%	1.2%	[15]
	2.7	0.19 - 0.26	76.6 - 137.6	2	-1.2%	1.2%	
	3.2	0.04 - 0.23	16.4 - 160.0	5	-1.2%	1.2%	
				9	-1.2%	1.2%	
348	1	0.25 - 0.52	37.9 - 97.9	3	-1.2%	1.2%	[15]
	2	0.14 - 0.37	43.1 - 132.7	3	-1.2%	1.2%	
	3	0.05 - 0.27	19.0 - 197.3	9	-1.2%	1.2%	
				15	-1.2%	1.2%	
				24	-1.2%	1.2%	[15]

Table H 28. Carbon Dioxide in Aqueous Na_2SO_4 Mixtures [16]

T(K)	Na_2SO_4 (mol/kg)	CO_2 (mol/kg)	P (Bar)	Pts	Bias	AAPD	REF
288	0.29 - 1.06	0.02 - 0.03	1.01 - 1.01	5	-7.4%	7.4%	[16]
298	0.21 - 2.21	0.01 - 0.03	1.01 - 1.01	14	-14.2%	14.2%	
308	0.22 - 1.76	0.01 - 0.02	1.01 - 1.01	7	-10.6%	10.6%	
				26	-11.9%	11.9%	

Table H 29. Carbon Dioxide in Aqueous $(NH_4)_2SO_4$ Mixtures [14]

T(K)	$(NH_4)_2SO_4$ (mol/kg)	CO_2 (mol/kg)	P (Bar)	Pts	Bias	AAPD	REF
313	2	0.08 - 0.73	6.3 - 89.7	8	-0.4%	1.0%	[14]
333	2	0.05 - 0.60	5.2 - 93.5	8	-0.6%	0.8%	
353	2	0.05 - 0.50	7.1 - 93.4	7	-0.6%	0.7%	
393	2	0.05 - 0.39	10.6 - 88.5	10	-0.2%	1.2%	
413	2	0.05 - 0.40	12.9 - 98.7	8	0.5%	0.8%	
433	2	0.05 - 0.38	15.9 - 97.5	8	1.0%	1.0%	
				49	-0.1%	0.9%	
313	4	0.06 - 0.55	7.1 - 89.7	7	-1.8%	2.3%	[14]
333	4	0.06 - 0.45	8.0 - 93.9	6	-1.4%	1.6%	
353	4	0.05 - 0.38	8.8 - 95.1	7	-0.7%	0.7%	
393	4	0.05 - 0.30	13.6 - 97.6	6	-0.6%	0.7%	
413	4	0.05 - 0.24	16.3 - 82.9	5	0.5%	1.4%	
				31	-0.9%	1.3%	
				80	-0.4%	1.1%	[14]

Table H 30. Carbon Dioxide in Aqueous $(NH_4)_2SO_4$ Mixtures [16]

T(K)	$(NH_4)_2SO_4$ (mol/kg)	CO_2 (mol/kg)	P (Bar)	Pts	Bias	AAPD	REF
288	0.32 - 3.35	0.01 - 0.04	1.01 - 1.01	9	-11.5%	11.5%	[16]
298	0.25 - 3.36	0.01 - 0.03	1.01 - 1.01	11	-11.0%	11.0%	
308	0.28 - 3.87	0.01 - 0.02	1.01 - 1.01	11	-10.2%	10.2%	
				31	-10.9%	10.9%	

Carbon Dioxide in Aqueous Na_2SO_4 + $(NH_4)_2SO_4$ Mixtures [14]

T(K)	Na_2SO_4 + $(NH_4)_2SO_4$ (mol/kg)	CO_2 (mol/kg)	P (Bar)	Pts	Bias	AAPD	REF
313	1+1	0.05 - 0.53	7.0 - 82.6	6	-1.8%	2.1%	[14]
333	1+1	0.05 - 0.47	7.0 - 96.7	7	-0.5%	0.9%	
353	1+1	0.05 - 0.37	9.4 - 81.4	5	-0.9%	0.9%	
393	1+1	0.05 - 0.31	13.0 - 82.6	4	-0.9%	0.9%	
413	1+1	0.05 - 0.32	15.3 - 89.9	6	0.4%	0.9%	
433	1+1	0.05 - 0.31	18.4 - 91.0	7	0.4%	0.6%	
				35	-0.5%	1.0%	

OTHER WEAK ELECTROLYTES AND SALT MIXTURES

Table H 32. Sulfur Dioxide in Aqueous Na_2SO_4 Mixtures [5, 17]

T (K)	Na_2SO_4	SO_2	P (Bar)	Pts	Bias	AAPD	REF
313	0.5	0.17 - 1.65	0.11 - 2.11	4	52.7%	53.7%	[5]
363	0.5	0.15 - 4.25	0.89 - 15.6	9	10.3%	11.6%	
393	0.5	0.30 - 5.19	3.53 - 27.7	13	1.5%	5.0%	
				26	12.4%	14.7%	
313	1.0	0.37 - 3.92	0.38 - 5.24	7	9.6%	15.3%	
333	1.0	0.19 - 4.03	0.38 - 8.92	6	15.2%	18.6%	
363	1.0	0.06 - 4.66	0.65 - 17.8	12	8.6%	10.8%	
393	1.0	0.15 - 5.80	2.15 - 32.8	14	1.5%	4.2%	
				39	7.2%	10.4%	
				65	9.3%	12.2%	

T (K)	Na_2SO_4	SO_2	P (Bar)	Pts	Bias	AAPD	REF
293	0.30 - 2.80	1.44 - 1.66	1.01 - 1.01	6	1.5%	3.7%	[17]
303	0.30 - 2.80	1.09 - 1.21	1.01 - 1.01	6	15.5%	15.5%	
313	0.40 - 2.80	0.88 - 0.93	1.01 - 1.01	6	26.5%	26.5%	
323	0.40 - 2.80	0.07 - 0.74	1.01 - 1.01	5	30.8%	32.2%	
				23	18.0%	18.9%	

Table H 33. Hydrogen Sulfide in Aqueous NaCl Mixtures [18]

T (K)	NaCl	H_2S	P (Bar)	Pts	Bias	AAPD	REF
299 - 368	1.0	0.01 - 0.08	1.01 - 1.01	31	-1.0%	4.7%	[18]
299 - 369	2.0	0.01 - 0.07	1.01 - 1.01	22	-2.5%	4.5%	
297 - 370	3.0	0.01 - 0.07	1.01 - 1.01	79	-1.3%	4.3%	
296 - 369	4.0	0.01 - 0.06	1.01 - 1.01	79	-0.3%	4.1%	
297 - 368	5.0	0.01 - 0.06	1.01 - 1.01	27	-1.8%	5.2%	
				238	-1.1%	4.4%	

Table H 34. Ammonia in Aqueous Na_2SO_4 and $(NH_4)_2SO_4$ Mixtures [19, 20]

T (K)	Na_2SO_4	NH_3	P (Bar)	Pts	Bias	AAPD	REF
333	1.0	1.73 - 16.13	0.44 - 2.02	10	-1.1%	1.1%	[19]
353	1.0	1.87 - 17.15	0.94 - 3.96	19	-1.1%	1.1%	
393	1.0	1.87 - 18.22	3.00 - 11.68	15	-1.2%	1.2%	
413	1.0	1.50 - 7.96	4.82 - 10.37	5	-1.2%	1.2%	
				49	-1.1%	1.1%	

T (K)	$(NH_4)_2SO_4$	NH_3	P (Bar)	Pts	Bias	AAPD	REF
303 - 319	0.4	6.1	0.22 - 0.47	9	-10.4%	10.4%	[20]
299 - 319	0.4	9.5	0.29 - 0.66	10	5.3%	5.3%	
301 - 320	0.4	10.3	0.43 - 0.89	14	-14.8%	14.8%	
				33			

T (K)	$(NH_4)_2SO_4$	NH_3	P (Bar)	Pts	Bias	AAPD	REF
333	1.0	2.28 - 23.67	0.52 - 3.64	10	-20.2%	20.2%	[19]
333	3.9	1.42 - 5.46	0.52 - 1.27	3	-33.9%	33.9%	
353	1.0	1.85 - 17.61	0.91 - 4.56	10	-18.1%	18.1%	
393	1.0	2.30 - 22.18	3.53 - 16.00	10	-5.0%	5.0%	
413	1.0	3.03 - 17.15	6.40 - 19.42	5	-2.5%	2.5%	
433	1.0	1.09 - 16.19	7.30 - 26.72	11	-2.7%	3.5%	
				49	-11.8%	11.9%	

AQUEOUS MULTICOMPONENT GAS AND SALT MIXTURES

Table H 35. Aqueous Carbon Dioxide - Ammonia Mixtures [21]

T (K)	P (Bar)	mNH_3	mCO_2		Pts	BIAS	AAD
333.15 - 393.15	0.78 - 70.27	0.5 - 16.5	0.2 - 13.0	P_{TOT}	541	2.3%	4.4%
				$ppNH_3$	350	4.4%	6.1%
				$ppCO_2$	505	-0.2%	7.3%
				ppH_2O	541	-0.3%	7.1%

Table H 36. Aqueous Carbon Dioxide - Ammonia Mixture Isotherms [21]

T (K)	P (Bar)	mNH_3	mCO_2		Pts	BIAS	AAD
333.15	0.78 - 68.18	0.7 - 11.8	0.6 - 12.7	P_{TOT}	77	0.7%	3.3%
				$ppNH_3$	10	13.0%	13.7%
				$ppCO_2$	77	-5.9%	9.4%
373.15	1.80 - 69.23	1.0 - 14.3	0.4 - 10.4	P_{TOT}	127	2.7%	5.0%
				$ppNH_3$	108	3.0%	5.4%
				$ppCO_2$	108	1.5%	6.2%
393.15	2.84 - 49.96	0.7 - 12.0	0.2 - 7.4	P_{TOT}	62	2.2%	3.8%
				$ppNH_3$	57	3.6%	4.6%
				$ppCO_2$	60	2.6%	5.2%
353.15	0.98 - 70.27	0.6 - 12.2	0.4 - 11.4	P_{TOT}	93	1.4%	3.6%
				$ppNH_3$	34	7.1%	7.7%
				$ppCO_2$	93	-3.0%	8.4%
360.15	1.15 - 70.15	0.5 - 16.5	0.2 - 13.0	P_{TOT}	182	3.1%	5.0%
				$ppNH_3$	141	4.6%	6.4%
				$ppCO_2$	167	1.9%	7.1%

Table H 37. Aqueous Carbon Dioxide - Ammonia Mixtures: Ammonia Concentration Ranges for 333 K [21]

T (K)	P (Bar)	mNH_3	mCO_2		NPTS	BIAS	AAD
333.15	0.78 - 44.19	0.7 - 0.7	0.6 - 1.3	P_{TOT}	12	-0.2%	1.2%
				$ppNH_3$			
				$ppCO_2$	12	-8.1%	8.1%
	1.43 - 44.97	1.0 - 1.1	0.8 - 1.6	P_{TOT}	11	-0.9%	1.7%
				$ppNH_3$	1	3.6%	3.6%
				$ppCO_2$	11	-7.9%	7.9%
	1.04 - 50.00	2.2 - 2.7	1.6 - 3.1	P_{TOT}	11	1.1%	3.4%
				$ppNH_3$	1	8.2%	8.2%
				$ppCO_2$	11	-6.0%	7.6%
	1.00 - 60.17	3.8 - 4.0	2.5 - 4.4	P_{TOT}	14	-1.5%	1.7%
				$ppNH_3$	1	2.6%	2.6%
				$ppCO_2$	14	-8.6%	8.9%
	1.00 - 60.15	8.1 - 8.1	4.8 - 8.5	P_{TOT}	14	1.7%	6.2%
				$ppNH_3$	3	18.8%	18.8%
				$ppCO_2$	14	-4.0%	12.1%
	1.02 - 68.18	11.7 - 11.8	6.6 - 12.7	P_{TOT}	15	3.2%	4.8%
				$ppNH_3$	4	16.6%	16.6%
				$ppCO_2$	15	-2.1%	11.0%

Table H 38. Aqueous Carbon Dioxide - Ammonia Mixtures: Ammonia Concentration Ranges for 353 K [21]

T (K)	P (Bar)	mNH_3	mCO_2		NPTS	BIAS	AAD
353.15	1.11 - 68.94	0.6 - 0.6	0.4 - 1.2	P_{TOT}	13	-0.2%	1.9%
				$ppNH_3$	2	-1.1%	1.3%
				$ppCO_2$	13	-6.7%	6.7%
	0.98 - 68.45	1.1 - 1.1	0.6 - 1.7	P_{TOT}	13	-1.8%	2.3%
				$ppNH_3$	1	-3.4%	3.4%
				$ppCO_2$	13	-8.8%	8.8%
	1.05 - 69.74	2.0 - 2.0	1.0 - 2.5	P_{TOT}	13	-1.5%	1.7%
				$ppNH_3$	2	-2.0%	2.3%
				$ppCO_2$	13	-7.9%	8.0%
	1.28 - 69.34	4.1 - 4.1	2.0 - 4.4	P_{TOT}	13	-0.7%	1.9%
				$ppNH_3$	5	2.4%	2.4%
				$ppCO_2$	13	-5.0%	6.8%
	1.83 - 70.27	5.9 - 5.9	3.1 - 5.9	P_{TOT}	15	3.6%	4.7%
				$ppNH_3$	9	8.2%	8.2%
				$ppCO_2$	15	1.4%	8.4%
	2.25 - 60.50	9.0 - 9.0	4.8 - 8.0	P_{TOT}	13	5.0%	5.9%
				$ppNH_3$	8	10.0%	10.0%
				$ppCO_2$	13	2.8%	9.4%
	1.58 - 69.65	12.2 - 12.2	5.1 - 11.4	P_{TOT}	13	5.3%	6.8%
				$ppNH_3$	7	12.5%	12.5%
				$ppCO_2$	13	2.5%	11.0%

Table H 39. Aqueous Carbon Dioxide - Ammonia Mixtures: Ammonia Concentration
Ranges for 360 K [21]

T (K)	P (Bar)	mNH$_3$	mCO$_2$		NPTS	BIAS	AAD
360.15	2.06 - 70.15	0.5 - 0.5	0.4 - 1.0	P$_{TOT}$	12	0.0%	2.2%
				ppNH$_3$	2	-1.5%	1.5%
				ppCO$_2$	12	-6.4%	6.4%
	1.16 - 68.22	0.9 - 1.8	0.5 - 2.2	P$_{TOT}$	29	-0.2%	1.8%
				ppNH$_3$	10	2.2%	3.4%
				ppCO$_2$	29	-4.8%	6.8%
	1.15 - 67.88	2.9 - 4.8	0.8 - 3.5	P$_{TOT}$	25	0.2%	3.1%
				ppNH$_3$	17	2.7%	4.3%
				ppCO$_2$	25	-1.3%	6.1%
	1.53 - 68.64	6.1 - 6.5	0.2 - 5.6	P$_{TOT}$	28	1.0%	4.1%
				ppNH$_3$	28	1.0%	4.9%
				ppCO$_2$	24	2.0%	4.9%
	1.67 - 11.10	7.7 - 7.8	0.8 - 5.3	P$_{TOT}$	13	4.4%	7.6%
				ppNH$_3$	13	4.4%	8.8%
				ppCO$_2$	11	6.7%	8.8%
	1.87 - 68.50	9.8 - 9.9	1.5 - 8.3	P$_{TOT}$	21	4.0%	5.9%
				ppNH$_3$	20	5.1%	6.8%
				ppCO$_2$	20	4.9%	7.0%
	2.13 - 68.55	12.3 - 12.5	1.3 - 10.0	P$_{TOT}$	22	5.5%	6.2%
				ppNH$_3$	22	5.5%	6.1%
				ppCO$_2$	19	6.3%	6.8%
	2.29 - 11.06	14.0 - 14.1	4.4 - 8.9	P$_{TOT}$	12	9.7%	9.7%
				ppNH$_3$	12	10.3%	10.3%
				ppCO$_2$	11	11.2%	11.2%
	2.54 - 56.59	16.0 - 16.5	0.9 - 13.0	P$_{TOT}$	20	7.9%	8.3%
				ppNH$_3$	17	8.4%	8.4%
				ppCO$_2$	16	6.1%	9.4%

Table H 40. Aqueous Carbon Dioxide - Ammonia Mixtures: Ammonia Concentration
Ranges for 373 K [21]

T (K)	P (Bar)	mNH_3	mCO_2		NPTS	BIAS	AAD
373.15	1.80 - 69.23	1.0 - 1.1	0.4 - 1.6	P_{TOT}	21	-1.0%	2.8%
				$ppNH_3$	11	0.7%	3.2%
				$ppCO_2$	21	-4.0%	6.0%
	1.88 - 49.78	1.9 - 2.0	0.6 - 2.1	P_{TOT}	12	-1.8%	2.8%
				$ppNH_3$	9	-0.3%	2.9%
				$ppCO_2$	12	-2.8%	4.7%
	1.91 - 53.81	3.9 - 4.0	0.5 - 3.7	P_{TOT}	18	-0.3%	3.6%
				$ppNH_3$	17	0.6%	4.8%
				$ppCO_2$	17	0.6%	4.7%
	2.71 - 58.37	7.8 - 8.2	0.4 - 6.5	P_{TOT}	33	4.1%	6.4%
				$ppNH_3$	32	3.7%	6.8%
				$ppCO_2$	27	4.3%	7.3%
	3.44 - 36.19	11.0 - 11.3	0.7 - 7.9	P_{TOT}	24	4.8%	5.1%
				$ppNH_3$	23	3.3%	4.3%
				$ppCO_2$	17	4.4%	5.1%
	3.87 - 69.05	14.0 - 14.3	0.8 - 10.4	P_{TOT}	19	7.2%	7.5%
				$ppNH_3$	16	6.9%	7.7%
				$ppCO_2$	14	5.4%	9.0%

Table H 41. Aqueous Carbon Dioxide - Ammonia Mixtures: Ammonia Concentration
Ranges for 393 K [21]

T (K)	P (Bar)	mNH_3	mCO_2		NPTS	BIAS	AAD
393.15	2.84 - 49.62	0.7 - 0.7	0.2 - 0.9	P_{TOT}	7	-3.8%	3.9%
				$ppNH_3$	4	-2.7%	3.7%
				$ppCO_2$	7	-6.3%	6.8%
	3.01 - 49.76	1.8 - 1.8	0.3 - 1.8	P_{TOT}	9	-0.8%	2.9%
				$ppNH_3$	7	0.8%	3.5%
				$ppCO_2$	9	-1.4%	4.8%
	3.74 - 49.91	3.8 - 3.9	0.6 - 3.0	P_{TOT}	9	1.8%	3.0%
				$ppNH_3$	9	3.1%	3.8%
				$ppCO_2$	9	3.1%	3.8%
	5.32 - 49.86	7.8 - 8.0	0.5 - 5.3	P_{TOT}	13	2.9%	3.1%
				$ppNH_3$	13	3.5%	3.5%
				$ppCO_2$	12	3.8%	3.8%
	6.08 - 39.27	9.7 - 10.0	0.5 - 6.1	P_{TOT}	14	5.7%	5.7%
				$ppNH_3$	14	6.4%	6.7%
				$ppCO_2$	13	7.1%	7.1%
	6.77 - 49.96	11.6 - 12.0	2.1 - 7.4	P_{TOT}	10	3.5%	3.5%
				$ppNH_3$	10	4.9%	4.9%
				$ppCO_2$	10	4.9%	4.9%

Table H 42. Aqueous Carbon Dioxide - Ammonia Mixtures [22]

T (K)	P (Bar)	mNH_3	mCO_2		Pts	BIAS	AAD
373.15 - 473.15	1.92 - 88.10	2.4 - 26.0	0.2 - 13.3	P_{TOT}	254	-0.2%	3.1%
				$ppNH_3$	254	1.1%	3.0%

Table H 43. Aqueous Carbon Dioxide - Ammonia Mixtures: Isotherms [22]

T (K)	P (Bar)	mNH_3	mCO_2		Pts	BIAS	AAD
373.15	1.92 - 9.36	3.8 - 26.0	0.3 - 13.3	P_{TOT}	61	0.8%	6.6%
				$ppNH_3$	61	2.1%	6.7%
393.15	3.28 - 27.33	2.8 - 25.9	0.2 - 12.7	P_{TOT}	42	0.8%	4.0%
				$ppNH_3$	42	2.1%	4.5%
413.15	5.78 - 46.60	2.5 - 25.3	0.2 - 11.6	P_{TOT}	72	-0.7%	1.7%
				$ppNH_3$	72	0.6%	1.6%
433.15	10.46 - 67.60	2.7 - 24.6	0.2 - 9.8	P_{TOT}	40	-1.1%	1.2%
				$ppNH_3$	40	0.2%	0.7%
453.15	16.53 - 79.50	2.5 - 12.7	0.2 - 3.8	P_{TOT}	23	-1.3%	1.4%
				$ppNH_3$	23	0.0%	0.9%
473.15	29.10 - 88.10	2.4 - 10.7	0.3 - 2.1	P_{TOT}	16	-1.0%	1.0%
				$ppNH_3$	16	0.3%	0.3%

Table H 44. Aqueous Carbon Dioxide - Ammonia Mixtures: Ammonia Concentration Ranges for 373 K [22]

T (K)	P (Bar)	mNH$_3$	mCO$_2$		Pts	BIAS	AAD
373.15	1.92 - 5.75	3.8 - 3.9	0.3 - 2.2	P$_{TOT}$	14	-5.0%	5.4%
				ppNH$_3$	14	-3.7%	4.8%
	2.38 - 7.37	5.6 - 6.4	0.4 - 3.6	P$_{TOT}$	13	-2.9%	6.6%
				ppNH$_3$	13	-1.6%	6.2%
	2.62 - 7.94	7.3 - 7.3	0.4 - 4.0	P$_{TOT}$	10	-2.8%	2.8%
				ppNH$_3$	10	-1.5%	2.1%
	3.16 - 3.50	9.6 - 9.6	0.7 - 2.2	P$_{TOT}$	3	-5.2%	5.2%
				ppNH$_3$	3	-4.0%	4.0%
	3.49 - 8.71	12.6 - 12.6	0.9 - 6.9	P$_{TOT}$	7	7.3%	7.3%
				ppNH$_3$	7	8.7%	8.7%
	4.44 - 9.32	18.3 - 18.4	1.3 - 9.7	P$_{TOT}$	7	10.6%	10.6%
				ppNH$_3$	7	12.1%	12.1%
	5.34 - 9.36	25.9 - 26.0	1.7 - 13.3	P$_{TOT}$	7	10.4%	10.4%
				ppNH$_3$	7	11.8%	11.8%

Table H 45. Aqueous Carbon Dioxide - Ammonia Mixtures: Ammonia Concentration
Ranges for 393 K [22]

T (K)	P (Bar)	mNH_3	mCO_2		Pts	BIAS	AAD
393.15	3.28 - 8.53	2.8 - 2.8	0.2 - 1.3	P_{TOT}	7	-5.4%	8.0%
				$ppNH_3$	7	-4.1%	7.2%
	5.37 - 14.74	8.1 - 8.1	0.6 - 4.1	P_{TOT}	7	1.5%	5.0%
				$ppNH_3$	7	2.9%	5.3%
	6.92 - 27.33	12.2 - 12.5	0.8 - 6.9	P_{TOT}	14	1.2%	2.3%
				$ppNH_3$	14	2.5%	2.9%
	10.80 - 22.16	20.4 - 20.5	1.3 - 10.1	P_{TOT}	7	2.5%	2.5%
				$ppNH_3$	7	-3.9%	3.9%
	11.87 - 22.33	25.7 - 25.9	1.8 - 12.7	P_{TOT}	7	3.6%	3.6%
				$ppNH_3$	7	5.0%	5.0%

Table H 46. Aqueous Carbon Dioxide - Ammonia Mixtures: Ammonia Concentration Ranges for 413 K [22]

T (K)	P (Bar)	mNH_3	mCO_2		Pts	BIAS	AAD
413.15	5.78 - 18.30	2.5 - 2.5	0.2 - 1.0	P_{TOT}	6	-2.5%	3.5%
				$ppNH_3$	6	1.2%	2.6%
	6.47 - 23.76	4.0 - 4.0	0.2 - 1.8	P_{TOT}	7	-2.4%	2.7%
				$ppNH_3$	7	-1.1%	1.8%
	8.74 - 35.90	7.2 - 8.2	0.4 - 3.8	P_{TOT}	20	-1.0%	1.2%
				$ppNH_3$	20	-0.3%	0.7%
	11.84 - 32.20	11.6 - 11.9	0.9 - 5.2	P_{TOT}	14	-0.8%	2.2%
				$ppNH_3$	14	0.6%	2.2%
	17.11 - 46.60	18.4 - 18.8	1.3 - 8.8	P_{TOT}	13	0.3%	1.2%
				$ppNH_3$	13	-1.6%	1.7%
	21.86 - 45.10	24.9 - 25.3	2.0 - 11.6	P_{TOT}	12	0.6%	0.9%
				$ppNH_3$	12	2.0%	2.0%

Table H 47. Aqueous Carbon Dioxide - Ammonia Mixtures: Ammonia Concentration
Ranges for 433 K [22]

T (K)	P (Bar)	mNH_3	mCO_2		Pts	BIAS	AAD
433.15	10.46 - 32.00	2.7 - 2.7	0.2 - 1.1	P_{TOT}	7	-1.8%	1.8%
				$ppNH_3$	7	-0.5%	0.5%
	15.11 - 51.50	7.7 - 7.7	0.7 - 3.1	P_{TOT}	6	-1.0%	1.0%
				$ppNH_3$	6	0.4%	0.7%
	20.35 - 57.40	12.7 - 12.7	0.9 - 4.9	P_{TOT}	6	-1.0%	1.1%
				$ppNH_3$	6	0.3%	0.6%
	25.34 - 54.60	17.9 - 18.5	0.9 - 6.4	P_{TOT}	14	-1.2%	1.3%
				$ppNH_3$	14	0.1%	0.7%
	32.50 - 67.60	24.6 - 24.6	1.3 - 9.8	P_{TOT}	7	-0.4%	0.7%
				$ppNH_3$	7	0.9%	1.0%

Table H 48. Aqueous Carbon Dioxide - Ammonia Mixtures: Ammonia Concentration Ranges for 453 K and 473 K [22]

T (K)	P (Bar)	mNH_3	mCO_2		Pts	BIAS	AAD
453.15	16.53 - 47.60	2.5 - 2.5	0.2 - 0.9	P_{TOT}	7	-2.0%	2.0%
				$ppNH_3$	7	-0.7%	0.7%
	21.96 - 70.40	6.9 - 6.9	0.2 - 2.1	P_{TOT}	7	-1.4%	1.4%
				$ppNH_3$	7	-0.1%	0.7%
	31.30 - 79.50	12.3 - 12.7	0.7 - 3.8	P_{TOT}	9	-0.6%	1.0%
				$ppNH_3$	9	-0.7%	1.1%
473.15	29.10 - 83.40	2.4 - 2.4	0.3 - 1.0	P_{TOT}	6	-0.9%	1.0%
				$ppNH_3$	6	0.4%	0.4%
	36.30 - 82.10	7.0 - 7.1	0.5 - 1.6	P_{TOT}	4	-1.1%	1.1%
				$ppNH_3$	4	0.2%	0.2%
	34.90 - 88.10	10.6 - 10.7	0.3 - 2.1	P_{TOT}	6	-1.0%	1.0%
				$ppNH_3$	6	0.3%	0.3%

REFERENCES

1.   Diamond, L.W. and N.N. Akinfiev, *Solubility of CO_2 in water from -1.5 to $100^o C$ and from 0.1 to 100 MPa: evaluation of literature data and thermodynamic modelling.* Fluid Phase Equilibria, 2003. 208: p. 265-290.

2.   Takenouchi, S. and G.C. Kennedy, *The binary system H_2O-CO_2 at high temperatures and pressures.* American Journal of Science, 1962. 262: p. 1053-1074.

3.   Nighswander, J.A., N. Kalogerakis, and A.K. Mehrotra, *Solubilities of Carbon Dioxide in Water and 1 wt % NaCl Solution at Pressures up to 10 MPa and Temperatures from 80 to 200 C.* J. Chem. Eng. Data, 1989. 34: p. 355-360.

4.   Rumpf, B., et al., *Simultaneous Solubility of Ammonia and Hydrogen Sulfide in Water at Temperatures from 313 K to 393 K.* Fluid Phase Equilibria, 1999. 158-160: p. 923-932.

5.   Hudson, J., *CLXXXIII.--The Solubility of Sulphur Dioxide in Water and in Aqueous Solutions of Potassium Chloride and Sodium Sulphate*, Imperial College: London. p. 1332-1347.

6.   Rabe, A.E. and J.F. Harris, *Vapor-Liquid-Equilibrium Data for the Binary System, Sulfur Dioxide and Water.* Journal of Chemical and Engineering Data, 1963. 8: p. 333-336.

7.   Lee, J.I. and A.E. Mather, Ber. Bunsenges. Phys. Chem., 1977. 8: p. 1021-1023.

8.   Onken, U., J. Ghmeling, and W. Arlt, *Vapor-Liquid Equilibrium Data Collection, Aqueous-Organic Systems*, ed. D. Bekrens and R. Eckermann. Vol. Vol 1, Part Ia. 1981: DECEMA.

9.   Rumpf, B. and G. Maurer, *Solubilities of Hydrogen Cyanide and Sulfur Dioxide in Water at Temperatures from 293.15 to 413.15 K and Pressures up to 2.5 MPa.* Fluid Phase Equilibria, 1992. 81: p. 241-260.

10.   Clifford, I.L. and E. Hunter, *The System Ammonia-Water at Temperatures up to 150°C. and at Pressures of up to Twenty Atmospheres*. p. 101-118.

11.   Takenouchi, S. and G.C. Kennedy, *The Solubility of Carbon Dioxide in NaCl Solutions at High Pressure Temperatures and Pressures.* American Journal of Science, 1965. 263(May): p. 445-454.

12.   Rumpf, B., et al., *Solubility of Carbon Dioxide in Aqueous Solutions of Sodium Chloride: Experimental Results and Correlation.* Journal of Solution Chemistry, 1994. 23(No. 3): p. 431-448.

13.   Prutton, C.F. and R.L. Savage, *The Solubility of Carbon Dioxide in Calcium Chloride-Water Solutions at 75, 100, 120 and High Pressures.* Am. Chem. Soc. J., 1945. 67: p. 1550-1554.

14.   Rumpf, B. and G. Maurer, *An Experimental and Theoretical Investigation on the Solubility of Carbon Dioxide in Aqueous Solutions of Strong Electrolytes.* Ber. Bunsenges. Phys. Chem., 1993. 97(No. 1): p. 85-97.

15.   Corti, H.R., et al., *Effect of a Dissolved Gas on the Solubility of an Electrolyte in Aqueous Solution.* 1990. 29: p. 1043-1050.

16.   Yasunishi, A. and Y. Fumitake, *Solubility of Carbon Dioxide in Aqueous Electrolyte Solutions.* Journal of Chemical and Engineering Data, 1979. 24(No. 1): p. 11-14.

17.   Rumpf, B. and G. Maurer, *Solubility of sulfur dioxide in aqueous solutions of sodium-and ammonium sulfate at temperatures from 313.15 K to 393.15 K and pressures up to 3.5 MPa.* Fluid Phase Equilibria, 1993. 91: p. 113-131.

18.   Barrett, T.J., G.M. Anderson, and J. Lugowski, *The solubility of hydrogen sulphide in 0-5 m NaCl solutions at 25-95 C and one atmosphere.* Geochimica et Cosmochimica Acta, 1988. 52: p. 807-811.

19.   Perman, E.P., *LXXXII.--Influence of Sodium Sulphate on the Vapour Pressure of Aqueous Ammonia Solution.* J. Chem. Soc., 1901. 79: p. 725-729.

20. Rumpf, B. and G. Maurer, *Solubility of Ammonia in Aqueous Solutions of Sodium Sulfate and Ammonium Sulfate at Temperatures from 333.15 K to 433.15 K and Pressures up to 3 MPa.* Ind. Eng. Chem. Res., 1993. 32: p. 1780-1789.

21. Goppert, U. and G. Maurer, *Vapor-Liquid Equilibria in Aqueous Solutions of Ammonia and Carbon Dioxide at Temperatures between 333 and 393 K and Pressures up to 7 MPa.* Fluid Phase Equilibria, 1988. 41: p. 153-185.

22. Muller, G., E. Bender, and G. Maurer, *Das Dampf-Flussigkeits-Gleichgewicht des ternaren System Ammoniak-Kohlendioxid-Wasser bei hohen Wassergehalten im Bereich zwischen 373 und 473 Kelvin.* Ber. Bunsenges. Phys. Chem., 1988. 92: p. 148-1660.

VITA

Eric Lawrence Maase

Candidate for the Degree of

Doctor of Philosophy

Dissertation: DEVELOPMENT OF A THERMODYNAMIC DATABASE,

EVALUATION OF EXPERIMENTAL ENTHALPY DEPARTURE DATA, AND

MODELING PHASE BEHAVIOR IN WEAK AQUEOUS ELECTROLYTE

MIXTURES

Major Field: Chemical Engineering

Biographical:

Personal Data: Born in Cincinnati, Ohio on August 21, 1970, the son of Shirley M. and David L. Maase.

Education: Received Bachelor of Science degree in Chemical Engineering from University of Maryland, College Park, Maryland in May and received a Master of Science degree in Chemical Engineering from Colorado School of Mines, Golden, Colorado in May 1995. Completed the requirements for the Doctor of Philosophy degree with a major in Chemical Engineering at Oklahoma State University in December 2004.

Experience: Teaching Fellow in Freshman Introduction to Engineering course 1992 at the University of Maryland, College Park Maryland. Research/Teaching Assistant 1993-95 at the Colorado School of Mines, Golden, Colorado. Research/Teaching Assistant at Oklahoma State University, Stillwater, Oklahoma. Associate Professor, Mathematics, 1999 at Chesapeake College, Wye Mills, Maryland. Computer/Programming Consultant 1994-Present on various contracts. Currently (2004) a Guest Lecturer and Post-Doctoral Student at Oklahoma State University, Stillwater, Oklahoma.

Professional Memberships: Member of American Institute of Chemical Engineers (AICHE), Omega Chi Epsilon, American Chemical Society, and American Association of Engineering Educators.